HAL
open science

Aspects moléculaires des hélicases de la famille de RecQ

Hua Ren

To cite this version:

Hua Ren. Aspects moléculaires des hélicases de la famille de RecQ. Sciences du Vivant [q-bio]. École normale supérieure de Cachan - ENS Cachan, 2009. Français. NNT : . tel-00448084

HAL Id: tel-00448084

https://theses.hal.science/tel-00448084v1

Submitted on 18 Jan 2010

HAL is a multi-disciplinary open access archive for the deposit and dissemination of scientific research documents, whether they are published or not. The documents may come from teaching and research institutions in France or abroad, or from public or private research centers.

L'archive ouverte pluridisciplinaire **HAL**, est destinée au dépôt et à la diffusion de documents scientifiques de niveau recherche, publiés ou non, émanant des établissements d'enseignement et de recherche français ou étrangers, des laboratoires publics ou privés.

N° ENSC-(n° d'ordre)

THESE DE DOCTORAT
DE L'ECOLE NORMALE SUPERIEURE DE CACHAN

Présentée par

Madame Hua REN

pour obtenir le grade de

DOCTEUR DE L'ECOLE NORMALE SUPERIEURE DE CACHAN

Domaine :

SCIENCES DE LA VIE ET DE LA SANTE

Sujet de la thèse:

Aspects moléculaires des hélicases de la famille de RecQ

Thèse présentée et soutenue à ECNU Chine le 28 / 09/ 2009 devant le jury composé de :

M. Marc BOUDVILLAIN Président/Rapporteur

M. Jie-min WENG Rapporteur

M. Duan MA Examinateur

Mme Min QIAN Co-Directrice de thèse

M. Xu-guang XI Co-Directeur de thèse

Nom du Laboratoire: LBPA

ENS CACHAN/CNRS/UMR 8113

61, avenue du Président Wilson, 94235 CACHAN CEDEX (France)

ACKNOWLEDGEMENT

This thesis would not have been done possibly without the support of many people.

Foremost, I would like to express my gratitude to my two co-supervisors, Prof. Min QIAN and Prof. Xu-guang XI. Thanks to Xu-guang XI for allowing me to join his team, sharing with me a lot of his expertise and research insight. He is extremely helpful and offering me invaluable assistance, support and guidance. I would like to thank Prof. Min QIAN for her expertise, kindness, patience and most of all, for her support.

My great appreciation also goes to my thesis committee members: Prof. Marc BOUDVILLAIN, Prof. Jie-min WENG, Prof. Duan MA, Prof. Jia LI and Prof. Xiang-huo HE. Without their knowledgeable and considerable assistances, this thesis would not have been successful.

I am greatly indebted to many teachers in the *Ecole normale supérieure de Cachan (ENS Cachan)*, *East China Normal University* and *Institute Curie of Orsay.* Especially thanks to Prof. Christian AUCLAIR, the director of the laboratories and institutes of ENS Cachan; Prof. Jean-francois MOUSCADET, the director of Laboratory and Applied Genetic Pharmacology Laboratory (LBPA); Prof. Giuseppe Baldacci, the president of Institute Curie of Orsay; Mesdames Bogdana NEUVILLE and Yu-hua QIAN; Mr. Hai-sheng LI.

And I am deeply grateful to the French government, the Chinese Scholarship Council and the Chinese Embassy in France for providing me the financial support during my PhD. Studies.

I am tempted to individually thank all of the members in the same team, Mesdames Rong-bing GUO, Min ZHOU, Françoise CHAMINADE, Mounira AMOR-GUERET, Rosine Onclercq-Delic, Emmanuelle Delagoutte; Messieurs Pascal Rigolet, Philippe FOSSE, Nicolas BAZEILLE, Jie-lin LIU, Bo ZHANG, Da-peng ZHANG.

It is never been overstated how much thanks I owes to all my friends who studied with me together in France. Thank you for your company which made my lives there enjoyable and beyond my expectation.

Last but not least, I want to show how grateful I am with my family: my husband Wei NIU who has been standing beside me and encouraging me as always; my mother Wan-ying ZHANG whose love is boundless and my father Hui-bin REN who is my role model. They have always been supporting and stimulating me to do my best in all matters of life. To them I heartily dedicate this thesis.

TABLE OF CONTENTS

SUMMARY IN CHINESE （中文摘要） **7**

SUMMARY IN FRENCH (RESUME) **11**

SUMMARY **13**

ABREVIATIONS **15**

CHAPTER 1 GENERAL INTRODUCTION **18**

1. DIFFERENT HELICASE FAMILIES **20**

SUPERFAMILY 1 21
SUPERFAMILY 2 21
SUPERFAMILY 3 22
SUPERFAMILY 4 24
OTHER SUPERFAMILIES 26

2. HELICASE-GENERAL PROPERTIES OF HELICASES AND MODE OF ACTION **27**

2.1 BIOCHEMICAL PROPERTIES OF HELICASES 27
2.1.1 NTP binding and hydrolysis of NTP *27*
2.1.2 Nucleic Acids binding *27*
2.1.3 Unwinding Activity and Mode of Action *28*
2.1.4 Annealing Activity *31*
2.2 THE MULTIPLE FUNCTIONS OF HELICASES 32
Helicase and DNA replication *32*
Helicase and DNA repair *33*
Helicase and RNA metabolism *33*

3. THE RECQ FAMILY OF DNA HELICASES **34**

3.1 GENERAL FEATURES AND STRUCTURAL ORGANISATION 34
3. 2 THE ESCHERICHIA COLI RECQ 39
3.2.1 Genetic Background *39*
3.2.2 Biochemical and structural Properties of E.coli RecQ *39*
3.2.3 Role in genomic stability *40*
3.2.4 RecQ helicases from other microorganisms *43*
3.3 YEAST RECQ FAMILY HELICASES 43
3.3.1 Saccharomyces cerevisiae Sgs1 ..... *43*
3.3.1.1 Sgs1 Cellular Phenotype *43*
3.3.1.2 Biochemical Properties of Sgs1 ..... *44*
3.3.1.3 Interaction Partners and Models for genome instability *44*
3.3.2 Schizosaccharomyces pombe Rqh1 ..... *46*
3.3.2.1 Biochemical properites 46
3.3.2.2 Function in telomere metabolism 46
3.4 RECQ HELICASES IN HUMAN 47
3.4.1 Human RECQ1 ..... *47*
Human RECQl and genome stability 47
Biochemical properties 50
Structure of human RECQl 50
3.4.2 BLM - The Bloom Syndrome Helicase *51*
Bloom's Syndrome (BS) 51
BS Cellular Phenotype 53
BLM protein and its interaction partners 53
3.4.3 WRN - The Werner Syndrome Helicase *57*
The Werner Syndrome 57
WS Cellular Phenotype 58
WRN protein and its interaction partners 60

3.4.4 RECQ4/RTS- The Rothmund-Thomson Syndrome Protein 62
The Rothmund-Thomson Syndrome (RTS) 62
RTS Cellular Phenotype 63
RECQ4 protein 64
3.4.5 RECQ5 ..... *66*
Discovery of RECQ5 66
Biochemical properties of RECQ5 67
RECQ5 and SCEs 70

4. PROPOSE 70

4.1 THE ENZYMATIC REGULATION ROLE OF ZINC FINGER MOTIF IN RECQ FAMILY HELICASE 70
4.2 THE FUNCTIONAL ASPECTS OF HRDC DOMAIN IN RECQ HELICASE FAMILY 71
4.3 THE SPECIAL STRUCTURAL FEATURE OF ARGININE FINGER IN RECQ FAMILY HELICASE 71

REFERENCES 73

CHAPTER 2 RESULTS 90

I ZINC BINDING MOTIF IN RECQ5B ACTS AS A MOLECULAR SWITCH TURNING STRAND ANNEALING INTO DNA UNWINDING 91

ACKNOWLEDGEMENTS 92

SUMMARY 93

INTRODUCTION 94

MATERIALS AND METHODS 97

PROTEINS AND DNA SUBSTRATES 97
QUANTIFICATION OF THE PROTEIN-BOUND ZN^{2+} IONS 100
ATP BINDING ASSAY 100
ATPASE ASSAY 101
DNA BINDING ASSAY 101
DNA HELICASE ACTIVITY ASSAY 102
DNA STRAND-ANNEALING ASSAY 103

RESULTS AND DISSCUSSION 104

RECQ5 HELICASE DOMAIN ALONE CATALYZES STRAND ANNEALING, BUT NOT STRAND SEPARATION 104
THE RECQ5 HELICASE DOMAIN BINDS ATP EFFICIENTLY, BUT DISPLAYS A POOR ATPASE ACTIVITY 111
A ZINC-BINDING MOTIF IS ESSENTIAL FOR THE HELICASE ACTIVITY OF RECQ5B 112
MOLECULAR MECHANISM OF INTRAMOLECULAR STIMULATION OF CATALYTIC ACTIVITY MEDIATED BY THE ZINC BINDING MOTIF 115
MODEL FOR THE ROLE OF THE ZINC-BINDING MOTIF IN THE FUNCTION OF RECQ HELICASES 116

CONCLUDING REMARKS 119

REFERENCES 120

II BIOCHEMICAL CHARACTERIZATION OF HELICASE ACTIVITY AND DNA SUBSTRATE SPECIFICITY OF *BACILLUS SUBTILIS* RECQ HELICASES 123

ACKNOWLEDGEMENT 124

SUMMARY 125

INTRODUCTON 126

MATERIALS AND METHODS 128

Reagents 128
Nucleic Acid Substrates 128
Template selection and amino acid sequence alignment 128
Protein Expression 131
Protein Purification 132
Quantification of Zinc Ion Bound to SubL and SubS helicases 132
Size Exclusion Chromatography of SubL 133
ATPase Assay 133
DNA helicase assay 133
Protein-DNA Binding Assay by EMSA 134
DNA strand-annealing and strand-exchange assay 134

RESULTS 136

Molecular modelling 136
Cloning, Production and Purification of RecQ Helicase from *Bacillus subtilis* 138
DNA-dependent ATPase Activity 140
DNA Unwinding Activities Assay versus *B. subtilis* RecQ Helicases Concentration 143
Polarity and processivity of the *B. subtilis* RecQ Helicases 143
B. subtilis RecQ Helicase Activity on Blunt-ended and Gapped DNA Substrates 148
B. subtilis RecQ Helicase Activity on Forked Duplex DNA with Increasing 3' and 5'- Tail Length 150
B. subtilis RecQ Helicases target DNA replication and repair intermediates 150
Binding of the putative *B. subtilis* RecQ to DNA substrates 155
B. subtilis RecQ helicases possess DNA strand-annealing activity and promote DNA exchange weakly 157

DISCUSSION 160

REFERENCES 165

III. THE ARGININE FINGER OF THE BLOOM SYNDROME PROTEIN: ITS STRUCTURAL ORGANIZATION AND ITS ROLE IN ENERGY COUPLING 169

ACKNOWLEDGEMENTS 170

SUMMARY 171

INTRODUCTION 172

MATERIALS AND METHODS 177

Plasmid construction and site-directed mutagenesis 177
Protein expression and purification 177
DNA substrates preparation 178
ATPase assay 178
DNA unwinding activity assay 179
DNA binding assay 180
DNA annealing activity by EMSA 181
ATP-binding assays 181
Preparation of orthovanadate solutions 183

RESULTS 184

Design, expression, and purification of BLM mutations 184
Vi inhibits and uncouples ATPase and DNA unwinding activities of $BLM^{642-1290}$ 186
Helicase and ATPase activities of the mutant enzymes 189
All mutants display normal ATP and DNA binding abilities 194
Arginine residues mutants display normal annealing abilities 201
Vi inhibition study reveals that R982 functions as an arginine finger 202

DISCUSSION 206

REFERENCES **211**

CHAPTER 3 GENERAL CONCLUSION AND PERSPECTIVE **214**

1 THE SPECIAL FUNCTION OF ZINC BINDING MOTIF IN RECQ FAMILY HELICASES **215**

2 THE FUNCTION OF THE HRDC DOMAIN IN RECQ HELICASE FAMILY **216**

3 THE SPECIAL STRUCTURAL FEATURE OF ARGININE FINGER OF RECQ FAMILY HELICASE **217**

4 PERSPECTIVE **217**

REFERENCES **219**

CHAPTER 4 APPENDIXES **220**

I. MATERIALS AND METHODS **221**

1. PLASMIDS CONSTRUCTION **221**

A. PCR AND GEL EXTRACTION **221**

REAGENTS AND INSTRUMENTS 221

PROTOCOL 221

B. PLASMID CONSTRUCTION **222**

REAGENTS AND INSTRUMENTS 222

PROTOCOL 223

2. PROTEIN EXPRESSION AND PURIFICATION **227**

REAGENTS AND INSTRUMENTS 227

PROTOCOL 228

3. WESTERN BLOT **230**

REAGENTS AND INSTRUMENTS 230

PROTOCOL 231

4. ATPASE ACTIVITY **233**

REAGENTS AND INSTRUMENTS 233

PROTOCOL 233

5. HELICASE ACTIVITY EXAMINATION **234**

REAGENTS AND INSTRUMENTS 234

PROTOCOL 235

6. DETERMINE ZINC ION CONCENTRATION OF HELICASE **237**

REAGENTS AND INSTRUMENTS 237

PROTOCOL 237

II. LIST OF PUBLICATIONS **239**

SUMMARY IN CHINESE （中文摘要）

Waston 和 Crick 提出 DNA 双螺旋结构后，不仅引导人们发现了 DNA 聚合酶，它作用于 DNA 以一条链为模板聚合形成一条新的 DNA 链；而且也让科学家们寻找到一种酶能够在 DNA 复制时破坏互补碱基对的氢键结构而打开 DNA 双螺旋结构。随后，相似功能的酶在 RNA 复制中也被发现。这类酶被科学家称为解旋酶。解旋酶是一类能解开核苷酸双链的酶，它广泛存在于从病毒到人类等多种生物体中。自 1976 年人类在大肠杆菌（*Esherichia Coli E.coli*）中发现了第一个解旋酶，至今已有上百种解旋酶被发现，而且这一酶家族成员还在不断扩大。

解旋酶广泛存在于多种生物体中，有些生物还同时具有多种不同类型的解旋酶。尽管解旋酶种类繁多，人们在研究过程中发现，这类蛋白酶在其氨基酸序列上有一定的同源性和相似性。分析表明，这些同源序列在进化过程中构成了几个高度保守的区域，这些区域执行不同的酶功能。人们根据酶的二维结构和一级序列，把解旋酶分为几大家族来分类研究。经过多年的研究，人们发现解旋酶具有多种功能，在细胞内它们参与 DNA 复制、修复、转录重组以及 RNA 接拼、核糖体组装、蛋白质翻译，端粒稳定。最近，还发现个别解旋酶甚至参与机体天然免疫反应机制。解旋酶已不仅仅只是分开核酸双链结构的一类酶，它的生物功能远不止此。

解旋酶第二大家族中的 RecQ 解旋酶亚家族在核酸代谢过程中起了关键的作用，这一家族参与 DNA 复制、DNA 修复、重组、转录甚至端粒稳定机制。人们发现在人体中存在 RECQ1、BLM、WRN、RECQ4 和 RECQ5 这五种 RecQ 解旋酶家族成员。其中，BLM、WRN、RECQ4 编码基因缺陷会导致人类相应的疾病发生，它们分别为 Bloom 综合症（BS）、Werner 综合症（WS）、Rothmund-Thomson 综合症（RTS）、RAPADILINO 综合症和 Baller-Gerold 综合症。这些疾病虽然在人类中都是极其罕见的隐形遗传疾病，但是在分子水平都表现为基因组高度不稳定性、染色体异常（染色体断裂、缺失、重排、姐妹染色体交换等）和对 DNA 损伤因子敏感性增加。在临床上表现为过早衰老、II 型糖尿病、骨质疏松、动脉硬化和极度容易发生癌症。大部分病人都是最终发生不同癌症而死亡。这一临床共同现象引起了人们的关注和研究热潮 。对解旋酶的结构功能、作用机制的研究不仅可以认清核酸代谢过

程，还能帮助我们揭示癌症发病的某些相关机理。同时了解病毒解旋酶的结构与功能，为抗病毒药物的研制提供了新的靶点和思路。

解旋酶具有四大基本生物化学活性：NTP 水解活性、DNA 或 RNA 结合活性、核酸链解链活性和核酸链退火配对活性。在二价金属离子（比如 Mg^{2+}）和 NTP 的存在下，解旋酶便表现出水解 NTP 的性质，大部分酶水解 ATP 和 dATP，一些酶则能水解其他的核苷酸，比如 TTP 和 GTP。当解旋酶与 DNA 或 RNA 结合后，利用水解核苷酸产生的能量，推动酶在核酸链上的移动，从而解开互补的两条核酸链。随着研究的深入，人们发现有些解旋酶在核酸修复过程中能促使核酸链配对重组。这使得我们意识到解旋酶在基因稳定过程中的作用越来越重要。但是并不是所有的解旋酶成员都表现出这四种基本生化功能，这与酶自身的结构有密切的关系，酶的结构决定了它所能表现的作用机制和生化活性。长期以来，科学家们一直研究探索解旋酶的结构与其功能间的相互关系，力求发现解旋酶本质的运作机制。

RecQ 解旋酶家族尽管蛋白种类繁多，在氨基酸序列上同源性不高，但有限的同源序列构成了数个典型的功能区域：从 N 端向 C 端方向，分别为位于氨基酸序列中间段的解旋酶核心区域，RecQ C 端区域（RecQ-Ct）和解旋酶 RNase D 保守区域（HRDC），这些区域具有不同的功能，并相互协调共同执行解旋酶的运作机制。解旋酶核心区域是解旋酶标志性结构，它由一段高度保守的氨基酸序列组成，含有 7 个保守区域， 负责结合 NTP、NTP 水解和 DNA 结合。RecQ-Ct 区域是 RecQ 解旋酶家族唯一含有的结构特征，但不是所有 RecQ 成员都含有这一结构域。RecQ-Ct 区域包含两个重要的亚结构域：由四个 α 螺旋和四个保守的半胱氨酸残基组成的结构平台，因能特异结合锌离子而被命名为锌结合区域或锌指结构（zinc-binding motif, zinc finger, ZBM）；序列上不太保守的翼型螺旋亚结构域（winged-helix, WH）。目前发现 RecQ-Ct 结构域主要负责酶与核酸的结合、酶自身的折叠作用。HRDC 区域位于解旋酶氨基酸序列的 C 端，在部分 RecQ 成员中缺失，对这一结构域的认识甚浅，一些研究表明 HRDC 区域能够增强解旋酶对 NTP 水解和解链活性。虽然解旋酶不同的结构域负责不同的酶功能，但解旋酶核心区域、RecQ-Ct 和 HRDC 区域并不是各自独立的，它们互相之间相互作用相互协调，共同完成酶的生理作用机制。

本文就以 RecQ 解旋酶家族中 BLM、RECQ5 和枯草杆菌 RecQ （*Bacillus subtilis* RecQ）为实验对象，来研究解旋酶不同结构域之间是如何相互影响、相互牵制。从而了解解旋酶结构与其功能相互间的关系，揭示解旋酶的作用机制。

首先我们把焦点放在 RecQ 解旋酶的 RecQ-Ct 区域，想了解这一区域是如何与解旋酶核心区域相互作用，相互之间存在何种联系，来共同维持解旋酶整体的酶活性平衡。我们以 RECQ5 为研究模型，RECQ5 是人体 5 种解旋酶之一，虽然至今未发现它与任何人类疾病有关，但是有实验证明 RECQ5 与 BLM 蛋白密切相关，能协助 BLM 蛋白维持染色体的平衡。而且 RECQ5 解旋酶天然存在三种异构体：RECQ5α 、REQ5β 和 RECQ5γ。其中 REQ5β 最大，含有解旋酶核心区域和 RecQ-Ct 区域，相对的 RECQ5α 最小，只含有解旋酶核心区域结构。这两种异构体成为研究 RecQ-Ct 结构域功能，和解旋酶核心结构域相互关系最理想的天然模型。实验结果揭示，RECQ5α 既没有 ATP 水解能力，也不表现解链活性，却展示出对互补核酸链的退火配对作用。REQ5β 则表现出较弱的退火配对能力和较强的解链活性。一系列实验证明，其中 RecQ-Ct 区域的保守结构—锌结合区域起到了重要作用，不仅增加酶对 DNA 的结合能力，而且起到了分子开关的作用，能够通过对 DNA 结合的增强来抑制解旋酶核心区域的退火配对活性，同时改变蛋白构型启动解链过程。我们率先提出 RecQ-Ct 区域锌指结构与解旋酶核心区域相互作用的机制模型，初步揭示两者之间的相互联系，了解 RecQ 解旋酶结构与结构之间，结构与功能间的相互关系。

在对 RecQ 解旋酶核心区域与 RecQ-Ct 区域认识的基础上，进一步研究位于氨基酸序列最 C 端的 HRDC 区域的功能，探究 HRDC 与解旋酶核心区域、RecQ-Ct 区域的相互关系。本文利用 RecQ 解旋酶家族中枯草杆菌 RecQ （*Bacillus subtilis* RecQ，SubRecQ）亚家族为研究模型，它由两个成员组成。这两种 RecQ 解旋酶的典型结构差异在于一个含有 HRDC 区域，而另一个则 HRDC 区域缺失。为研究提供了理想的天然结构模型。 结果表明，具有 HRDC 区域的 SubRecQ 酶，表现出解旋酶基本的生化活性，并能有效地解开一些 DNA 复制与修复中 DNA 错误结构甚至是 Holliday 结构。相对地，SubRecQ 如果缺失 HRDC 区域，虽能具有较弱 ATP 水解活性，解链活性，但无法解开某些复杂的 DNA 复制与修复中间体结构，同时也不具有解开 Holliday 结构的能力。两种解旋酶的 DNA 结合活性与 DNA 退火配对活性无明显差异。分析认为，HRDC 结构能辅助增强解旋酶的 ATP 水解活性与解链活性，在解开复杂的 DNA 结构过程中起到了关键的作用。

RecQ 解旋酶家族中的 BLM 蛋白是迄今在人体中发现的 5 种解旋酶之一，BLM 编码基因的缺陷会导致疾病 Bloom 综合症的发生。而且 BLM 蛋白具有 RecQ 解旋酶家族典型的结构特征，因此它成为理想的研究模型。本实验室致力于 BLM 蛋白生化

活性的研究已有多年，发现完整的 BLM 蛋白能表现出解旋酶全部的基本生物功能，也了解了其各个结构区域负责哪些酶功能。在研究其结构与功能的相互关系的过程中我们发现，BLM 蛋白的解旋酶核心区域含有高度保守的精氨酸残基靠近于与其结合的 ATP γ 磷酸位置，称为精氨酸指结构。我们推测这一结构负责 ATP 的结合与水解活性。蛋白结构分析表明，BLM 蛋白解旋酶核心区域还有两个保守的精氨酸残基—R979 与 R982。突变这两个残基位点后，发现 BLM 对 ATP 的水解能力明显下降，同时丧失解链能力，但对 ATP 结合与 DNA 结合能力并无影响。R982 突变体的 ATP 水解和解链活性减弱幅度比 R979 突变体更为明显。运用目前公认的精氨酸指检测试剂—原钒酸盐（Vi）探测 BLM 蛋白的精氨酸指结构，Vi 能与镁离子、ADP 和酶形成复合物，从而抑制酶对核苷酸 5’端三磷酸催化活性，试验结果表明 Vi 能非竞争性抑制 R982 精氨酸残基对 ATP 的水解作用，对 R979 精氨酸无抑制作用，从而确定 BLM 蛋白 R982 氨基酸残基形成了精氨酸指结构。我们还发现 R982 精氨酸指能与其周围其他一些解旋酶核心区域的重要残基相互作用，促进对 ATP 的招募和水解。在此我们也从一个新的角度揭示解旋酶是如何与 ATP 和核酸结合启动 ATP 的水解，随后引起蛋白构型变化并将水解产生的化学能源用于解链过程的作用机制。

解旋酶的结构是其生化活性的前提，不同保守功能区域分别具有不同的功能，彼此之间相互作用，互相协调，来完成酶的整个运作机制。除了解旋酶核心区域外，RecQ-Ct 与 HRDC 区域也是解旋酶重要的结构，结构的缺失与突变会不同程度影响酶的功能，增加或者减弱某些酶活性。解旋酶结构特征的完整保证了其在细胞中维持核酸代谢稳定的重要地位。

SUMMARY IN FRENCH (RESUME)

Dans les cellules, le déroulement de l'ADN double-brin est catalysé par une famille de protéines appelées hélicases. Ces protéines sont présentes chez tous les organismes des virus jusqu'à l'homme. Parmi ces hélicases, celles de la famille RecQ jouent un rôle essentiel dans le métabolisme de l'ADN en facilitant de nombreux processus cellulaires tels que la réplication, la réparation, la recombinaison, la transcription et la maintenance des télomères. Chez l'homme, il existe cinq membres de la famille RecQ identifiés comme RECQ1, BLM, WRN, RECQ4 et RECQ5. Les mutations dans BLM, WRN et RECQ4 sont associées à une prédisposition au cancer. En plus du domaine hélicase très conservé et contenant sept motifs bien distincts, la plupart des hélicases de la famille RecQ possèdent également un domaine RecQ C-terminal (RecQ-Ct) et un domaine hélicase RNase D (HRDC). Au cours de ce travail, nous nous concentrons sur les mécanismes intra-fonctionnels de certains membres de la famille RecQ des hélicases.

Tout d'abord, nous avons utilisé deux isoformes naturels de l'hélicase RECQ5 humain comme modèle pour étudier la modulation fonctionnelle du domaine hélicase avec le doigt de zinc. Ici, nous montrons que la variante tronquée RECQ5α de l'hélicase RECQ5β issue d'un épissage alternatif et composée uniquement du domaine hélicase ne possède ni l'activité ATPase ni l'activité de déroulement de l'ADN. A l'inverse, et ce de matière étonnante, cette protéine est dotée d'une forte activité de réhybridation du brin déroulé. Les mesures quantitatives indiquent que l'amélioration de l'affinité de la protéine pour l'ADN que lui confère le doigt de zinc est à l'origine de ses activités ATPase et hélicase. Le plus important est que l'on constate que le doigt de zinc est capable d'agir comme un facteur moléculaire à même de supprimer l'activité de re-synthèse du brin déroulé par le domaine hélicase et de déclencher l'activité de déroulement d'ADN à travers une modulation de la fixation à l'ADN.

Ensuite, nous avons analysé les propriétés biochimiques de deux isoformes de l'hélicase RecQ de *Bacillus subtilis* : SubL et SubS. Parmi elles, SubS ne dispose pas du domaine HRDC. Nos études montrent que le domaine HRDC est crucial pour *Bacillus subtilis* RecQ hélicases dans la résolution des intermédiaires de réplication et / ou de réparation de l'ADN tels que les jonctions de Holliday et la jonction de kappa. Les activités ATPase, hélicase et l'activité de rehybridation du brin déroulé sont plus importantes en présence du domaine HRDC. Ces résultats nous permettent de spéculer sur l'importance du domaine HRDC des activités de la famille de RecQ hélicase. Nous avons découvert que dans la famille RecQ, le

domaine HRDC peut augmenter les activités ATPases et hélicases. De manière intéressante, le domaine HRDC de *Bacillus subtilis* joue un rôle critique dans la résolution des intermédiaires de réplication ou de réparation de l'ADN et des jonctions de Holliday. Nous suggérons l'hypothèse que le domaine HRDC des hélicases RecQ participe à exposer leurs fonctions dans le processus de réparation de l'ADN.

Dans la dernière partie, nous nous sommes intéressés à l'existence et au rôle du doigt d'arginine dans la protéine BLM. Ces études ont été menées afin de démontrer son rôle dans l'hydrolyse d'ATP et dans la conversion en mouvement mécanique permettant à la protéine de progresser le long de l'ADN. Nos études démontrent que le résidu R982, situé à proximité du γ-phosphate de l'ATP, fonctionne comme un doigt d'arginine dans la protéine BLM. Nos conclusions indiquent en outre que ce doigt d'arginine interagit avec d'autres motifs conservés situés autour du γ-phosphate des nucléotides et qu'ils effectuent ensemble les fonctions enzymatiques au sein d'un réseau complexe.

Mots-clés : RecQ hélicase, le doigt de zinc, le domaine HRDC, le doigt d'arginine, RECQ5, *Bacillus subtilis*, BLM

SUMMARY

In the cells, the unwinding of double-stranded polynucleotides is catalyzed by helicases that exist in all kingdoms of life from virus to human. RecQ family helicases play essential roles in nucleic acid metabolism by facilitating cellular processes including genome replication, DNA repair, recombination, transcription and telomere maintenance. In human, five RecQ family members named RECQ1, BLM, WRN, RECQ4 and RECQ5, have been identified. Defects in BLM, WRN and RECQ4 will give rise to autosomal recessive disorders and predisposition to cancer. In addition to the highly conserved helicase core domain containing seven helicase motifs, most RecQ family helicases have a unique RecQ C-terminal domain (RecQ-Ct) and the Helicase RNase D conserved domain (HRDC). In the present studies, we focus on the intra-functional mechanisms of some important members of RecQ family helicases.

Firstly, we have chosen two natural isoforms of human RECQ5 helicase as models to study the functional modulation of the helicase core domain by the zinc-binding domain. Here we show that a truncated variant of the human RECQ5β helicase comprised of the conserved helicase domain only, a splice variant named RECQ5α, possesses neither ATPase nor DNA unwinding activities, but surprisingly displays a strong strand annealing activity. Quantitative measurements indicate that the regulatory role of the zinc-binding motif of RECQ5β is achieved by enhancing the DNA binding affinity of the helicase. More important, the zinc-binding motif of RECQ5β is found to act as a molecular switch that suppresses the strand-annealing activity of the helicase domain and triggers DNA-unwinding activity of the enzyme through enhancing DNA binding.

Subsequently, we analyzed the biochemical properties of two isoforms of *Bacillus subtilis* RecQ helicases: SubL and SubS. Between them, SubS naturally lacks the HRDC domain. Our studies demonstrate that the HRDC domain is crucial in Bacillus subtilis RecQ helicases in unwinding of DNA replication/repair intermediates such as Holliday junction and kappa junction. The enzyme with HRDC domain shows stronger ATPase activity and DNA unwinding and annealing activities than the other one. These results allow us to speculate on the importance of HRDC domain in the basic activities of RecQ family helicases.

In the last part, we investigated the existence and role of the arginine finger in the Bloom syndrome protein (BLM) in ATP hydrolysis and energy coupling. Our studies demonstrate that R982 is the residue located near the γ-phosphate of ATP which functions as a BLM

arginine finger. Our finding further indicates that the arginine finger interacts with other conserved motifs around γ-phosphate of the nucleotide to carry out the functions as a complex network.

Key words: RecQ helicase, the zinc binding domain, the HRDC domain, the arginine finger, RECQ5, *Bacillus subtilis*, BLM,

ABREVIATIONS

3D	Three dimension
ADP	adenine diphosphate
ADPNP	5′-adenylyl-β,γ-imidodiphosphate
ALT	alternative lengthening of telomeres
APH	aphidicolin
ATM	ataxia-telangiectasia mutated
ATP	adenine triphosphate
ATRx	alpha thalassemia/mental retardation syndrome X-linked
BACH1	BTB and CNC homology 1, basic leucine zipper transcription factor 1
BAS	bovine serum albumin
BLAP	BLM-associated polypeptide
BLM	protein expressed by the gene related to BS
BS	Bloom's syndrome
BTB	BLM-Topo IIIα-BLAP75 complex
dsDNA	double-stranded DNA
BRCA1	Breast cancer 1, early onset
Dda	DNA dependent ATPase
DHJ	Double Holliday junctions
DNA	deoxyribonucleotide acid
DnaB	a replicative DNA helicase of *E.coli*
DNA-PK	DNA dependent protein kinase
DNP	nucleotide diphosphate
DSBs	DNA double-strand breaks
DTT	dithiothreitol
EDTA	ethylene diamine tetracetic acid
eIF4B	eukaryotic initiation factor 4B
EMSA	Electrophoretic mobility shift assay
ERCC	excision repair cross-complementing rodent repair deficiency
FANCD2	A factor associated with breast cancer
FEN1	flap structure-special endonuclease 1
FRET	fluorescence resonance energy transfer
FPLC	fast protein liquid chromatography
G4	G-quadruplex structure

GC	gene conversion
GFP	green fluorescence protein
HerA	a bipolar DNA helicase
HJ	Holliday junction
HPLC	High fast protein liquid chromatography
HR	Homologous recombination
HRDC	Helicase RNase D conserved domain
HU	hydroxy urea
ICL	induced cross link
IPTG	isopropyl-β-D-thiogalactopyranoside
LSD1	Lysine demethylase 1
mantATP	2′(3′)-*O*-(*N*-methlanthraniloyl) adenosine-5′-triphosphate
MLH1	Mut L homolog 1
MMR	mismatch repair
MMS	methyl methanesulfonate
NHEJ	non-homologous end join
NLS	nuclear localization signals sequence
NS3	nonstructural 9.5 kDa protein, an RNA helicase of hepatitis B virus
NTP	Nucleoside triphosphate
p53	protein 53, encoded by the *TP53* gene
PAGE	polyacrilamide gel electrophoresis
PARP-1	Poly (ADP ribose) polymerase 1
PCR	polymerase chain reaction
PcrA	an ATP-dependent DNA helicase
PML NB	promyolocytic leukemia nuclear body
PMS2	postmeiotic segregation increased 2
PMSF	Phenylmethylsulfonyl fluoride
QU663	(N’-(pyrazin-ecarbonyl)-N’’-(7-ethoxy-2-methylquinolin-4-yl) hydrazine)
RAP	4-(2-pyridylazo)resorcinol
RDP	ribavirin-5' diphosphate
RecQ-Ct	RecQ helicase C-terminal domain
Rep	a replication related DNA helicase, ssDNA-dependent ATPase
RMN	RAD50/MRE11/NBS1 complex
RNA	ribonucleotide acid
RNAPII	RNA polymerase II

RPA	replication protein A
RTP	ribavirin-5'-triphosphate
RTS	Rothmund-Thomson syndrome
SCC	sister-chromatid conversion
SCE	sister chromatid exchange
SDS	sodium dodecylsulfate
SETX	senataxin
SF	superfamily
SNPs	single nucleotide polymorphism
SUMO	small ubiquitin like modification
ssDNA	single-stranded DNA
TRF2	telomere repeat binding factor 2
UvrD	DNA dependent ATPase I and helicase II in *E.coli*
WH	winged helix-turn-helix
WRN	Protein expressed by the gene related to WS
WS	Werner's syndrome

Chapter 1
GENERAL INTRODUCTION

In 1953, Watson and Crick set forth their hypothesis for the double-helical nature of DNA. The Watson-Crick model had an immediate effect on the emerging discipline of molecular biology (1). It was a remarkable feat in the history of genetics and biology. The discovery of the DNA structure was a pivotal event in modern biology. The double helical DNA structure must be unwound transiently and the two complementary strands must be separated, at least partially, in order to form single-stranded DNA during the processes of DNA replication, repair, recombination, and DNA transfer during conjugation. In the course of these biochemical metabolisms, several enzymes are required to attend the processes. So the Watson-Crick DNA model enables us to discover some enzymes which are used to synthesize the new DNA strand or to separate the DNA double helical structure during DNA replication, repair and recombination. Helicase is one of these important enzymatic tools for the cellular DNA metabolisms.

The first helicase was identified in 1976 in *Escherichia coli* (2;3). From then on, dozens more of DNA or RNA helicases have been identified from different organisms including bacteria, bacteriophages, viruses, yeasts, cows, frogs, *drosophila*, mice, humans, and plants. It is not surprising that helicases exist ubiquitously in prokaryotes and eukaryotes as well as in bacteriophages and viruses because these proteins play an essential role in nucleic acid metabolism. While DNA helicases are described as molecular 'motor' enzymes that are involved in most DNA metabolism, RNA helicases were found to play essential roles in RNA metabolic processes, including RNA genome replication for RNA virus, ribosome biogenesis, messengers RNA transcription, pre-mRNA splicing, RNA maturation, RNA export and degradation and RNA translation (4;5). So helicase is pivotal for cellular genome stability and integrity. But up to now, the precise molecular mechanisms of helicases are still poorly understood.

1. Different Helicase families

Since the discovery of the first helicase in *Escherichia coli* 30 years ago, more and more helicases have been isolated from different organisms. Helicases can be classified according to sequence homology and directionality. The directionality is defined with respect to the nucleic acid strand on which the enzyme translocates (3'-5' or 5'-3'). Based on amino acid sequence homology, helicases are classified into several major groups, denoted superfamilies 1-6 (SF1-6) (Table 1). SF1 and SF2 are the largest and are characterised by a set of similar amino acid motifs called I, Ia, TxGx and II-VI (Figure 1). SF3 helicases harbour only three different conserved helicase motifs called A, B and C and the SF4 helicases are known to have the five motifs called 1, 1a and 2-4. The motifs of the SF5 and SF6 members have not been well described (6).

Table 1 Classification of helicases

Six superfamilies of helicases are shown in the left row. Some typical members of each superfamily are listed in the table. The natures of the substrates and the polarities of unwinding are also indicated.

Helicase family	Helicase name	Species	Substrate	Reference
	Rep	*Escherichia coli*	3' to 5' DNA	(7;8)
SF1	PcrA	*Bacillus stearothermophilus*	3' to 5' DNA	(9)
	UvrD	*Escherichia coli*	3' to 5' DNA	(10;11)
	RecD	*Escherichia coli*	5' to 3' DNA	(12)
SF2	RecQ	*Escherichia coli*	3' to 5' DNA	(13;14)
	NS3	HCV virus	3' to 5' RNA	(15)
SF3	T antigen	Simian virus 40	3' to 5' DNA/RNA	(16)
SF4	DnaB	*Escherichia coli*	5' to 3' DNA	(17)
SF5	Rho	*Escherichia coli*	5' to 3' DNA/RNA	(18)
SF6	RuvB	*Escherichia coli*	5' to 3' DNA	(19)

Superfamily 1 (SF1): In this family, PcrA and Rep are two typical members (20;21). The conserved amino-acid sequences of SF1 helicases are distributed into seven motifs which carry out different biochemical functions. Superfamily1 can further be fallen into two groups according to the polarity of translocation along the DNA or RNA: SF1A (3' to 5') and SF1B (5' to 3'). Extensive biochemical and structural studies have been performed to understand molecular mechanisms of SF1A family helicases such as RepA, PcrA, UvrD, while the precise molecular aspects of SF1B family helicases including Red, Upf1 (22), Rrm3 (23) and Dda, still need to be clarified (24). Structural analysis shows that the SF1 helicases fold into two prominent domains, named 1 and 2, that are separated by a deep cleft and each domain contains two subdomains called A and B (Fig.1). The cleft is a site for ATP binding. Most of the conserved sequences motifs are found in domain 1A and 2A which take charge of binding nucleotides. These two subdomains composed of parallel β-sheet flanked by α-helices are located at the centre of the enzyme. The seven conserved motifs are distributed in subdomain 1A, 2A and 1B (25). They carry out different biochemical functions. The domain 2B is variable among different SF1 members. It may be involved in translocation of helicase along the DNA. The crystal structures of Rep and PcrA showed that the enzymes will be in two different conformations (termed 'open' and 'close' state) alternatively during biochemical processes (9). The conformational change is considered an important aspect of the mechanism of helicase.

Superfamily 2 (SF2): This is the largest family among all the helicases families. It has been identified in diverse organisms from virus to human beings. The representative helicases in this family are RecQ helicases (26), DEAD-box RNA helicases, the Snf2-like helicases and so on (27). The first revealed crystal structure of SF2 helicase was the non-structural protein 3 (NS3) of hepatitis C virus RNA which is involved in viral replication process (28). It is shown that the conserved helicase motifs of SF1 and SF2 share some similarities with one another. There are also seven conserved motifs (Motif1, Ia, II-VI) in the helicase core domain of helices in SF2 (25). The crystal structure of NS3 demonstrated that the seven motifs mainly reside in domain 1 and domain 2 which are homologues to the 1A and 2A domains of SF1 helicases (Fig. 2) (25;29). The domain 1 contains motif I, motif Ia, motif II and motif III. Structure-function studies indicated that motif I and II are implicated in NTP binding (Fig 1) (30). Unlike the motif III of SF1, that of SF2 forms a flexible loop that connects the domain 1 and 2 and may help couple ATP hydrolysis to a conformational change in order to cause the translocation along the substrates (31). The motifs IV to VI

residing in domain 2 contribute to couple ATP hydrolysis and nucleotide binding. The domain 3 is a unique special structure of SF2 containing α-helical feature which has poor similarity but is essential for ATP hydrolysis and unwinding of nucleic acids (32). Recently, new motifs have been found continuously (motif Q, TxGx motif, motif 4a and TRG) in some SF2 members (6). For example, motif Q which is unique in DEAD-box helicase, locates before motif I in the N-terminus (Fig. 1). Motif Q is involved in ATP binding and hydrolysis (33). The RecQ helicase family is a representative member of SF2 helicases which exists in all kinds of organisms. It is a highly conserved DNA helicase that plays a key role in chromosomal maintenance and genome integrity. We will discuss RecQ helicase in detail in the following section.

Superfamily 3 (SF3): The SF3 helicases which are distinct from the SF1 and SF2 originally identified in the genomes of small DNA and RNA viruses which (6). They are involved in multiple biological activities, such as genome replication, origin recognition and unwinding. There are four common conserved motifs in SF3 protein named A, B, B' and C (6;34). The motif A and B correspond to the Walker A and B ATPase boxes while motif C is specific in SF3. The typical structural difference among SF1, SF2 and SF3 families is that SF1 and SF2 helicases contain a RecA-like core fold, while SF3 helicases have a novel modified AAA+ core (ATPase associated with diverse cellular activities) relatively (35). The small poorly conserved AAA+ domain containing α-helice/β-sheet structure may be involved in stabilizing the hexameric form and NTP binding activity. Several crystal structures of proteins from this family, for example simian virus 40 (SV40), the bovine papillomavirus (BPV-1) E1 helicase (36), adeno-associated virus type 2 (AAV2) (6;37) and HPV18 (38), were solved in recent years.

Figure 1

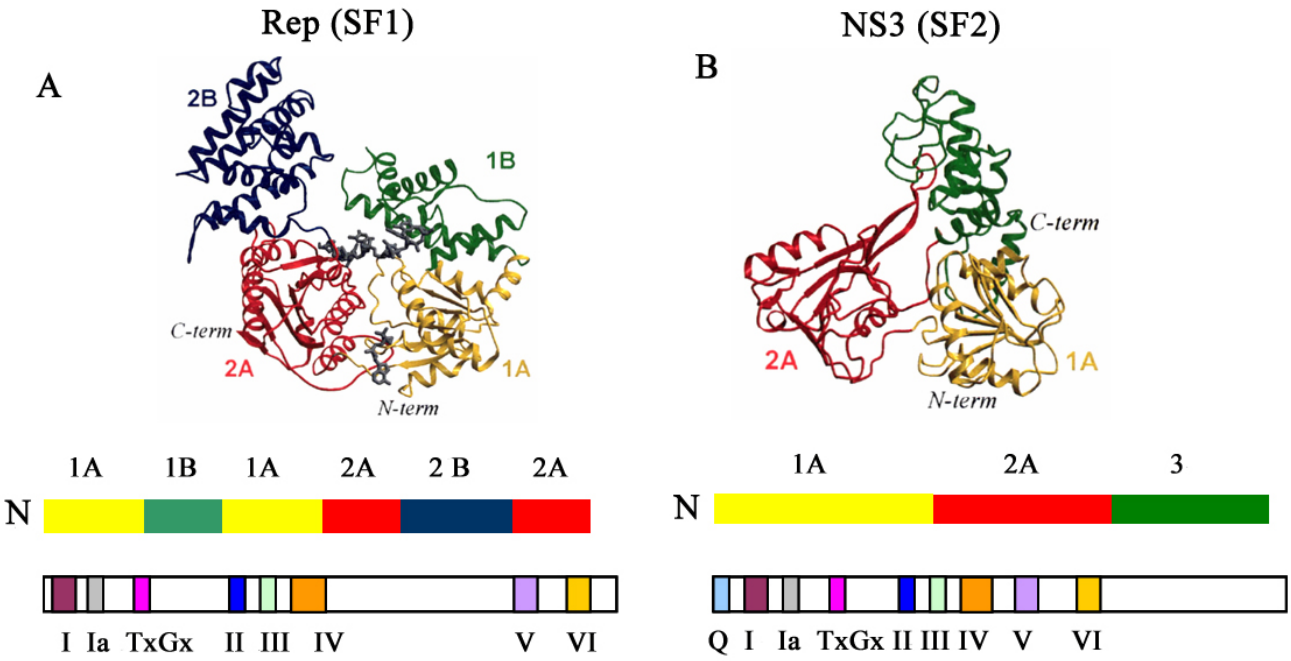

Fig. 1 Ribbon representations of Rep (SF1) and NS3 (SF2)

(A): The ribbon diagram of the open conformer of Rep in Superfamily 1. Domain 1A is indicated in yellow, 2A in red, 1B in green, and 2B in blue. DNA and ADP are indicated in gray. The middle panel is the location of the domains in the amino acid sequences of Rep indicated by the same colour coding as in the upper panel. The low panel shows the conserved amino acid motifs in the helicase domain. From N-terminal to C-terminal, the motif I, Ia, TxGx, II-VI are labelled in different colours. **(B)**: The upper panel is the ribbon diagram of HCV NS3 helicase belonging to Superfamily 2. The structural homologue to domain 1A of Rep is indicated in yellow, and that of 2A in red. The C-terminal domain 3 is indicated in green. The middle panel indicates three domains of NS3 helicase in the same colour as the upper panel. The low panel is the position and function of seven conserved motifs of helicase domain. From N-terminal to C-terminal of amino acid sequence, the helicase core domain contains motif I, Ia, TxGx, II-VI. Each motif has special biochemical function. Motif Q before motif I is an expanded motif found in DEAD-box helicases.

Structures reveal that most SF3 helicases form a sixfold symmetric collar that stabilized the hexamer, with the AAA+ domain shown from exact radial symmetry (Fig. 2). The hexamer forms a two-tiered assembly with a hole to bind the substrates. The central channel of hexamer binds with nucleic acid via interactions between a loop in the B' motif and the phosphodiester backbone. It's not surprising that the SF3 helicases are different in structure from SF1 and SF2 because their consensus patterns of the helicase motifs are not conserved.

Superfamily 4 (SF4): Helicases from the SF4 family act as replicative enzymes which were first identified in bacteria and bacteriophages. Up to the present, few members have been classified in this superfamily. One member named DnaB helicase is a replicative helicase of eubacteria (39). This family also includes other replicative helicases of the T4 and T7 bacteriophages showing a RecA-type core fold. All members of SF4 contain five conserved motifs (H1, H1a, H2, H3 and H4) that are located in the C-terminal region of the protein. Motifs H1 and H2 are equivalent to the Walker A and B motifs in the helicase domain of SF1 and SF2 helicases, but H1a, H3 and H4 have no obvious counterparts in any other superfamily (Fig. 2). H3 has a conserved glutamine or histidine which is the functional equivalent of motif III of SF1 family. Motif 4 forms a loop that projects into the central channel of the hexamer. The hexamer shows deviations from six fold symmetry with the consequence that the subunit interfaces, DNA-binding loops and arginine fingers are in non-equivalent conformations in different subunits. Comparisons of their respective RecA-like folds showed that although the Walker A and Walker B motifs are similarly positioned, the DNA-binding elements are located in different regions of the fold. But in the quaternary structures, the DNA-binding elements are still found at the centre of the ring of each helicase. The N-terminal region of these helicases is usually less well conserved (40).

Figure 2

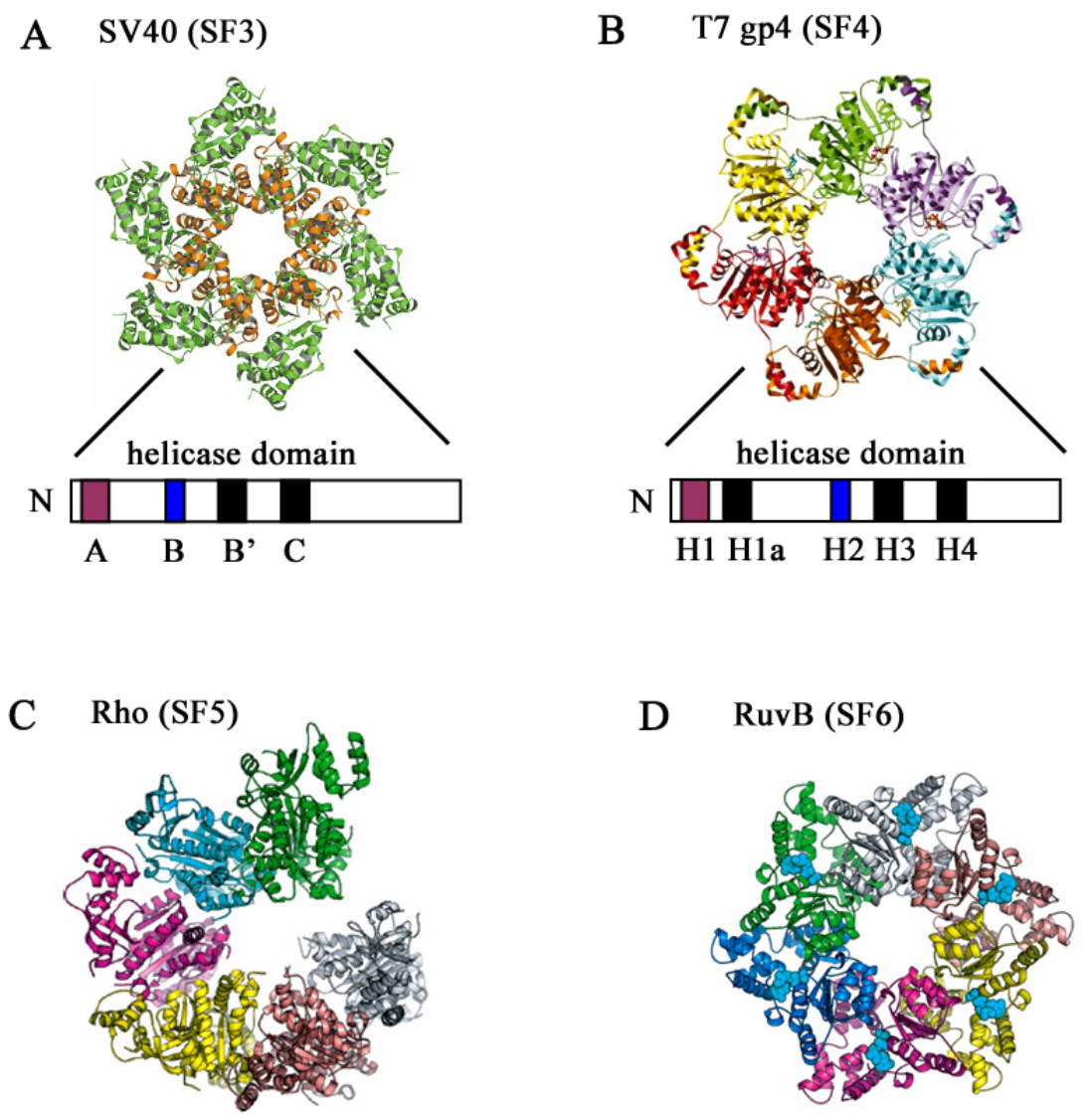

Fig. 2 Ribbon diagrams of hexameric helicases from SF3 to SF6 (Ribbon diagrams of helicases are adapted from Reference 6) **(A)** The SV40 Tag hexamer (SF3), looking down through the central channel. The N-terminal a-helical domains (in gold) form a ring resting upon a larger ring formed by AAA+ domains (in green). Below the hexamer, it is shown the helicase domain. From N-terminal, the conserved motifs of SF3, motif A, A', B and C, are indicated in different colours. The motif A and B correspond to the Walker A and B of SF1 and SF2. **(B)** Schematic of the hexamers of T7 gp4. Its helicase domain contains five conserved motifs (H1, H1a, H2, H3 and H4) from N-terminal to C-termainl. Motif H1 and H2 are equal to Walker A and B. **(C, D)** Hexamers of *E.coli* Rho and *T. maritima* RuvB from SF5 and SF6 respectively. The monomers of the hexameric helicase are shown in different colours.

Other Superfamilies: There are several helicases that are distributed into other families according to their different amino-acids sequences. Crystal structure analysis revealed that most of them form as hexamers. Rho, a kind of transcription termination factor in bacteria belongs to superfamily 5. It takes role in the termination of transcription by binding to a specific sequence on the nascent RNA and then unwinds the DNA/RNA hybrid (41). The crystal structure of Rho shows a hexamer and RNA binds to each six subunits (42;43). Two crystallographic structures of the Rho hexamer from *Escherichia coli* have been solved. In one structure, the Rho ring is split open which gives rise to a global shape with RNA bound to the RNA-binding domain (Fig. 2). This conformation is different from DNA hexameric helicases (44). The other structure of Rho is a close hexamer ring with the RNA bound to both the RNA-binding and the ATPase domain (45). The mechanism of regulation of Rho closing or opening is still unclear.

According to the sequence alignments and structural information, a number of hexameric motor helicases containing the AAA+ like fold form the SF6 family. Comparing with the structures of SF3 helicases, they contain an additional β-hairpin insertion that disrupts helix α2 (46). The RuvB helicase, a member in this family, interacting with RuvA and RuvC proteins is responsible for promoting branch migration during bacterial recombination. The dsDNA strands of Holliday junctions bind to the central channel of the hexameric ring of RuvB in an ATP-dependent manner (Fig. 2) (47). The mini chromosome maintenance protein (MCM) is a helicase involved in the eukaryotic replication. It forms a hexameric ring complex (MCM2-7) with a large central channel to connect with dsDNA which is essential for replication initiation and elongation (48).

Although helicases are different in sequence, structure and function, they share common biochemical properties, including nucleic acid binding, nucleoside triphosphate (NTP) binding, NTP hydrolysis, and unwinding of nucleic acid duplexes. The structure of helicase is tightly associated with their functions. So understanding the structure of helicase clearly will help us to find out the mechanism of its biochemical functions.

2. Helicase-General properties of helicases and Mode of Action

2.1 Biochemical properties of Helicases

Helicases have several common biochemical properties: nucleic acid binding, nucleotide triphosphate (NTP) binding, NTP hydrolysis and NTP hydrolysis-dependent unwinding of nucleic acid helices.

2.1.1 NTP binding and hydrolysis of NTP

Up to now, all the analysed helicases exhibit NTP binding and NTP hydrolysis activity (49;50). Most helicases preferentially hydrolyze ATP than three other nucleotides (TTP, GTP and CTP). Usually, a magnesium ion binds specially to the beta and gamma phosphates of the NTP. This metal ion is an essential component of the overall reaction for ATP binding and hydrolysis. The NTPase activity of a helicase is stimulated by binding of nucleic acid (DNA or RNA) generally. However several helicases display ATPase activity even in the absence of nucleic acids. For example, Anasuya Roychowdhury recently found that the *E. coli* replicative helicase, the DnaB protein, can hydrolyze all the NTPs independent of DNA substrates (51). Crystal structures of many helicases reveal highly conserved arginine residues in the helicase core domain which are located near the γ-phosphate of ATP and may sense the ATP hydrolysis. The arginine finger contributes to ATP hydrolysis through stabilization of the transition state of the reaction and it is also used as a trigger for conformational change after release of pyrophosphate (49;52). Although it is accepted that helicases convert the chemical energy into mechanical force for translocation and unwinding nucleic acid strands, the mechanism of energy conversion still remains to be elucidated.

2.1.2 Nucleic Acids binding

Helicase binding to nucleic acids is an important step towards nucleic acids separations. The crystal structures of helicases bound to DNA or RNA revealed that helicases bind to DNA or RNA through their phosphate backbones or nucleotide bases. The binding mechanism of nucleic acids substrate differs in various helicases families. For most helicases, nucleic acids bind to helicase with the conserved motifs in the helicase core domain. However, there is a special domain named the zinc-binding motif which also has

been found in some helicases to contribute to nucleic acid binding (53;54). Most DNA helicases display stronger binding affinity for ssDNA than dsDNA. To date, the most noticeable feature of nucleic acids binding is that the binding of nucleic acids and NTP triggers a significant conformational change in the helicase domain. This change is absolutely necessary for ATPase and DNA/RNA unwinding. For example, when the DEAD box helicase YxiN binds to RNA, it will induce the closer conformational change of two helicase subdomains for RNA unwinding (55). Similar structure changes also have been indicated in PcrA and Rep helicases (9;56).

2.1.3 Unwinding Activity and Mode of Action

Double-strand separation by helicase is a complex process. There are certain common features of which can be described such as polarity, processivity, step-size and mode of action.

The polarity of unwinding is defined as the direction of helicase moving on initially bound single strand template with respect to the polarity of the sugar phosphate backbone. It is determined as 5' to 3' polarity when helicase, such as FANCJ, XPD and RecD helicases, unwinds the duplex possessing the 5' single strand; whereas if the helicase unwinds the other single-end strand, it displays 3' to 5' polarity such as RecQ helicase family. However, for some helicases, RecBCD (57), PcrA of *Bacillus anthracis* (58) and herA *of thermophilic archaea* and so on (59), they can show bipolar unwinding activity. There are major differences in DNA or RNA substrate specificity among various helicases. A single tail of duplex strands is required for most DNA helicases. Several helicases, such as BLM and *E.coli* RecQ, even can unwind blunt-end duplex DNA structures.

Processivity is another measure of the number of base pairs unwound before the helicase dissociates from the substrate, and varies largely among the different helicases. Some helicases exhibit a high processivity with a separation of several kilo base-pairs per second (60), while other helicases can only unwind just few bases before dissociating from the substrate.

Today, several models have been proposed to explain the mechanism by which helicases catalyze the unwinding of nucleic acid duplexes. Each model envisions a different assembly state for the active protein. There are three accepted unwinding models by which helicase forms different oligomerization. When helicase separates nucleic acids in monomer or dimer, the model of action is described as 'inchworm model' or 'rolling model' (61) (Fig.

3). The inchworm model is based on an active monomeric protein such as PcrA (9) and Rep (62). ATP binding, hydrolysis and product release cycle the protein through a series of conformational states as the protein 'inches', one step along the substrates. Two subdomains of helicase both bind single strand. After binding ATP, they are closer to each other and consequently cause the substrates to be tumbled through the binding pocket. The 'rolling model' requires a dimerized helicase in which each monomer has the different affinity for single-strand or double-strand of the substrate. NTP binding and hydrolysis provide the energy for protein conformation. Binding NTP brings the closed form of two monomers from the open state and then the dimeric enzyme can be envisioned to 'roll' through duplex substrates with subunits alternate of utilizing cycles of NTP binding (61). Some helicases form a hexameric complex when they separate DNA or RNA substrates such as human BLM (63), T7 gp4 (64), *E.coli* Rho (65), SV40 (66) and so on. The unwinding model of hexameric helicases proposed that a single strand passes through the centre of a ring-shaped protein while the complementary single strand passes along the outside of the ring. The protein moving along one strand of the substrate has a corkscrew-like motion with alternating subunits catalysing ATP hydrolysis (Fig. 3). The unwinding model of hexameric helicases can further be classified into three models according to the different manners in which they bind to nucleic acids (67).

However, the detailed molecular mechanism of unwinding models such as the energy of NTP hydrolysis coupled to the separation of double-strands is still not well known. More information is needed to explain the unwinding models of helicases.

Figure 3

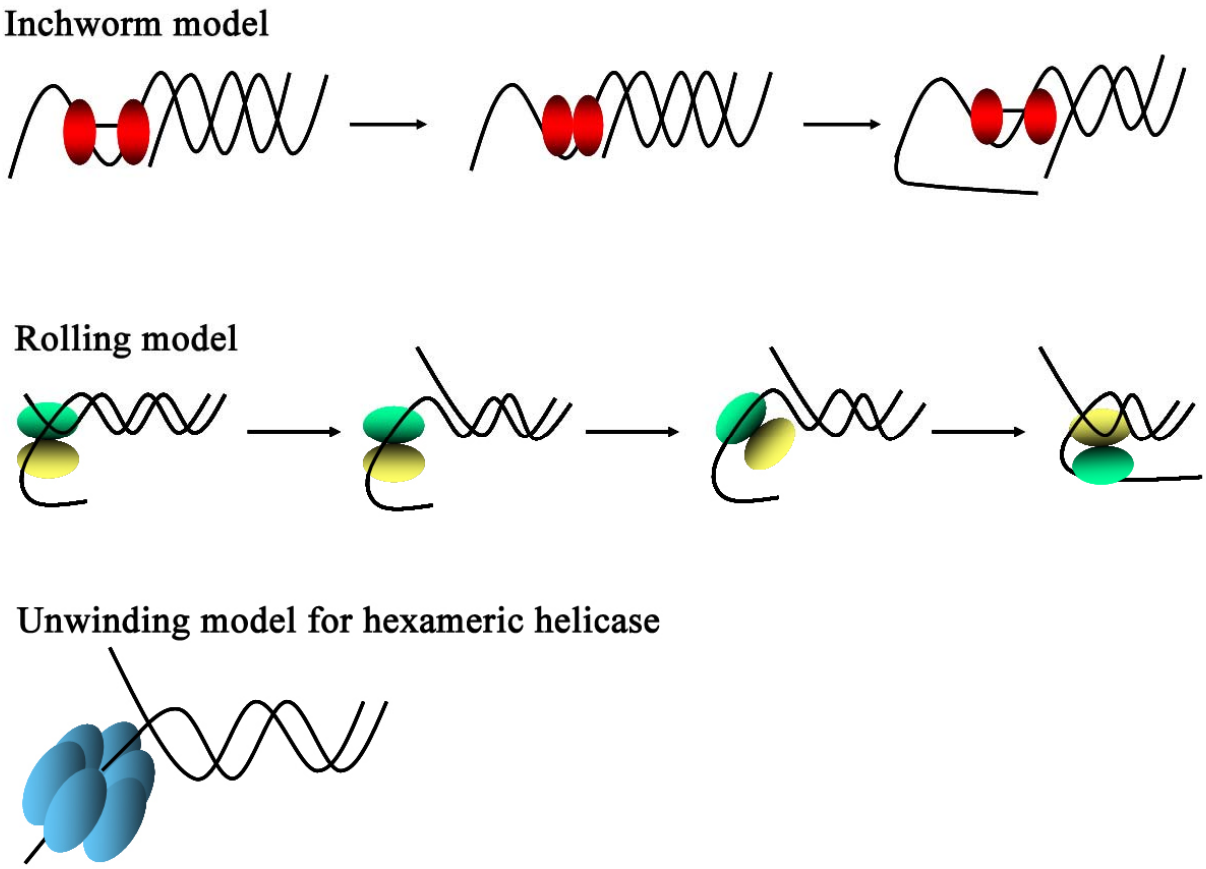

Fig. 3 Unwinding models of helicases

Top view shows the inchworm model in which helicase binds to substrates with two subunits. Helicase transfers between 'open' and 'close' situation alternately. The rolling model involves dimer of helicase. Each monomer binds to single or double stranded substrate alternately. For hexameric helicase, the substrate passes through the core of enzyme. The unwinding model of hexameric helicase is shown on the bottom of figure.

2.1.4 Annealing Activity

Although helicase is a kind of enzyme which can separate nucleic acid duplexes, the increasing evidence has shown that they also possess strand-annealing activity and even strand-exchange activities. For example, in RecQ helicase family such as human RecQ5 (68), RECQ4 (69), the Bloom Syndrome helicase (BLM) (70), the Werner Syndrome helicase (WRN) (71) and other family helicases including Dna2 and T4 helicase (72) display significant strand annealing activity. Single stranded DNA annealing by BLM, WRN or Dna2 suggest that they may play roles in the processing of Okazaki fragments (73). Some RNA helicases also have the ability to mediate the RNA secondary structure including yeast nuclear DEAD-box RNA helicases (p68 and p72) (74), the redox-regulated cyanobacterial RNA helicase (CrhR) (75) and the nucleolar DExD-box RNA helicase II/Gu (76). For RNA helicases, while p68/p72 and RNA helicase II/Gu carry out the unwinding function in the presence of ATP, these helicases also have the annealing ability independent of ATP (77). Some laboratories have found that DNA helicases carried out annealing activities in the absence of ATP. ATP will even reduce this ability to a certain extent. It is possible that this activity simply reflects the ability of binding two single complementary strands. When helicase binding to ATP, it will cause a conformational change in helicase and stimulate unwinding process, which, in turn, inhibit its annealing ability. The stimulatory effect of replication protein A (RPA) and single-stranded DNA binding protein (SSB) on unwinding ability were also found to prevent annealing of single strand DNA in some RecQ members (78). RPA and SSB can bind with single stranded DNA and then inhibit re-annealing. As the unwinding process, annealing ability of helicase also is influenced by structure and length of substrate. The 3' oligo(U)-tail and 3' stem-loop of RNA is necessary for annealing ability of gBP21 RNA helicase (79). When the length of duplex or region of complementary is increased, the annealing is also increased in the cases of BLM and WRN (80).

In theory, unwinding and annealing activities in the same helicase will tend to work against one another. So the competition and balance of these two opposite processes of helicase *in vivo* is deserved to be understood well. The redox-regulated cyanobacterial RNA helicase (CrhR) was found that its annealing ability is stronger than unwinding ability *in vitro*. In addition, CrhR couples these two activities to effect RNA rearrangements via strand exchange which is crucial for cellular activities (81). By contrast, the unwinding activities of BLM and WRN are significantly stronger than annealing functions. But BLM and WRN carry out the unwinding and annealing together on three or four stranded DNA

structures to perform strand exchange and branch migration during DNA repair pathway, especially in resolving the double Holliday junctions. The balance between annealing and unwinding seems to be regulated by other proteins which are important in DNA metabolism such as RPA and SSB (80).

The structural basis of helicase mediated-annealing is not well understood. Several lines of evidence have shown that oligomeric state of helicases is responsible for annealing activity. For example, both BLM and RECQ1 helicase need oligomerisation to perform their strands annealing activity. It's worth noting that the helicase core domain which takes charge of binding DNA or RNA is not responsible of annealing activity in the cases of most studied helicases. This conserved domain is not enough for executing out annealing ability. Some laboratories found the C-terminal region of helicase is required for the annealing ability (82). The C-terminal 79 amino acids region between the RecQ C-terminal (RecQ-Ct) and the Helicase and RNAse D C-terminal (HRDC) domains of WRN is required for ssDNA annealing process (83). Similarly a 60-amino-acids sequence in the HRDC domain of BLM is critical for annealing (84). Very surprisingly, we found that an isoform of RecQ5 helicase which only has the helicase core domain can efficiently catalyze nucleic acid strand annealing. We will discuss this in detail in the Chapter II.

2.2 The multiple functions of Helicases

Helicase and DNA replication

Helicases are conserved enzymes from bacteria to human. Since they have multiple biochemical functions, helicases have diverse roles in genomic metabolism. DNA helicases are required for the maintenance of genome integrity including DNA replication, repair, recombination and transcription (50). During the DNA replication, helicase acts as a roadblock remover. Helicases function as a checkpoint and a surveillance mechanism to remove structural roadblock in S-phase of DNA replication. Some DNA replication intermediates such as DNA hairpins, D-loop, triple junctions, Holliday junctions can be solved by helicase (85). Additionally, helicase also probably assist in the re-initiation of replication at sites of replication-fork demise.

Helicase and DNA repair

Chemical agents and UV light can create replication blocking lesions and DNA damage. One of the fatal damages is DNA double-strand breaks (DSBs). Cells repair DSBs primarily by nonhomologous end-joining (NHEJ) and homologous recombination (HR). XPB and XPD helicases were found to play important roles in nucleotide extension repair (NER) pathway (85;86). RecQ helicases have been found to play key roles in DSBs repair pathway interacting with several proteins (87). FAND1 (fanconi anemia-associated proteins with helicase motifs) helicase regulates the homologous recombination repair by interacting with RAD51 recombinase. Some helicases are also involved in nucleic acid repair process to mediate strand separation at the site of lesion and separate the forked DNA structure. Some members in RecQ family have been found to play a part in transcription and regulation of chromatin structure (88). WRN, the Werner Syndrome helicase, might play a role in DNA mismatch repair. This helicase can move a mismatched nucleotide incorporated by a DNA polymerase during DNA replication and DNA repair (89). It is also noticeable that DNA strand annealing activity of helicase is important for their functions at blocked DNA fork. Helicase can disrupt the forked structure and promote strand exchange to facilitate the procession of DNA process.

Helicases and RNA metabolism

RNA helicases are involved in various cellular processes of RNA by catalyzing the alteration of higher-order RNA structures, for example, secondary structure melting, strand separation and RNA-protein dissociation. The DEAD-Box RNA helicases belonging to Superfamily 2 can regulate many aspects of RNA metabolism, including transcription, splicing, transport, translation and degradation of mRNA and ribosome biogenesis (90;91). Vasa, the first identified DEAD-box helicase, has been characterized in oogenesis and germ-cell specification in *Drosophila*. It functions in translocation of specific mRNA targets and recruitment of the 60S ribosomal subunit to the translational start site by interacting with elF5B, a kind of translocation factor (92;93). Interestingly, some evidences indicated that helicases are implicated in the mediation of the position and density of histone congregates along the DNA in reconstituted nucleosomes. Snf2, a kind of ATP-dependent chromatin remodeler in fission yeast, can convert the local chromatin into transcriptional active and repressed state. Snf2 plays an essential role in cell viability including chromosome segregation and centromere functions (94). Human DDX3 is another

famous RNA helicase which is implicated in nuclear mRNA export, cell growth and even cancer progression. Human DDX3 participates in the replication of human immunodeficiency virus Type1 (HIV-1) and in the pathogenesis of hepatitis C virus (HCV) (95;96). So Human DDX3 is a potential target of antiviral agent for HIV. More recently, an RNA helicase, RIG-I has been identified to be involved in the innate immune response in human. RIG-I recognizes viral dsRNA and transmits signals that induce type I interferon-mediated host immunity against virus infection (96). This is a new signal transduction and regulatory pathway for host against virus infection. Further research in this domain will contribute to understanding of the molecular aspects of RIG-I signal pathway.

All these evidences indicated that helicases are very critical in maintenance of the genome stability. Since helicases are very essential to genomic metabolisms from virus to human, resolving the structures of helicases will help us to understand their biochemical functions and molecular actions deeply.

3. The RecQ family of DNA helicases

3.1 General Features and Structural Organisation

The RecQ helicases, named after the DNA helicase RecQ of *Escherichia coli*, are highly conserved from bacteria to man. Defective functions of these proteins lead to genomic instability that generally manifests as hyperrecombination. In humans, defects in the BLM, WRN and RTS/RECQ4 genes are associated with the autosomal recessive, cancer-prone diseases Bloom syndrome (BS) (97), Werner syndrome (WS) (98) and Rothmund Thompson syndrome (RTS) (99), respectively. Higher organisms contain several RecQ homologues, with five homologues identified in humans. These proteins presumably play specialised roles in genome maintenance since distinctions in the clinical as well as the cellular manifestations of BS, WS and RTS have been observed. Furthermore, the multiple RecQ homologues also display differences at the biochemical level with overlapping, but also very distinct substrate specificities mostly due to the presence of various additional functional domains. The diverse protein interaction partners observed further implicate different human RecQ homologues in different DNA transactions. It seems that the cellular functions of the sole RecQ homologues in unicellular organisms are divided up into and extended on several homologues in higher organisms.

Figure 4

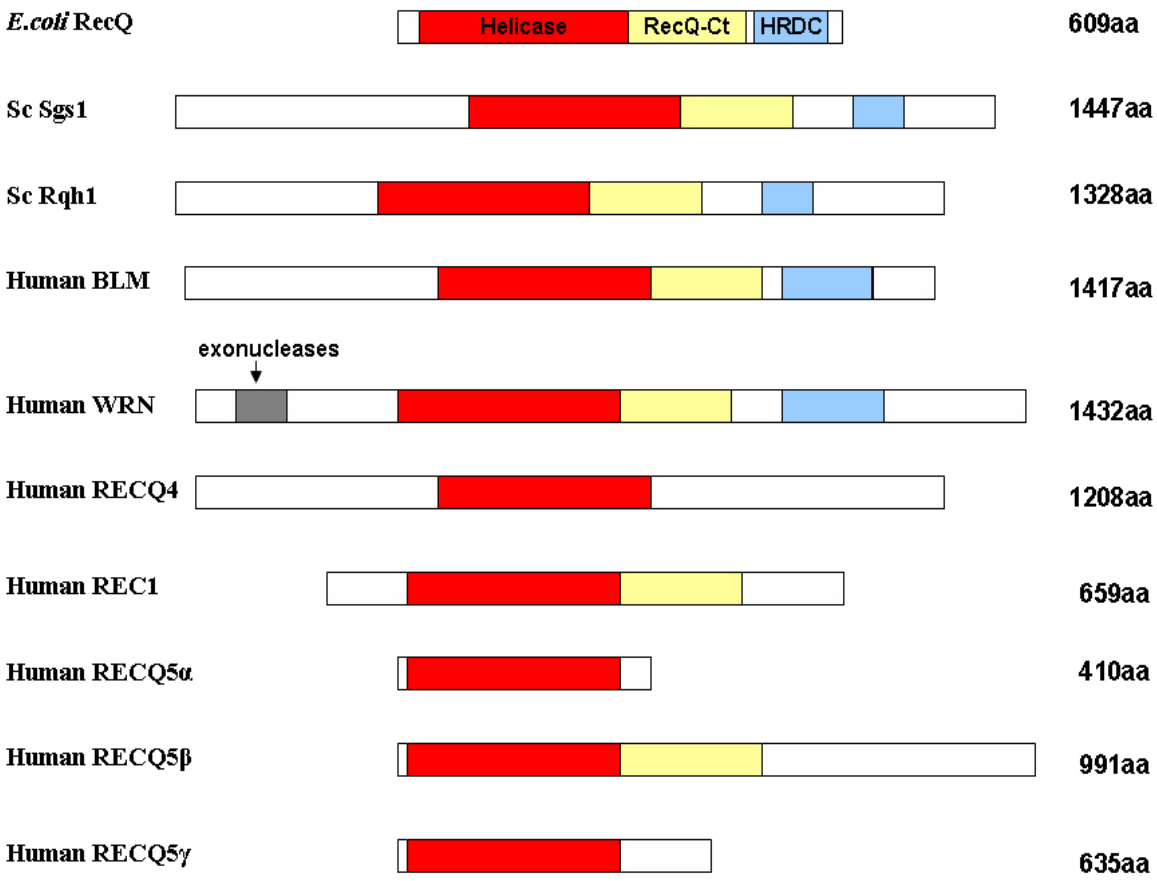

Fig. 4 Schematic diagram of selected members of the RecQ family of DNA helicases

The color scheme matches the scheme shown in the figure of the structures of the protein domains. The helicase core domains are shown in red, and the RecQ-Ct domain including the zinc finger is shown in yellow. The HRDC domain is depicted in blue, and the exonuclease domain of WRN is shown in gray. The lengths of the amino acid sequences of the RecQ helicases are indicated after each schematic diagram.

Figure 4 shows schematically some selected RecQ helicases. All RecQ members contain the helicase domains characteristic of the DEAH subgroup of SF2 helicases (6). The RecQ helicase domain is defined by the presence of seven highly conserved helicase motifs which is centrally located in the amino-acids sequences (Fig. 1). Biochemical analysis indicated that motifs Ia, III and V take charge of contacting with DNA. Motifs I, II-IV and VI form a pocket for interacting with ATP. The RecQ-Ct domain is a characteristic of the RecQ family and is involved in mediating protein-protein interactions and DNA binding, but this domain is absent in some members or its sequence has diverged significantly enough to make its identification less straight forward (Fig. 4). The RecQ-Ct domain is composed of two sub-domains: One is a structure of four α-helices that ligand a Zn^{2+} ion by four highly conserved cysteine side chains named as zinc binding motif or zinc finger (Fig. 5). The adjacent Zn^{2+} binding domain has been found in all RecQ helicases examined, except for RECQ4. Our researches on the structures and functions of *E.coli* RecQ, BLM and RECQ5β have demonstrated that the zinc binding motif plays critical role in protein-folding and DNA binding activity (54;68;100).

Another characteristic of the RecQ members is the winged helix (WH) domain, which is a less conserved winged-helix sub-domain and has only been found to be absent in the human RECQ4 and RECQ5 and their orthologues (Fig 5). The HRDC domains of *E.coli* RecQ and WRN have been found to take charge of binding DNA but are not required for catalytic activity (101). The three-dimensional structure of the HRDC domain of *Saccharomyces Cerevisiae* Sgs1 is used as a basis for establishing a general structural model for studying on its function (Fig. 5) (101;102). It also does not show independent enzymatic activity and it provides an auxiliary function in substrate recognition (Fig. 5).

Furthermore, distal to the WH domain, the Helicase and RNAse D C-terminal (HRDC) domain is found. This domain is absent in RECQ1, RECQ4 and REQ5. The WRN helicase contains an additional 3'-5' exonuclease at the amino-terminus of the protein and a 27 amino acids repeat between the exonuclease and the helicase domains (Fig. 4) (26). All unicellular organisms examined contain a single RecQ homologue that harbours all the common conserved motifs, such as the helicase domains, the Zn^{2+} binding domain, the WH domain and the HRDC domain (50).

The DNA helicase of RecQ family can unwind various DNA strands in the 3' to 5' direction. The helicase activity depends on the hydrolysis of ATP. The hydrolysis of ATP provides energy for the processive translocation of the helicase along the substrates. The

substrates are specific for different RecQ helicase members. Table 2 schematically shows some substrates that have been used to study RecQ family helicases.

Figure 5

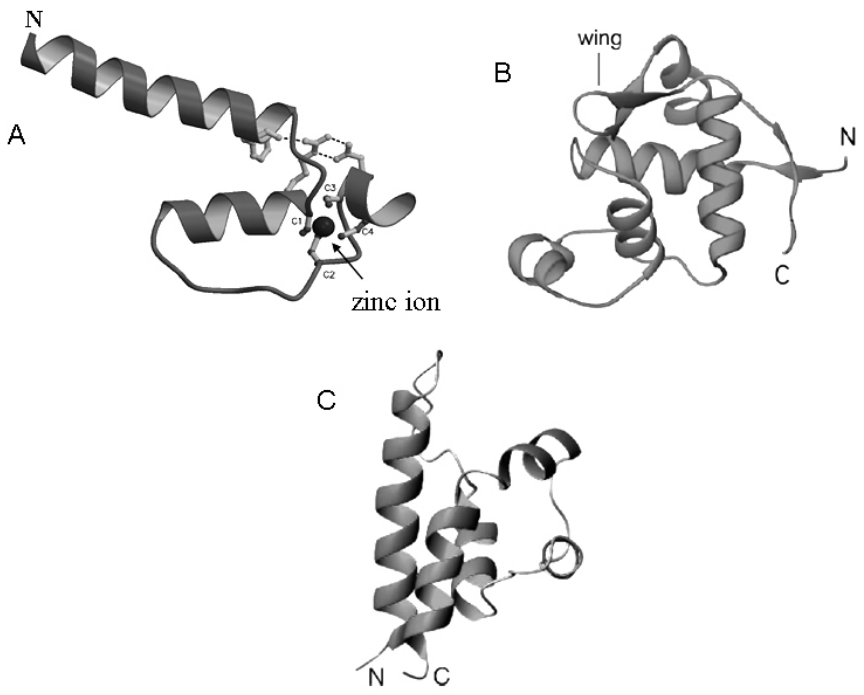

Fig. 5 High-resolution structures of some important domains in RecQ family helicases

(A) Structure of just the zinc finger of the RecQ-Ct domain from the *E. coli* RecQ catalytic core (Adapted from Reference 100). Side chains of cysteine metal ligands labelled with C1 to C4 are shown and labelled, and the bound zinc ion is indicated. **(B)** Structure of just the WH domain of the RecQ-Ct domain from the *E. coli* RecQ catalytic core (Adapted from Reference 29). **(C)** The three-dimensional structure of the HRDC domain of Sgs1 RecQ helicase (Adapted from Reference 102).

Table 2 Substrate specificity of RecQ helicases (26;103-107)

Structure of Substrate	Name of substrate	Note of substrate	Helicase
5' 3'	Blunt duplex		*E.coli* RecQ, RECQ4
5'	5' tailed duplex		*E.coli* RecQ
3'	3' tailed duplex	B-form duplex DNA intermediates in replication and repair	*E.coli* RecQ, Sgs1, REQ1, BLM, WRN RECQ4, RECQ5
	'Bubble' substrate		BLM, WRN, RECQ4
5' 3'	Forked duplex		*E.coli* RecQ, Sgs1, RECQ1, BLM, WRN, RECQ4, RECQ5
5' or 3'	'Kappa' structrue		*E.coli* RecQ, Sgs1, RECQ5
5' 3'	Duplex fork		WRN, RECQ5
5' or 3'	D-loop	DNA intermediates in recombination	BLM, WRN
	3-way junctions		BLM, WRN
	Triple helix		*E.coli* RecQ, Sgs1, RECQ1, BLM, WRN
	Holliday junction		BLM, WRN
17-30nt	Holliday junction α-strucutre	Circle phage M13 hybridized with different length single–strand DNA	Sgs1, RECQ1, BLM, WRN, RECQ5
33-40nt			Rqh1, WRN
42-100nt			*E.coli* RecQ, Sgs1, BLM, RECQ5
109-343nt			*E.coli* RecQ, Sgs1,
5' or 3'	M13 substrate	Alternate DNA structures formed in triplet and G-rich repeat sequences (telomeric DNA)	*E.coli* RecQ, BLM, WRN
	G-quadruplex structure		*E.coli* RecQ, Sgs1, BLM, WRN

3. 2 The *Escherichia coli* RecQ

3.2.1 Genetic Background

The RecQ protein from *Escherichia coli* is the founding member of the RecQ DNA helicase family and was discovered in 1984 by Nakayama in a screen for mutations that confer resistance to thymineless death (13). RecQ acts in the RecF pathway of homologous recombination that operates in the repair of stalled replication forks. RecQ mutations in a recBC sbcB background lead to an enhanced UV sensitivity and lower the efficiency of conjugal recombination (13). RecQ and RecJ are required for lagging strand degradation at stalled replication forks (108). RecQ is involved in the supression of illegitimate recombination, which is enhanced 30-300 fold in *recQ* mutants (109). A recent study shows that RecQ is needed for the fast degradation of the LexA repressor in response to UV irradiation to induce the SOS response (109). The SOS response is a mechanism of bacteria strongly enhanced by the formation of RecA filaments and induces the expression of roughly 30 DNA repair genes as a response to DNA damage (110).

3.2.2 Biochemical and structural Properties of *E.coli* RecQ

The first isolated helicase, *E.coli* RecQ, is a protein of 610 amino acids (molecular mass, 68,920 Da) (111). Sequences alignment of *E.coli* RecQ with other RecQ family members reveals that it has high conservation of the helicase domain. Analysis of the amino acid sequence of *E.coli* RecQ indicated that it contains the helicase core, RecQ-Ct, HRDC domains and a short N-terminus (112). *E.coli* RecQ shows a wider DNA substrates specificity and higher processivity than that of other RecQ family members (14). It can unwind longer partial duplexes, blunt-ending DNA, DNA with 5' or 3' overhangs, nicked or forked DNA, and three- or four-way junctions including G4 structure (a guanine-rich parallel four-stranded DNA structure) efficiently (13) (Table 2). It displays a 3' to 5' polarity in DNA unwinding and DNA-depending ATP hydrolysis.

The previous results in our laboratory indicated that *E.coli* RecQ functions as a monomer and unwinds DNA substrates in the inchworm model putatively (111). *E.coli* RecQ possesses both ssDNA and dsDNA binding abilities, but it prefers to ssDNA than dsDNA. Steady-state fluorescence anisotropy measurements of fluorescein-labelled oligonucleotides revealed that *E.coli* RecQ binds DNA with high affinity and low cooperativity of one protein monomer per ten nucleotides (113). It can bind ssDNA or dsDNA at the same site.

The concentration of salt influences the DNA binding ability of *E.coli* RecQ significantly (113). The affinity to substrate will decrease with salt concentration increasing and this phenomenon has been found in many other RecQ family members. Nucleotide cofactors not only provide energy for DNA unwinding ability but also regulate its affinity for DNA binding. It was further determined that *E.coli* RecQ unwinds DNA duplexes rapidly, independent of the ssDNA tail length, with a step size of 4 base pairs and a rate reaching as high as 84 bp/s (14).

Bernstein and Keck have crystallized the catalytic core domain of the *E. coli* RecQ protein and resolved its structure (112). The crystal structure of RecQ is shown in Figure 6. In this work, the authors show that there are two additional structural motifs adjacent to the helicase domains which are not present in other helicases. One is called zinc binding motif and the other is the winged helix motif (WH). The zinc binding motif contains four highly conserved cysteines which coordinate a zinc ion. Adjacent to that lies the winged helix motif forming a helix-turn-helix fold, found to act as a DNA binding motif in many proteins (101). The HRDC domain was not present on the polypeptide crystallized and its function is not yet fully elucidated. Liu *et al.* have resolved the three-dimensional structure of the HRDC of Sgs1 from *Saccharomyces cervisiae*, but was not able to draw functional conclusions from this work (102). Recently, our laboratory have characterised the importance of the zinc binding motif. We show that the highly conserved cysteines form a complex with the Zn^{2+}. This complex is essential for DNA binding and helicase activity, but not for ATP binding (114). Furthermore, we show that this zinc binding motif is important in maintaining the integrity of the protein structure.

3.2.3 Role in genomic stability

Based on genetic and biochemical evidences, four roles of RecQ in the maintenance of genomic stability in *E. coli* have been proposed (115) (Figure 7): 1) In a model for the initiation of recombination, RecQ unwinds DNA at gaps (in wild-type cells) or double-strand breaks (in $recBC^-$ cells) allowing RecA filament formation to initiate recombination and D-loop formation (116). 2) In the anti-recombination model, RecQ can disrupt D-loops formed by RecA (116). 3) RecQ is very likely to perform the double Holliday junction (DHJ) dissolution, as it has been shown that RecQ in concert with Topo III can catenate/decatenate

Figure 6

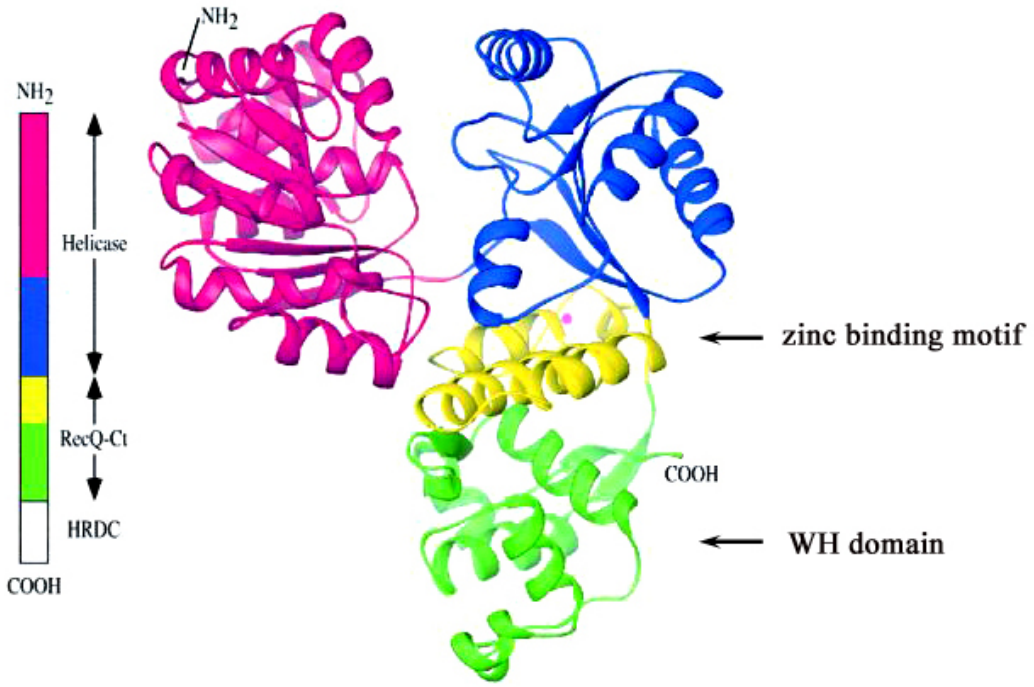

Fig. 6 High resolution structure of the *E.coli* RecQ catalytic core (Adapted from Reference 29)

The schematic diagram of *E.coli* RecQ is shown on the left. The catalytic core of *E.coli* RecQ includes only the helicase domain (labelled in red and blue) and RecQ-Ct domain (labelled in yellow and green). In the middle, it is the ribbon diagram of the crystal structure of *E.coli* RecQ catalytic core region which are labelled in the same colour as in the schematic diagram. The zinc binding motif is indicated in yellow and the WH domain is in the green respectively. A bound Zn^{2+} ion is shown as a magenta sphere.

duplex DNA (117). It is likely that RecQ can, together with Topo III perform this reaction as well *in vivo*. 4) In the SOS model of Hishida *et al.* (118), RecQ binds a gap on the leading strand of a stalled replication fork and unwinds the duplex template ahead of the fork, in a 3'-5' direction (119). The ensuing topological stress may be relieved by the combined action with a type I topoisomerase such as Topo III. Subsequently, RecQ switches to the lagging strand template, generating a single-stranded DNA gap on the lagging strand, on which a RecA filament is assembled in the 3' direction, leading to SOS induction. Subsequent repair of the blocking lesion, trans-lesion synthesis, or recombinational restart may lead to the resumption of DNA replication.

Figure 7

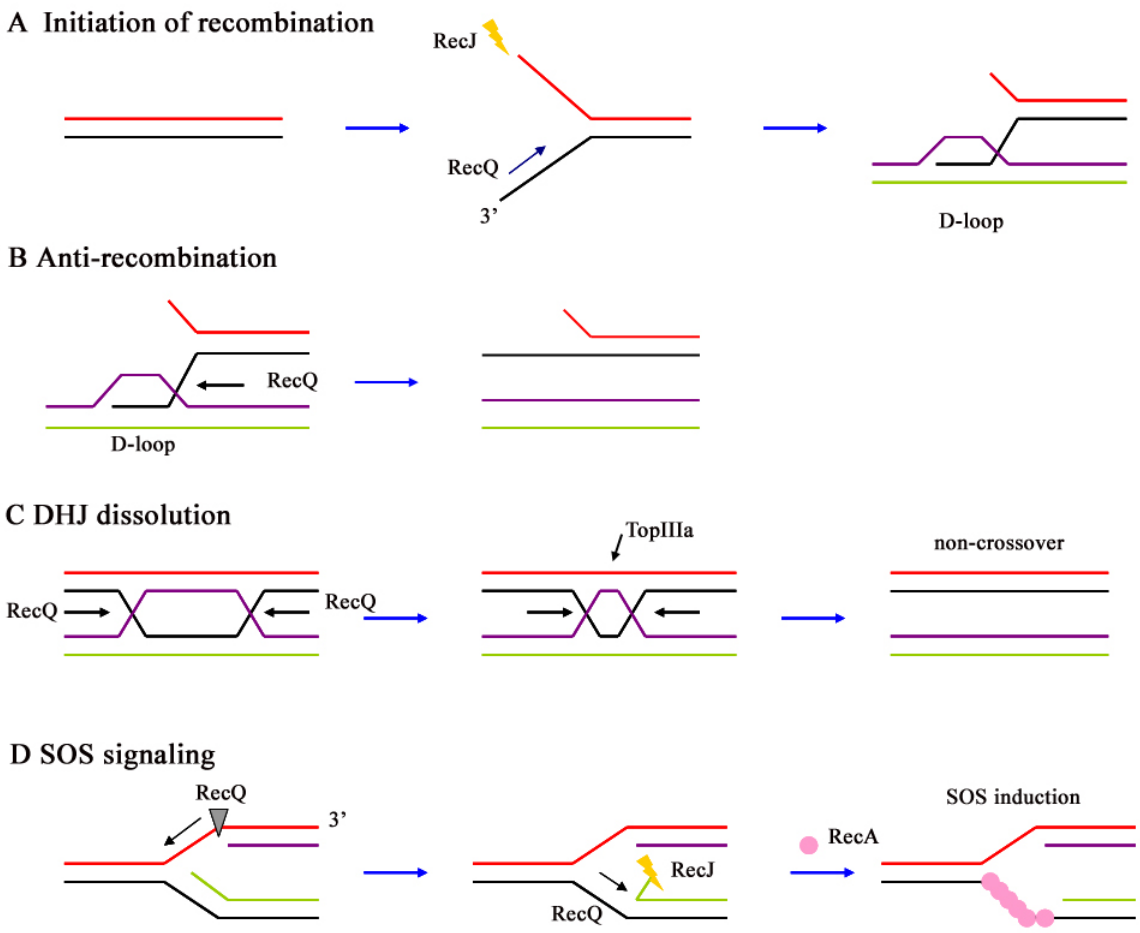

Fig. 7 Roles of the RecQ DNA helicase in genomic maintenance (Adapted from Reference 115)

(A) Initiation of recombination. RecQ helicase can unwind DNA at replication gaps or double strand breaks to initiate recombination and D-loop formation. In this process, RecJ, a single-strand DNA exonulease, digests the displaced 5'-end strand to allow formation of the RecA filament on the 3'-end stand. **(B)** Anti-recombination. RecQ also can disrupt D-loop structure formed by RecA protein. **(C)** DHJ dissolution. RecQ solves the double Holliday junctions interacting with TopIIIα topoisomerase. **(D)** The SOS model. RecQ binds a gap on the leading strand and unwinds the duplex template ahead of the fork in the indirection of 3' to 5'. Then RecQ moves to the lagging strand template to generate a single strand DNA gap on the lagging strand. RecA binds to the single strand region on the lagging strand which leads to SOS induction.

3.2.4 RecQ helicases from other microorganisms

In addition to *E.coli*, there are also a lot of other prokaryotic organisms such as *Haemophilus influenzae* and *Bacillus subtilis* which are good models for studying DNA mechanisms. The *recQ* genes of *H. influenzae* and *B. subtilis* are homologous to that of *E.coli* and the putative RecQ in these two bacteria share about 40% identities with *E.coli* RecQ (120). *B. subtilis* has proven highly amenable to genetic manipulation, and therefore has become widely used as a model organism for laboratory studies equivalent of *Escherichia coli*, especially of cellular differentiation, DNA replication and DNA repair pathways (121). *E.coli*, *B. subtilis* and *H. influenzae* are all suitable objects for research on DNA metabolizable mechanisms and enzymes interrelated in these processes. Scientists have found that RecU and RecS helicases are required for DNA repair and intramolecular recombination and the RecF and RecS provide overlapping activities that compensate for the effects of single mutation. Recently, in *H. influenzae*, the RecJ, RecG have been found to be involved in maintenance of its genome (121;122). However, the structures and functions of the RecQ helicases in these two bacteria are still not well known. Since the amino acid sequences of RecQ are similar among them, we presume that their enzymatic features are similar each other and they participate in DNA repair and recombination pathway possibly. We are interested in functions of *H. influenzae* and *B. subtilis* RecQ in DNA replication and repair pathway.

3.3 Yeast RecQ family helicases

Yeast is an extremely important model organism in molecular biology and cytology. Advanced studies have shown that RecQ helicases in yeast also play an essential role in genomic stability, especially *Saccharomyces cerevisiae* Sgs1 which is considered as homologous human BLM in yeast.

3.3.1 *Saccharomyces cerevisiae* Sgs1

3.3.1.1 Sgs1 Cellular Phenotype

Sgs1 was identified as a suppressor of the slow growth phenotype of top3 mutants (123). The *sgs1* mutant budding yeast cells show a 40% decrease in lifespan compared to wild-type cells (124). McVey *et al*. have shown that sgs1 mutants in fact arrest in G2 or in G1

(125). The *sgs1* mutants do not show differences in telomere lengths, compared to wild-type cells, but the double mutants *sgs1 tlc1* and *sgs1 est2* show an elevated rate of telomere shortening compared to the single tlc1 mutant, indicating a role in telomere maintenance (126). The *sgs1* cells show increased sensitivity to treatment with MMS (127), UV light (128) and HU (127), but not to γ-radiation (129). At the chromosomal level, *sgs1* mutants display a wide variety of defects as marker loss (130), an elevated rate of sister chromatid exchanges (SCEs) (131), gross chromosomal rearrangements (132), a higher rate of loss of heterozygosity (133) and an increased level of illegitimate recombination (134). MMS-induced interchromosomal recombination was found to be reduced in sgs1 cells and UV light exposure of these mutants only induced little of those events (135).

3.3.1.2 Biochemical Properties of Sgs1

Sgs1 codes for a protein of 1447 amino acids, but has not been purified at the full length yet. Biochemical assays were performed with a deletion variant Sgs1400-1268, which is as the other RecQ helicases an ATP-dependent 3'-5' helicase being able to unwind a wide variety of abnormal DNA structures including Holliday junctions (HJ) and D-loops (136). Not only Sgs1 is able to unwind DNA duplexes, it also can disrupt RNA/DNA hybrid molecules (137). The abundance of Sgs1 is cell-cycle regulated, with low levels in M and G1, a peak in S and degradation in G2. Sgs1 forms S-phase specific nuclear foci which partially co-localise with Rad53 and the origin recognition complex. Sinclair *et al*. have reported that Sgs1 localizes into the nucleolus (124), while Frei and Gasser did not observe this phenomenon (124;138).

3.3.1.3 Interaction Partners and Models for genome instability

DNA topoisomerases are enzymes that alter the state of supercoiling of DNA by a strand-passage mechanism involving transient DNA breaks. According to their models of action, they are classified into the type I topoisomerases which generate ssDNA breaks and into type II topoisomerases that create dsDNA breaks to mediate strand-passage. The *S. cervisiae* Sgs1 was identified by three different groups independently, but always in the context of either a topoisomerase gene or protein. Gangloff *et al.* discovered Sgs1 in a screen for suppressors of the top3 slow-growth phenotype (123). Watt *et al.* identified Sgs1 in a search for interaction partners of Top2 (139) and Lu *et al.* found Sgs1 because of

genetic interaction with Top1 (Type I) (140). Sgs1 interacts physically and genetically with all three nuclear topoisomerases. Yeast Top1 is required for DNA replication, mitotic chromosome condensation and general transcriptional repression in stationary phase (141). Under normal conditions, a deletion of *top1* has no effect on cellular growth. Top1 has been reported to interact with Sgs1, but the role of this complex has not been identified yet (124). Top2 (Type II) is required for the resolution of intertwined chromosomes during mitosis and meiosis (142). Genetically, Top2 and Sgs1 have been reported to be epistatic with regard to reducing chromosome non-disjunction, suggesting that they are involved in the same pathway for chromosome segregation (143). *Top3* mutants of the yeast *Saccharomyces cerevisiae* grow poorly (144), are sensitive to DNA damaging agents (137), have severe meiotic defects (145) and exhibit hyper-recombination between repetitive sequences such as telomeres and rDNA (137). The G2 delay, elevated frequency of marker loss and altered morpholgy of a *top3* mutant is suppressed by mutations in the Sgs1 gene (143;146). Recombinant Top3 (Type I) only acts on negatively supercoiled dsDNA (147). Ira *et al.* have shown that the deletion of Sgs1 increases crossovers in yeast cells 2-3 fold (136). The overexpression of Srs2 nearly eliminates crossovers, whereas overexpression of Rad51 in *srs2* cells almost completely eliminates the noncrossover recombination products. It is very likely that Sgs1 in concert with Top3 performs the same reaction as BLM/TOPOIIIα on DHJs (Fig. 7C).

Furthermore, the *sgs1 srs2* double mutant shows a severe growth which is alleviated upon blocking recombination by mutating Rad51, Rad52, Rad55 or Rad57 (128). A recent study from Liberi *et al.* shows that in *sgs1* mutants, recombination-dependent DNA intermediates accumulate at damaged forks, a phenomenon that requires the Rad51 protein, which is counteracted by the Srs2 protein and does not prevent fork movement (145). Sgs1, but not Srs2, promotes the resolution of these recombination intermediates. The integrity of these DNA structures at sister chromatid junctions is protected by the Rad53 checkpoint kinase. They also show that *top3* and *top3 sgs1* mutants accumulate the same structures as *sgs1* cells, arising from defective maturation of the recombination intermediates (148). The accumulation of HJs arising from fork reversal in *rad53* mutants has been shown by Sogo *et al.* (149).

3.3.2 *Schizosaccharomyces pombe* Rqh1

3.3.2.1 Biochemical properites

Schizosaccharomyces pombe Rqh1 protein is a member of the RecQ DNA helicase family. The Rqh1 helicase is a 1328 amino acid protein with a predicted molecular mass of 149kDa, which is homologue to human BLM helicase (Fig. 4). Like other RecQ family members, the Rqh1 protein displays 3' to 5' DNA helicase activity (150).

In the fission yeast, disruption of the *rqh1* gene encoding the single *Saccharomyces cerevisiae* RecQ-related helicase causes cells to display reduced viability and elevated levels of chromosome loss. Cells lacking functional Rqh1 are hypersensitive to DNA damaging agents and defective in recovery from S phase arrest. After S-phase arrest or DNA damage, *rqh1* mutant cells display elevated levels of homologous recombination and defective chromosome segregation (150). *Rqh1* mutation can cause a retarded growth rate and decrease viability. The mutant cells exhibit greatly increased sensitivity to some DNA damage factors, UV and γ-irradiation. Rqh1 helicase has been identified in screens for radiation and hydroxyurea (HU) sensitive mutants. So, Rqh1 is required for the S phase DNA damage as a checkpoint. It is reported that high cellular levels of Rqh1 result in lethal chromosome segregation defects, while more moderate levels of Rqh1 cause significantly elevated rates of chromosome loss. In wild-type cells, DSBs are repaired preferentially through gene conversion (GC) and this pathway is regulated by the action of Rqh1 by suppressing sister-chromatid conversion (SCC) leading to increased GC (151). Rqh1 can operate in the suppression of recombination of sister-chromatid during DSBs repair. Gareth A. Cromie found that Rqh1 extends hybrid DNA and biases the recombination outcome toward crossing over (152). All these results indicated that the Fission Yeast BLM Homolog, Rqh1, plays essential roles in DNA damage repair and meiosis.

3.3.2.2 Function in telomere metabolism

In fission yeast, the telomere binding protein Taz1 protects telomeres and negatively regulates telomerase. Moreover, the replication protein A (RPA) in yeast was found to be required for DNA replication, recombination repair and telomere maintenance. Telomere loss in the $Taz1^-/PRA^-$ double mutants can be suppressed by additional mutation of the helicase domain in Rqh1 enzyme (153). Rhq1 mutant cells show dramatically increased rates of HR after replication arrest or DNA damage. Deletion of *Rqh1* gene may activate a recombination-based and telomerase-independent telomere elongation mechanism. Rqh1 interacts directly with RPA to form a complex at telomere. In Tatsuya Kibe laboratory, they

found that mutation in the helicase domain of Rqh1 will suppress telomere loss on the base of *taz1* and *rpa* double mutations (153). From these studies, we can find that Rqh1 is involved in the telomere metabolism during crisis. All these findings demonstrate that controlling the activity of Rqh1 is critical for telomeres metabolism and therefore for the prevention of genomic instability (154). This provides clues about mechanisms of telomere maintenance in higher eukaryotes.

3.4 RecQ helicases in human

Up to now, five RecQ helicase members have been identified in humans, RECQ1, BLM, WRN, RECQ4 and RECQ5. Defections of WRN, BLM and RECQ4 helicases will give rise to the BS (Bloom's syndrome), WS (Werner's syndrome) and RTS (Rothmund-Thomson syndrome) respectively. RECQ4 deficiency also can lead to the RAPADILINO syndrome and Baller-Gerold syndrome (155). WS and RTS are characterized by premature aging. BS patients have a less pronounced and premature aging phenotype, but have a strong predisposition to several types of cancer. RecQ helicases are considered to be tumour suppressors which suppress neoplastic transformation through control of chromosomal stability.

3.4.1 Human RECQ1

Human RECQl and genome stability

Human RECQ1 (also named as DNA helicase Q1-like protein, RECQL) is the first found RecQ family helicase in human beings. The gene was cloned in 1994 by two laboratories, separately (156;157). These two groups got two different RECQ1 gene sequences resulted from alternative mRNA splicing (158). There is no disease which has been discovered involved in mutation of *RECQ1* gene thus far.

The sequence homology is highly conserved between the mouse and human RECQ1 helicases. To gain insight into the physiological function of human RECQ1, the gene *recql* has been disrupted in mice (159). On the cellular level, the RECQ1 deficient cells were hypersensitive to ionizing radiation and DNA damage agents (160). In addition, embryonic fibroblasts from *RecQ1* gene knockout mice displayed chromosomal structural aberrations including rearrangements, translocations and aneuploidy (159). RECQ1 mutation also results in elevation of sister-chromatid exchanges in both mice cells and human cells, which

may be due to unsuccessful attempts to repair damaged replication forks of Holliday junctions at DNA double-strand breaks (DSBs) (Fig.8A) (159). RECQ1 cooperates with some nuclear DNA metabolic factors including Topoisomerase IIIα and mismatch repair factors (MSH2/6, EXO-1) that serve to suppress crossover of sister chromatids during DNA replication and mismatch repair pathway (161). These studies showed that human RecQ1 has a profound role in the maintenance of chromosomal stability in primary fibroblasts. Mutant in RECQ1 will cause accumulation of DNA strand breaks and persistent Rad51 foci which are the same in BLM and WRN mutations (162). The presence of Rad51 foci corresponding to nucleoprotein filaments is necessary for early strand invasion during homologous recombination (HR). However, unlike *BLM* and *WRN* deficient cells, the *RecQ1* knockout cells have normal telomere lengths compared with normal cells. Although these studies have shown that RECQ1 is necessary for genomic stability, RECQ1-deficient mice did not exhibit any apparent phenotypic differences compared to wild type mice. It is explained that other human helicases, BLM, WRN, RECQ4 or RECQ5, may compensate the absence of RECQ1 (159). So it is supposed that RECQ1 may be an important back support to other human helicases and some key factors of DNA metabolism. In chicken B-lymphocyte line DT40 cells, the *RECQ1*$^{-}$*/BLM*$^{-}$ cells grew more slowly than *BLM*$^{-/-}$ cells because of the increase in the population of dead cells, indicating that RecQ1 are somehow involved in cell viability under the BLM function-impaired condition (163). Combination with the descriptions above about human RECQ1, it is indicated that RECQ1 plays an essential role in DNA repair to disrupt inappropriate recombination intermediates (164).

The amino acids sequence analysis indicated that human RECQ1 is high homologous to *E.coli* RecQ helicase in the seven conserved regions. The encoding gene of RECQ1 is located on the short arm of human chromosome 12p12 (165). This chromosome has been found to coincide with aberrations in testicular germ-cell tumours. Loss of heterozygosity of 12p12 chromosome, some diseases will occur such as haematological malignancies, solid tumours and a rare chronic myeloid leukaemia-like syndrome. RECQ1 is highly expressed in the lungs, and primary non-small-cell lung cancer caused by deletions at chromosome 12p12 (166). So RECQ1 may be involved in the risk of lung cancer although no any human disease and cancer have been found to link with RECQ1 directly. From these results, it is supposed that RECQ1 may play an important role in preventing chromosome instability and predisposition to cancer.

Figure 8

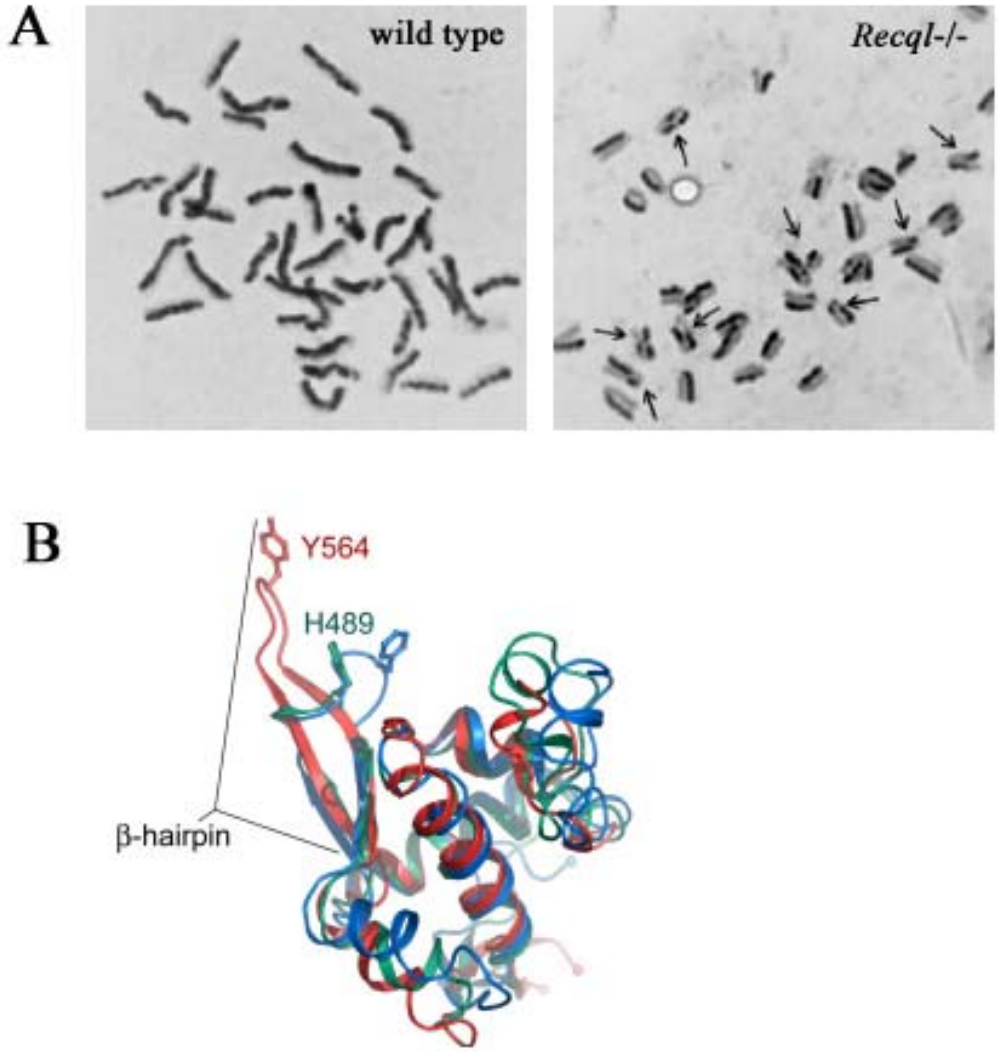

Fig. 8 (A) Elevated SCEs in *Req1-/-* mouse embryo fibroblasts. Metaphase chromosomes were prepared from BrdU-labelled, Giemsa-stained primary wild-type and *Req1-/-* fibroblasts. SCEs are marked with arrows. *Req1-/-* cells show higher frequency SCEs than the wild-type cells. (124)

(B) Ribbon overlay of the WH domains of RECQ1 (red), *E.coli* RecQ (green) and WRN (blue) was adapted from Reference 171. The hairpin structure of RECQ1 is longer and less conserved than that of other two RecQ helicases.

Biochemical properties

As most RecQ helicases, human RECQ1 also has a DNA-dependent ATPase activity and exhibits unwinding activity in the direction of 3' to 5' (167). Up to now, it has been discovered that RECQ1 can separate forked DNA substrates and even Holliday junctions, but it is less active on tailed-duplex DNA, blunt-ended duplex DNA and G-quadruplex DNA which all can be unwound by *E.coli* RecQ (168) (Table 2). RECQ1 has a DNA strand annealing activity influenced by ATP concentration (167). The ATP or hydrolysable analog ATPγS can strongly inhibit the strands annealing ability of RECQ1 whereas ADP has no any affection (169). The purified RECQ1 helicase probably exists as a dimmer in solution, suggesting it may work as a dimmer manner (170). But recent study indicated that RECQ1 carried out its different activities with distinct oligomeric forms. A form as monomer or dimmer of RECQ1 is responsible for DNA unwinding and DNA binding activities, whereas higher order oligomeric forms, hexamers or pentamers, are associated with its annealing ability. RECQ1 is a helicase of low processivity and it is unable to resolve the DNA substrates with long length (171). Like helping BLM and WRN, the human RPA will also stimulate RECQ1 helicase ability by helping it unwind long partial duplexes. RECQ1 involved in Holliday junction separation and DNA strand annealing process suggests that it is required for the homologous recombination. Several aspects of the mechanism of RECQ1 are still unsolved and further research should be carried out to insight to its functions in detail.

Structure of human RECQl

The structure of human RECQ1 seems resemble that of *E.coli* RecQ helicase, but there is a little difference from other RecQ helicases. Like most members in Superfamily 2, all functional domains of RECQ1 are conserved, including the helicase core domain, the zinc binding motif and winged-helix domain. In the helicase core domain, there is an arginine residue as arginine finger to cooperate ATP hydrolysis just like that in other RecQ helicase. The nucleotide binding site is conventional for RECQ1. But the winged-helix (WH) motif of RECQ1 presents different functions from that in other RecQ helicase (171). At first, the structures of WH are different between RECQ1 and *E.coli* RecQ. The changes in position and orientation of the WH domain change all the overall shape of the protein and will mediate it to bind to other proteins and recognition. In most RecQ helicase, this WH domain interacts with the helicase core domain and the zinc-binding motif involved in DNA binding ability. For RECQ1, this motif is much more important in DNA strand separation.

Analysis of the structure of WH domain indicated that the β-hairpin structure which forms part of this domain is significantly longer in RECQ1 than in other bacteria RecQ helicases (Fig. 8B). Deletion of portions of the hairin will severely reduce RECQ1 unwinding of forked DNA substrates but not affect ATPase activity. This function of the hairpin is similar with the HRDC domain of *E.coli* RecQ. So the WH domain is special for RECQ1 and the same function has not been found in other RecQ helicase up to now (172). RECQ1 helicase possesses different mechanistic model from other members in RecQ family. It would be interesting to explore how these differences relate to biological specificity or catalytic efficiency of RecQ enzymes.

3.4.2 BLM - The Bloom Syndrome Helicase

Bloom's Syndrome (BS)

Bloom's syndrome (BS) is an extremely rare, autosomal recessive genetic disorder of humans. Since this syndrome was first described by New York dermatologist David Bloom in 1954, more than 170 individuals have been recognized as being affected (173). This disease is more common in Ashkenazi Jews (at least 1 in 100 Ashkenazi Jews is a carrier of this syndrome) and also has been reported rarely in other countries such as Japan. This disease is caused by mutation of BLM gene located on chromosome 15q26.1 (174). The BS patient is a compound heterozygote emerging from an intragenic somatic recombination event. Major clinical features of BS patient are innate immune deficiency, bacterial infections of the ear and lung commonly and Type II diabetes mellitus which even observed in young patients. Several abnormalities are happened in BS patients including slow growth, proportional dwarfism, small head, unusual skull and facial configuration, but the body proportions are normal. The patients are sunlight sensitivity and their skins show erythema on the noses and cheeks (Fig. 9 low and right). The level of intelligence is low than averages accompanied by learning disabilities and occasional moderate mental deficiency. There is a very high incidence of cancers of most types including rare lung and prostate cancers with an early average age of onset (173). Wilms tumour, medulloblastoma and meningioma are popular in BS patients. Leukaemias predominate occurs in childhood of BS cases, lymphomas and carcinomas appear during adolescence.

Figure 9

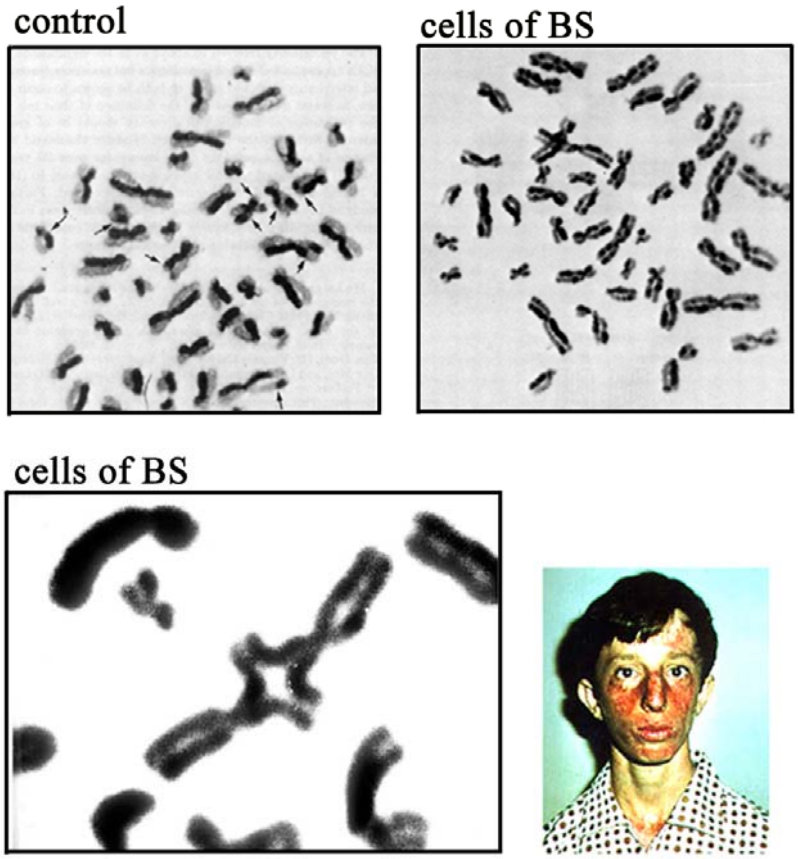

Fig. 9 (Up) Chromosomes of lymphocytes are from a BS case (right picture) and a normal person (left picture). The cells were cultured for two cell-division cycles in BrdU-containing medium, harvested at mitosis, and stained so that the two sister chromatids of each chromosome are stained with 33258 Hoechst and Giemsa differently, one dark, one light (142). **(Low and left)** The Chromatid interchange configuration composed of two probably homologous chromosomes, from a Bloom's syndrome lymphocyte (Adapted from Reference 175). **(Low and right)** The figure of a patient with Bloom's Syndrome exhibits the characteristic symptoms including sunlight sensitivity and discolored skin. (Found at http://web.mit.edu/biology/guarente/human/human.html.)

BS Cellular Phenotype

Cells derived from BS patients display higher frequencies of spontaneously occurring chromosomal aberrations in comparison to normal cells. The most striking cyto-morphological feature of BS cells is much higher frequency of sister-chromatid exchanges (SCEs) when differentially stained following incorporation of various thymidine analogs (175;176). As early as 1974, R.S.K.Chaganti and his colleagues isolated lymphocytes cells form BS patients. The cells were grown in bromodeoxyuridine and stained with 33258 Hoechst and Giemsa. The shapes of chromosomes were studied by fluorescence microscopy. The results indicated that higher frequency of SCEs happened in BS cells than in normal cells, in the cells of the Fanconi's anemia syndrome and Louis-Bar (ataxia telangiectasia) syndrome (177). It was also found that the increase of SCEs in the *BLM* knock-down mice and *BLM*$^{-/-}$ DT40 cells (178). The abnormal increase of SCEs exist commonly in blood lymphocytes from harvested individuals with BS (97). So the extremely high SCEs are considered as a key feature of Bloom's Syndrome (Fig. 9).

In addition, some abnormal conformations of chromosomes such as gaps, breaks, structurally rearranged forms also were found in BS cells. The SCEs present homologous recombination (HR) events occurring between sister-chromosomes during S or G2 phases of cell division (179). Not only HR events in BS cells, but also NHEJ (non-homologous end-joining) event is abnormal which is an error-prone repair process for DNA double-strand breaks (DSBs) (180). An inaccurate rejoining of DSBs is higher and chain elongation during DNA synthesis is lower in BS cells than in normal control cells (181). Most mutations in the *BLM* gene resulting in Bloom's Syndrome is due to either a nonsense mutation or a frameshift event leading to a premature termination codon. Research data shows that about 15% of BS cases are due to missense mutations in *BLM* map to exons encoding the helicase domain of the enzyme which render the enzyme catalytically inactive (26).

BLM protein and its interaction partners

The BLM protein has 1417 amino acids in length (molecular mass, 159 kDa) and native molecular mass of human BLM protein is very large (over 900kDa), which is the result of its hexameric structure. Survey by electron micrograph, Julia K. Karow found that purified recombinant BLM protein is in the close hexameric state (182). The same oligomer forms were testified by size-exclusion chromatography research. BLM protein expresses in all tissues where active cell proliferation occurs including most tumour cells, and that it is

restricted to the actively dividing cells. BLM, in common with *E.coli* RecQ, Sgs1 and Rqh1 helicases, contains three typical conserved domains of RecQ family helicase (Fig. 4). The helicase core domain, RecQ-Ct domain and HRDC domain are laid in all BLM species. Moreover human BLM enzyme contains a nuclear localization signals sequence (NLS) close to C-terminus. This domain of BLM is involved in the location in both the nucleus and cytoplasm, and it helps BLM migrate into nucleus (183). Biochemical and biophysical studies showed that RecQ-Ct and HRDC domains function as auxiliary DNA binding sites. The HRDC domain of BLM is also required for disruption of double Holliday junctions (184).

As most RecQ helicases, BLM utilizes the energy derived from the hydrolysis of ATP dependent on DNA to catalyse DNA strands separation in a 3' to 5' polarity (185). In addition, it has the ATP-independent annealing ability which can be blocked by ssDNA-binding proteins such as RPA (186). The C-terminal domain of BLM is essential for DNA strand annealing ability. One feature of BLM helicase is the ability to recognize and unwind a large array of substrates of different shapes and lengths. It includes forked duplexes, bubble structures, D-loop structures, synthetic three- way junctions and Holliday junctions (Table 2). Interestingly, a fully double-stranded, blunt-end structure is not a substrate for BLM helicase (187). There is an apparent preference for the unwinding of synthetic G-quadruplex DNA structures by BLM (105). It is suggested that BLM may take a role in disruption of telomeric quadruplexes to maintain telomere stability. RPA can enhance the processivity of BLM but not affect on its ATPase activity (188).

In our laboratory, we have analysed several disease-causing missense mutations localized in the BLM helicase core region. Our work revealed that structural elements implicated in DNA binding, ATP hydrolysis and DNA unwinding. These findings will help us explain the mechanism underlying BLM catalysis and interpreting new BLM causing mutations identified in future.

In human cells, arrays of factors have been found to interact with BLM protein physically or functionally to regulate genomic metabolism together *in vivo*. We discuss some BLM partners below briefly.

TopIIIα: Topisomerases which catalyse the passage of intact DNA strands through transient breaks in other DNA strands are mainly cooperative factors for RecQ helicase family. Topisomerase IIIα and BLM co-localize on the intermediates of DNA replicaion, where DNA structures generated by BLM are required to be resolved by TopIIIα (Fig. 10).

Summarily, TopIIIα helps BLM helicase suppress the hyper-recombination such as SCEs during DNA replication and repair processes.

Figure 10

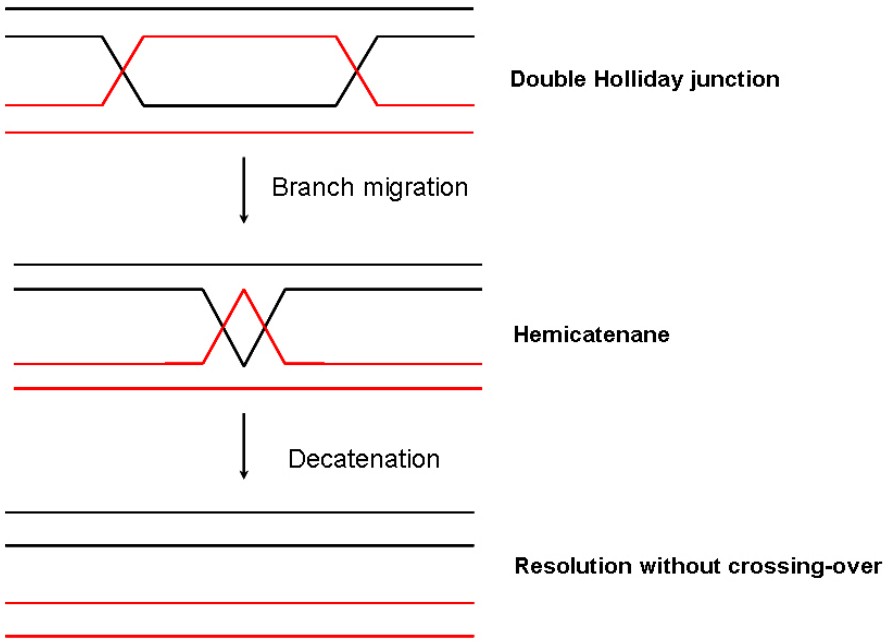

Fig. 10 Model for the resolution of DHJ structure of BLM with non crossing-over
The two recombining strands are indicated in black and red. The double Holliday junction (top) is converted by branch migration of the junctions to a hemicatenane (middle). Then topoisomerase IIIα resolves it by single-strand DNA decatenation. The resolved DNA products without crossing-over are shown in the bottom.

BLAP75 (BLM associated polypeptide, 75kDa): In Hela cells, BLAP75 was found always present in near-equal molar amounts compared to components such as BLM and Topo IIIα. It is an integral component of BLM complexes and essential for a BLM-Topo IIIα-BLAP75 complex (BTB complex) stability *in vivo*. Loss of BLAP75 resulted in destabilization of BLM complexes and genomic instability (189). In a recent study, it was found that BLAP75 binds DNA, associates with BLM and Topo IIIα and enhances the ability of BTB complex to branch migrate the Holliday junctions and dissolve the double Holliday junction structure

to yield non-crossover recombinants (182;190;191). I.D. Hickson provided experimental evidences to demonstrate that BLM and topoisomerase IIIα catalyse a novel reaction for the resolution of double Holliday junctions (DHJ). BLM helicase pushes two junctions of DHJ towards one another to form a single interwined structure called hemicatenance and then topoisomerase IIIα will resolve this product through a strand passage mechanism called decatenation to generate recombinant products (Fig. 10). This process completely depending on BLAP75 factor requires the hydrolysis of ATP by BLM helicase and active site tyrosine residue of topoisomerase IIIα.

RAD51: RAD51 protein is high similar to bacterial RecA protein structurally and functionally which assists in repair of DNA double strand break and homologous recombination. BLM forms a complex with recombinase RAD51 to act upon DNA intermediates during homologous recombination (HR) pathway (192). In early meiotic prophase cells, RAD51 co-localizes with BLM to the sites of interhomologue DNA interactions, and it helps BLM promote Holliday junction branch migration. RAD51 catalyses pairing between a ssDNA tail and a homologous stretch of dsDNA, and promotes DNA strand exchange to initiate DNA homologous recombination (193). Further research should be carried out to find out the relationship between BTB complex and RAD51 during HR.

BRCA1 (breast cancer 1, early onset): BRCA1 belongs to a class of proteins known as tumor suppressors which maintain genomic integrity to prevent uncontrolled proliferation. Some mutations of BRCA1 are associated with a significant increase in the risk of cancers, especially breast cancer. The BLM helicase interacts with BRCA1 factor to response to DNA damage or replication.

p53 (protein 53): The p53 factor is a tumour suppressor protein that acts to regulate gene expression under conditions of cellular stress. BLM and p53 are involved together in regulating cell growth and apoptosis. p53 can inhibit the unwinding of Holliday junction catalyzed by BLM by binding the HJ structure at its crossover point which may represent ssDNA arising due to breathing of the junction. It suggests that p53 regulates homologous recombination through its modulation of interaction of BLM with recombination intermediates (194).

The BRAFT Complex: Upon immunoprecipitation of BLM from HeLa cells, Meetei *et al.* identified by masspectrometric methods a complex called BRAFT which includes BLM, TOPOIIIα, RPA and the five core Fanconi anemia (FA) proteins (FANCA, FANCC, FANCE, FANCF and FANCG). BLM is responsible for the unwinding of DNA substrates

in this complex (195). Pichierri *et al*. have shown that BLM and FANCD2 co-localize and co-immunoprecipitate upon treatment with DNA crosslinkers or agents inducing replication fork arrest, again indicating a functional interaction (196). The features of the BS are very different to those of the FA, but some aspects of genomic instability in these diseases are similar. For a review on the Fanconi anemia proteins, see references (197;198) .

TRF2: In telomerase-negative cells, there is a different mechanism called alternative lengthening of telomeres (ALT) by which maintaining the telomeres. In this mechanism, BLM co-localizes with the telomere repeat binding factor 2 (TRF2) in atypical, telomere-associated PML bodies. Also, TRF2 and BLM could be co-immunoprecipitated, suggesting a role of this association *in vivo* (199). TRF2 also interacts with BLM physically and stimulates its helicase activity on forked duplexes with or without two telomeric repeats. TRF2 is unable to bind these structures, as it requires more telomeric repeats (200).

WRN: WRN and BLM have been reported to interact directly *in vivo* and *in vitro.* This interaction has a functional consequence in regulating the exonuclease activity of WRN. This interaction is certainly not the only way for the two proteins to function, as only a small portion of WRN could be co-immunoprecipitated with BLM (201) and Bloom Syndrome is quite different from the Werner syndrome.

3.4.3 WRN - The Werner Syndrome Helicase

The Werner Syndrome

Like Bloom Syndrome, the WRN Syndrome (WS) is an autosomal recessive disorder with an estimated frequency of 1~22 cases per million of the population word-wide. Interestingly, the majority of WS patients happen in Japan. There are about 3 cases per million of Japanese population. The *WRN* gene is located in human chromosome 8p-12 (98). The first WS case was found in 1904 by Otto Werner and he described the clinical features in his doctoral thesis. The condition becomes apparent in WS adolescence of short stature due to lack of the usual growth spurt. Changes are especially pronounced on the faces of patients which include thinning and sharpening of the noses, called a bird-like appearance. One of the typical features of WS patients is premature aging disorder with greying, thinning and loss of hair. It begins in adolescence or early adulthood and results in the appearance of old age (Fig. 11A). The similarity of some symptoms of WS and normal aging process makes it become a suitable model to study premature mechanism. WS patients are often shown atherosclerosis, arteriosclerosis, hypermelanosis, cerebral cortical

atrophy, lymphoid depletion and thymic atrophy. Higher incidence of early onset malignancies and Type II diabetes happen in several cases of WS. Most importantly, WS is associated with an excess of cancers and sarcomas, especially in soft tissues. Some data indicated that 10-fold ratio of epithelial and mesenchymal cancers occured in WS cases comparing to normal population (98).

WS Cellular Phenotype

The *WRN* gene has been positionally cloned and is located in the p11-p12 region on human chromosome 8, spanning 180 kb (202). In culture, WS cells have been shown to undergo replicative senescence at a faster rate than normal cells, which is considered to be the hallmark of WS cells with an average lifespan of only 27% of normal cells (203). A recent study has shown that the WS cells are defective in lagging strand synthesis of telomeres. Therefore it will suffer from a single telomere loss and further argues for WRN being involved in replication, presumably by disrupting quadruplex DNA that may form on the G-rich lagging strand template (Fig.11B) (204). Furthermore, the growth defects of WS cells are retained after transformation (205). The expression of telomerase hTERT reverses the poor growth and the entry into premature senescence phenotypes of WS cells, but it seems not quite sufficient to immortalise the cells (206). WS cells have been reported to be sensitive to 4-nitroquinoline 1-oxide (4NQO). This effect can be reverted by expressing hTERT in SV40-transformed WS cells (207). WS cells have further been reported to be sensitive to DNA cross-linking drugs such as mitomicin C and cisplatin (208;209). Furthermore, WRN-deficient human and murine cells are sensitive to camptothecin, an inhibitor of Topoisomerase I (210). Sensitivity to γ-radiation and radiomimetic drugs is debated, since several groups have shown different responses of WS cells to these treatments (128;178). The hallmark of WS cells at the chromosomal level is the elevated rate of extensive somatic deletions and translocations which can vary in different clones (211). Furthermore, WS cells display a higher number of RAD51 foci than normal cells, which probably indicates the persistence of unprocessed recombination intermediates (212). Unlike in BS cells, no any increase in SCE-frequency has been discovered in WS cells (213). WRN seems not to be involved in homologous recombination. Instead, its strong interaction with Ku rather suggests a role in non-homologous end-joining, in a manner that Ku regulates the WRN exonuclease in resection of DNA at non-homologous ends (213;214). This action is likely not to be the sole on DNA ends, as WS cells do not show an obvious DNA double strand break (DSB) repair defect.

Figure 11

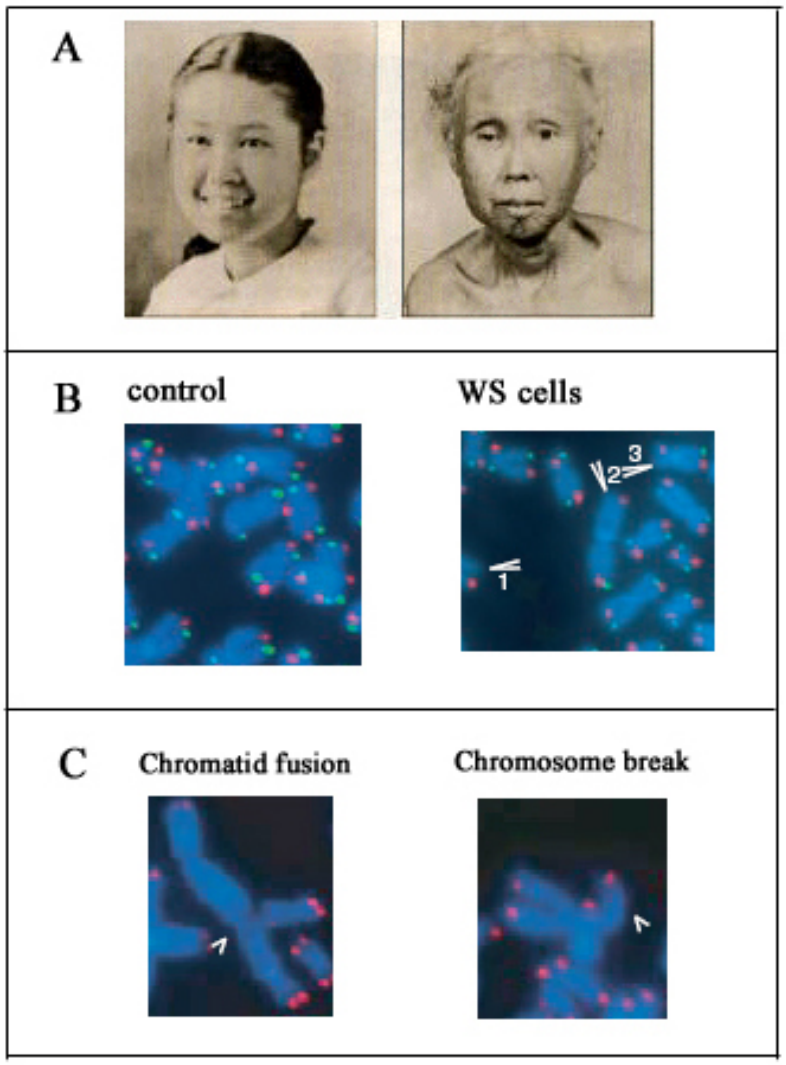

Fig. 11 (A) The case of Werner syndrome. A teenager (left) looked normal, but when she was 48 years old, the effects of Werner syndrome were apparent. (Photo comes from www.pathology.washington.edu) **(B) Loss of lagging strand telomeres in WS cells.** Leading strand telomeres were shown in red with a FITC probe and lagging strand telomeres in green with a TRITC probe using CO-FISH technique. DNA was stained with DAPI (blue). The arrows indicated missing sister telomeres. **(C) Chromosome fusions in WS cells.** Telomeres were shown with a FITC probe (red) and DNA was stained with DAPI (blue). Arrows indicated chromatid fusions and chromosome breaks. (Permission pending for images B and C are from Reference 217)

WRN protein and its interaction partners

The WRN protein is 1432 amino acids long and contains two functional domains: the central helicase domain and the N-terminal exonuclease domain. Furthermore, it carries an unusual direct repeat of 27 amino acids located between the exonuclease and the helicase domains. WRN displays an ATP-dependent 3'-5' helicase activity. As most other RecQ helicases, it is able to unwind D-loops, G-quadruplex DNA and to migrate Holliday junctions (Table 2). The N-terminal nuclease domain displays 3'-5' polarity and shows low processivity (215;216). One of the most important functions of WRN is that WRN can efficiently disrupt quadruplex DNA structures (also called G4 tetraplex DNA) *in vitro*, which may be widely distributed throughout the genome. G-quadruplex (G4) DNA, a highly stable DNA structure can form in guanine-rich loci such as within the c-myc gene promoter, where it seems to regulate gene expression, and within the G-rich strand of telomeres (Fig. 12). WRN acts as a 'roadblock remover', eliminating DNA secondary structures or other obstacles that would otherwise impede the progress of translocating protein complexes. In the absence of WRN, forks would stall or be disrupted, and this would lead to genomic instability during the attempted rescue of the blockade (217) (Fig.11C).

It has been suggested that the helicase and exonuclease activities of WRN appear to act co-ordinately to disrupt some DNA intermediates formed during DNA transaction (218;219). Recent biochemical researches indicate that WRN possesses ssDNA annealing ability required of a special C-terminal region (82). Furthermore, the activity appears to correlate with DNA binding and oligomerization status of the protein. Orren *et al.* have observed that WRN *in vitro* will as helicase unwind the duplex of the invading strand in a D-loop structure and as 3'-5' exonuclease digest the invading strand (218). WRN has also been reported to mediate strand exchange *in vitro* (220) , but the activity observed may be debated as the reaction conditions which were far from physiological environments.

The bipartite and bifunctional natures of WRN, as well as different symptoms in WS patients suggest that WRN is a versatile enzyme in diverse cellular processes and DNA mechanism. Shiratori and co-workers demonstrated that WRN may participate in either or both RNA polymerase I and polymerase II dependent transcription. It also plays an important role in DNA replication and repair (221).

Figure 12

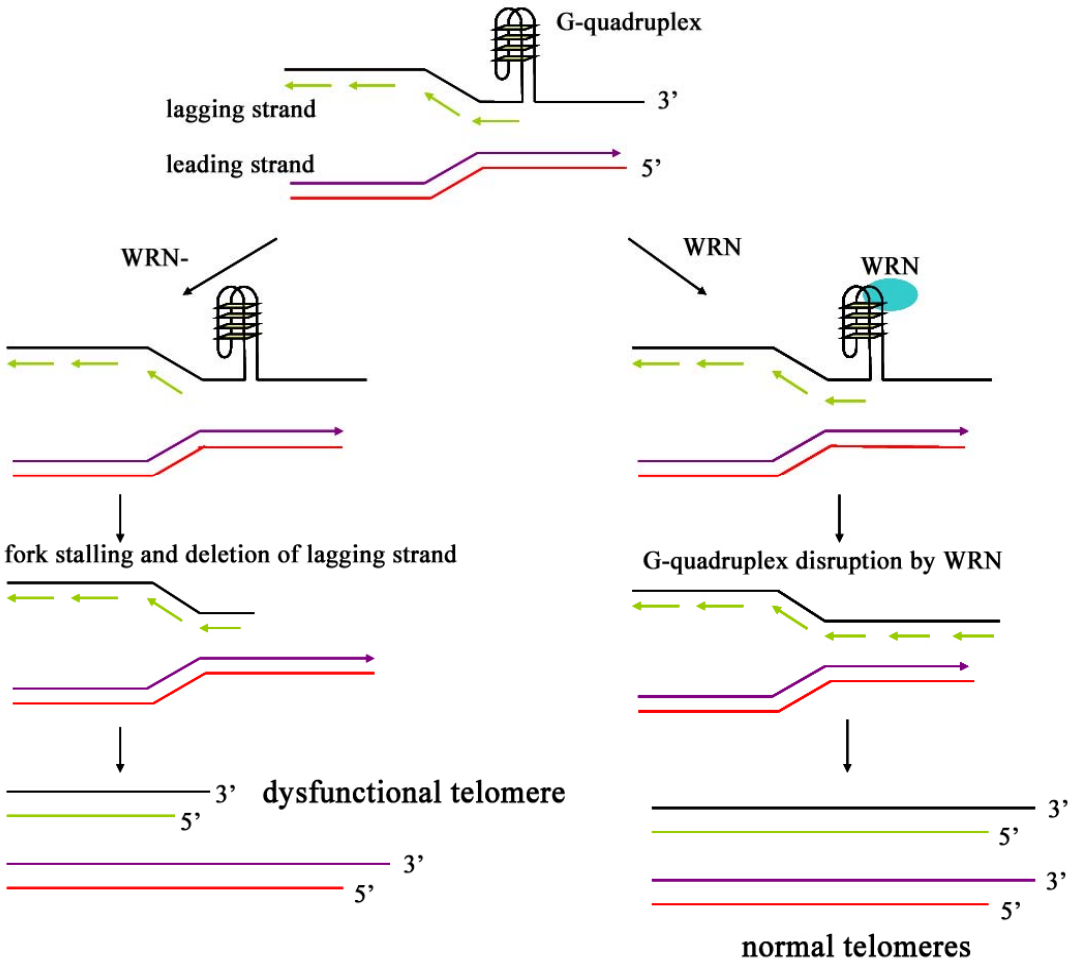

Fig. 12 Model for WRN to remove the G-quadruplex of telomere

An intrastrand G-quadruplex lying in the telomere is shown in the figure. WRN can disrupt this structure permitting smooth replisome progression of lagging strand G-rich telomeres. In the absence of WRN, G-quadruplex on the lagging telomere leads to replication fork stalling and deletion of lagging strand. Dysfunctional telomere can further induce a p53-dependent DNA damage response to premature onset of replicative senescence.

WRN is a versatile enzyme in different aspects because it interacts physically and functionally with several other proteins required for DNA metabolism. In the DNA replication process, some replication factors such as DNA polymeraseδ (222), toposomerase I (210), PRA (223) and proliferating cell nuclear antigen (PCNA) (224) can form a physical complex with WRN. WRN can remove the atypical DNA secondary structures to let DNA polymeraseδ process DNA synthesis normally. FEN1 (flap structure-special endonuclease 1) cooperates with WRN to resolve the 5'- flap structure which is a DNA intermediate product during DNA replication (225). Some data suggested that RPA markedly stimulates the DNA helicase activity of WRN. Interestingly, WRN interacts with TRF1, TRF2, RAD52 and some other factors to supervise the telomere maintenance together (204). Interaction between some tumour suppressors and WRN revealed the potential reason of the high incidence of cancers in WS patients. It's worth noting that BLM has been found to inhibit WRN exonuclease function in a concentration-dependent manner *in vitro* (87). Most importantly, the hyper-recombination and high SCEs phenotype of the *BLM* mutant cells can be partially suppressed and be disrupted by WRN (178). But BLM and WRN contribute different roles on special DNA metabolic pathways.

3.4.4 RECQ4/RTS- The Rothmund-Thomson Syndrome Protein

The Rothmund-Thomson Syndrome (RTS)

The Rothmund-Thomson syndrome (RTS) is a rare autosomal recessive disorder with roughly 200 reported patients worldwide. RTS was first described in 1868 by Rothmund, a german ophtalmologist. Patients from a german family suffered from unusual skin degeneration and cataracts, a condition where the lens of the eye gradually turns opaque and results in a blurred view (26). 68 years later, Thomson, a British dermatologist described a syndrome with skin abnormalities and skeletal malformations and called it Poikiloderma congenitale (226). In 1957, Taylor recognised that the two syndromes are manifestations of the same disease and called it therefore RTS syndrome (26). Through a number of patients studies it is known that RTS confers a high incidence of malignancies, mainly osteosarcomas (227). Patients suffer from retarded postnatal growth and skin abnormalities that manifest as poikiloderma and sun-sensitive rash. Most patients also have sparse hair, eyebrows and eyelashes. The RST patients have clinic features of slow growth and small

stature; abnormalities of the teeth and nails; and gastrointestinal problems in infancy, such as chronic diarrhea and vomiting.

Furthermore, diverse skeletal abnormalities arise, such as a decrease in bone density (osteopenia), pathological fractures, dislocations and metaphysis. In many cases, the so-called "radial ray defect" is immediately apparent, which manifests as appendages of the thumb or small, missing or bifid thumbs. Often, cataracts appear, whereas mental or gonadal problems are varying from patient to patient. RTS has been found in some cases to be associated with a defect in the RECQ4 gene (228). Unlike BS and WS patients, RTS cases are very frequently associated with one characteristic type of cancer, osteosarcoma. Wang *et al.* have later classified RTS into RTS type I which represents RTS without a predisposition to osteosarcomas and RTS type II that is characterised by a defective RECQ4 and a high predisposition to osteosarcomas (229).

Another disease associated with a defective RECQ4 gene has been recently identified: the RAPADILINO syndrome, characterised by radial hypoplasia, patella hypoplasia and cleft or arched palate, diarrhea and dislocated joints, little size and limb malformation, nose slender and normal intelligence. Unlike the RTS, RAPADILINO does not display the same high predisposition for malignancies (155). Interestingly, the distinction between the two syndromes is also seen at the genetic level, as RTS patients with a defective RECQ4 gene are mainly compound heterozygotes of nonsense or frameshift mutations, resulting in a RECQ4 polypeptide lacking a large part of the helicase domains (229), whereas most of the RAPADILINO patients are compound heterozygotes in which at least one of two defective RECQ4 alleles contains a deletion that causes, upon pre-mRNA splicing, the skipping of exon 7 without frameshift leading to a polypeptide with an intact putative helicase domain of RECQ4 (155).

RTS Cellular Phenotype

RTS cells have been reported to be genetically unstable, displaying a high frequency of chromosomal abnormalities such as translocations and trisomies (230;231). Cultured cells from RTS patients show normal sensitivity to mitomicin C, bleomycin, vincristine, methotrexate, cisplatin and adriamycin (228;232;233). The rate of sister chromatid exchanges is also normal in RTS cells (213). However, RTS cells show an increased sensitivity to ionizing radiation , probably due to a reduced level of DNA repair synthesis and an abnormally low rate of the removal of radiationinduced DNA lesions (234). The low

DNA repair capacity is also an explanation for the UV sensitivity and reduced unscheduled DNA synthesis after UVC exposure observed in RTS cells (228).

RECQ4 protein

The RECQ4 gene has been cloned by Kitao *et al.* before it was known to be associated with RTS. It lies on the p-arm of chromosome 8 at 24.3 spanning 6.5 kb and includes 21 exons (228;235). The RECQ4 protein of 1208 amino acids harbours the helicase domains, but seems to lack the zinc binding domain as well as the WH and HRDC domains (99) (Fig. 4).

The RECQ4 protein is present in all phases of the cell cycle, but apparently peaks in S and G2, again indicating replicative or postreplicative roles of RECQ4 (236). Yin *et al.* have recently shown that the RECQ4 protein is present in the nucleus as well as in the cytoplasm of HeLa cells and preliminarly characterised biochemical activities of the immunoprecipitated protein. They could observe an ATPase activity with ssDNA or dsDNA as co-effectors but the protein failed to displace synthetic DNA duplexes (99;236) or to melt a triple helix. The authors concluded that RECQ4 may be similar to the SWI/SNF chromatin-remodelling factors, members of the SF2 family that show ATPase activity but not helicase activity *in vitro*. The absence of the zinc binding domain remains enigmatic even in this context.

Using Xenopus laevis as a model system, Sangrithi *et al.* have found that xRTS, the X. laevis homologue of RECQ4, is essential for DNA replication in egg extracts (237). They observed that xRTS accumulates on chromatin during replication initiation after establishment of the prereplication-complex but before the recruitment of replicative polymerases. Furthermore, xRTS depletion suppressed the loading of RPA that marks unwound origins before polymerase recruitment. The authors concluded that xRTS functions after the formation of the prereplication-complex to promote loading of replication factors, an activity previously unrecongnised but apparently necessary for initiation of replication (238). This role in replication initiation may explain the cause of chromosomal abberations of type II RTS cells.

A previous study has shown that the purified RECQ4 helicase displayed only DNA annealing activity, but DNA unwinding activity was not observed (99). Recently, it showed that under the appropriate experimental conditions, RECQ4 was found to be capable of unwinding different DNA structures such as forked, bubbled and blunt-end duplex DNA (103). Because of its high DNA strand annealing activity, its DNA unwinding activity is

hidden under usually experimental conditions. More importantly, two distinct regions of the protein, the conserved helicase motifs and the Sid2-like N-terminal domain display ATP-dependent DNA unwinding activity. This balance mechanism between annealing and unwinding is different from that of RECQ5 discovered in our laboratory (68).

Like BLM and WRN helicases, the RECQ4 also has some interacting partners in cells. RECQ4 has been proposed to function in the initiation of DNA replication required for the recruitment of DNA polymerase α. Petkovic found that RECQ4 cooperates RAD51 in homologous recombination of double strand break repair pathway. In the repair of UV DNA damage, RECQ4 can remove the DNA lesion through interaction with nucleotide excision repair factor: Xeroderma Pigmentosum Group A (XPA) (239).

It has been demonstrated that RECQ4 form a stable complex with UBR1 and UBR2 in the cell. UBR1 and UBR2 are very similar proteins that are the components of ubiquitin (Ub) ligases (E3) of the N-end rule pathway, one pathway of the Ub-proteasome system. Yin *et al* (155) could isolate a protein complex consisting of RECQ4, UBR1 and UBR2 mainly from the cytoplasm and observed that the complex displayed DNA-stimulated ATPase activity, but failed to display helicase or translocation activities. Furthermore, they showed that RECQ4 is not ubiquitylated *in vivo* and is a long-lived protein in HeLa cells (155). Recently, p53 has been shown to repress the transcription of RECQ4 in G1-arrested cells, both in the absence and presence of DNA damage. Tumour-derived mutant forms of p53 were not able to repress the transcription of RECQ4. Arresting the cells by the topoisomerase-inhibitors etoposide (arrest in G2) or camptothecin (arrest in S) led to further accumulation of p53 and concomitant decrease in the amount of RECQ4. Histone deacetylase 1 (HDAC1) was shown to be normally recruited to the RECQ4 and p21 promoter. Trichostatin A (TSA), an inhibitor of all histone deacetylases (HDACs) inhibited the p53-mediated repression of the RECQ4 promoter, probably due to a conformational change of HDAC1 as it was observed that it was no longer bound to the promoter upon camptothecin treatment. The authors of this work proposed that the p53-mediated repression of RECQ4 transcription during DNA damage results from the modulation of the RECQ4 promoter occupancy by transcription activators and repressors (236) .

3.4.5 RECQ5

Discovery of RECQ5

RECQ5 is the fifth human homologue of the *E. coli* RecQ and has not been associated with any syndrome yet. Kitao *et al.* identified a small isoform of RECQ5, which was later denoted RECQ5 alpha (235). In this work, they cloned a cDNA with homology of 48% to the helicase domain of RecQ. The cloned gene encoded for a 410 amino acids long polypeptide. Because of the relatively small size compared to the other human RecQ homologues, the authors classified this RECQ5 variant as a member of a small group. FISH analysis revealed the corresponding gene to be located on the q arm of chromosome 17 at the 25 region. The gene was found to be expressed ubiquitously with the highest levels in testis and ovary (235).

A year later, Sekelsky *et al.* reported their work on cloning the *Drosophila* melanogaster RecQ5 (DmRecQ5) (240). The discovery of the DmRecQ5 was coincidental, as they found it while cloning an unrelated cell-cycle checkpoint gene by screening a *Drosophila* embryo cDNA library. They found two RECQ5 isoforms of 54 kDa and 121 kDa generated by alternative splicing. The shorter one consists of the conserved helicase domains and is similar to the previously reported human RECQ5 protein and the longer one, in addition to the helicase region, contains a long C-terminal part bearing many charged residues without homology to any other RecQ helicase. Furthermore, they showed that the long isoform of DmRecQ5 localises to the nucleus. The authors also extended their study to the human RECQ5 and observed that the cDNA from Kitao *et al.* was incomplete at the 5' end and used this clone to screen a brain cDNA library. They found a cDNA coding for a protein of 49 kDa, which would be a bit longer than the 46 kDa protein identified by Kitao *et al.* As both cDNAs contained a polyadenylation signal at the 3'-end, it was assured that both constructs were from genuine coding mRNA. Although the two cDNAs were almost identical, the one identified by Sekelsky *et al.* was slightly longer than the other at the 3' end. It was concluded that the resulting protein would be generated from a different alternative splicing to yield a protein containing additional 25 amino acids. The protein variant Sekelsky *et al.* had discovered in this work was actually later denoted RECQ5γ (240;241). Furthermore, they speculated on the existence of two additional variants, of which one was later cloned and named RECQ5β. Another attempt to clone RECQ5 DNA from human testis mRNA revealed three different splice variants named alpha (α), beta (β) and gamma (γ) (242). The structures of these transcripts are shown in Figure 4. Furthermore, it has been shown that RECQ5β localises to the nucleus, whereas the short isoforms

RECQ5α and RECQ5γ are only present in the cytoplasm. The authors also report an interaction of RECQ5β with the topoisomerases IIIα and IIIβ (243).

Biochemical properties of RECQ5

The human RECQ5 gene encodes three isoforms naturally by different mRNA splicing, designated RECQ5α, RECQ5β and RECQ5γ (Fig. 4) (68). RecQ5α is the shortest variant including only the helicase domain (410 amino acids). RECQ5β contains the helicase domain and a putative RecQ-Ct domain, which is followed by a long C-terminal region that shows no homology with the other RecQ helicases. RecQ5γ includes the helicase domain followed by a C-terminal extension of 25 amino acids which is not present in RECQ5β. The three isoforms expressing in different tissues show they may carry out different functions in cells. The amino acid homology search indicates that a NLS sequence existing in the C-terminal of RECQ5β will help it migrate into the nucleus like other human RecQ helicases. So RECQ5β may play essential role in the genomic metabolism. The RecQ5α and RECQ5γ which are lack of this domain stay in the cytoplasm, and the functions of these two smaller isoforms remain to be clarified.

At present, only RECQ5β has been biochemical characterized completely. RECQ5β exists as a monomer manner. Patrick described human RECQ5β not only functions as an ssDNA or dsDNA-dependent ATPase, an ATP-dependent DNA helicase with 3' to 5' polarity, but also has an annealing activity which can be restrained by ATP binding (244). It suggested that RECQ5β may mediate DNA transactions that require a coordinated action of helicase and strand-annealing activities such as replication fork regression. The biochemical and structure studies revealed that RECQ5β unwind only the lagging strand arm of the fork and this reaction can be enhanced in the presence of hRPA protein (244). It was proposed that a mechanism in which RECQ5β binds to the fork junction and translocates along the lagging strand duplex from 3' to 5' direction to unwind this fork substrate (243). At the same time, RECQ5β also has the ability to promote strand exchange ability. So when the moving junction meets the leading strand, RECQ5β carried out strand exchange ability resulting in the displacement of the leading strand and its annealing to the displaced lagging strand to form a four-way junction. The mechanism of RECQ5β solves the DNA forked structure during DNA replication and repair is complicated because of its multiple helicase capabilities including unwinding, annealing and exchange of forked substrates. Some results indicate that the C-terminal sequence is important for the annealing and unwinding activities of RECQ5β (68). How this enzyme balances its different functions during DNA

metabolisms remain to be solved. In our research, we found out the relationship between annealing and unwind abilities of RECQ5β, and it is also the first time to put insight into the functions of RECQα. We used human RECQ5α and RECQ5β to reveal the relationship between unwinding and annealing abilities and brought forward a cooperative model which is different from previous results.

The co-immunoprecipitation results indicated that RECQ5β interacts with topoisomerases 3α and 3β which are important factors during DNA replication (242). Then, it was found that RECQ5β also can associate with DNA replication factories in S phase nuclei and persists at the sites of stalled replication forks after exposure of cells to UV irradiation (243). Moreover, it can interact physically with the polymerase processivity factor proliferating cell nuclear antigen (PCNA) *in vitro* and *in vivo*. All these findings suggest that RECQ5β plays important roles in DNA replication and repair pathways.

Figure 13

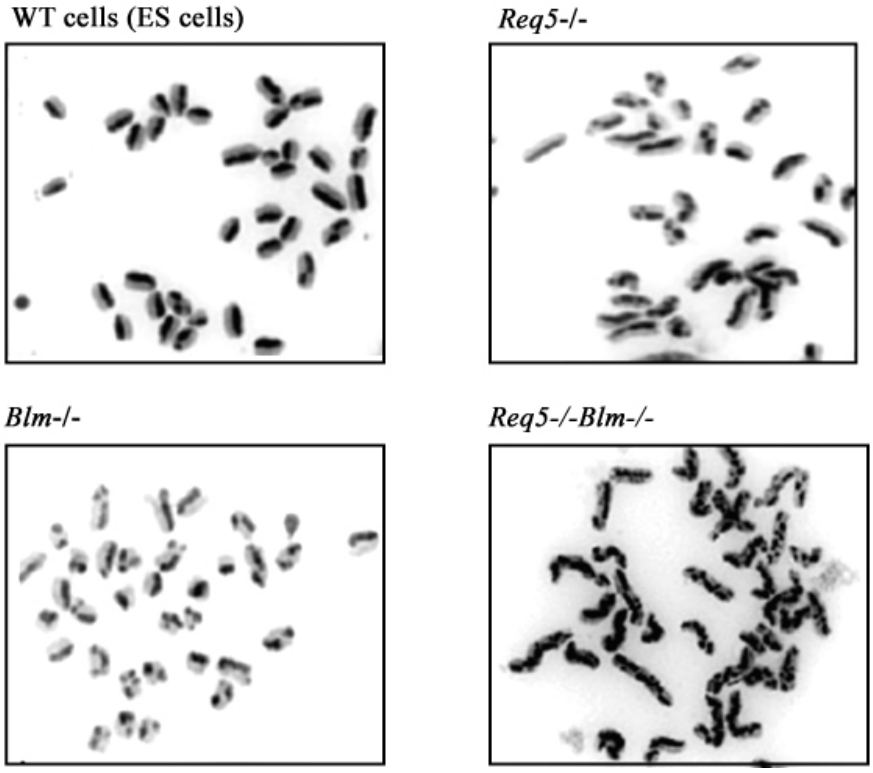

Fig. 13 Spontaneous SCEs in mouse embryonic stem cells (ES cells)
The chromosomes of wild type of ES cells are normal. Either *Recq5*$^{-/-}$ or *BLM*$^{-/-}$ cells has an elevated frequency of SCEs. The higer SCEs can be found in both *Recq5*$^{-/-}$ and *BLM*$^{-/-}$ cells than single mutation of these two genes. (Adapted from Reference 246)

Figure 14

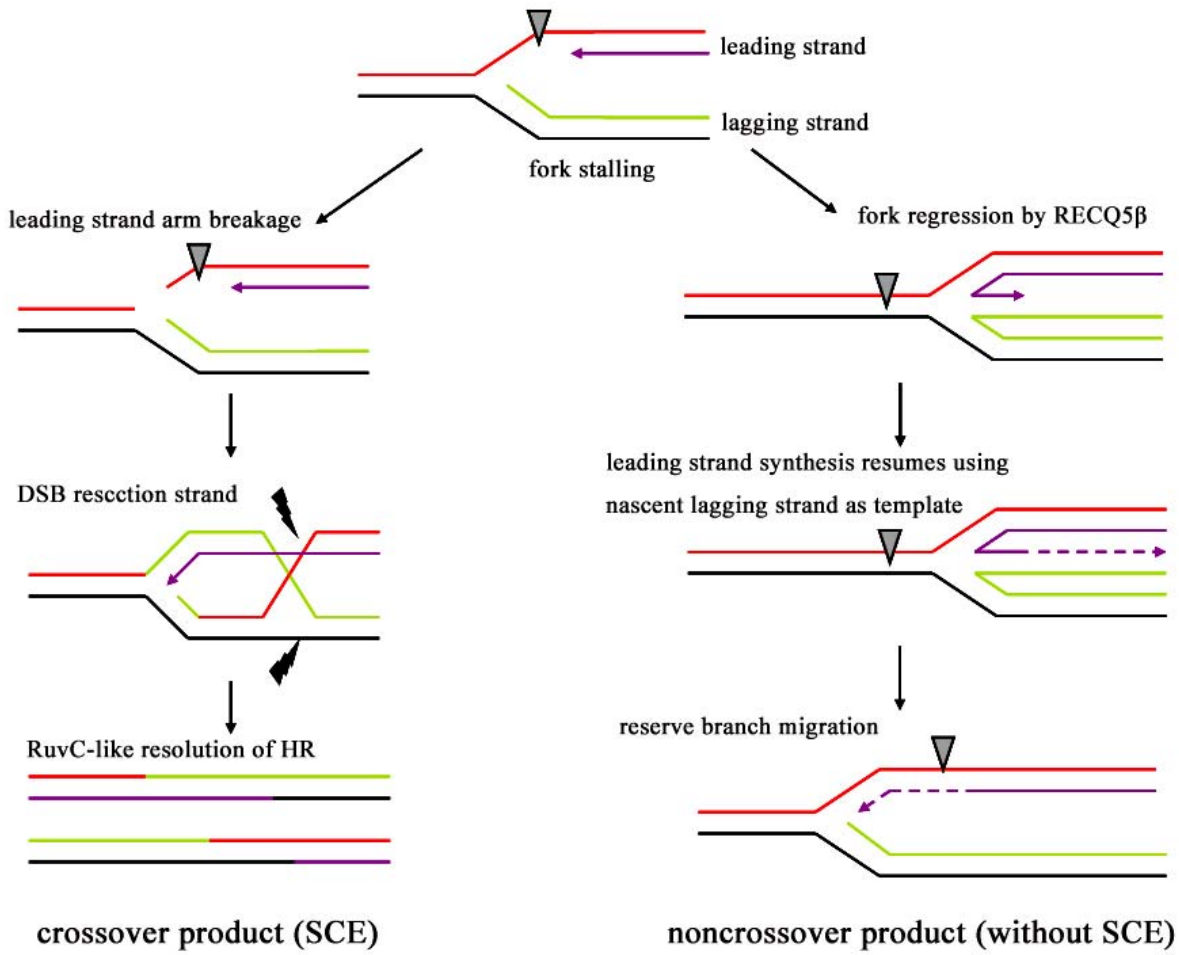

Fig. 14 A mechanism presumably of RECQ5β in suppressing on overcorss

During DNA replication, when a DNA lesion on the leading strand causes replication fork stalling, RECQ5β promotes regression of stalled replication forks, which allows template switching to the undamaged chromatid. This prevents fork breakage and subsequent recombinational repair of DSBs that can result in SCEs.

RECQ5 and SCEs

It is known that cells from Bloom syndrome exhibit a high frequency of sister chromatid exchanges (SCEs). In contrast, cells from Werner and Rothmund-Thomson syndrome patients do not exhibit the SCEs phenotype. Wang and colleagues deleted the chicken RECQ5 homologue in DT40 cells. The authors found that no effect of *RECQ*5 deletion on the frequency of SCEs (245). However, the *RECQ*5 deletion on the $BLM^{-/-}$ background can increase SCEs. This result led the authors conclude that *RECQ*5 suppresses SCEs but only under *BLM* function-impaired conditions. Recently, a significant increase of SCEs has been found initiated by only inactivation of the *Recq5* genes in mouse embryonic stem cells (ES cells) and cells from *Drosophia* (240;246) (Fig. 13). Moreover, mutant of both *Blm* and *RecQ5β* in mouse ES cells will show much higher levels of SCEs than mutating either one of these two genes alone. This indicates that RECQ5β may serve as a partner for BLM to regulate DNA homologous recombination which is an essential step in replications intermediate processing (246). Radhakrishnan supposed that RECQ5β may suppress crossover products of HR mediated repair of broken replication forks. RECQ5β binds to the fork junction and subsequently translocates along the lagging-strand template to unwind the lagging-strand duplex (Fig. 14). Crossover and SCEs resulting from repair events can lead to DNA rearrangements and increase the risk of developing cancer. So it is shown that the potential roles of RECQ5 in maintaining of genomic stability and reducing the probability of cancer.

4. Propose

The aim of our research is to understand, at molecular level, the mechanisms of action of RecQ family helicases, especially, human RecQ family helicases, with special emphasis on the structural elements implicated in enzymatic regulation.

4.1 The enzymatic regulation role of zinc finger motif in RecQ family helicase

Our laboratory has previously identified a zinc finger motif which plays an essential role in protein folding and DNA binding (54;114). In order to further study its role in human RecQ family helicase, we analyzed the human RecQ5 helicase. In this study, we take the

advantage that RECQ5 exists in three different isoforms, namely RECQ5α, RECQ5β and RECQ5γ, which result from alternative splicing of the RECQ5 transcript. RECQ5α is the shortest variant including only the helicase domain (410 amino acids). RECQ5β contains the helicase domain and a putative RecQ-Ct domain, which is followed by a long C-terminal region that shows no homology with the other RecQ helicases. RECQ5γ includes the helicase domain followed by a C-terminal extension of 25 amino acids that is not present in RECQ5β.

The RECQ5α and RECQ5β proteins offer attractive model systems to characterize the enzymatic activities of a RecQ helicase domain in isolation and in association with other sub-domains on the same polypeptide. This unique property allows us to address some interesting and important questions that have not yet been resolved with any DNA helicase, especially, the regulation effect between the zinc finger motif and helicase core domain in RecQ family helicase.

4.2 The functional aspects of HRDC domain in RecQ helicase family

As we have discussed above, most unicellular organisms have only one RecQ family gene. However, we found that *bacillus subtilis* possesses two potential RecQ helicases, identified by BLAST analysis. In addition, the great differences between the two proteins are that one potential RecQ helicase is shorter in the C-terminal region motif although the both proteins display very high sequence homology with *E. coli* RecQ helicase in helicase core domain. We therefore analyzed the two helicases of *Bacillus subtilis*, with emphasis on the roles of zinc finger motif and HRDC domain in helicase activity. Moreover, the conserved cysteine residues that constitute the zinc finger motif are different from their sites locating in the amino acid sequence between these two helicases in *bacillus subtilis*.

4.3 The special structural feature of arginine finger in RecQ family helicase

It is well documented that deficiency of RecQ helicases in human lead to autosomal recessive genetic diseases. The clinical observations demonstrated that only homozygote displays disease phenotypes while the heterozygote appears healthy. Moreover, the biochemical and biophysical studies revealed that both purified BLM and WRN proteins are hexamers or oligomers in solution. If the BLM functions as a hexamer in cell, the

possibility that BLM protein to be assembled into active hexamer in heterozygote is as low as 7-8%. This is in contradictory with the fact that the heterozygote does not display disease phenotype. A previous study indicated that oligomeric WRN protein dissociate into monomer during catalysis. This leads us to investigate if BLM could function as a monomer. Towards this end, we analyzed the structural feature of an essential arginine residue, which is implicated in ATP binding and hydrolysis. More importantly, this residue, named "arginine finger" is usually localized in the interface of subunits of oligomeric helicases. Therefore, the isolated monomer from such hexamer could not hydrolyse ATP and is inactive. We found that the arginine finger of BLM is localized between the two domains of one monomer, not the interface between the subunits of molecule. This special feature of the arginine finger provides a structural proof that RecQ family helicase could function as a monomer.

REFERENCES

1. WATSON,J.D. and CRICK,F.H. (1953) Genetical implications of the structure of deoxyribonucleic acid. *Nature*, **171**, 964-967.

2. bdel-Monem,M., Durwald,H. and Hoffmann-Berling,H. (1976) Enzymic unwinding of DNA. 2. Chain separation by an ATP-dependent DNA unwinding enzyme. *Eur. J. Biochem.*, **65**, 441-449.

3. bdel-Monem,M. and Hoffmann-Berling,H. (1976) Enzymic unwinding of DNA. 1. Purification and characterization of a DNA-dependent ATPase from Escherichia coli. *Eur. J. Biochem.*, **65**, 431-440.

4. Barhoumi,M., Tanner,N.K., Banroques,J., Linder,P. and Guizani,I. (2006) Leishmania infantum LeIF protein is an ATP-dependent RNA helicase and an eIF4A-like factor that inhibits translation in yeast. *FEBS J.*, **273**, 5086-5100.

5. Luking,A., Stahl,U. and Schmidt,U. (1998) The protein family of RNA helicases. *Crit Rev. Biochem. Mol. Biol.*, **33**, 259-296.

6. Singleton,M.R., Dillingham,M.S. and Wigley,D.B. (2006) Structures and Mechanism of Helicases and Nucleic Acid. *Annu. Rev. Biochem*.

7. Korolev,S., Hsieh,J., Gauss,G.H., Lohman,T.M. and Waksman,G. (1997) Major domain swiveling revealed by the crystal structures of complexes of E. coli Rep helicase bound to single-stranded DNA and ADP. *Cell*, **90**, 635-647.

8. Cheng,W., Hsieh,J., Brendza,K.M. and Lohman,T.M. (2001) E. coli Rep oligomers are required to initiate DNA unwinding in vitro. *J. Mol. Biol.*, **310**, 327-350.

9. Velankar,S.S., Soultanas,P., Dillingham,M.S., Subramanya,H.S. and Wigley,D.B. (1999) Crystal structures of complexes of PcrA DNA helicase with a DNA substrate indicate an inchworm mechanism. *Cell*, **97**, 75-84.

10. Cheng,W., Hsieh,J., Brendza,K.M. and Lohman,T.M. (2001) E. coli Rep oligomers are required to initiate DNA unwinding in vitro. *J. Mol. Biol.*, **310**, 327-350.

11. Hickson,I.D., Arthur,H.M., Bramhill,D. and Emmerson,P.T. (1983) The E. coli uvrD gene product is DNA helicase II. *Mol. Gen. Genet.*, **190**, 265-270.

12. Lovett,S.T., Luisi-DeLuca,C. and Kolodner,R.D. (1988) The genetic dependence of recombination in recD mutants of Escherichia coli. *Genetics*, **120**, 37-45.

13. Umezu,K., Nakayama,K. and Nakayama,H. (1990) Escherichia coli RecQ protein is a DNA helicase. *Proc. Natl. Acad. Sci. U. S. A*, **87**, 5363-5367.

14. Zhang,X.D., Dou,S.X., Xie,P., Hu,J.S., Wang,P.Y. and Xi,X.G. (2006) Escherichia coli RecQ is a rapid, efficient, and monomeric helicase. *J. Biol. Chem.*, **281**, 12655-12663.

15. Tai,C.L., Chi,W.K., Chen,D.S. and Hwang,L.H. (1996) The helicase activity associated with hepatitis C virus nonstructural protein 3 (NS3). *J. Virol.*, **70**, 8477-8484.

16. Wiekowski,M., Schwarz,M.W. and Stahl,H. (1988) Simian virus 40 large T antigen DNA helicase. Characterization of the ATPase-dependent DNA unwinding activity and its substrate requirements. *J. Biol. Chem.*, **263**, 436-442.

17. LeBowitz,J.H. and McMacken,R. (1986) The Escherichia coli dnaB replication protein is a DNA helicase. *J. Biol. Chem.*, **261**, 4738-4748.

18. Brennan,C.A., Dombroski,A.J. and Platt,T. (1987) Transcription termination factor rho is an RNA-DNA helicase. *Cell*, **48**, 945-952.

19. renas-Licea,J., van Gool,A.J., Keeley,A.J., Davies,A., West,S.C. and Tsaneva,I.R. (2000) Functional interactions of Mycobacterium leprae RuvA with Escherichia coli RuvB and RuvC on holliday junctions. *J. Mol. Biol.*, **301**, 839-850.

20. Gorbalenya,A.E., Koonin,E.V. and Wolf,Y.I. (1990) A new superfamily of putative NTP-binding domains encoded by genomes of small DNA and RNA viruses. *FEBS Lett.*, **262**, 145-148.

21. Subramanya,H.S., Bird,L.E., Brannigan,J.A. and Wigley,D.B. (1996) Crystal structure of a DExx box DNA helicase. *Nature*, **384**, 379-383.

22. Zhang,D.H., Zhou,B., Huang,Y., Xu,L.X. and Zhou,J.Q. (2006) The human Pif1 helicase, a potential Escherichia coli RecD homologue, inhibits telomerase activity. *Nucleic Acids Res.*, **34**, 1393-1404.

23. Schmidt,K.H., Derry,K.L. and Kolodner,R.D. (2002) Saccharomyces cerevisiae RRM3, a 5' to 3' DNA helicase, physically interacts with proliferating cell nuclear antigen. *J. Biol. Chem.*, **277**, 45331-45337.

24. Saikrishnan,K., Griffiths,S.P., Cook,N., Court,R. and Wigley,D.B. (2008) DNA binding to RecD: role of the 1B domain in SF1B helicase activity. *EMBO J.*, **27**, 2222-2229.

25. Korolev,S., Yao,N., Lohman,T.M., Weber,P.C. and Waksman,G. (1998) Comparisons between the structures of HCV and Rep helicases reveal structural similarities between SF1 and SF2 super-families of helicases. *Protein Sci.*, **7**, 605-610.

26. Bachrati,C.Z. and Hickson,I.D. (2003) RecQ helicases: suppressors of tumorigenesis and premature aging. *Biochem. J.*, **374**, 577-606.

27. Gorbalenya,A.E., Koonin,E.V., Donchenko,A.P. and Blinov,V.M. (1989) Two related superfamilies of putative helicases involved in replication, recombination, repair and expression of DNA and RNA genomes. *Nucleic Acids Res.*, **17**, 4713-4730.

28. Yao,N., Hesson,T., Cable,M., Hong,Z., Kwong,A.D., Le,H.V. and Weber,P.C. (1997) Structure of the hepatitis C virus RNA helicase domain. *Nat. Struct. Biol.*, **4**, 463-467.

29. Bernstein,D.A., Zittel,M.C. and Keck,J.L. (2003) High-resolution structure of the E.coli RecQ helicase catalytic core. *EMBO J.*, **22**, 4910-4921.

30. Frick,D.N. (2007) The hepatitis C virus NS3 protein: a model RNA helicase and potential drug target. *Curr. Issues Mol. Biol.*, **9**, 1-20.

31. Kim,J.L., Morgenstern,K.A., Griffith,J.P., Dwyer,M.D., Thomson,J.A., Murcko,M.A., Lin,C. and Caron,P.R. (1998) Hepatitis C virus NS3 RNA helicase domain with a bound oligonucleotide: the crystal structure provides insights into the mode of unwinding. *Structure.*, **6**, 89-100.

32. Frick,D.N. (2007) The hepatitis C virus NS3 protein: a model RNA helicase and potential drug target. *Curr. Issues Mol. Biol.*, **9**, 1-20.

33. Tuteja,N. and Tuteja,R. (2004) Unraveling DNA helicases. Motif, structure, mechanism and function. *Eur. J. Biochem.*, **271**, 1849-1863.

34. Hickman,A.B. and Dyda,F. (2005) Binding and unwinding: SF3 viral helicases. *Curr. Opin. Struct. Biol.*, **15**, 77-85.

35. Hanson,P.I. and Whiteheart,S.W. (2005) AAA+ proteins: have engine, will work. *Nat. Rev. Mol. Cell Biol.*, **6**, 519-529.

36. Rangasamy,D., Woytek,K., Khan,S.A. and Wilson,V.G. (2000) SUMO-1 modification of bovine papillomavirus E1 protein is required for intranuclear accumulation. *J. Biol. Chem.*, **275**, 37999-38004.

37. James,J.A., Escalante,C.R., Yoon-Robarts,M., Edwards,T.A., Linden,R.M. and Aggarwal,A.K. (2003) Crystal structure of the SF3 helicase from adeno-associated virus type 2. *Structure.*, **11**, 1025-1035.

38. Titolo,S., Brault,K., Majewski,J., White,P.W. and Archambault,J. (2003) Characterization of the minimal DNA binding domain of the human papillomavirus e1 helicase: fluorescence anisotropy studies and characterization of a dimerization-defective mutant protein. *J. Virol.*, **77**, 5178-5191.

39. Bailey,S., Eliason,W.K. and Steitz,T.A. (2007) The crystal structure of the Thermus aquaticus DnaB helicase monomer. *Nucleic Acids Res.*, **35**, 4728-4736.

40. Ilyina,T.V., Gorbalenya,A.E. and Koonin,E.V. (1992) Organization and evolution of bacterial and bacteriophage primase-helicase systems. *J. Mol. Evol.*, **34**, 351-357.

41. Gogol,E.P., Seifried,S.E. and von Hippel,P.H. (1991) Structure and assembly of the Escherichia coli transcription termination factor rho and its interaction with RNA. I. Cryoelectron microscopic studies. *J. Mol. Biol.*, **221**, 1127-1138.

42. Richardson,J.P. (2003) Loading Rho to terminate transcription. *Cell*, **114**, 157-159.

43. Canals,A. and Coll,M. (2009) Cloning, expression, purification and crystallization of the Rho transcription termination factor from Thermotoga maritima. *Protein Expr. Purif.*.

44. Skordalakes,E. and Berger,J.M. (2003) Structure of the Rho transcription terminator: mechanism of mRNA recognition and helicase loading. *Cell*, **114**, 135-146.

45. Skordalakes,E. and Berger,J.M. (2006) Structural insights into RNA-dependent ring closure and ATPase activation by the Rho termination factor. *Cell*, **127**, 553-564.

46. Erzberger,J.P. and Berger,J.M. (2006) Evolutionary relationships and structural mechanisms of AAA+ proteins. *Annu. Rev. Biophys. Biomol. Struct.*, **35**, 93-114.

47. West,S.C. (1996) The RuvABC proteins and Holliday junction processing in Escherichia coli. *J. Bacteriol.*, **178**, 1237-1241.

48. Labib,K., Tercero,J.A. and Diffley,J.F. (2000) Uninterrupted MCM2-7 function required for DNA replication fork progression. *Science*, **288**, 1643-1647.

49. Matson,S.W., Bean,D.W. and George,J.W. (1994) DNA helicases: enzymes with essential roles in all aspects of DNA metabolism. *Bioessays*, **16**, 13-22.

50. Tuteja,N. and Tuteja,R. (2004) Prokaryotic and eukaryotic DNA helicases. Essential molecular motor proteins for cellular machinery. *Eur. J. Biochem.*, **271**, 1835-1848.

51. Roychowdhury,A., Szymanski,M.R., Jezewska,M.J. and Bujalowski,W. (2009) Mechanism of NTP Hydrolysis by the Escherichia coli Primary Replicative Helicase DnaB Protein. II. Nucleotide and Nucleic Acid Specificities. *Biochemistry*.

52. Ren,H., Dou,S.X., Rigolet,P., Yang,Y., Wang,P.Y., mor-Gueret,M. and Xi,X.G. (2007) The arginine finger of the Bloom syndrome protein: its structural organization and its role in energy coupling. *Nucleic Acids Res.*, **35**, 6029-6041.

53. Alberts,I.L., Nadassy,K. and Wodak,S.J. (1998) Analysis of zinc binding sites in protein crystal structures. *Protein Sci.*, **7**, 1700-1716.

54. Guo,R.B., Rigolet,P., Zargarian,L., Fermandjian,S. and Xi,X.G. (2005) Structural and functional characterizations reveal the importance of a zinc binding domain in Bloom's syndrome helicase. *Nucleic Acids Res.*, **33**, 3109-3124.

55. Karow,A.R. and Klostermeier,D. (2009) A conformational change in the helicase core is necessary but not sufficient for RNA unwinding by the DEAD box helicase YxiN. *Nucleic Acids Res.*.

56. Korolev,S., Hsieh,J., Gauss,G.H., Lohman,T.M. and Waksman,G. (1997) Major domain swiveling revealed by the crystal structures of complexes of E. coli Rep helicase bound to single-stranded DNA and ADP. *Cell*, **90**, 635-647.

57. Dillingham,M.S., Spies,M. and Kowalczykowski,S.C. (2003) RecBCD enzyme is a bipolar DNA helicase. *Nature*, **423**, 893-897.

58. Naqvi,A., Tinsley,E. and Khan,S.A. (2003) Purification and characterization of the PcrA helicase of Bacillus anthracis. *J. Bacteriol.*, **185**, 6633-6639.

59. Constantinesco,F., Forterre,P., Koonin,E.V., Aravind,L. and Elie,C. (2004) A bipolar DNA helicase gene, herA, clusters with rad50, mre11 and nurA genes in thermophilic archaea. *Nucleic Acids Res.*, **32**, 1439-1447.

60. Bianco,P.R., Brewer,L.R., Corzett,M., Balhorn,R., Yeh,Y., Kowalczykowski,S.C. and Baskin,R.J. (2001) Processive translocation and DNA unwinding by individual RecBCD enzyme molecules. *Nature*, **409**, 374-378.

61. Waksman,G., Lanka,E. and Carazo,J.M. (2000) Helicases as nucleic acid unwinding machines. *Nat. Struct. Biol.*, **7**, 20-22.

62. Yarranton,G.T. and Gefter,M.L. (1979) Enzyme-catalyzed DNA unwinding: studies on Escherichia coli rep protein. *Proc. Natl. Acad. Sci. U. S. A*, **76**, 1658-1662.

63. Karow,J.K., Newman,R.H., Freemont,P.S. and Hickson,I.D. (1999) Oligomeric ring structure of the Bloom's syndrome helicase. *Curr. Biol.*, **9**, 597-600.

64. Johnson,D.S., Bai,L., Smith,B.Y., Patel,S.S. and Wang,M.D. (2007) Single-molecule studies reveal dynamics of DNA unwinding by the ring-shaped T7 helicase. *Cell*, **129**, 1299-1309.

65. Walmacq,C., Rahmouni,A.R. and Boudvillain,M. (2006) Testing the steric exclusion model for hexameric helicases: substrate features that alter RNA-DNA unwinding by the transcription termination factor Rho. *Biochemistry*, **45**, 5885-5895.

66. Enemark,E.J. and Joshua-Tor,L. (2008) On helicases and other motor proteins. *Curr. Opin. Struct. Biol.*, **18**, 243-257.

67. Patel,S.S. and Picha,K.M. (2000) Structure and function of hexameric helicases. *Annu. Rev. Biochem.*, **69**, 651-697.

68. Ren,H., Dou,S.X., Zhang,X.D., Wang,P.Y., Kanagaraj,R., Liu,J.L., Janscak,P., Hu,J.S. and Xi,X.G. (2008) The zinc-binding motif of human RECQ5beta suppresses the intrinsic strand-annealing activity of its DExH helicase domain and is essential for the helicase activity of the enzyme. *Biochem. J.*, **412**, 425-433.

69. Macris,M.A., Krejci,L., Bussen,W., Shimamoto,A. and Sung,P. (2006) Biochemical characterization of the RECQ4 protein, mutated in Rothmund-Thomson syndrome. *DNA Repair (Amst)*, **5**, 172-180.

70. Cheok,C.F., Wu,L., Garcia,P.L., Janscak,P. and Hickson,I.D. (2005) The Bloom's syndrome helicase promotes the annealing of complementary single-stranded DNA. *Nucleic Acids Res.*, **33**, 3932-3941.

71. Brosh,R.M., Jr., Opresko,P.L. and Bohr,V.A. (2006) Enzymatic mechanism of the WRN helicase/nuclease. *Methods Enzymol.*, **409**, 52-85.

72. Masuda-Sasa,T., Polaczek,P. and Campbell,J.L. (2006) Single strand annealing and ATP-independent strand exchange activities of yeast and human DNA2: possible role in Okazaki fragment maturation. *J. Biol. Chem.*, **281**, 38555-38564.

73. Bartos,J.D., Wang,W., Pike,J.E. and Bambara,R.A. (2006) Mechanisms by which Bloom protein can disrupt recombination intermediates of Okazaki fragment maturation. *J. Biol. Chem.*, **281**, 32227-32239.

74. Muller,U.F., Lambert,L. and Goringer,H.U. (2001) Annealing of RNA editing substrates facilitated by guide RNA-binding protein gBP21. *EMBO J.*, **20**, 1394-1404.

75. Chamot,D., Colvin,K.R., Kujat-Choy,S.L. and Owttrim,G.W. (2005) RNA structural rearrangement via unwinding and annealing by the cyanobacterial RNA helicase, CrhR. *J. Biol. Chem.*, **280**, 2036-2044.

76. Valdez,B.C., Henning,D., Perlaky,L., Busch,R.K. and Busch,H. (1997) Cloning and characterization of Gu/RH-II binding protein. *Biochem. Biophys. Res. Commun.*, **234**, 335-340.

77. Chamot,D., Colvin,K.R., Kujat-Choy,S.L. and Owttrim,G.W. (2005) RNA structural rearrangement via unwinding and annealing by the cyanobacterial RNA helicase, CrhR. *J. Biol. Chem.*, **280**, 2036-2044.

78. Machwe,A., Lozada,E.M., Xiao,L. and Orren,D.K. (2006) Competition between the DNA unwinding and strand pairing activities of the Werner and Bloom syndrome proteins. *BMC. Mol. Biol.*, **7**, 1.

79. Muller,U.F., Lambert,L. and Goringer,H.U. (2001) Annealing of RNA editing substrates facilitated by guide RNA-binding protein gBP21. *EMBO J.*, **20**, 1394-1404.

80. Machwe,A., Lozada,E.M., Xiao,L. and Orren,D.K. (2006) Competition between the DNA unwinding and strand pairing activities of the Werner and Bloom syndrome proteins. *BMC. Mol. Biol.*, **7**, 1.

81. Chamot,D., Colvin,K.R., Kujat-Choy,S.L. and Owttrim,G.W. (2005) RNA structural rearrangement via unwinding and annealing by the cyanobacterial RNA helicase, CrhR. *J. Biol. Chem.*, **280**, 2036-2044.

82. Muftuoglu,M., Kulikowicz,T., Beck,G., Lee,J.W., Piotrowski,J. and Bohr,V.A. (2008) Intrinsic ssDNA annealing activity in the C-terminal region of WRN. *Biochemistry*, **47**, 10247-10254.

83. Muftuoglu,M., Kulikowicz,T., Beck,G., Lee,J.W., Piotrowski,J. and Bohr,V.A. (2008) Intrinsic ssDNA annealing activity in the C-terminal region of WRN. *Biochemistry*, **47**, 10247-10254.

84. Cheok,C.F., Wu,L., Garcia,P.L., Janscak,P. and Hickson,I.D. (2005) The Bloom's syndrome helicase promotes the annealing of complementary single-stranded DNA. *Nucleic Acids Res.*, **33**, 3932-3941.

85. Hickson,I.D. (2003) RecQ helicases: caretakers of the genome. *Nat. Rev. Cancer*, **3**, 169-178.

86. Coin,F., Bergmann,E., Tremeau-Bravard,A. and Egly,J.M. (1999) Mutations in XPB and XPD helicases found in xeroderma pigmentosum patients impair the transcription function of TFIIH. *EMBO J.*, **18**, 1357-1366.

87. Bohr,V.A. (2008) Rising from the RecQ-age: the role of human RecQ helicases in genome maintenance. *Trends Biochem. Sci.*, **33**, 609-620.

88. Bohr,V.A. (2008) Rising from the RecQ-age: the role of human RecQ helicases in genome maintenance. *Trends Biochem. Sci.*, **33**, 609-620.

89. Harrigan,J.A., Fan,J., Momand,J., Perrino,F.W., Bohr,V.A. and Wilson,D.M., III (2007) WRN exonuclease activity is blocked by DNA termini harboring 3' obstructive groups. *Mech. Ageing Dev.*, **128**, 259-266.

90. Linder,P. and Stutz,F. (2001) mRNA export: travelling with DEAD box proteins. *Curr. Biol.*, **11**, R961-R963.

91. Linder,P. and Daugeron,M.C. (2000) Are DEAD-box proteins becoming respectable helicases? *Nat. Struct. Biol.*, **7**, 97-99.

92. Linder,P. and Lasko,P. (2006) Bent out of shape: RNA unwinding by the DEAD-box helicase Vasa. *Cell*, **125**, 219-221.

93. Sengoku,T., Nureki,O., Nakamura,A., Kobayashi,S. and Yokoyama,S. (2006) Structural Basis for RNA Unwinding by the DEAD-Box Protein Drosophila Vasa. *Cell*, **125**, 287-300.

94. Yamada,K., Hirota,K., Mizuno,K., Shibata,T. and Ohta,K. (2008) Essential roles of Snf21, a Swi2/Snf2 family chromatin remodeler, in fission yeast mitosis. *Genes Genet. Syst.*, **83**, 361-372.

95. Ariumi,Y., Kuroki,M., Abe,K., Dansako,H., Ikeda,M., Wakita,T. and Kato,N. (2007) DDX3 DEAD-box RNA helicase is required for hepatitis C virus RNA replication. *J. Virol.*, **81**, 13922-13926.

96. Franca,R., Belfiore,A., Spadari,S. and Maga,G. (2007) Human DEAD-box ATPase DDX3 shows a relaxed nucleoside substrate specificity. *Proteins*, **67**, 1128-1137.

97. German,J., Schonberg,S., Louie,E. and Chaganti,R.S. (1977) Bloom's syndrome. IV. Sister-chromatid exchanges in lymphocytes. *Am. J. Hum. Genet.*, **29**, 248-255.

98. Goto,M., Miller,R.W., Ishikawa,Y. and Sugano,H. (1996) Excess of rare cancers in Werner syndrome (adult progeria). *Cancer Epidemiol. Biomarkers Prev.*, **5**, 239-246.

99. Macris,M.A., Krejci,L., Bussen,W., Shimamoto,A. and Sung,P. (2005) Biochemical characterization of the RECQ4 protein, mutated in Rothmund-Thomson syndrome. *DNA Repair (Amst)*.

100. Liu,J.L., Rigolet,P., Dou,S.X., Wang,P.Y. and Xi,X.G. (2004) The zinc finger motif of Escherichia coli RecQ is implicated in both DNA binding and protein folding. *J. Biol. Chem.*, **279**, 42794-42802.

101. Kitano,K., Yoshihara,N. and Hakoshima,T. (2007) Crystal structure of the HRDC domain of human Werner syndrome protein, WRN. *J. Biol. Chem.*, **282**, 2717-2728.

102. Liu,Z., Macias,M.J., Bottomley,M.J., Stier,G., Linge,J.P., Nilges,M., Bork,P. and Sattler,M. (1999) The three-dimensional structure of the HRDC domain and implications for the Werner and Bloom syndrome proteins. *Structure.*, **7**, 1557-1566.

103. Xu,X. and Liu,Y. (2009) Dual DNA unwinding activities of the Rothmund-Thomson syndrome protein, RECQ4. *EMBO J.*, **28**, 568-577.

104. Opresko,P.L., Cheng,W.H. and Bohr,V.A. (2004) Junction of RecQ helicase biochemistry and human disease. *J. Biol. Chem.*, **279**, 18099-18102.

105. Cheok,C.F., Bachrati,C.Z., Chan,K.L., Ralf,C., Wu,L. and Hickson,I.D. (2005) Roles of the Bloom's syndrome helicase in the maintenance of genome stability. *Biochem. Soc. Trans.*, **33**, 1456-1459.

106. Popuri,V., Bachrati,C.Z., Muzzolini,L., Mosedale,G., Costantini,S., Giacomini,E., Hickson,I.D. and Vindigni,A. (2008) The Human RecQ helicases, BLM and RECQ1, display distinct DNA substrate specificities. *J. Biol. Chem.*, **283**, 17766-17776.

107. Ozsoy,A.Z., Ragonese,H.M. and Matson,S.W. (2003) Analysis of helicase activity and substrate specificity of Drosophila RECQ5. *Nucleic Acids Res.*, **31**, 1554-1564.

108. Courcelle,J., Donaldson,J.R., Chow,K.H. and Courcelle,C.T. (2003) DNA damage-induced replication fork regression and processing in Escherichia coli. *Science*, **299**, 1064-1067.

109. Hishida,T., Han,Y.W., Shibata,T., Kubota,Y., Ishino,Y., Iwasaki,H. and Shinagawa,H. (2004) Role of the Escherichia coli RecQ DNA helicase in SOS signaling and genome stabilization at stalled replication forks. *Genes Dev.*, **18**, 1886-1897.

110. Hishida,T., Han,Y.W., Shibata,T., Kubota,Y., Ishino,Y., Iwasaki,H. and Shinagawa,H. (2004) Role of the Escherichia coli RecQ DNA helicase in SOS signaling and genome stabilization at stalled replication forks. *Genes Dev.*, **18**, 1886-1897.

111. Xu,H.Q., Deprez,E., Zhang,A.H., Tauc,P., Ladjimi,M.M., Brochon,J.C., Auclair,C. and Xi,X.G. (2003) The Escherichia coli RecQ helicase functions as a monomer. *J. Biol. Chem.*, **278**, 34925-34933.

112. Bernstein,D.A., Zittel,M.C. and Keck,J.L. (2003) High-resolution structure of the E.coli RecQ helicase catalytic core. *EMBO J.*, **22**, 4910-4921.

113. Dou,S.X., Wang,P.Y., Xu,H.Q. and Xi,X.G. (2004) The DNA binding properties of the Escherichia coli RecQ helicase. *J. Biol. Chem.*, **279**, 6354-6363.

114. Liu,J.L., Rigolet,P., Dou,S.X., Wang,P.Y. and Xi,X.G. (2004) The zinc finger motif of Escherichia coli RecQ is implicated in both DNA binding and protein folding. *J. Biol. Chem.*, **279**, 42794-42802.

115. Heyer,W.D. (2004) Damage signaling: RecQ sends an SOS to you. *Curr. Biol.*, **14**, R895-R897.

116. Harmon,F.G. and Kowalczykowski,S.C. (1998) RecQ helicase, in concert with RecA and SSB proteins, initiates and disrupts DNA recombination. *Genes Dev.*, **12**, 1134-1144.

117. Harmon,F.G., DiGate,R.J. and Kowalczykowski,S.C. (1999) RecQ helicase and topoisomerase III comprise a novel DNA strand passage function: a conserved mechanism for control of DNA recombination. *Mol. Cell*, **3**, 611-620.

118. Hishida,T., Han,Y.W., Shibata,T., Kubota,Y., Ishino,Y., Iwasaki,H. and Shinagawa,H. (2004) Role of the Escherichia coli RecQ DNA helicase in SOS signaling and genome stabilization at stalled replication forks. *Genes Dev.*, **18**, 1886-1897.

119. Courcelle,J., Donaldson,J.R., Chow,K.H. and Courcelle,C.T. (2003) DNA damage-induced replication fork regression and processing in Escherichia coli. *Science*, **299**, 1064-1067.

120. Fernandez,S., Sorokin,A. and Alonso,J.C. (1998) Genetic recombination in Bacillus subtilis 168: effects of recU and recS mutations on DNA repair and homologous recombination. *J. Bacteriol.*, **180**, 3405-3409.

121. Frenkiel-Krispin,D. and Minsky,A. (2006) Nucleoid organization and the maintenance of DNA integrity in E. coli, B. subtilis and D. radiodurans. *J. Struct. Biol.*, **156**, 311-319.

122. Kumar,G.A., Woodhall,M.R., Hood,D.W., Moxon,E.R. and Bayliss,C.D. (2008) RecJ, ExoI and RecG are required for genome maintenance but not for generation of genetic diversity by repeat-mediated phase variation in Haemophilus influenzae. *Mutat. Res.*, **640**, 46-53.

123. Gangloff,S., McDonald,J.P., Bendixen,C., Arthur,L. and Rothstein,R. (1994) The yeast type I topoisomerase Top3 interacts with Sgs1, a DNA helicase homolog: a potential eukaryotic reverse gyrase. *Mol. Cell Biol.*, **14**, 8391-8398.

124. Sinclair,D.A., Mills,K. and Guarente,L. (1997) Accelerated aging and nucleolar fragmentation in yeast sgs1 mutants. *Science*, **277**, 1313-1316.

125. McVey,M., Kaeberlein,M., Tissenbaum,H.A. and Guarente,L. (2001) The short life span of Saccharomyces cerevisiae sgs1 and srs2 mutants is a composite of normal aging processes and mitotic arrest due to defective recombination. *Genetics*, **157**, 1531-1542.

126. Watt,P.M., Hickson,I.D., Borts,R.H. and Louis,E.J. (1996) SGS1, a homologue of the Bloom's and Werner's syndrome genes, is required for maintenance of genome stability in Saccharomyces cerevisiae. *Genetics*, **144**, 935-945.

127. Miyajima,A., Seki,M., Onoda,F., Shiratori,M., Odagiri,N., Ohta,K., Kikuchi,Y., Ohno,Y. and Enomoto,T. (2000) Sgs1 helicase activity is required for mitotic but apparently not for meiotic functions. *Mol. Cell Biol.*, **20**, 6399-6409.

128. Gangloff,S., Soustelle,C. and Fabre,F. (2000) Homologous recombination is responsible for cell death in the absence of the Sgs1 and Srs2 helicases. *Nat. Genet.*, **25**, 192-194.

129. Frei,C. and Gasser,S.M. (2000) The yeast Sgs1p helicase acts upstream of Rad53p in the DNA replication checkpoint and colocalizes with Rad53p in S-phase-specific foci. *Genes Dev.*, **14**, 81-96.

130. Watt,P.M., Hickson,I.D., Borts,R.H. and Louis,E.J. (1996) SGS1, a homologue of the Bloom's and Werner's syndrome genes, is required for maintenance of genome stability in Saccharomyces cerevisiae. *Genetics*, **144**, 935-945.

131. Onoda,F., Seki,M., Miyajima,A. and Enomoto,T. (2000) Elevation of sister chromatid exchange in Saccharomyces cerevisiae sgs1 disruptants and the relevance of the disruptants as a system to evaluate mutations in Bloom's syndrome gene. *Mutat. Res.*, **459**, 203-209.

132. Myung,K., Datta,A., Chen,C. and Kolodner,R.D. (2001) SGS1, the Saccharomyces cerevisiae homologue of BLM and WRN, suppresses genome instability and homeologous recombination. *Nat. Genet.*, **27**, 113-116.

133. Ajima,J., Umezu,K. and Maki,H. (2002) Elevated incidence of loss of heterozygosity (LOH) in an sgs1 mutant of Saccharomyces cerevisiae: roles of yeast RecQ helicase in suppression of aneuploidy, interchromosomal rearrangement, and the simultaneous incidence of both events during mitotic growth. *Mutat. Res.*, **504**, 157-172.

134. Yamagata,K., Kato,J., Shimamoto,A., Goto,M., Furuichi,Y. and Ikeda,H. (1998) Bloom's and Werner's syndrome genes suppress hyperrecombination in yeast sgs1 mutant: implication for genomic instability in human diseases. *Proc. Natl. Acad. Sci. U. S. A*, **95**, 8733-8738.

135. Onoda,F., Seki,M., Miyajima,A. and Enomoto,T. (2001) Involvement of SGS1 in DNA damage-induced heteroallelic recombination that requires RAD52 in Saccharomyces cerevisiae. *Mol. Gen. Genet.*, **264**, 702-708.

136. Ira,G., Malkova,A., Liberi,G., Foiani,M. and Haber,J.E. (2003) Srs2 and Sgs1-Top3 suppress crossovers during double-strand break repair in yeast. *Cell*, **115**, 401-411.

137. Wagner,M., Price,G. and Rothstein,R. (2006) The absence of Top3 reveals an interaction between the Sgs1 and Pif1 DNA helicases in Saccharomyces cerevisiae. *Genetics*, **174**, 555-573.

138. Frei,C. and Gasser,S.M. (2000) The yeast Sgs1p helicase acts upstream of Rad53p in the DNA replication checkpoint and colocalizes with Rad53p in S-phase-specific foci. *Genes Dev.*, **14**, 81-96.

139. Watt,P.M., Louis,E.J., Borts,R.H. and Hickson,I.D. (1995) Sgs1: a eukaryotic homolog of E. coli RecQ that interacts with topoisomerase II in vivo and is required for faithful chromosome segregation. *Cell*, **81**, 253-260.

140. Lu,J., Mullen,J.R., Brill,S.J., Kleff,S., Romeo,A.M. and Sternglanz,R. (1996) Human homologues of yeast helicase. *Nature*, **383**, 678-679.

141. Sadoff,B.U., Heath-Pagliuso,S., Castano,I.B., Zhu,Y., Kieff,F.S. and Christman,M.F. (1995) Isolation of mutants of Saccharomyces cerevisiae requiring DNA topoisomerase I. *Genetics*, **141**, 465-479.

142. Uemura,T. and Tanagida,M. (1986) Mitotic spindle pulls but fails to separate chromosomes in type II DNA topoisomerase mutants: uncoordinated mitosis. *EMBO J.*, **5**, 1003-1010.

143. Watt,P.M., Louis,E.J., Borts,R.H. and Hickson,I.D. (1995) Sgs1: a eukaryotic homolog of E. coli RecQ that interacts with topoisomerase II in vivo and is required for faithful chromosome segregation. *Cell*, **81**, 253-260.

144. Kim,R.A. and Wang,J.C. (1992) Identification of the yeast TOP3 gene product as a single strand-specific DNA topoisomerase. *J. Biol. Chem.*, **267**, 17178-17185.

145. Fabre,F., Chan,A., Heyer,W.D. and Gangloff,S. (2002) Alternate pathways involving Sgs1/Top3, Mus81/ Mms4, and Srs2 prevent formation of toxic recombination intermediates from single-stranded gaps created by DNA replication. *Proc. Natl. Acad. Sci. U. S. A*, **99**, 16887-16892.

146. Onodera,R., Seki,M., Ui,A., Satoh,Y., Miyajima,A., Onoda,F. and Enomoto,T. (2002) Functional and physical interaction between Sgs1 and Top3 and Sgs1-independent function of Top3 in DNA recombination repair. *Genes Genet. Syst.*, **77**, 11-21.

147. Seki,T., Seki,M., Onodera,R., Katada,T. and Enomoto,T. (1998) Cloning of cDNA encoding a novel mouse DNA topoisomerase III (Topo IIIbeta) possessing negatively supercoiled DNA relaxing activity, whose message is highly expressed in the testis. *J. Biol. Chem.*, **273**, 28553-28556.

148. Liberi,G., Maffioletti,G., Lucca,C., Chiolo,I., Baryshnikova,A., Cotta-Ramusino,C., Lopes,M., Pellicioli,A., Haber,J.E. and Foiani,M. (2005) Rad51-dependent DNA structures accumulate at damaged replication forks in sgs1 mutants defective in the yeast ortholog of BLM RecQ helicase. *Genes Dev.*, **19**, 339-350.

149. Sogo,J.M., Lopes,M. and Foiani,M. (2002) Fork reversal and ssDNA accumulation at stalled replication forks owing to checkpoint defects. *Science*, **297**, 599-602.

150. Win,T.Z., Mankouri,H.W., Hickson,I.D. and Wang,S.W. (2005) A role for the fission yeast Rqh1 helicase in chromosome segregation. *J. Cell Sci.*, **118**, 5777-5784.

151. Hope,J.C., Mense,S.M., Jalakas,M., Mitsumoto,J. and Freyer,G.A. (2006) Rqh1 blocks recombination between sister chromatids during double strand break repair, independent of its helicase activity. *Proc. Natl. Acad. Sci. U. S. A*, **103**, 5875-5880.

152. Cromie,G.A., Hyppa,R.W. and Smith,G.R. (2008) The fission yeast BLM homolog Rqh1 promotes meiotic recombination. *Genetics*, **179**, 1157-1167.

153. Kibe,T., Ono,Y., Sato,K. and Ueno,M. (2007) Fission yeast Taz1 and RPA are synergistically required to prevent rapid telomere loss. *Mol. Biol. Cell*, **18**, 2378-2387.

154. Wilson,S., Warr,N., Taylor,D.L. and Watts,F.Z. (1999) The role of Schizosaccharomyces pombe Rad32, the Mre11 homologue, and other DNA damage response proteins in non-

homologous end joining and telomere length maintenance. *Nucleic Acids Res.*, **27**, 2655-2661.

155. Yin,J., Kwon,Y.T., Varshavsky,A. and Wang,W. (2004) RECQL4, mutated in the Rothmund-Thomson and RAPADILINO syndromes, interacts with ubiquitin ligases UBR1 and UBR2 of the N-end rule pathway. *Hum. Mol. Genet.*, **13**, 2421-2430.

156. Seki,M., Miyazawa,H., Tada,S., Yanagisawa,J., Yamaoka,T., Hoshino,S., Ozawa,K., Eki,T., Nogami,M., Okumura,K. *et al.* (1994) Molecular cloning of cDNA encoding human DNA helicase Q1 which has homology to Escherichia coli Rec Q helicase and localization of the gene at chromosome 12p12. *Nucleic Acids Res.*, **22**, 4566-4573.

157. Puranam,K.L. and Blackshear,P.J. (1994) Cloning and characterization of RECQL, a potential human homologue of the Escherichia coli DNA helicase RecQ. *J. Biol. Chem.*, **269**, 29838-29845.

158. Zhang,A.H. and Xi,X. (2002) Molecular cloning of a splicing variant of human RECQL helicase. *Biochem. Biophys. Res. Commun.*, **298**, 789-792.

159. Sharma,S., Stumpo,D.J., Balajee,A.S., Bock,C.B., Lansdorp,P.M., Brosh,R.M., Jr. and Blackshear,P.J. (2007) RECQL, a member of the RecQ family of DNA helicases, suppresses chromosomal instability. *Mol. Cell Biol.*, **27**, 1784-1794.

160. Sharma,S. and Brosh,R.M., Jr. (2008) Unique and important consequences of RECQ1 deficiency in mammalian cells. *Cell Cycle*, **7**, 989-1000.

161. Doherty,K.M., Sharma,S., Uzdilla,L.A., Wilson,T.M., Cui,S., Vindigni,A. and Brosh,R.M., Jr. (2005) RECQ1 helicase interacts with human mismatch repair factors that regulate genetic recombination. *J. Biol. Chem.*, **280**, 28085-28094.

162. Bugreev,D.V., Brosh,R.M., Jr. and Mazin,A.V. (2008) RECQ1 possesses DNA branch migration activity. *J. Biol. Chem.*, **283**, 20231-20242.

163. Wang,W., Seki,M., Narita,Y., Nakagawa,T., Yoshimura,A., Otsuki,M., Kawabe,Y., Tada,S., Yagi,H., Ishii,Y. *et al.* (2003) Functional relation among RecQ family helicases RecQL1, RecQL5, and BLM in cell growth and sister chromatid exchange formation. *Mol. Cell Biol.*, **23**, 3527-3535.

164. Sharma,S., Stumpo,D.J., Balajee,A.S., Bock,C.B., Lansdorp,P.M., Brosh,R.M., Jr. and Blackshear,P.J. (2007) RECQL, a member of the RecQ family of DNA helicases, suppresses chromosomal instability. *Mol. Cell Biol.*, **27**, 1784-1794.

165. Seki,M., Miyazawa,H., Tada,S., Yanagisawa,J., Yamaoka,T., Hoshino,S., Ozawa,K., Eki,T., Nogami,M., Okumura,K. *et al.* (1994) Molecular cloning of cDNA encoding human DNA helicase Q1 which has homology to Escherichia coli Rec Q helicase and localization of the gene at chromosome 12p12. *Nucleic Acids Res.*, **22**, 4566-4573.

166. Grepmeier,U., Dietmaier,W., Merk,J., Wild,P.J., Obermann,E.C., Pfeifer,M., Hofstaedter,F., Hartmann,A. and Woenckhaus,M. (2005) Deletions at chromosome 2q and 12p are early and frequent molecular alterations in bronchial epithelium and NSCLC of long-term smokers. *Int. J. Oncol.*, **27**, 481-488.

167. Sharma,S., Sommers,J.A., Choudhary,S., Faulkner,J.K., Cui,S., Andreoli,L., Muzzolini,L., Vindigni,A. and Brosh,R.M., Jr. (2005) Biochemical analysis of the DNA unwinding and strand annealing activities catalyzed by human RECQ1. *J. Biol. Chem.*, **280**, 28072-28084.

168. Popuri,V., Bachrati,C.Z., Muzzolini,L., Mosedale,G., Costantini,S., Giacomini,E., Hickson,I.D. and Vindigni,A. (2008) The Human RecQ helicases, BLM and RECQ1, display distinct DNA substrate specificities. *J. Biol. Chem.*, **283**, 17766-17776.

169. Muzzolini,L., Beuron,F., Patwardhan,A., Popuri,V., Cui,S., Niccolini,B., Rappas,M., Freemont,P.S. and Vindigni,A. (2007) Different quaternary structures of human RECQ1 are associated with its dual enzymatic activity. *PLoS. Biol.*, **5**, e20.

170. Muzzolini,L., Beuron,F., Patwardhan,A., Popuri,V., Cui,S., Niccolini,B., Rappas,M., Freemont,P.S. and Vindigni,A. (2007) Different quaternary structures of human RECQ1 are associated with its dual enzymatic activity. *PLoS. Biol.*, **5**, e20.

171. Pike,A.C., Shrestha,B., Popuri,V., Burgess-Brown,N., Muzzolini,L., Costantini,S., Vindigni,A. and Gileadi,O. (2009) Structure of the human RECQ1 helicase reveals a putative strand-separation pin. *Proc. Natl. Acad. Sci. U. S. A*, **106**, 1039-1044.

172. Story,R.M. and Steitz,T.A. (1992) Structure of the recA protein-ADP complex. *Nature*, **355**, 374-376.

173. German,J. (1997) Bloom's syndrome. XX. The first 100 cancers. *Cancer Genet. Cytogenet.*, **93**, 100-106.

174. McDaniel,L.D. and Schultz,R.A. (1992) Elevated sister chromatid exchange phenotype of Bloom syndrome cells is complemented by human chromosome 15. *Proc. Natl. Acad. Sci. U. S. A*, **89**, 7968-7972.

175. Chaganti,R.S., Schonberg,S. and German,J. (1974) A manyfold increase in sister chromatid exchanges in Bloom's syndrome lymphocytes. *Proc. Natl. Acad. Sci. U. S. A*, **71**, 4508-4512.

176. Korenberg,J.R. and Freedlender,E.F. (1974) Giemsa technique for the detection of sister chromatid exchanges. *Chromosoma*, **48**, 355-360.

177. Chaganti,R.S., Schonberg,S. and German,J. (1974) A manyfold increase in sister chromatid exchanges in Bloom's syndrome lymphocytes. *Proc. Natl. Acad. Sci. U. S. A*, **71**, 4508-4512.

178. Imamura,O., Fujita,K., Itoh,C., Takeda,S., Furuichi,Y. and Matsumoto,T. (2002) Werner and Bloom helicases are involved in DNA repair in a complementary fashion. *Oncogene*, **21**, 954-963.

179. Langlois,R.G., Bigbee,W.L., Jensen,R.H. and German,J. (1989) Evidence for increased in vivo mutation and somatic recombination in Bloom's syndrome. *Proc. Natl. Acad. Sci. U. S. A*, **86**, 670-674.

180. Gellert,M. (2002) V(D)J recombination: RAG proteins, repair factors, and regulation. *Annu. Rev. Biochem.*, **71**, 101-132.

181. Gaymes,T.J., North,P.S., Brady,N., Hickson,I.D., Mufti,G.J. and Rassool,F.V. (2002) Increased error-prone non homologous DNA end-joining--a proposed mechanism of chromosomal instability in Bloom's syndrome. *Oncogene*, **21**, 2525-2533.

182. Karow,J.K., Newman,R.H., Freemont,P.S. and Hickson,I.D. (1999) Oligomeric ring structure of the Bloom's syndrome helicase. *Curr. Biol*, **9**, 597-600.

183. Hayakawa,S., Kaneko,H., Fukao,T., Kasahara,K., Matsumoto,T., Furuichi,Y. and Kondo,N. (2000) Characterization of the nuclear localization signal in the DNA helicase responsible for Bloom syndrome. *Int. J. Mol. Med.*, **5**, 477-484.

184. Wu,L., Chan,K.L., Ralf,C., Bernstein,D.A., Garcia,P.L., Bohr,V.A., Vindigni,A., Janscak,P., Keck,J.L. and Hickson,I.D. (2005) The HRDC domain of BLM is required for the dissolution of double Holliday junctions. *EMBO J.*, **24**, 2679-2687.

185. Guo,R.B., Rigolet,P., Ren,H., Zhang,B., Zhang,X.D., Dou,S.X., Wang,P.Y., mor-Gueret,M. and Xi,X.G. (2007) Structural and functional analyses of disease-causing missense mutations in Bloom syndrome protein. *Nucleic Acids Res.*, **35**, 6297-6310.

186. Cheok,C.F., Wu,L., Garcia,P.L., Janscak,P. and Hickson,I.D. (2005) The Bloom's syndrome helicase promotes the annealing of complementary single-stranded DNA. *Nucleic Acids Res.*, **33**, 3932-3941.

187. Mohaghegh,P., Karow,J.K., Brosh,J.R., Jr., Bohr,V.A. and Hickson,I.D. (2001) The Bloom's and Werner's syndrome proteins are DNA structure-specific helicases. *Nucleic Acids Res.*, **29**, 2843-2849.

188. Brosh,R.M., Jr., Li,J.L., Kenny,M.K., Karow,J.K., Cooper,M.P., Kureekattil,R.P., Hickson,I.D. and Bohr,V.A. (2000) Replication protein A physically interacts with the Bloom's syndrome protein and stimulates its helicase activity. *J. Biol. Chem.*, **275**, 23500-23508.

189. Yin,J., Sobeck,A., Xu,C., Meetei,A.R., Hoatlin,M., Li,L. and Wang,W. (2005) BLAP75, an essential component of Bloom's syndrome protein complexes that maintain genome integrity. *EMBO J.*, **24**, 1465-1476.

190. Raynard,S., Zhao,W., Bussen,W., Lu,L., Ding,Y.Y., Busygina,V., Meetei,A.R. and Sung,P. (2008) Functional role of BLAP75 in BLM-topoisomerase IIIalpha-dependent holliday junction processing. *J. Biol. Chem.*, **283**, 15701-15708.

191. Raynard,S., Bussen,W. and Sung,P. (2006) A double Holliday junction dissolvasome comprising BLM, topoisomerase IIIalpha, and BLAP75. *J. Biol. Chem.*, **281**, 13861-13864.

192. Wu,L., Davies,S.L., Levitt,N.C. and Hickson,I.D. (2001) Potential role for the BLM helicase in recombinational repair via a conserved interaction with RAD51. *J. Biol. Chem.*, **276**, 19375-19381.

193. Ding,S.L., Yu,J.C., Chen,S.T., Hsu,G.C., Kuo,S.J., Lin,Y.H., Wu,P.E. and Shen,C.Y. (2009) Genetic variants of BLM interact with RAD51 to increase breast cancer susceptibility. *Carcinogenesis*, **30**, 43-49.

194. Yang,Q., Zhang,R., Wang,X.W., Spillare,E.A., Linke,S.P., Subramanian,D., Griffith,J.D., Li,J.L., Hickson,I.D., Shen,J.C. *et al.* (2002) The processing of Holliday junctions by BLM and WRN helicases is regulated by p53. *J. Biol. Chem.*, **277**, 31980-31987.

195. Singh,T.R., Ali,A.M., Busygina,V., Raynard,S., Fan,Q., Du,C.H., Andreassen,P.R., Sung,P. and Meetei,A.R. (2008) BLAP18/RMI2, a novel OB-fold-containing protein, is an essential component of the Bloom helicase-double Holliday junction dissolvasome. *Genes Dev.*, **22**, 2856-2868.

196. Pichierri,P., Franchitto,A. and Rosselli,F. (2004) BLM and the FANC proteins collaborate in a common pathway in response to stalled replication forks. *EMBO J.*, **23**, 3154-3163.

197. Meetei,A.R., Levitus,M., Xue,Y., Medhurst,A.L., Zwaan,M., Ling,C., Rooimans,M.A., Bier,P., Hoatlin,M., Pals,G. *et al.* (2004) X-linked inheritance of Fanconi anemia complementation group B. *Nat. Genet.*, **36**, 1219-1224.

198. Joenje,H. and Patel,K.J. (2001) The emerging genetic and molecular basis of Fanconi anaemia. *Nat. Rev. Genet.*, **2**, 446-457.

199. Stavropoulos,D.J., Bradshaw,P.S., Li,X., Pasic,I., Truong,K., Ikura,M., Ungrin,M. and Meyn,M.S. (2002) The Bloom syndrome helicase BLM interacts with TRF2 in ALT cells and promotes telomeric DNA synthesis. *Hum. Mol. Genet.*, **11**, 3135-3144.

200. Opresko,P.L., von,K.C., Laine,J.P., Harrigan,J., Hickson,I.D. and Bohr,V.A. (2002) Telomere-binding protein TRF2 binds to and stimulates the Werner and Bloom syndrome helicases. *J. Biol. Chem.*, **277**, 41110-41119.

201. von,K.C., Karmakar,P., Dawut,L., Opresko,P., Zeng,X., Brosh,R.M., Jr., Hickson,I.D. and Bohr,V.A. (2002) Colocalization, physical, and functional interaction between Werner and Bloom syndrome proteins. *J. Biol. Chem.*, **277**, 22035-22044.

202. Yu,C.E., Oshima,J., Fu,Y.H., Wijsman,E.M., Hisama,F., Alisch,R., Matthews,S., Nakura,J., Miki,T., Ouais,S. *et al.* (1996) Positional cloning of the Werner's syndrome gene. *Science*, **272**, 258-262.

203. Salk,D., Bryant,E., Au,K., Hoehn,H. and Martin,G.M. (1981) Systematic growth studies, cocultivation, and cell hybridization studies of Werner syndrome cultured skin fibroblasts. *Hum. Genet.*, **58**, 310-316.

204. Multani,A.S. and Chang,S. (2007) WRN at telomeres: implications for aging and cancer. *J. Cell Sci.*, **120**, 713-721.

205. Saintigny,Y., Makienko,K., Swanson,C., Emond,M.J. and Monnat,R.J., Jr. (2002) Homologous recombination resolution defect in werner syndrome. *Mol. Cell Biol.*, **22**, 6971-6978.

206. Choi,D., Whittier,P.S., Oshima,J. and Funk,W.D. (2001) Telomerase expression prevents replicative senescence but does not fully reset mRNA expression patterns in Werner syndrome cell strains. *FASEB J.*, **15**, 1014-1020.

207. Hisama,F.M., Chen,Y.H., Meyn,M.S., Oshima,J. and Weissman,S.M. (2000) WRN or telomerase constructs reverse 4-nitroquinoline 1-oxide sensitivity in transformed Werner syndrome fibroblasts. *Cancer Res.*, **60**, 2372-2376.

208. Poot,M., Yom,J.S., Whang,S.H., Kato,J.T., Gollahon,K.A. and Rabinovitch,P.S. (2001) Werner syndrome cells are sensitive to DNA cross-linking drugs. *FASEB J.*, **15**, 1224-1226.

209. Poot,M., Gollahon,K.A., Emond,M.J., Silber,J.R. and Rabinovitch,P.S. (2002) Werner syndrome diploid fibroblasts are sensitive to 4-nitroquinoline-N-oxide and 8-methoxypsoralen: implications for the disease phenotype. *FASEB J.*, **16**, 757-758.

210. Lebel,M. and Leder,P. (1998) A deletion within the murine Werner syndrome helicase induces sensitivity to inhibitors of topoisomerase and loss of cellular proliferative capacity. *Proc. Natl. Acad. Sci. U. S. A*, **95**, 13097-13102.

211. Fukuchi,K., Martin,G.M. and Monnat,R.J., Jr. (1989) Mutator phenotype of Werner syndrome is characterized by extensive deletions. *Proc. Natl. Acad. Sci. U. S. A*, **86**, 5893-5897.

212. Pichierri,P., Franchitto,A., Mosesso,P. and Palitti,F. (2001) Werner's syndrome protein is required for correct recovery after replication arrest and DNA damage induced in S-phase of cell cycle. *Mol. Biol. Cell*, **12**, 2412-2421.

213. Darlington,G.J., Dutkowski,R. and Brown,W.T. (1981) Sister chromatid exchange frequencies in Progeria and Werner syndrome patients. *Am. J. Hum. Genet.*, **33**, 762-766.

214. Li,B. and Comai,L. (2000) Functional interaction between Ku and the werner syndrome protein in DNA end processing. *J. Biol. Chem.*, **275**, 28349-28352.

215. Mohaghegh,P., Karow,J.K., Brosh,J.R., Jr., Bohr,V.A. and Hickson,I.D. (2001) The Bloom's and Werner's syndrome proteins are DNA structure-specific helicases. *Nucleic Acids Res.*, **29**, 2843-2849.

216. Constantinou,A., Tarsounas,M., Karow,J.K., Brosh,R.M., Bohr,V.A., Hickson,I.D. and West,S.C. (2000) Werner's syndrome protein (WRN) migrates Holliday junctions and co-localizes with RPA upon replication arrest. *EMBO Rep.*, **1**, 80-84.

217. Crabbe,L., Verdun,R.E., Haggblom,C.I. and Karlseder,J. (2004) Defective telomere lagging strand synthesis in cells lacking WRN helicase activity. *Science*, **306**, 1951-1953.

218. Orren,D.K., Theodore,S. and Machwe,A. (2002) The Werner syndrome helicase/exonuclease (WRN) disrupts and degrades D-loops in vitro. *Biochemistry*, **41**, 13483-13488.

219. Hickson,I.D., Davies,S.L., Li,J.L., Levitt,N.C., Mohaghegh,P., North,P.S. and Wu,L. (2001) Role of the Bloom's syndrome helicase in maintenance of genome stability. *Biochem. Soc. Trans.*, **29**, 201-204.

220. Machwe,A., Xiao,L., Lloyd,R.G., Bolt,E. and Orren,D.K. (2007) Replication fork regression in vitro by the Werner syndrome protein (WRN): holliday junction formation, the effect of leading arm structure and a potential role for WRN exonuclease activity. *Nucleic Acids Res.*, **35**, 5729-5747.

221. Shiratori,M., Suzuki,T., Itoh,C., Goto,M., Furuichi,Y. and Matsumoto,T. (2002) WRN helicase accelerates the transcription of ribosomal RNA as a component of an RNA polymerase I-associated complex. *Oncogene*, **21**, 2447-2454.

222. Kamath-Loeb,A.S., Johansson,E., Burgers,P.M. and Loeb,L.A. (2000) Functional interaction between the Werner Syndrome protein and DNA polymerase delta. *Proc. Natl. Acad. Sci. U. S. A*, **97**, 4603-4608.

223. Brosh,R.M., Jr., Orren,D.K., Nehlin,J.O., Ravn,P.H., Kenny,M.K., Machwe,A. and Bohr,V.A. (1999) Functional and physical interaction between WRN helicase and human replication protein A. *J. Biol. Chem.*, **274**, 18341-18350.

224. Lebel,M., Spillare,E.A., Harris,C.C. and Leder,P. (1999) The Werner syndrome gene product co-purifies with the DNA replication complex and interacts with PCNA and topoisomerase I. *J. Biol. Chem.*, **274**, 37795-37799.

225. Brosh,R.M., Jr., Driscoll,H.C., Dianov,G.L. and Sommers,J.A. (2002) Biochemical characterization of the WRN-FEN-1 functional interaction. *Biochemistry*, **41**, 12204-12216.

226. Siitonen,H.A., Kopra,O., Kaariainen,H., Haravuori,H., Winter,R.M., Saamanen,A.M., Peltonen,L. and Kestila,M. (2003) Molecular defect of RAPADILINO syndrome expands the phenotype spectrum of RECQL diseases. *Hum. Mol. Genet.*, **12**, 2837-2844.

227. el-Khoury,J.M., Haddad,S.N. and Atallah,N.G. (1997) Osteosarcomatosis with Rothmund-Thomson syndrome. *Br. J. Radiol.*, **70**, 215-218.

228. Lindor,N.M., Furuichi,Y., Kitao,S., Shimamoto,A., Arndt,C. and Jalal,S. (2000) Rothmund-Thomson syndrome due to RECQ4 helicase mutations: report and clinical and molecular comparisons with Bloom syndrome and Werner syndrome. *Am. J. Med. Genet.*, **90**, 223-228.

229. Kitao,S., Lindor,N.M., Shiratori,M., Furuichi,Y. and Shimamoto,A. (1999) Rothmund-thomson syndrome responsible gene, RECQL4: genomic structure and products. *Genomics*, **61**, 268-276.

230. Der,K., V, McGill,J.J., Vekemans,M. and Kopelman,H.R. (1990) Clonal lines of aneuploid cells in Rothmund-Thomson syndrome. *Am. J. Med. Genet.*, **37**, 336-339.

231. Ying,K.L., Oizumi,J. and Curry,C.J. (1990) Rothmund-Thomson syndrome associated with trisomy 8 mosaicism. *J. Med. Genet.*, **27**, 258-260.

232. Varughese,M., Leavey,P., Smith,P., Sneath,R., Breatnach,F. and O'Meara,A. (1992) Osteogenic sarcoma and Rothmund Thomson syndrome. *J. Cancer Res. Clin. Oncol.*, **118**, 389-390.

233. Shinya,A., Nishigori,C., Moriwaki,S., Takebe,H., Kubota,M., Ogino,A. and Imamura,S. (1993) A case of Rothmund-Thomson syndrome with reduced DNA repair capacity. *Arch. Dermatol.*, **129**, 332-336.

234. Smith,P.J. and Paterson,M.C. (1982) Enhanced radiosensitivity and defective DNA repair in cultured fibroblasts derived from Rothmund Thomson syndrome patients. *Mutat. Res.*, **94**, 213-228.

235. Kitao,S., Ohsugi,I., Ichikawa,K., Goto,M., Furuichi,Y. and Shimamoto,A. (1998) Cloning of two new human helicase genes of the RecQ family: biological significance of multiple species in higher eukaryotes. *Genomics*, **54**, 443-452.

236. Sengupta,S., Shimamoto,A., Koshiji,M., Pedeux,R., Rusin,M., Spillare,E.A., Shen,J.C., Huang,L.E., Lindor,N.M., Furuichi,Y. *et al.* (2005) Tumor suppressor p53 represses transcription of RECQ4 helicase. *Oncogene*, **24**, 1738-1748.

237. Sangrithi,M.N., Bernal,J.A., Madine,M., Philpott,A., Lee,J., Dunphy,W.G. and Venkitaraman,A.R. (2005) Initiation of DNA replication requires the RECQL4 protein mutated in Rothmund-Thomson syndrome. *Cell*, **121**, 887-898.

238. Matsuno,K., Kumano,M., Kubota,Y., Hashimoto,Y. and Takisawa,H. (2006) The N-terminal noncatalytic region of Xenopus RecQ4 is required for chromatin binding of DNA polymerase alpha in the initiation of DNA replication. *Mol. Cell Biol.*, **26**, 4843-4852.

239. Fan,W. and Luo,J. (2008) RecQ4 facilitates UV light-induced DNA damage repair through interaction with nucleotide excision repair factor xeroderma pigmentosum group A (XPA). *J. Biol. Chem.*, **283**, 29037-29044.

240. Sekelsky,J.J., Brodsky,M.H., Rubin,G.M. and Hawley,R.S. (1999) Drosophila and human RecQ5 exist in different isoforms generated by alternative splicing. *Nucleic Acids Res.*, **27**, 3762-3769.

241. Ozsoy,A.Z., Sekelsky,J.J. and Matson,S.W. (2001) Biochemical characterization of the small isoform of Drosophila melanogaster RECQ5 helicase. *Nucleic Acids Res.*, **29**, 2986-2993.

242. Shimamoto,A., Nishikawa,K., Kitao,S. and Furuichi,Y. (2000) Human RecQ5beta, a large isomer of RecQ5 DNA helicase, localizes in the nucleoplasm and interacts with topoisomerases 3alpha and 3beta. *Nucleic Acids Res.*, **28**, 1647-1655.

243. Kanagaraj,R., Saydam,N., Garcia,P.L., Zheng,L. and Janscak,P. (2006) Human RECQ5beta helicase promotes strand exchange on synthetic DNA structures resembling a stalled replication fork. *Nucleic Acids Res.*, **34**, 5217-5231.

244. Garcia,P.L., Liu,Y., Jiricny,J., West,S.C. and Janscak,P. (2004) Human RECQ5beta, a protein with DNA helicase and strand-annealing activities in a single polypeptide. *EMBO J.*, **23**, 2882-2891.

245. Wang,W., Seki,M., Narita,Y., Nakagawa,T., Yoshimura,A., Otsuki,M., Kawabe,Y., Tada,S., Yagi,H., Ishii,Y. *et al.* (2003) Functional relation among RecQ family helicases RecQL1, RecQL5, and BLM in cell growth and sister chromatid exchange formation. *Mol. Cell Biol.*, **23**, 3527-3535.

246. Hu,Y., Lu,X., Barnes,E., Yan,M., Lou,H. and Luo,G. (2005) Recql5 and Blm RecQ DNA helicases have nonredundant roles in suppressing crossovers. *Mol. Cell Biol.*, **25**, 3431-3442.

Chapter 2

RESULTS

I Zinc binding motif in RECQ5β acts as a molecular switch turning strand annealing into DNA unwinding

The abbreviations used are: dsDNA, double-stranded DNA; ssDNA, single-stranded DNA; EMSA, electrophoretic mobility shift assay; FRET, fluorescence resonance energy transfer; HRDC, helicase-and-ribonuclease D-C-terminal domain; mantATP, 2′(3′)-*O*-(*N*-methlanthraniloyl) adenosine-5′-triphosphate; PAR, 4-(2-pyridylazo)resorcinol; RPA, replication protein A; RQC, RecQ carboxy-terminal conserved; WH, winged helix-turn-helix.

ACKNOWLEDGEMENTS

In this chapter, we thank Dr. Pascal Rigolet (Department of Biochemistry, ENS de Cachan, France) for help with molecular modelling, Dr. Robert Pansu and Dr. Loussiné Zargarian (Department of Biochemistry, ENS de Cachan, France) for assistance in the fluorescence measurements. We are grateful to Yan He (Department of Pharmacy, Guiyang Medical College, China) and Nicolas Bazeille (Section de Recerche, Institut Curie, France) for carrying out some preliminary studies. This research was supported by grants from Institut National du Cancer and La Ligue Contre Le Cancer to X. G. X.; the National Natural Science Foundation of China and the Innovation Project of the Chinese Academy of Sciences, the Swiss National Science Foundation to P. J., and the grants from the American Cancer Society (RSG-03-238-01) and the American Heart Association (0335253N) to J.-S. H.

SUMMARY

RecQ family helicases, functioning as caretakers of genomic integrity, contain a zinc binding motif which is highly conserved among these helicases, but does not have substantial structural similarity with any other known zinc finger folds. In the present study, we show that a truncated variant of the human RECQ5β helicase comprised of the conserved helicase core domain only, a splice variant named RECQ5α, possesses neither ATPase nor DNA-unwinding activities, but surprisingly displays a strong strand-annealing activity. In contrast, fragments of RECQ5β including the intact zinc-binding motif, which is located immediately down-stream of the helicase domain, exhibit much reduced strand-annealing activity but are proficient in DNA unwinding interacting with helicase core domain. Quantitative measurements indicate that the regulatory role of the zinc-binding motif to helicase core domain achieved by enhancing the DNA-binding affinity of the enzyme. The novel intramolecular modulation of RECQ5β catalytic activity mediated by the zinc-binding motif may represent a universal regulation mode for all RecQ family helicases.

INTRODUCTION

DNA helicases are molecular motors that transduce the chemical energy derived from NTP hydrolysis into mechanical force to unwind dsDNA (double-stranded DNA) (1; 2). Therefore helicases display both DNA-stimulated ATPase and ATP-dependent helicase activities. Structural studies revealed that helicases from SF1 and SF2 (superfamily 1 and 2) contain a structural module that consists of two RecA-related domains (3;4). Residues involved in ATP binding/hydrolysis and DNA binding are located in the cleft separating the two RecA-like domains. It is postulated that theses domains serve as a DNA translocation motor (4).

The RecQ family DNA helices are highly conserved from bacteria to man and play essential roles in the maintenance of genomic stability (5-8). In human, five family members, named RECQ1 (9;10), BLM (11), WRN (12), RECQ4 (13) and RECQ5 (14), have been identified. Defects in BLM, WRN and RECQ4 lead to human hereditary disorders: BS (Bloom syndrome), WRN (Werner syndrome) and RTS (Rothumund-Thompson syndrome), respectively, that are characterized by genome instability and cancer predisposition (15). In addition to the highly conserved DexH helicase domain containing seven helicase motifs, most RecQ family helicases contain a unique RQC (RecQ conserved) domain which is composed of a conserved zinc binding motif and a WH (winged helix-turn-helix) motif (16;17). RecQ helicase activity is highly regulated not only through inter-molecular protein-protein interactions (18), but also through intramolecular interactions between the different domains (19). In the present study, we have chosen human RecQ5 protein as a model to study the function modulation of the DexH-helicase core by the zinc-binding domain. The striking feature of human RecQ5 is that it exists in three isoforms, namely RECQ5α, RECQ5β and RECQ5γ, which result from alternative splicing of the RECQ5 transcript (14;20). The three proteins are identical within the N-terminal regions of 410 residues which constitutes the helicase motifs (Fig. 1). RecQ5α is the shortest variant including only the helicase domain (410 amino acids). RECQ5β contains the helicase domain and a putative RecQ-Ct domain, which is followed by a long C-terminal region that shows no homology with the other RecQ helicases. RecQ5γ includes the helicase domain followed by a C-terminal extension of 25 amino acids that is not present in RECQ5β. At present, only RECQ5β has been biochemically characterized (21). It possesses both DNA-unwinding and DNA strand-annealing activities (21). However, the molecular mechanism

that underlies the co-ordination of DNA unwinding and strand-annealing activities of RECQ5β remains largely elusive.

The RECQ5α and RECQ5β proteins offer an attractive model system to characterize the enzymatic activities of a RecQ helicase domain in isolation and in association with other sub-domains on the same polypeptide. This unique property allows us to address some interesting and important questions that have not yet been resolved with any DNA helicase. These questions include: (i) is the DNA helicase domain sufficient to catalyze dsDNA separation; (ii) does the helicase domain have an intrinsic strand-annealing activity as suggested by its structural similarity to the stand-exchange protein RecA; (iii) what is the role of the accessory domain, namely the zinc-binding domain, in the helicase activity of the enzyme. In the present study, we found that the helicase domain of RECQ5 does not possess DNA-unwinding capability, but exhibits an intrinsic strand-annealing activity. More importantly, the zinc-binding motif is found to act as a molecular switch that suppresses the strand-annealing activity of the helicase domain and triggers DNA-unwinding activity through modulating DNA binding.

Figure 1

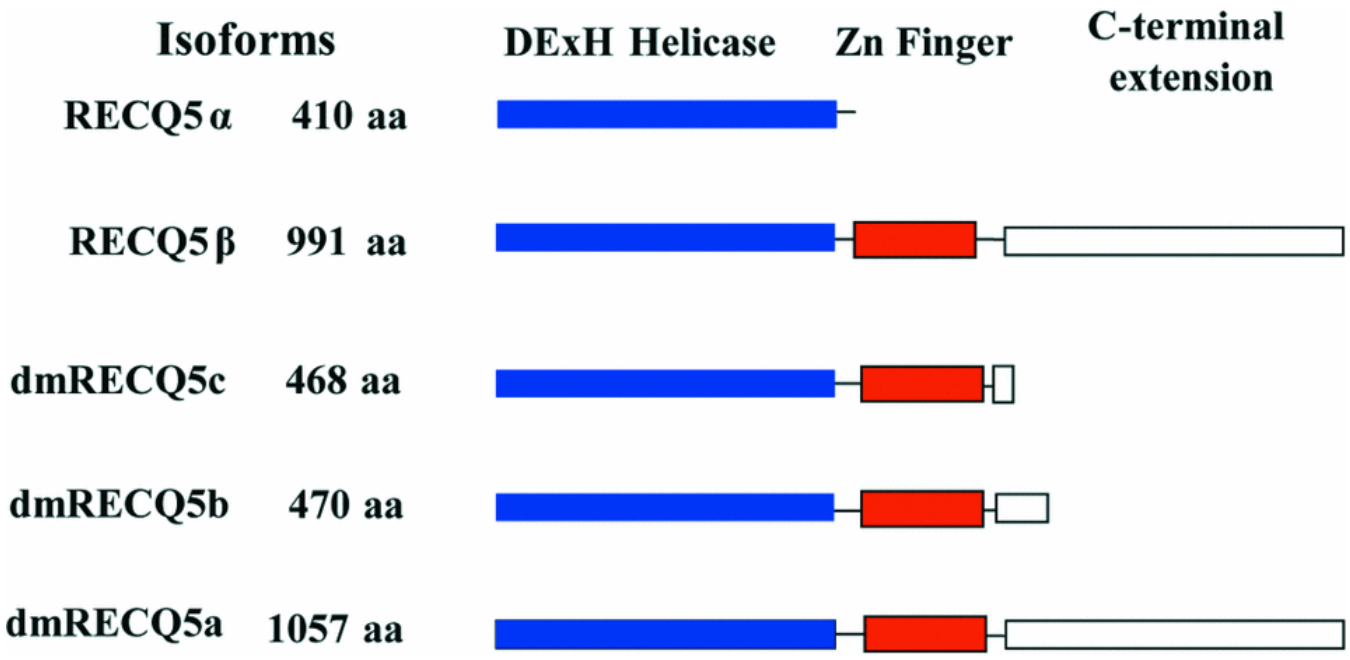

Fig. 1 The determination of DNA binding affinity of the RECQ5 isoforms and their derived protein fragments under equilibrium conditions

The anisotropy based binding isotherms were obtained by varying protein concentration in the presence of 5nM 3'-fluorescent labelled (A and C) ssDNA (BA) and (B and D) dsDNA (BA/BB) (Table 1), and then were fitted to Michaelis-Mentens or Hill equation. The apparent K_d values are summarized in Table 2.

MATERIALS AND METHODS

Proteins and DNA substrates

The human RECQ5α and RECQ5β protein were produced as C-terminal fusion with a self-cleaving chitin-binding domain and purified as described previously (21). The truncation mutants of RECQ5β were amplified by PCR and cloned into pET15b as N-terminal fusions with a hexahistidine tag. The resulting plasmids were transformed into the *Escherichia coli* strain BL21-codonPlus (Stratagene). The cells were grown to the mid-exponential phase (A_{600} of 0.5-0.6) at 37°C and the protein expression was induced by 0.25mM IPTG (isopropyl β-D-thiogalactoside) at 15°C for 18 h. The cells were lysed in buffer containing 50mM Tris/HCl (pH 7.5), 500mM NaCl, 0.1% Triton X-100, 0.1μM PMSF and 10% ethylene glycerol). The cell lysate was clarified by centrifugation (23 000 *g* for 45 min at 4°C) and the supernatant was applied to a 20 ml Ni^{2+}-column connected to an ÄKTA FPLC system. The bound proteins were eluted with a linear gradient of imidazole (0.02-0.4M, 300 ml. Fractions containing the proteins of interest were identified by SDS-PAGE (Fig. 2). Protein was further purified using size-exclusion chromatography (Superdex 200, Amersham). Human RPA (replication protein A) was produced and prified according to a procedure described previously (23).

PAGE-purified DNA oligonucleotides (Table 1) were purchased from Proligo. The DNA duplex substrates were prepared as described previously (24). Briefly, 250μM component oligonucleotides were denatured in the 1 × TE buffer [10mM Tris/HCl(pH7.5) and 1mM EDTA] containing 1M NaCl or KCl by heating at 95°C for 10 min. The denatured DNA was then annealing at 37°C for 48h. The annealed products were separated on native-PAGE (8% gel) containing 10mM KCl run at 4°C for 12 h with a constant current of 20mA.

Figure 2

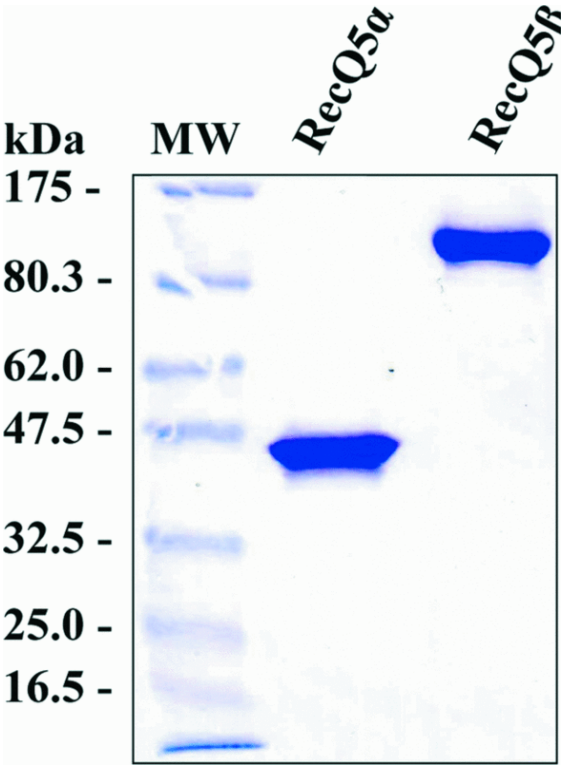

Fig. 2 Coomassie-Blue-stained SDS/PAGE (10% gel) of purified RECQ5α and RECQ5β The molecular-mass (MW) standards (in kDa) are shown on the left-hand side.

Table 1 DNA oligonucleotides used in the present study

F and H represent fluorescein and hexachlorofluoresein groups respectively.

Oligonucleotide name	Length (nucleotides)	Sequence (5′–3′)
BA	36	AATCCGTCGAGCAGAGTTAGGGTTAGGGTTAGGGTT
BB	36	AACCCTAACCCTAACCCGAAGTCTGCTCGACGGATT
UA	44	GCACTGGCCGTCGTTTTACTTGG TGACTGGGAAAACCCTGGCG
UB	44	TTTTTTTTTTTTTTTTTTTTCCAAGTAAAACGACGGCCAGTGC
UFA	56	H-AATCCGTCGAGCAGAG (dT_{40})
UFB	16	CTCTGCTCGACGGATT-F
SPA	50	TCAAAGTCACGACCTAGACACTGCGAGCTCGAATTCACTGGAGTGACCTC
SPB	50	GAGGTCACTCCAGTGAATTCGAGCTCGCAGTGTCTAGGTCGTGACTTTGA
SPFA	45	AGATCCCTCAGACCCTTTTAGTCAGTGTGGAAAATCTCTAGCAGT-F
SPFB	45	H-ACTGCTAGAGATTTTCCACACTGACTAAAAGGGTCTGAGGGATCT
SPC	23	GCACTGGCCGTCGTTTTACTTGG

Quantification of the protein-bound Zn^{2+} ions

Protein-bound Zn^{2+} ion was measured using PAR [4-(2-pyridyl-azo) resorcinol], a reporter dye that absorbs light at 490 nm when bound to Zn^{2+}. To precisely quantify the Zn^{2+} content, all buffers were treated with Chelex®-100 resins (Bio-Rad). The proteins were dialysed against the EDTA-free Chelex®-treated buffer, passed over a 10-cm column of Chelex®-100 and re-concentrated. To facilitate the Zn^{2+} release, the protein (approx.1 nmol in 40 µl) was first denatured with Chelex®-treated 7 M guanidine/HCl, and then transferred to a 1 ml curvette. PAR was added to the cuvette to a final concentration of 100 µM and the volume was adjusted to 1 ml with the containing 20mM Tris/HCl (pH 8.0) and 150mM NaCl. The absorbance was recorded from 300 to 600 nm on a UVIKON spectrophotometer 941 (Kontron) at 25°C. The quantity of Zn^{2+} was determined using the absorbance coefficient for the $Zn(PAR)_2$ complex ($\varepsilon 500 = 6.6\times10^4\ M^{-1}cm^{-1}$). As a control, 20nmol of the pure $ZnCl_2$ was quantified under the identical conditions.

ATP binding assay

mantATP [2'(3')-O-(N-methylanthraniloyl) adenosine-5'-triphosphate], a fluorescent nucleotide analogue of ATP, was used to determine the apparent dissociation constant of ATP binding by RECQ5 proteins. For that purpose, fluorescence spectra of the proteins at a concentration of 0.5 µM were first measured using a FluoroMax-2 spectrofluorimeter (Jobin Yvon, Spex Instruments S.A.) at 25°C. In a 10mm × 10mm × 40mm quartz cuvette, the protein was excited at 280nm and their intrinsic fluorescence emission near 350nm was montiored. This measurement was useful for confirming the overlap of the fluorescence emission spectra of the protein and the excitation spectrum of mantATP near 350nm. When exctied at 280nm, this overlap would result in an enhancement of the emission of mantATP at 440nm after its binding to the proteins due to FRET (fluorescence resonance energy transfer).

The mantATP-binding assay was performed using a Bio-Logic auto-titrator (TCU-250) and a Bio-Logic optical system (MOS450/AF-CD) in fluorescence mode. Various amounts of mantATP were added to 1ml of binding buffer [20mM Tris/HCl, 50mM NaCl, 1mM $MgCl_2$ and 0.1mM DTT (dithiothreitol)] containing 0.5µM protein. After 1 min incubation, fluorescence at 440nm was measured. Titrations were performed in a temperature-

controlled cuvette at 25°C. The solution was stirred continuously using a magnetic stir bar during the whole titration process. The apparent dissociation constant K_d was determined by fitting the fluorescence intensity at 440nm (corrected for the inner filter effect) with eqn (1):

$$F = F_s c_d + f_d x + f_c \frac{(x + 0.5c_d + K_d) - \sqrt{(x + 0.5c_d + K_d)^2 - 4 \times 0.5c_d \times x}}{2}, \quad (1)$$

where, F_s is the starting fluorescence of the reaction mixture, f_d is the fluorescence coefficient of free mantATP, f_c is the fluorescence coefficient of the complex formed and x is the total concentration of mantATP. $c_d = V_0 / (V_0 + V_i) \equiv 1 - x/[\text{mantATP}]$ is included to correct accurately for the sample dilution effect, where V_0 is the initial sample volume, V_i is the volume of titrant added, and [mantATP] is the mantATP concentration of the titrant.

ATPase assay

The ATPase activity of the RECQ5 proteins was detected by measuring the concentration of Pi produced by ATP hydrolysis (25). The reaction was carried out in ATPase reaction buffer [50mM Tris/HCl (pH 8.0), 3mM $MgCl_2$, and 0.5mM DTT] at 37°C in a volume of 100 µl. The reactions were initiated by the addition of enzyme into a reaction mixture containing 1.5µM heat-denatured Hind III-cut pGEM-7Zf linear DNA and the mixture of ATP and [γ-^{32} P]ATP. The reaction was stopped by adding 0.2ml of stopping buffer consisting of 8.1mM ammonium molybdate and 0.8 M HCl. The liberated ^{32}Pi was extracted with a solution of 2-butanol/benzene/acetone/ammonium molybdate (750:750:15:1) saturated with water. An aliquot of 60µl was removed from the organic phase and the radioactivity was quantified using a liquid-scinitillation counter.

DNA binding assay

DNA binding of RECQ5 proteins was analysed using a fluorescence polarization anisotropy assay as described previously (24). The DNA-binding assay was performed using the Bio-Logic auto-titrator (TCU-250) and the Bio-Logic optical system (MoS450/AF-CD) in fluorescence anisotropy mode. Various amounts of proteins were added to 1ml of binding buffer (as above) containing 1nM DNA substrate. After 1 min incubation, the fluorescence polarization anisotropy was measured. The temperature was controlled at 25°C and the solution was stirred continuously during the whole titration

process. The equilibrium dissociation constant was determined by fitting the data to the Michaelis-Menten or Hill equation using the program KaleidaGraphy (Synergy Software).

DNA helicase activity assay

DNA-unwinding reactions were carried out at 37°C in 20 μl of the mixture containing 25 mM Hepes/NaOH (pH7.5), 25mM NAOAc, 7.5mM $Mg(OAc)_2$, 2mM ATP, 1mM DTT and 0.1mg/ml BSA, and indicated ^{32}P-labelled partial DNA duplex substrate (10 fmol, 3000 c.p.m/fmol). Where required, RPA was added at the indicated concentration. The reaction was initiated by the addition of the indicated concentration of the RECQ5 protein and incubated at 37°C for 30 min. Reactions were terminated by the addition of 5μl of 5 × loading buffer (50mM EDTA, 0.5% SDS, 0.1% xylene cyanol, 0.1% Bromophenol Blue and 50 % glycerol.) The reaction producs were resolved on PAGE [12% (w/v) gel] run in 1 ×TBE buffer (89mM Tris-Base, 89mM Boric acid, 2mM EDTA, pH8.0) at 100V for 2h at 4°C. Radiolabelled species were visualized using a Storm 860 Phosphoimager (Amersham Biosciences).

A stopping –flow DNA-unwinding assay was performed according to Zhang *et al.* (26). Briefly, the experiment was carried out using a Bio-logic SFM-400 mixer with a 1.5mm× 1.5mm cell (Bio-Logic, FC-15) and a Bio-Logic MOS450/AF-CD optical system equipped with a 150W mercury-xenon lamp. Fluorescein was excited at 492nm, and its emission was monitored at 525nm. The unwinding assay was performed in a two-syringe- mixing bated in syringe # 1for 5 min, while ATP was present in syringe # 4. Both syringe contained the unwinding reaction buffer [25mM Tris/HCl (pH7, 5), 50mM NaCl, 1mM $MgCl_2$ and 0.1 mM DTT]. The unwinding reaction was initiated by a rapid mixing of the contents of the two syringes. The dsDNA substrates had both strands labelled with fluorescein and hexachlorofluorescein respectively, and their sequences are listed in Supplementary Table S1. During the unwinding process, the fluorescein emission signal at 525nm was enhanced due to the loss of FRET, i.e. the separation of the two dye molecules on the two ssDNA (single-stranded DNA). For converting the output signal change from volts into performed in a four-syringe-mixing mode, where there was the helicase in syringe #1, hexachlorofluorescein-labelled ssDNA in syinge #2, fluorescein-labelled ssDNA in syringe #3 and ATP in syringe #4, all incubated in unwinding reaction buffer. The fluorescent signal of the mixed solution from the four syringe corresponded to 100% unwinding. The standard reaction was carried out at 25°C.

DNA strand-annealing assay

The DNA annealing activity of the RECQ5 isoforms was assayed using complementary synthetic oligonucleotides (0.5nM) with one strand 5′-end labelled using [γ-^{32}P] ATP and T4 polynucleotide kinase. In this assay, the labelled oligonuclotide was added to reaction buffer (20µl) containing 20 mM Tris/acetate, (pH 7.9), 50 mM KOAc, 10 mM $Mg(OAc)_2$, 1 mM DTT and 50 µg/ml BSA and the indicated protein concentration. Where required, ATP, ATP[S] (adenosine 5'-[γ-thio] triphosphate), p[NH]ppA (adenosine 5'-[β,γ-imido]triphophate) or ADP were also added to a final concentration of 2mM. The reaction was initiated by adding the unlabelled oligonuclotide and incubated at 37°C for 30 min. The resulting DNA products were analysed as described for the helicase reactions.

The stopped-flow DNA strand-annealing assay was carried out under similar conditions as the helicase assay. The reaction was performed in a three-syringe-mixing mode, where the helicase was in syringe #1 while fluorescein- and hexachlorofluorescein-labeled complementary ssDNA were in syringe #2 and syringe #3 respectively, in buffer containing 25mM Tris/HCl (pH 7.5), 50mM NaCl, 1mM $MgCl_2$ and 0.1mM DTT. The sequences of the two 45-mer ssDNA substrates are indicated in the Supplementary Table 1. The reaction was initiated by rapidly mixing the contents of the three syringes. During the annealing process, the fluorescein emission signal at 525nm was reduced due to FRET from fluorescein to hexachlorofluorescein on the two ssDNA. For converting the output signal change from volts into percentage of annealing, we performed another experiment in a two-syringe-mixing mode, where the helicase was in the syringe #1, and the annealed dsDNA in the syringe #4, both in the same buffer as indicated above. The fluorescent signal of the mixed solution from the two syringes corresponded to 100% annealing. The reaction was carried out 25°C.

RESULTS AND DISSCUSSION

RECQ5 helicase domain alone catalyzes strand annealing, but not strand separation

To analyse the function of an isolated helicase domain of RecQ DNA helicases, we investigated the biochemical properties of the human RECQ5α protein. We first compared the unwinding activities of RECQ5α and RECQ5β using a gel-shift-based helicase assay. The results showed that RECQ5β efficiently unwound a partial DNA duplex in a dose-dependent manner, whereas RECQ5α displayed hardly any detectable helicase activity (Fig. 3A), even in the presence of human RPA (results not shown), which was reported to stimulate RECQ5β-mediated DNA unwinding (21). To confirm this result, we employed a FRET-based helicase assay, which allowed the helicase-mediated DNA unwinding to be monitored in real-time in a stop-flow experiment (26). Consistent with earlier studies, RECQ5α displayed non-detectable helicase activity, whereas RECQ5β unwound the DNA substrate efficiently (Fig. 3B). Under multiple turn over conditions, the unwinding kinetics of RECQ5β was biphasic. The fitting using a sum of two exponential terms gave two rate constants of 4.54 and 0.84 min^{-1} for the fast and slow phases respectively (Fig. 3B and Table 2).

Next, we tested RECQ5α and RECQ5β for the ability to promote strand-annealing using two complementary 50-mer oligonucleotides. Remarkably, RECQ5α was found to promote strand annealing as efficiently as RECQ5β (Fig. 4A). This result was rather surprising, since the strand-annealing activity of RECQ5β was previously shown to reside in the C-terminal portion of the RECQ5β polypeptide (21). We then examined the effect of ATP on the annealing activities of the RECQ5 proteins. Consistent with previously published results (21), we found that ATP had no effect on the annealing activity of RECQ5β, whereas ATP[S], a poorly hydrolysable analogue of ATP, dramatically suppressed this reaction (Fig. 4B, lanes 2 and 3). In contrast, ATP dramatically inhibited the annealing activity of RECQ5α as it did ATP[S] (Fig. 4B, lanes 8 and 9).We also examined the effect of ADP on the strand-annealing activities ofRECQ5α andRECQ5β. We found that ADP partially inhibited the annealing activity of RECQ5β, but had no effect on the annealing activity of RECQ5α (Fig. 4B, lanes 4 and 10). Since previous studies showed that RPA efficiently inhibited the strand-annealing activities of RECQ5β and RECQ1 (21;27), we also tested the effect of this single-strand binding protein on the strand-annealing activity of RECQ5α.

Figure 3

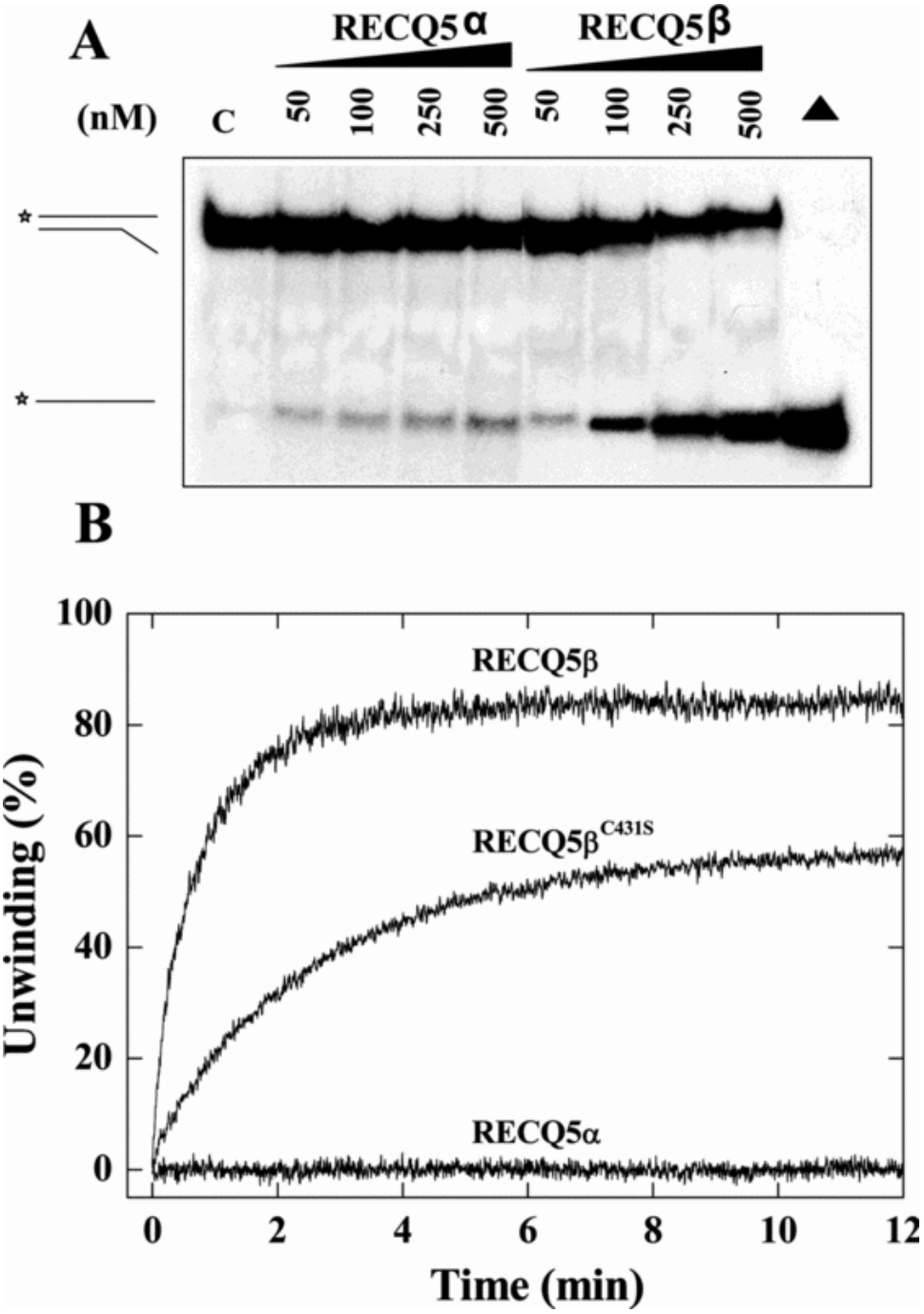
A
RECQ5α
RECQ5β
(nM)
C
50
100
250
500
50
100
250
500
B
RECQ5β
RECQ5β^C431S
RECQ5α
Unwinding (%)
Time (min)
0
20
40
60
80
100
0
2
4
6
8
10
12

Fig. 3 Helicase assays of RECQ5α and RECQ5β

(**A**) Gel-based assay of DNA unwinding using 0.5 nM 5'-^{32}P-labelled 23-base DNA duplex (UA/UB). Reactions were carried out at 37°C for 30 min under conditions as described in the Materials and methods section. The reaction products were analysed by non-denaturing PAGE (12% gels). (**B**) Stopped-flow DNA-unwinding assay. As described in the Materials and methods section, 1 nM 56:16-mer DNA substrate (UFA/UFB) was pre-incubated with 20 nM helicase for 5 min at 25°C. The unwinding reaction was initiated by mixing with 1 mM ATP. The increase of the fluorescence signal of fluorescein at 525 nm (excited at 492 nm) during unwinding was monitored. The fraction of DNA unwound was obtained by normalization of the fluorescence signal F using the value F_{max} as obtained from the calibration measurement that corresponded to 100% unwinding (see the Materials and methods section), i.e. fraction unwound=$(F - F_s)/(F_{max} - F_s)$, where F_s is the fluorescence signal at the start of unwinding.

Table 2 Summary of the measured parameters for RECQ5 isoforms and mutants

Protein	$[Zn^{2+}]/[P]$	ATP binding K_d (μM)	Annealing (%)	ATPase k_{cat} (s^{-1})	Helicase activity		DNA binding	
					%	k_{obs} (min^{-1})	K_d for ssDNA (nM)	K_d for dsDNA (nM)
RECQ5α	0.03±0.02	48.4±2.5	95.2±8.6	ND	ND	ND	1.0×10^6±219[2]	1.8×10^6±267[2]
RECQ5β	0.98±0.18	51.0±4.9	57.3±5.6	15.6±1.4	84.1±3.5	4.54 and 0.84[1]	46.6±2.5	59.3±2.0
$RECQ5\beta^{C431S}$	0.35±0.12		78.6±3.5	4.8±0.6	58.3±2.8	0.50 and 0.03[1]	67.5±12.1	201±23.4
$RECQ5\beta^{1–475}$	0.96±0.11		25.5±6.5	14.8±1.1	90.3±4.9	5.03 and 0.87[1]	64.2±5.4	79.8±2.4
$RECQ5\beta^{1–662}$	1.02±0.15		55.3±10.5	16.3±1.3	92.5±5.6	5.65 and 0.92[1]	55.8±2.5	70.3±3.2
$RECQ5\beta^{379–662}$	1.01±0.14						680±63	149±6.7
$RECQ5\beta^{454–662}$							1308±116	1539±32

[1]Values corresponding to the fast-rate constant and the slow-rate constant respectively.

[2] DNA-binding affinity is determined with K_d (app)=218.2±7.8nM and Hn=2.68±0.18 for dsDNA and K_d (app)=149.8nM and Hn=2.76 for ssDNA using the equation $K_d=[K_d\ (app)]^{(Hn)}$.

Figure 4

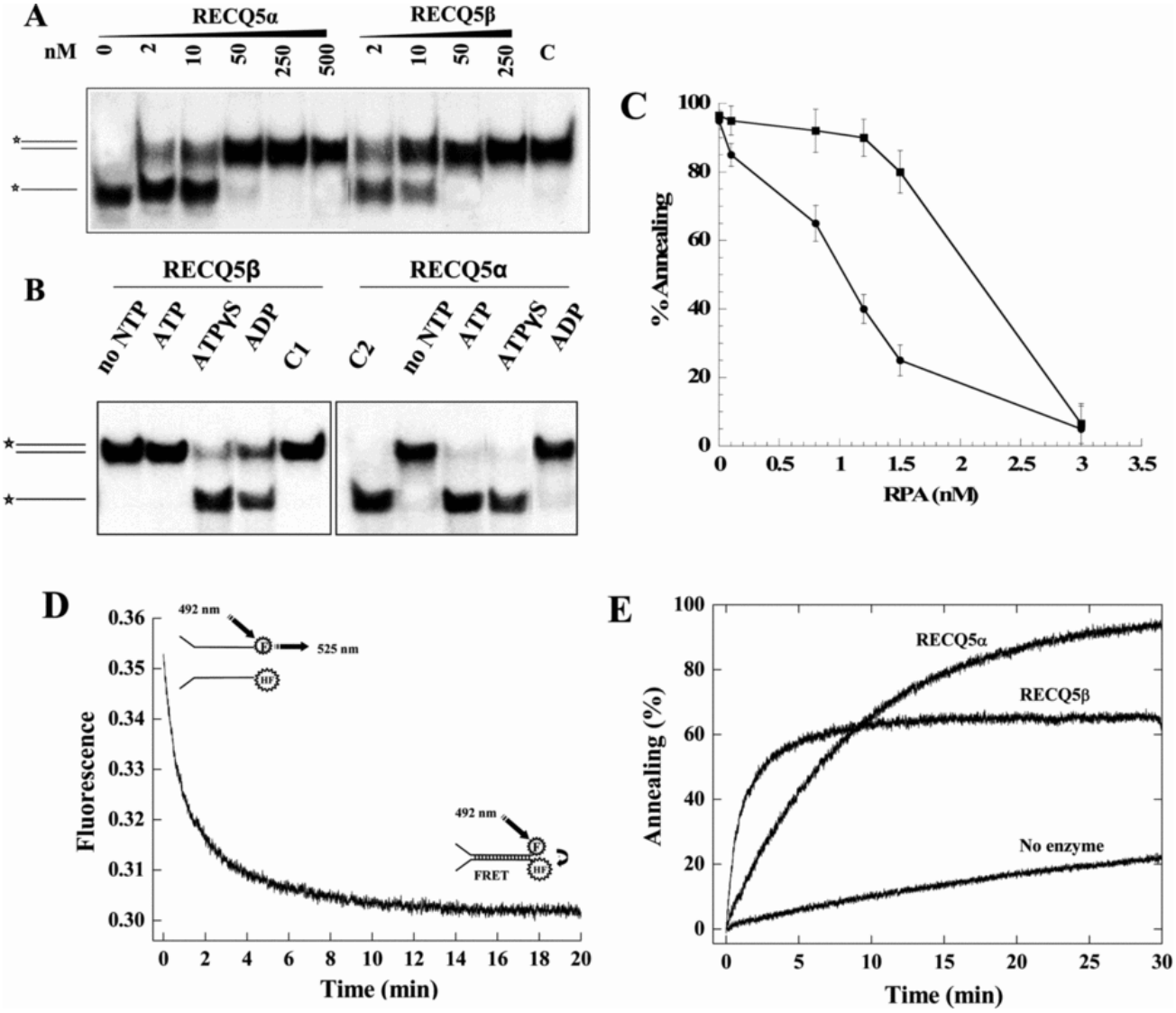
A
RECQ5α
RECQ5β
nM
0
2
10
50
250
500
2
10
50
250
C
B
RECQ5β
RECQ5α
no NTP
ATP
ATPγS
ADP
C1
C2
no NTP
ATP
ATPγS
ADP
C
% Annealing
RPA (nM)
D
492 nm
525 nm
HP
Fluorescence
Time (min)
FRET
E
RECQ5α
RECQ5β
No enzyme
Annealing (%)
Time (min)

Fig. 4 RECQ5-mediated ssDNA annealing

(A) Annealing of the 5'-^{32}P-labelled SPA (0.5nM) and SPB ssDNA substrates by RECQ5α and RECQ5β. Reactions were incubated with the indicated protein concentrations for 30 min at 37°C. The reaction products were separated by non-denaturing PAGE (12% gels) and visualized by a PhosphoImager. **(B)** Effect of nucleotides on the RECQ5-mediated ssDNA annealing. The reactions contained 50nM RECQ5α or RECQ5β and were carried out under the same conditions as in (A). Preformed 50bp duplex and 50-mer ss-oligonucleotide were loaded as markers (C1 and C2 respectively). The indicated nucleotides were present at a concentration of 2mM. **(C)** Strand-annealing activity of RECQ5α (black dot) and RECQ5β (black square) in the presence of the increasing concentration of RPA. The complementary 50-mer oligonucleotides (0.5nM) were incubated with or without RPA for 5 min at room temperature (25°C). The RECQ5 proteins were added to a final concentration of 40nM and incubation was continued at 37°C for 20 min. Reaction products were analysed as in (A) and quantified using ImageQuant software. The results are the average of three independent experiments. **(D)** FRET-based ssDNA-annealing assay. The annealing was measured by monitoring the decrease in fluorescence at 525nm caused by FRET between fluorescein and hexachlorofluorescein labels on the oligonuclotide substrates as indicated. The reaction mixture contained 0.5 nM fluorescein-labelled SPFA DNA, 0.5nM hexachlorofluorescein-labelled complementary SPFB DNA and 30nM RECQ5β. **(E)** Time course of ssDNA annealing by RECQ5α and RECQ5β proteins measured by the assay in (C). Proteins were present at a concentration of 30nM. The fraction of annealed DNA (**Table 2**) was obtained by normalization of fluorescence signal F using the value F_{min} as obtained from the calibration measurement that corresponded to 100% annealing (see the Materials and methods section), i.e. fraction annealed=$(F_s - F)/(F_s - F_{min})$, where F_s is the fluorescence signal at the start of annealing.

Table 3 Summary of gel-filtration experiments

The experiments were performed using a Superdex75™ gel-filtration column run on an AKTA Purifier system (GE Healthcare). The column was equilibrated at a flow rate of 0.5ml/min with 20 mM Tris (pH 7.5), 150mM KCl and 1mM DTT. When required, 2mM $MgCl_2$, 1mM ATP or ATP[S] was added to the elution buffer. Approx. 30µg of recombinant RECQ5α was loaded. Proteins were detected at $A_{260/280}$. The experiments in the presence of ssDNA were performed by pre-incubating RECQ5α (2µM) with 2-fold molar excess of oligo SPC (see Supplementary Table 1) with or without 1mM nucleotide and 2mM $MgCl_2$ for 20 min at 25°C. Calibration of the column was performed with the pre-mixed standard proteins of known molecular masses (Sigma).

Sample	Apparent molecular mass (kDa)
23-mer	29.8±3.5
RECQ5α	42.6±6.4
RECQ5α+23-mer	93.9±16.9
RECQ5α+Mg^{2+}+ATP[S]	45.9±9.2
RECQ5α+Mg^{2+}+ATP[S]+23-mer	102.5±19.5

We found that, similar to RECQ5β, RECQ5α- mediated strand-annealing activity was inhibited by RPA in a dose-dependent manner (Fig. 4C). To quantitatively compare the DNA-annealing kinetics of the RECQ5 isoforms, a FRET based assay was used, which was essentially identical with the stop-flow helicase assay described above. The only difference was that the annealing assay monitored the decrease, instead of the increase, in the fluorescence emission due to FRET (Fig. 4D). The measured annealing reaction rates were 0.95 min^{-1} and 0.14 min^{-1} for RECQ5β and RECQ5α respectively. Thus RECQ5β promoted strand annealing approx. 7-fold faster than RECQ5α (Figure 2E). However, when evaluated by the extent of annealing, RECQ5α was more active than RECQ5β (Fig. 4E and Table 2).

In order to understand the molecular basis of the RECQ5α- mediated strand annealing, we studied the quaternary structure of RECQ5α in the absence and in the presence of ATP and/or ssDNA by means of size-exclusion chromatography on a Superdex™ 75 column. These experiments (Table 3) revealed an apparent molecular mass of 40~70kDa at all conditions tested, indicating that RECQ5α promotes strand annealing as a monomer (the predicted molecular mass of monomeric RECQ5α is 46.3kDa).

The RECQ5 helicase domain binds ATP efficiently, but displays a poor ATPase activity

To understand why RECQ5α does not catalyse DNA unwinding, we analysed its ATP-binding and ATPase activities relative to RECQ5β. To quantify ATP-binding of RECQ5α and RECQ5β, mantATP, a fluorescent analogue of ATP, was used. The apparent dissociation constants (*K*d) measured were 48.4±2.5 and 51.0±4.9μM for RECQ5α and RECQ5β respectively (Fig. 5A and Table 2), indicating that the two isoforms bind ATP with a similar affinity.

The ATPase activities of the RECQ5 proteins were determined by measuring the release of inorganic ^{32}Pi from ATP in the presence of denatured dsDNA (2.9 kb) (Fig. 5B). In agreement with previously published results (21), RECQ5β was found to exhibit a robust ATPase activity, with a k_{cat} of 15.6±1.4s^{-1}. However, under identical conditions, RECQ5α had no measurable ATPase activity (Fig. 5B and Table 2). These data indicate that the inability of RECQ5α to unwind DNA is caused by its failure to hydrolyse ATP. Moreover, these results provide an explanation for the differential effect of ATP on the strand-annealing activities of RECQ5α and RECQ5β (Fig. 5B). As RECQ5α cannot hydrolyse

ATP, it would persist in ATP-bound form, which is not proficient in strand annealing (21). In the case of RECQ5β, this inhibitory effect can be seen only with poorly hydrolysable ATP[S].

A zinc-binding motif is essential for the helicase activity of RECQ5β

The observation that the isolated helicase domain of RECQ5β failed to unwind dsDNA suggested a role for a C-terminal part of RECQ5β in performing its helicase function. Therefore C-terminal truncation mutants of RECQ5β, including RECQ5β$^{1-475}$ and RECQ5β$^{1-662}$, were assayed to identify the C-terminal region responsible for the intramolecular stimulation of the helicase activity of RECQ5β. We found that these two mutants had essentially identical ATPase and DNA-unwinding activities with respect to the full-length RECQ5β protein (Fig. 5B and Table 2). Together, these observations suggest that the region of RECQ5β spanning amino acid residues 410–475 that constitute the putative zinc-binding domain (Fig. 6A) play an essential role in the ATPase and helicase activities of the enzyme. Molecular modelling of the zinc-binding motif of RECQ5β revealed the distances between the cysteine side-chain sulfur groups and the zinc atom for Cys^{411} [2.46 Å (1 Å=0.1 nm)], Cys^{427} (2.36 Å), Cys^{431} (2.42 Å) and Cys^{434} (2.39 Å)] are close to the ideal distance (2.35± 0.09 Å) for structural metal zinc-co-ordination sites (28) (Fig. 6B). In agreement with this prediction, using a PAR assay, we found that RECQ5β contains 0.98± 0.18mol of Zn^{2+} ion (Fig. 6C and Table 2). Similar results were obtained for RECQ5β$^{1-475}$ and RECQ5β$^{1-662}$ deletion mutants (Table 2). In contrast, the PAR assay indicated that RECQ5α did not contain any Zn^{2+} ion, with a measured Zn^{2+} value of 0.03± 0.02 (Table 2). To evaluate further the role of the zinc-binding motif in the helicase function of RECQ5β, we generated a panel of mutants in which one or more of the four conserved cysteine residues were replaced by serine residues. However, these mutant proteins either formed aggregates or were degraded except for the C431S mutant, which was subjected to biochemical analysis. We found that the replacement of Cys^{431} with serine reduced the protein bound Zn^{2+} to 0.35±0.12mol (Table 2). Accordingly, this mutant had significantly reduced ATPase and helicase activities relative to wild-type RECQ5β (Fig. 3B and 5B, and Table 2). Taken together, these results suggest that the zinc-binding motif modulates the enzymatic activity of RECQ5β: it suppresses the strand-annealing function of the helicase domain and promotes strand separation.

Figure 5

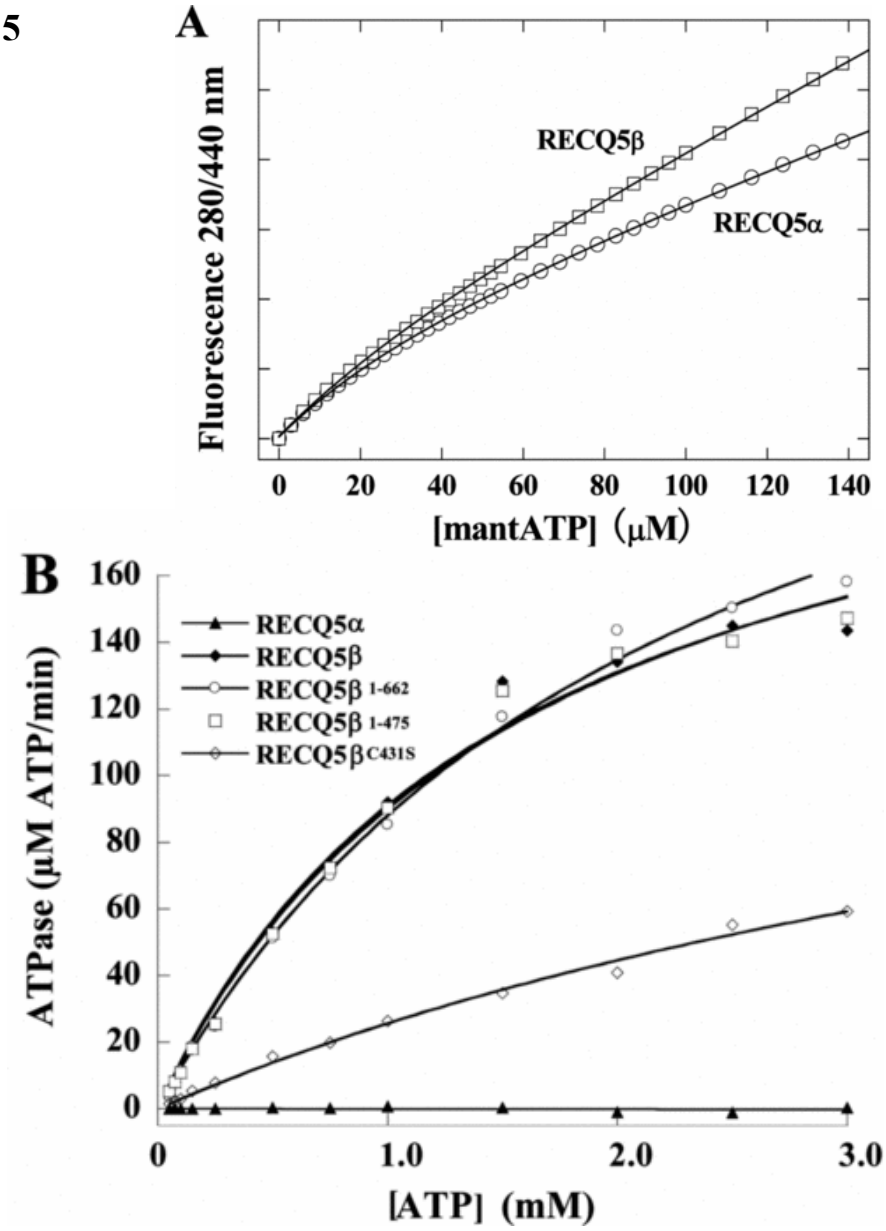

Fig. 5 ATP-binding affinity and ATPase activity of RECQ5 proteins

(A) Changes in fluorescence intensity at 440nm as 0.5μM RECQ5α and RECQ5β were titrated with an increasing concentration of mantATP. Solid lines represent the best fit of the data to eqn (1). Apparent K d values are summarized in Table 1. **(B)** ATPase activities of wild-type and mutant RECQ5 proteins. The initial rate of ATP hydrolysis by RECQ5 proteins is plotted as a function of the ATP concentration. Reactions contained 250nM RECQ5 proteins and 1.5μM heated dsDNA and were carried out as described in the Materials and methods section. The lines in the graph correspond to the best fits by Michaelis–Menten equation: $V = V_{max}$ [ATP]/(K_m +[ATP]), where V is the initial reaction rate, [ATP] is the concentration of ATP and k m is the Michaelis–Menten constant. Each value represents the mean of at least three independent measurements.

Figure 6

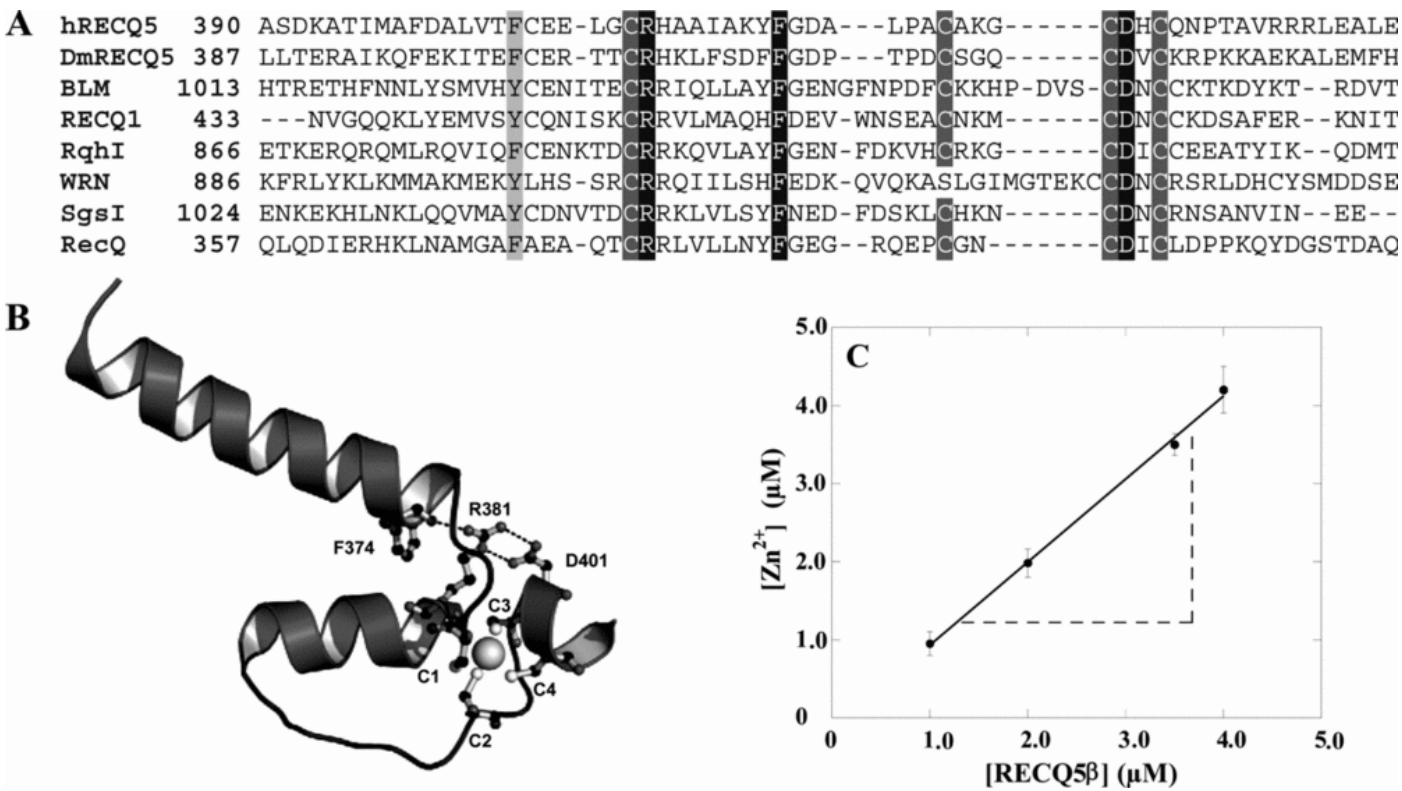

Fig. 6 Identification of the zinc-binding motif of RECQ5β helicase

(A) Amino-acid-sequence alignment of the zinc-binding domains of RecQ family helicases. The multiple sequence alignment was performed using ClustalW software and refined manually. The conserved cysteine residue and other residues are highlighted. **(B)** Ribbon diagram showing the zinc-binding domain of the RECQ5β helicase as revealed by molecular modelling based on the crystal structure of *E. coli* RecQ. The zinc ion is shown as a sphere. The positions of the four conserved cysteine residues are labelled as C1–C4. The conserved arginine, aspartic acid and aromatic residues, involved in three very important hydrogen bonds (broken lines) that stabilize the conformation of the zinc-binding domain, are shown in ball and stick representation. (**C**) Plot of the concentration of protein-bound Zn^{2+} against RECQ5β protein concentration as determined using the PAR assay. The absorption spectra were scanned from 300 to 600 nm at 25°C. As a control, 20 nmol of $ZnCl_2$ complexed with PAR was scanned under identical conditions.

Molecular mechanism of intramolecular stimulation of catalytic activity mediated by the zinc binding motif

In order to understand the molecular mechanism underlying the essential role of the zinc-binding motif in the helicase activity of RECQ5β, we compared the DNA-binding properties of RECQ5α and RECQ5β using a fluorescence polarization assay with fluorescently labelled oligonucleotide substrates (24). This method allows direct measurement of DNA binding in solution under equilibrium conditions. K_d values for RECQ5α and RECQ5β determined from protein titration curves indicated that RECQ5α displayed much lower binding affinities for ssDNA and dsDNA than RECQ5β (Fig. 7 and Table 2).

It has been shown that ATP binding stimulates DNA binding of some helicases, which in turn triggers ATP hydrolysis (29–32). Therefore we measured the DNA-binding activities of RECQ5 proteins in the presence of a non-hydrolysable ATP analogue, p[NH]ppA and/or ATP[S]. We found that the ssDNA-binding affinity of RECQ5β was enhanced approx. 2–3-fold in the presence of 2mM Mp[NH]ppA, whereas no noticeable effect could be observed with RECQ5α, even in the presence of ATP (ATP cannot be hydrolysed by RECQ5α; results not shown). These results imply that in RECQ5α there is no co-operativity between the ATP and DNA-binding sites.

To further explore the role of the zinc-binding motif in DNA binding by RECQ5β, the RECQ5β$^{1-475}$ and RECQ5β$^{1-662}$ truncation mutants were assayed for their DNA-binding activities. We found that these two mutants had similar DNA-binding affinities to the wild-type RECQ5β protein, suggesting that the non-conserved C-terminal region of RECQ5β does not play a role in DNA binding by the enzyme and that the zinc-binding motif confers the DNA-binding proficiency to the RECQ5β helicase core (Fig. 7A and 7B, and Table 2).

To determine whether the zinc-binding motif of RECQ5β is directly involved in DNA binding, we sought to examine the DNA-binding properties of the isolated zinc-binding domain. Our first attempts to generate a fragment including only the zinc-binding fold (RECQ5β$^{379-454}$) failed because this protein was found to be rapidly degraded. We then performed DNA binding experiments with RECQ5β$^{379-662}$ and RECQ5β$^{454-662}$ that could be purified to homogeneity. We found that RECQ5β$^{379-662}$, which contains the intact zinc-binding motif, was bound to DNA showing a preference for dsDNA (K_d values of 149± 6.7 nM and 680± 63nM for dsDNA and ssDNA respectively). In contrast, RECQ5β$^{454-662}$ with a truncated zinc-binding motif displayed hardly any detectable DNA-binding activity

(Figures 7C and 7D). Together, these experiments revealed that the zinc-binding domain enhances the DNA-binding affinity of the RECQ5β helicase core through direct DNA binding.

Model for the role of the zinc-binding motif in the function of RecQ helicases

Based on the results presented above, in combination with structural information for SF2 helicases, we proposed a model for the function of the zinc-binding motif of RecQ DNA helicases in DNA unwinding (Fig. 8). Crystal structures of several DNA helicases including the E. coli RecQ helicase core suggested that ATP is bound at the top of domain 1A, while the ssDNA substrate is bound at the bottom of domains 1A and 2A (Fig. 8). Since more residues in domain 1A are implicated in DNA binding than in domain 2A, as revealed by the crystal structures of NS3 helicase (33) and DEAD-Box helicase Vasa (34), it is likely that DNA may be bound more tightly to domain 1A than to domain 2A. Consequently, the portion of DNA that is bound to domain 2A may undergo large conformational fluctuation. In this case, the distance between the two helicase domains is too far to interact with each other to form the functional ATPase site that is essential for DNA unwinding. However, it is conceivable that while domain 1Abinds ssDNA tightly; domain 2A can capture another ssDNA molecule. Thus RECQ5α would function as a 'molecular crowding agent' (35) that increases the effective concentrations of ssDNA substrates, thereby promoting the hybridization between complementary ssDNA molecules (Fig. 8). However, in the presence of the zinc-binding motif, the double-stranded part of the DNA substrate would be tightly bound to the enzyme, enhancing the ssDNA binding to domain 2A (Fig. 8). The tight binding of DNA to domains 1A and 2A, in collaboration with ATP binding, brings the domains into the closed form. In this structure, ATP is efficiently hydrolysed and the energy is coupled to DNA unwinding.

Figure 7

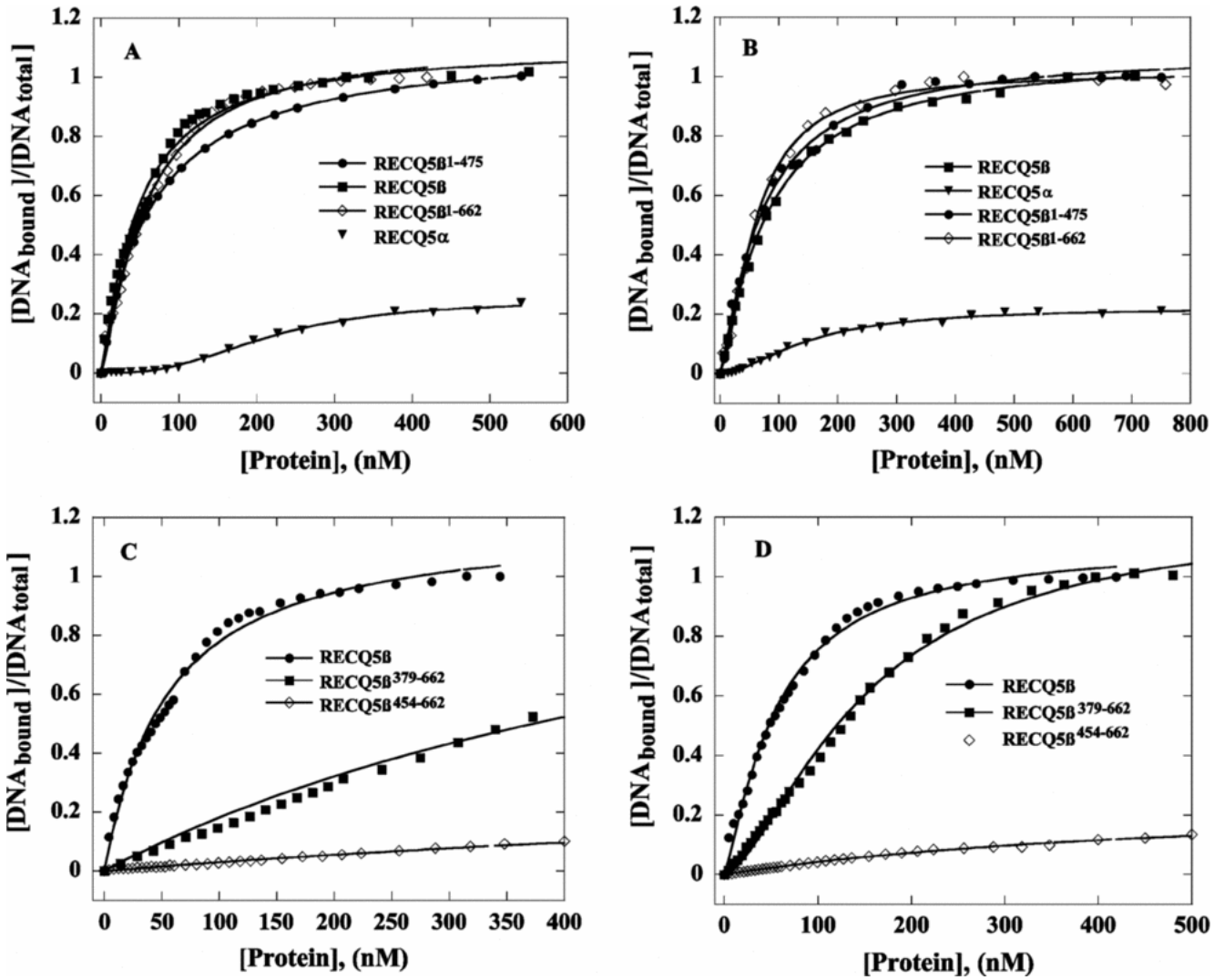

Fig. 7 DNA-binding activities of wild-type and mutant RECQ5 proteins

The anisotropy-based binding isotherms were obtained by varying the protein concentration in the presence of 5nM 3'-fluorescently labelled (**A** and **C**) ssDNA (BA) and (**B** and **D**) dsDNA (BA/BB). The data were fitted by Michaelis–Menten or Hill equations. The apparent K_d values are summarized in Table 2.

Figure 8

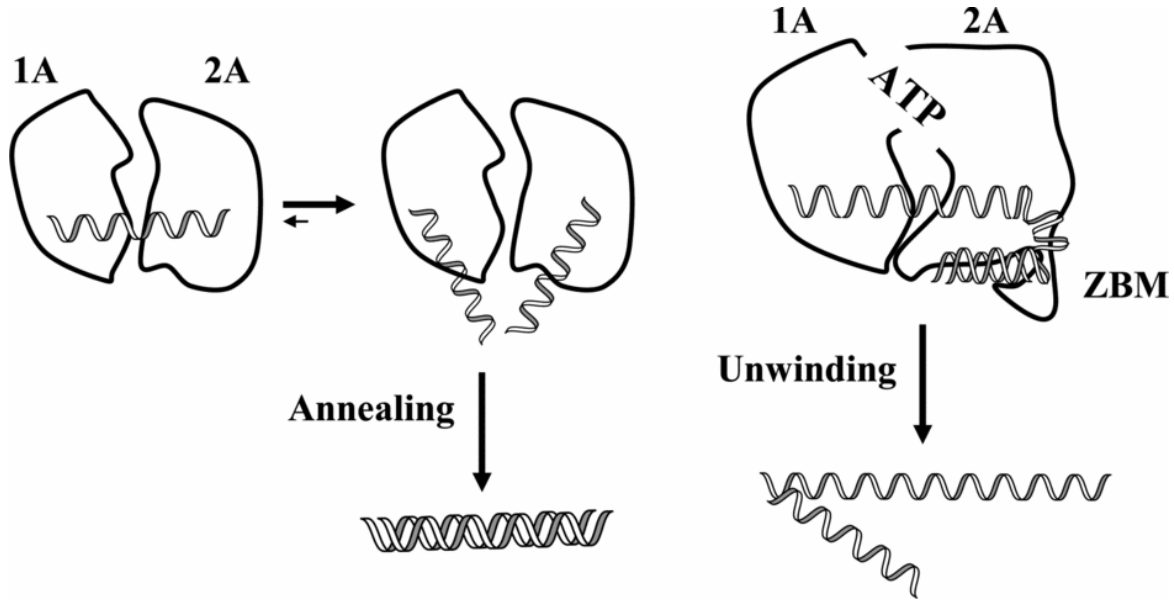

Fig. 8 Model for the role of the zinc-binding motif in the function of a RecQ helicase

In the absence of the zinc-binding motif (left-hand side), the helicase domains bind ssDNA with low affinity. Although one part of the ssDNA binds relatively tightly to domain 1A, the other part of the ssDNA may dissociate from domain 2A due to thermal fluctuation, providing an opportunity for domain 2A to capture a complementary ssDNA. In this situation, RECQ5α brings the two complementary strands into close proximity, promoting the hybridization of the complementary ssDNA. In this state, although ATP is bound tightly to domain 1A, the distance between domains 1A and 2A is too long to form a functional ATPase site. In the presence of the zinc-binding motif (ZBM; right-hand side), the DNA substrate is tightly bound to the enzyme through an additional interaction between the zinc-binding motif and the duplex region of the substrate, which stabilizes ssDNA binding to the domains 1A and 2A. This tight DNA binding induces conformational changes in the protein that bring the two helicase sub-domains into a closed form, allowing ATP hydrolysis, a prerequisite for helicase function.

CONCLUDING REMARKS

The zinc-binding motif conserved among the RecQ family helicases does not have substantial structural similarity with any other known zinc-finger folds. It is therefore important to determine its specific function in the RecQ helicase family. We have previously shown that the zinc-binding motifs of *E. coli* RecQ and human BLM are important for DNA binding and protein folding of these helicases (25, 36). Thus there is a clear correlation between the presence of the zinc-binding motif and the helicase activity of RecQ helicases. Interestingly, the human RECQ4 protein, the only RecQ family member without a zinc-binding motif, fails to unwind DNA, but catalyses DNA annealing, which is in agreement with our results obtained with RECQ5α (37). Thus all of these studies establish the RecQ-specific zinc-binding motif as an essential DNA-binding module required for RecQ family helicase activity.

REFERENCES

1. Lohman, T. M. and Bjornson, K. P. (1996) Mechanisms of helicase-catalyzed DNA unwinding. *Annu. Rev. Biochem*., **65,** 169–214.

2. Soultanas, P. and Wigley, D. B. (2000) DNA helicases: 'inching forward'. *Curr. Opin. Struct. Biol.,* **10,** 124–128.

3. Caruthers, J. M. and McKay, D. B. (2002) Helicase structure and mechanism. *Curr. Opin. Struct. Biol.*, **12,** 123–133.

4. Singleton, M. R. and Wigley, D. B. (2002) Modularity and specialization in superfamily 1 and 2 helicases. *J. Bacteriol.,* **184,** 1819–1826.

5. Yamagata, K., Kato, J., Shimamoto, A., Goto, M., Furuichi, Y. and Ikeda, H. (1998) Bloom's and Werner's syndrome genes suppress hyperrecombination in yeast sgs1 mutant: implication for genomic instability in human diseases. *Proc. Natl. Acad. Sci. U.S.A*, **95,** 8733–8738.

6. Hanada, K., Ukita, T., Kohno, Y., Saito, K., Kato, J. and Ikeda, H. (1997) RecQ DNA helicase is a suppressor of illegitimate recombination in Escherichia coli. *Proc. Natl. Acad. Sci. U.S.A.,* **94,** 3860–3865.

7. Hickson, I. D. (2003) RecQ helicases: caretakers of the genome. *Nat. Rev. Cancer,* **3,** 169–178.

8. Mankouri, H. W. and Hickson, I. D. (2004) Understanding the roles of RecQ helicases in the maintenance of genome integrity and suppression of tumorigenesis. *Biochem. Soc. Trans.,* **32,** 957–958.

9. Puranam, K. L. and Blackshear, P. J. (1994) Cloning and characterization of RECQL, a potential human homologue of the Escherichia coli DNA helicase RecQ. *J. Biol. Chem.,* **269,** 29838–29845.

10. Seki, M., Miyazawa, H., Tada, S., Yanagisawa, J., Yamaoka, T., Hoshino, S., Ozawa, K., Eki, T., Nogami, M., Okumura, K. et al. (1994) Molecular cloning of cDNA encoding human DNA helicase Q1 which has homology to Escherichia coli Rec Q helicase and localization of the gene at chromosome 12p12. *Nucleic Acids Res.,* **22,** 4566–4573.

11. Ellis, N. A., Groden, J., Ye, T. Z., Straughen, J., Lennon, D. J., Ciocci, S., Proytcheva, M. and German, J. (1995) The Bloom's syndrome gene product is homologous to RecQ helicases. *Cell,* **83,** 655–666.

12. Yu, C. E., Oshima, J., Fu, Y. H., Wijsman, E. M., Hisama, F., Alisch, R., Matthews, S., Nakura, J., Miki, T., Ouais, S. et al. (1996) Positional cloning of the Werner's syndrome gene. *Science,* **272,** 258–262.

13. Kitao, S., Ohsugi, I., Ichikawa, K., Goto, M., Furuichi, Y. and Shimamoto, A. (1998) Cloning of two new human helicase genes of the RecQ family: biological significance of multiple species in higher eukaryotes. *Genomics*, **54,** 443–452.

14. Shimamoto, A., Nishikawa, K., Kitao, S. and Furuichi, Y. (2000) Human RecQ5β, a large isomer of RecQ5 DNA helicase, localizes in the nucleoplasm and interacts with topoisomerases 3α and 3β. *Nucleic Acids Res.,* **28,** 1647–1655.

15. Karow, J. K., Wu, L. and Hickson, I. D. (2000) RecQ family helicases: roles in cancer and aging. Curr. Opin. *Genet. Dev.,* **10,** 32–38.

16. Morozov, V., Mushegian, A. R., Koonin, E. V. and Bork, P. (1997) A putative nucleic acid-binding domain in Bloom's and Werner's syndrome helicases. *Trends Biochem. Sci.* **22,** 417–418.

17. Bernstein, D. A., Zittel, M. C. and Keck, J. L. (2003) High-resolution structure of the E. coli RecQ helicase catalytic core. *EMBO J.,* **22,** 4910–4921.

18. Bachrati, C. Z. and Hickson, I. D. (2003) RecQ helicases: suppressors of tumorigenesis and premature aging. *Biochem. J.*, **374,** 577–606

19. Hu, J. S., Feng, H., Zeng, W., Lin, G. X. and Xi, X. G. (2005) Solution structure of a multifunctional DNA- and protein-binding motif of human Werner syndrome protein. *Proc. Natl. Acad. Sci. U.S.A.,* **102,** 18379–18384.

20. Sekelsky, J. J., Brodsky, M. H., Rubin, G. M. and Hawley, R. S. (1999) Drosophila and human RecQ5 exist in different isoforms generated by alternative splicing. *Nucleic Acids Res.*, **27,** 3762–3769.

21. Garcia, P. L., Liu, Y., Jiricny, J., West, S. C. and Janscak, P. (2004) Human RECQ5β, a protein with DNA helicase and strand-annealing activities in a single polypeptide. *EMBO J.,* **23,** 2882–2891

22. Kanagaraj, R., Saydam, N., Garcia, P. L., Zheng, L. and Janscak, P. (2006) Human RECQ5β helicase promotes strand exchange on synthetic DNA structures resembling a stalled replication fork. *Nucleic Acids Res.,* **34,** 5217–5231.

23. Henricksen, L. A., Umbricht, C. B. and Wold, M. S. (1994) Recombinant replication protein A: expression, complex formation, and functional characterization. *J. Biol. Chem.,* **269,** 11121–11132.

24. Dou, S. X., Wang, P. Y., Xu, H. Q. and Xi, X. G. (2004) The DNA binding properties of the Escherichia coli RecQ helicase. *J. Biol. Chem.,* **279**, 6354–6363.

25. Guo, R. B., Rigolet, P., Zargarian, L., Fermandjian, S. and Xi, X. G. (2005) Structural and functional characterizations reveal the importance of a zinc binding domain in Bloom's syndrome helicase. *Nucleic Acids Res.,* **33,** 3109–3124.

26. Zhang, X. D., Dou, S. X., Xie, P., Wang, P. Y. and Xi, X. G. (2005) RecQ helicase- catalyzed DNA unwinding detected by fluorescence resonance energy transfer. Acta *Biochim. Biophys. Sin. (Shanghai),* **37,** 593–600.

27. Sharma, S., Sommers, J. A., Choudhary, S., Faulkner, J. K., Cui, S., Andreoli, L., Muzzolini, L., Vindigni, A. and Brosh, Jr, R. M. (2005) Biochemical analysis of the DNA unwinding and strand annealing activities catalyzed by human RECQ1. *J. Biol. Chem.,* **280,** 28072–28084.

28. Alberts, I. L., Nadassy, K. and Wodak, S. J. (1998) Analysis of zinc binding sites in protein crystal structures. *Protein Sci.,* **7,** 1700–1716.

29. Wong, I. and Lohman, T. M. (1992) Allosteric effects of nucleotide cofactors on Escherichia coli Rep helicase-DNA binding. *Science,* **256,** 350–355.

30. Jezewska, M. J. and Bujalowski, W. (1996) Global conformational transitions in Escherichia coli primary replicative helicase DnaB protein induced by ATP, ADP, and single-stranded DNA binding. Multiple conformational states of the helicase hexamer. *J. Biol. Chem.,* **271,** 4261–4265.

31. Jezewska, M. J. and Bujalowski, W. (2000) Interactions of Escherichia coli replicative helicase PriA protein with single-stranded DNA. *Biochemistry* **39,** 10454–10467.

32. Bujalowski, W. and Jezewska, M. J. (2000) Kinetic mechanism of nucleotide cofactor binding to Escherichia coli replicative helicase DnaB protein. Stopped-flow kinetic studies using fluorescent, ribose-, and base-modified nucleotide analogues. *Biochemistry,* **39,** 2106–2122.

33. Kim, J. L., Morgenstern, K. A., Griffith, J. P., Dwyer, M. D., Thomson, J. A., Murcko, M. A., Lin, C. and Caron, P. R. (1998) Hepatitis C virus NS3 RNA helicase domain with a bound oligonucleotide: the crystal structure provides insights into the mode of unwinding. *Structure,* **6,** 89–100.

34. Sengoku, T., Nureki, O., Nakamura, A., Kobayashi, S. and Yokoyama, S. (2006) Structural basis for RNA unwinding by the DEAD-box protein Drosophila Vasa. *Cell,* **125,** 287–300.

35. Minton, A. P. (1997) Influence of excluded volume upon macromolecular structure and associations in 'crowded' media. *Curr. Opin. Biotechnol.,* **8,** 65–69.

36. Liu, J. L., Rigolet, P., Dou, S. X., Wang, P. Y. and Xi, X. G. (2004) The zinc finger motif of Escherichia coli RecQ is implicated in both DNA binding and protein folding. *J. Biol. Chem.,* **279,** 42794–42802.

37. Macris, M. A., Krejci, L., Bussen, W., Shimamoto, A. and Sung, P. (2006) Biochemical characterization of the RECQ4 protein, mutated in Rothmund–Thomson syndrome. *DNA Repair (Amst),* **5,** 172–180.

II Biochemical Characterization of Helicase Activity and DNA Substrate Specificity of *Bacillus subtilis* RecQ Helicases

Running title: Biochemical properties of RECQ helicases from *Bacillus subtillis*

The abbreviations used are: dsDNA, double-stranded DNA; ssDNA, single-stranded DNA; PAGE, polyacrylamide gel electrophoresis; AMP-PNP, 5'-adenyl-β,γ-imidodiphosphate; FPLC, fast protein liquid chromatography; NTP, nucleotide triphosphate; DNP, nucleotide diphosphate; PAR, 4-(2-Pyridylazo)resorcinol;

ACKNOWLEDGEMENT

In this party, we thank Drs. P.fosse, F.Chaminade and Y.Y.Zhang for help analysis EMSA and autoradiography experiments, Drs. E. Deprez, P. Tauc and J.-C. Brochon for help with TFA experiments, Dr. H. Leh for help with FPLC, and A. Vignes for preparation of the figures. We thank Professor C. Auclair for his continuous support. This work was supported by the China Scholarship Council.

SUMMARY

RecQ DNA helicases function during DNA replication and are essential for the maintenance of genome stability. The Bacteria *Bacillus subtilis* SubL and SubS proteins are two members of the RecQ DNA helicase family which includes the *Escherichia coli.* RecQ, BLM, WRN and RECQ4. Here we report biochemical characterizations of these two RecQ helicases from *Bacillus subtilis*. To study the enzymatic characteristics of the proteins, the recombinant SubL and SubS proteins have been over expressed in *E.coli* and purified to near homogeneity. These two recombinant SubL and SubS protein possessed ATPase activity in the presence of single- or double-stranded DNA, but single-stranded DNA is more effective cofactor. Moreover, they exhibit ATP- and Mg^{2+}-dependent DNA helicase activity that occur in the in the 3' to 5' direction with respect to the single-stranded DNA to which the SubRecQ binds. The efficiency of unwinding was found to correlate inversely with the length of the duplex region of DNA. In addition, the recombinant SubRecQ helicases were found to bind more tightly to a forked double DNA substrate than to single-stranded DNA and SubS can bind more tightly with single-stranded DNA than SubL. The SubRecQ helicases are not capable of unwinding duplex DNA from a blunt-ended terminus, but SubL was found to possess an intrinsic DNA strand-annealing activity. However, it's the SubL not SubS that can unwind the same blunt-ended duplex containing a synthetic X-structure (a model for the Holliday junction recombination intermediate) and an internal nick DNA structure. SubL can recognize the fork structure and unwind two important intermediates of replication/repair, a 5'-ssDNA flap substrate and a synthetic replication fork.

INTRODUCTON

The RecQ helicase family plays an important role in nearly all DNA metabolic processes, including DNA replication, recombination and repair (1). These family members are found in diverse organisms, such as bacteria (1;4;5), yeast (1;6-8), fungi (1;9), flies (1;10), frogs (1;11), and humans (1;12-16). RecQ helicases are highly conserved from bacteria to humans. Proteins belonging to the RecQ family contain an about 450 amino acids core sequence harbouring the seven helicase motifs: I, Ia, II, III, IV and VI. The motifs I and II are the highly conserved Walker A and B sequences characteristic of ATPase activities. RecQ helicase family also contains a C-terminal extension that is divided into two domains called the RecQ-Ct (RecQ C-terminal) domain and the HRDC (helicase and RNase D-C terminal) domain. The proximal domain, RecQ-Ct domain, appears to be unique to RecQ family helicases and contains a Zn^{2+}-binding site and a poorly conserved winged helix-trun-helix (WH) motif (17). The distal domain, HRDC domain, is similar to domains in RNase D and eukaryotic homologues.

In all organisms, defective RecQ helicase is associated with genomic instability, which is generally manifested as an increase in the frequency of inappropriate recombination events. Mutations in genes encoding the human RecQ helicases BLM (18), WRN (19) and RecQ4 (20) will give rise to the hereditary disorders Bloom's syndrome, Werner's syndrome and Rothmund-Thomson syndrome, respectively (21). These diseases are associated with cancer predisposition and variable signs of premature aging. Although the precise DNA metabolism mediated by RecQ helicase remains elusive, the enzyme has been implicated in DNA replication, recombination and repair (22).

The RecQ helicases BLM, WRN and RECQ5β have the strand-annealing activity and catalyze strand exchange by combining DNA-unwinding and strand-annealing activities (23;24). However, we couldn't find this phenomenon in *E.coli* RecQ helicase. Unliked *E.coli* containing only one RecQ protein with DNA helicase activity, higher species could possess more than one such putative helicase (25;26). It's similar with the fact that human cells contain five RecQ helicases (RecQ1, BLM, WRN, RecQ4 and RecQ5) (27;28). Although the amino acids sequence of *Bacillus subtilis* has not yet been tested, it seems to be nonessential for cell viability (28;29).

Bacillus subtilis is a Gram-positive, spore-forming bacterium. BLAST analysis identifies a sequence in the chromosome of *B. subtilis* RecQL encoding a 591-amino-acid protein that shares 61% identity and 76% similarity with the *E. coli* RecQ helicase (Fig.1) that may be a RecQ homologue. The protein sequence of SubS is 496 amino acids long which 46%

consistent and 66% similar with the RecQ helicase of *E.coli* (Fig.1). We studied whether this putative *B. subtilis* RecQ helicases have biochemical activities similar to those of *E. coli* RecQ helicase. We overproduced and purified these two proteins as a fusion with a histidine tag (His_6) and investigated their biochemical activities. The putative *B. subtilis* RecQL and RecQS helicases appear to be DNA-dependent ATPases and 3'to 5' DNA helicases, and *B. subtilis* RecQL has many of the biochemical characteristics of a RecQ family helicase. But *B. subtilis* RecQS does not show these biochemical activities as *E.coli* RecQ helicase. So the protein probably makes an essential contribution to maintaining chromosome stability. According to the amino acid sequence of these two *B. subtilis* RecQ helicases, there is both a RecQ-Ct motif containing zinc finger domain and HRDC motif in SubL protein. This phenomenon is homologous to the structures of most SF2 helicases such as *E.coli* RecQ (30-32). But interestingly we found that SubS helicase doesn't have the HRDC motif. The previous studies indicated that the zinc binding site of RecQ-Ct and HRDC motif are very important for the protein structure and the enzyme function of the RecQ helicases (3;33). In this part, we will discover some important helicase characters and functions of SubL and SubS. Moreover we want to indicate the roles of zinc finger domain and HRDC motif in the *Bacillus subtilis* RecQ family.

MATERIALS AND METHODS

Reagents

Chemicals were reagent grade and all solutions were prepared using ELGA pure water. [γ-^{32}P] ATP was purchased from PerkinElmer. EDTA, 2-mercaptoethanol, nucleotides, deoxynucleotides, AMPPNP and *E.coli* single strand DNA binding protein (ESSB) were obtained from Sigma. T4 polynucleotide kinase was from New England Biolabs. TE: 10mM Tris-HCl (pH8.0), 1mM EDTA (pH8.0). Unstained protein Molecular Weight Marker (#SM0431) was purchased from Fermentas. TBE buffer: 89mM Tris-Base, 89mM Boric acid, 2mM EDTA, pH8.0.

Nucleic Acid Substrates

Oligonucleotides were purchased from Eurogentec and further purified by polyacrylamide gel electrophoresis. The phiX174 virion circle ssDNA was obtained from Biolabs. The sequences and the structures of the oligonucleotides used for helicase activity measurement in this study are listed in Tables 1 and 2, respectively. A single oligonucleotide was 5'-end-labbelled with [γ-^{32}P] ATP using T4 polynucleotide kinase and purified with Sephadex-G25-TE column. The labelled oligonucleotide was annealed to their unlabelled complementary strands at a 1:1-2 molar ratios by incubation at 95 ℃ for 5 min followed by slow cooling to room temperature. For purification of the substrates, the annealed oligonucleotides were purified with Sephadex-G50, G75, and G100 TE columns respectively, according to their length. The DNA or RNA used for a cofactor of ATPase activity of *Bacillus subtilis* helicase are: 53nt ssDNA, 7kb PN6 DNA linear, 5.5kb GC70-plasmid DNA, 5.5kb GC70-plasmid DNA denatured, 678nt RNA.

Template selection and amino acid sequence alignment

A template search was performed by comparing the sequences of interest in *B. subtilis* RecQ helicases with the *E.coli* RecQ using NCBI Blast (34). The sequence of *E.coli* RecQ could be aligned with 39% identity and 58% similarity with the sequence of *B. subtilis* putative RecQL helicase. And it showed 42% identity and 66% similarity to the sequence of SubS.

Table 1 Oligonucleotides used for helicase measurement in this chapter

Name	Length (nt)	Sequence (5'-3')
1	44	GCACTGGCCGTCGTTTTACGGTCGTGACTGGGAAAACCCTGGCG
2	45	TTTTTTTTTTTTTTTTTTTTTCCAAGTAAAACGACGGCCAGTGC
3	19	GTAAAACGACGGCCAGTGC
4	20	AGTAAAACGACGGCCAGTGC
5	24	TCCAAGTAAAACGACGGCCAGTGC
6	29	TTTTTTCCAAGTAAAACGACGGCCAGTGC
7	20	GCACTGGCCGTCGTTTTACG
8	24	GCACTGGCCGTCGTTTTACGGTCG
9	29	GCACTGGCCGTCGTTTTACGGTCGTGACT
10	44	GCACTGGCCGTCGTTTTACGGTCGTGACTGGGAAAACCCTGGCG
11	25	CGCCAGGGTTTTCCCAGTCACGACC
12	44	CGCCAGGGTTTTCCCAGTCACGACCAACCCCTTTTTTTTTCAA
13	20	TTGGAAAAAAAAAAAAAAAAAAAAAA
14	70	TGCAGTAGCGCCAATATGAGAAGAGCCATACCGCTGATTCTGCGTTTGCTGATGAACTAAGTCAACCTCA
15	19	GCACTGGCCGTCGTTTTACG
16	19	GCACTGGCCGTCGTTTTACGGTCG
17	40	ACGTGGGCAAAGGTTCGTCAATGGACTGACAGCTGCATGG
18	19	GACGAACCTTTGCCCACGT
19	21	CCATGCAGCTGTCAGTCCATT
20	19	CCATGCAGCTGTCAGTCCA
21	16	CCATGCAGCTGTCAGT
22	50	TCAAAGTCACGACCTAGACACTGCGAGCTCGAATTCACTGGAGTGACCTC
23	50	GAGGTCACTCCAGTGAATTCGAGCTCGCAGTGTCTAGGTCGTGACTTTGA
24	41	GCCGTGATCACCAATGCAGATTGACGAACCTTTGCCCACGT
25	41	GACGTGGGCAAAGGTTCGTCAATGGACTGACAGCTGCATGG
26	41	GCCATGCAGCTGTCAGTCCATTGTCATGCTAGGCCTACTGC
27	41	GGCAGTAGGCCTAGCATGACAATCTGCATTGGTGATCACGG
28	5386	PhiX 174 circle ssDNA
29	20	TCAGCACCAGCACGCTCCCA
30	35	TCAGCACCAGCACGCTCCCATTTTTTTTTTTTTTT
31	35	AAAAAAAAAAAAAAATCAGCACCAGCACGCTCCCA

Table 2 Structures of substrates

Name	Structure	Oligos
A		1*+2
B		1*+3
C		1*+4
D		1*+5
E		1*+6
F		3*+7
G		3*+8
H		3*+9
I		3*+10
J		1*+2+11

Name	Structure	Oligos
K		1*+2+12
L		1*+2+11+14
M		14*+15
N		14*+16
O		17*+18+19
P		17*+18+20
Q		17*+18+21
R		22*+23
S		24*+25+26+27

Protein Expression

The full coding region of *Bacillus subtilis* RecQL and RecQS helicases DNA were prepared by PCR using *Bacillus subtilis* strain QST713 chromosome DNA as template. A 1.8-kb PCR product and 1.5-kb PCR product were cloned into pGEM®-T easy vector respectively, and the sequences of these inserts were shown to be identical to the published *Bacillus subtilis* RecQ helicase gene sequence (Genebank No: F69901 and No: L47648).

The DNA corresponding to the coding sequence of the *Bacillus subtilis* RecQL helicase gene was amplified again by PCR-mediated amplification, using a set of oligonucleotides corresponding to the 5'- and 3'-ends of the gene. These primers had additional bases at each end for creation of restriction sites: *NdeI* at the 5'-end (5'-CAT ATG TTA CAT AGA GCC CAA TCC CTT CTG GCT CAT-3') and *XhoI* at the 3'-end of the gene (5'-ATA CAG GCT TAT GCA AGG ATG ACA GAC TAA CTC GAG-3') for expression of the *Bacillus subtilis* RecQL helicase bearing a hexahistidine tag at the N-terminal end. The DNA corresponding to the 5'- and 3'-ends of gene. These primers had additional bases at each end for creation of restriction sites: *NdeI* at 5'-end (5'-CAT ATG ACT AAA TTA CAG CAA ACG TTA TAT CAG TTT-3') and *XhoI* at the 3'-end of the gene (5'-AGC TTG CAG ACT GTA GGT GAG CTG AAC TGA CTC GAG-3') for expression of the SubS helicase bearing a hexahistidine tag at the NH_2-terminal end. The amplified products were digested with *NdeI* and *XhoI* enzymes, and the appropriate size fragments (1776 bp and 1488bp, respectively) were gel-purified and then subcloned into *NdeI/XhoI* sites of the vector pET-15b. The pET-15b vector encodes a hexa-histidine tag at the amino terminus that allows purification of the expressed protein on a nickel-chelating column. A thrombin cleavage site was adjacent to the histidine tag. The constructed plasmids were transformed in *E. coli* strain Rosetta and BL21 (DE3)/TrxB, respectively. The bacteria containing SubL protein were grown at 37°C in terrific broth supplemented with 100μg/mL ampicillin and 34μg/mL chloramphenicol. However, the bacteria which contain SubS helicase were grown at 37°C in terrific broth supplemented with 50μg/mL ampicillin and 15μg/mL kanamycin. Before inducing the SubS helicase expression, we hot shock the bacteria at 42°C for 1 hour. The expressions of these two proteins were induced by adding isopropylthio-D-galactoside to 0.3mM at low log phase (A600 = 0.6). The cultures were then incubated for 12-14 h at 15-18°C. Cells were harvested by centrifugation at 3,000 × g for 15 min at 4°C.

Protein Purification

His-tagged *Bacillus subtilis* RecQL and RecQS helicases were overexpressed in *E. coli* Rosetta and BL21 (DE3)/TrxB purified under native conditions. Briefly, harvested cells were suspended in 30 ml of suspension buffer (20mM Tris-HCl, pH 8.0, 5mM imidazole, 500mM NaCl) per 1 L culture and were lysed using a French pressure cell. The lysate was then sonicated in order to shear DNA into small fragments. The lysate was cleared by centrifugation at 7,000 ×g for 30 min at 4°C. The supernatant was applied to the column charged with histidine binding resin (Novagen). The column was washed with 20mM Tris-HCl (pH 8.0) buffer containing 500mM NaCl, 5mM imidazole. The proteins bound to the column were eluted stepwise using 20mM Tris-HCl (pH 8.0) buffer containing 5, 60, 80, 200, or 500mM imidazole. The *Bacillus subtilis* RecQ helicase-containing fractions, identified by both DNA-dependent ATP hydrolysis and helicase activity assays, were pooled. The *Bacillus subtilis* RecQ helicases were further purified by HPLC size exclusion chromatography (Superdex 200; Amersham Biosciences). The active fractions were pooled, dialyzed against storage buffer (20mM Tris-HCl, pH 8.0, 500mM NaCl, 1mM dithiothreitol, 10% glycerol), and stored at –80°C. The proteins were pure as judged by Coomassie staining and electrospray mass spectrometry. Proteins concentrations were determined spectrophotometrically using a Bio-Rad Protein Assay.

Quantification of Zinc Ion Bound to SubL and SubS helicases

We measured the zinc content of SubL and SubS helicases by the PAR (4-(2-Pyridylazo) resorcinol) assay according to Hunt *et al*. PAR has a low absorbance at 490nm in the absence of zinc ion due to the formation of the $(PAR_2)\cdot Zn^{2+}$ complex. To facilitate zinc release; the volume of zinc was adjusted to 0.5ml with buffer A (20mM Tris-HCl at pH8.0, 500mM NaCl). PAR was added into the cuvette for a final concentration of 100μM. The absorbance at 500 nm was measured. The quantity of zinc was determined from a standard curve of $ZnCl_2$ samples in a range of concentrations using the sample preparation procedure as described above with the *B. Subtilis* helicase omitted. Then we measured the zinc ion concentration using the absorbance coefficient for the $(PAR_2)\cdot Zn^{2+}$ complex. ($\varepsilon_{490nm}=6.6 \times 10^4\ M^{-1}\ cm^{-1}$)

Size Exclusion Chromatography of SubL

Size exclusion chromatography was performed at 18°C using an HPLC system (ÄKTA Purifier, GE Healthcare) on a Superdex 200 (analytical grade) column equilibrated with elution buffer. Fractions of 0.5 ml were collected at a flow rate of 0.4ml/min, and absorbance was measured at 280 and 260 nm. The partition coefficient K_{av} was calculated using the formula $K_{av} = (V_e - V_0)/(V_t - V_0)$, where V_e is the elution volume of the sample, V_0 is the excluded volume of the column; V_t is the total volume of the column. The excluded volume, V_0 (7.52ml) and the total volume, V_t (23.5ml) were measured by calibration with Dextran blue and thymidine. The calibration graph of log Rs versus K_{av} was constructed using a high and low molecular weight calibration kit from Sigma : cytochrome c (Mw=12.4 kDa; Rs=12 Å), carbonic anhydrase (Mw=29 kDa; Rs=22.5 Å), albumin (Mw=67 kDa; Rs=35.5 Å), phosphorylase b (Mw=97.4 kDa; Rs=38.75 Å), thyroglobulin (Mw=669 kDa; Rs=85 Å). Assuming similar shape factors, the plot calibration of log Mw versus K_{av} allowed the determination in first approximation of the molecular weight of helicase. Gel filtration chromatography was performed using a standard elution buffer (50mM Tris-Cl (pH 7.5), 400mM NaCl, and 0.1mM EDTA).

ATPase Assay

The ATPase activity was determined in an assay by measuring the radioactive ^{32}Pi liberated during hydrolysis. The measurement was carried out at 37°C for 30 min in a 40µl reaction mixture (50mM Tris-HCl pH8.0, 25mM NaCl, 5mM $MgCl_2$, 50µg/ml BSA and 1mM DTT) containing the indicated concentration of DNA or RNA. The reactions were initiated by the addition of an appropriate concentration of RecQ helicase into 40µl of reaction mixture and stopped by transferring 35µl of aliquots from the reaction mixture every 20s into a hydrochloric solution of ammonium molybdate. The liberated radioactive ^{32}Pi was extracted with a solution of 2-butanol-cyclohexane-acetone-ammonium molybdate (250:250:50:0.1) saturated with water. An aliquot of the organic phase was counted.

DNA helicase assay

The helicase assay measures the unwinding of a γ-^{32}P-labeled DNA fragment from a partial duplex DNA molecule. The 20µl reaction mixture contained 50mM Tris–HCl pH 8.0, 1mM DTT, 6mM NaCl, 5mM $MgCl_2$, 2.5mM ATP, 50µg/ml BSA and ^{32}P-labeled helicase

substrate (~0.45nM). The recombinant *Bacillus subtilis* RecQ proteins at the indicated concentrations were added to the mixture and incubated at 37°C for 30 min. The reaction was terminated by the addition of 0.5%SDS, 20mM EDTA, 50% glycerol and 0.05% bromphenol blue (unwinding-stopping buffer). The products of the reaction were fractionated by electrophoresis on a 12% non-denaturing polyacrylamide gel (acrylamide to bis-acrylamide, 19:1 (w/w)) and ran in 1 × TBE buffer for 2 hours at 200V at 10°C. The gel was dried and exposed using a phosphorimager and analysed with ImageQuant softwave (Molecular Dynamics).

Protein-DNA Binding Assay by EMSA

0.45nM 5'-32P-lablled DNA substrate and appropriate concentration of the protein were incubated at 37°C for 20 minutes in DNA binding buffer (50mM Tris–HCl (pH 8,0), 1mM DTT, 20mM NaCl, and 10% (v/v) glycerol). Samples were subsequently subjected to electrophoresis through a non-denaturing 6% polyacrylamide gel (acrylamide to bis-acrylamide, 19:1 (w/w)) run in 1 X TBE buffer at 200V at 10°C for 2 hours to separate protein–DNA complex from free DNA substrates. Gels were dried and visualized using a phosphorimager and analysed with ImageQuant softwave (Molecular Dynamics).

DNA strand-annealing and strand-exchange assay

The DNA strand-annealing activity of the *Bacillus subtilis* RecQL and RecQS were assayed using complementary synthetic oligonucleotides (each at a concentration of 0.2nM) of which one was labelled at the 5′-end using [γ-^{32}P]ATP and T4 polynucleotide kinase. In a standard strand-annealing assay, the labelled oligonucleotide (oligonucleotide 22) was added to a reaction buffer (20µl) containing 50mM Tris-HCl (pH8,0), 5mM $MgCl_2$, 20mM NaCl, 1mM DTT, 50µg/ml BSA and the indicated protein concentration. The reaction was initiated by adding the unlabelled oligonucleotide (oligonucleotide 23), immediately followed by incubation at 37°C for 10 min. The resulting DNA products were analysed as described for the helicase reactions. The strand-exchange assays were performed essentially as described by Machwe *et al.* with some modifications (35). Briefly, the labelled forked substrate (oligonucleotides 1 and 2) and ssDNA (oligonucleotide 11) (1nM) were incubated with 400nM protein in a 20µl helicase reaction buffer for increasing time from 5 min to 30

min. After addition of 2.5mM ATP, the DNA products were subsequently monitored over time.

RESULTS

Molecular modelling

We constructed a homology model for the *B. subtilis* RecQ helicases for which a template structure was available. The models was for the putative SubL and based on the crystal structures of the *E. coli* helicase (36). The relatively high homology between the three amino acid sequences of (39% of identity and 58% of similarity over the whole sequence length between *E.coli* RecQ and SubL; 42% of identity and 66% of similarty between *E.coli* RecQ and SubS, see Fig. 1) allowed us to obtain reasonable models, with the same overall features as the *E. coli* RecQ helicase template (Fig. 1).

This homology modelling predicted the existence of a zinc-binding domain in the SubL and SubS. Indeed, the crystal structure of the template helicase and RecQ-Ct domains of *E. coli* RecQ (Fig. 2A) reveals a zinc-binding domain formed by a platform of four α-helices that bind a zinc ion via the side chains of four highly conserved cysteine residues (3;37). The four cysteine residues are all conserved in the SubL (Cys-374, Cys-391, Cys-394 and Cys-397) (Fig. 2B) and in SubS (Cys-431, Cys-453, Cys-454 and Cys-457) (date not shown), and our three-dimensional model suggests that the platform of four α-helices is probably also conserved. Therefore, it is likely that the proteins bind a zinc ion via the SH group of the four conserved cysteine residues, conforming to the classical C4 zinc-binding domain topology observed in the template (Fig. 2). Quantitative analysis by the PAR (4-(2-Pyridylazo) resorcinol) assay method indicated that *B. subtilis* RecQ helicases both harbour zinc ions with about a 1:1 stoichiometry (Fig. 2). This is consistent with the putative that each molecule of SubL or SubS contains one zinc ion.

Fig. 1 Sequence alignment of the putative SubL (591 residues, second row), SubS (496 residues, third row) with the *E. coli* RecQ helicase (610 residues, first row) by software VectorNTI8

Identical residues shadowed in yellow are highly similar residues and in green shadowed are lower similar among the three sequences. The conservative sequences are shadowed in blue. The sign '-'presents gaps between the sequences. The HRDC domains are labelled from the sign arrow. The pentacles mean the conserved residues cysteines which form the zinc fingers of *E.coli* RecQ and SubL. The black triangles present the putative cysteines that form the zinc finger of SubS.

Figure 1

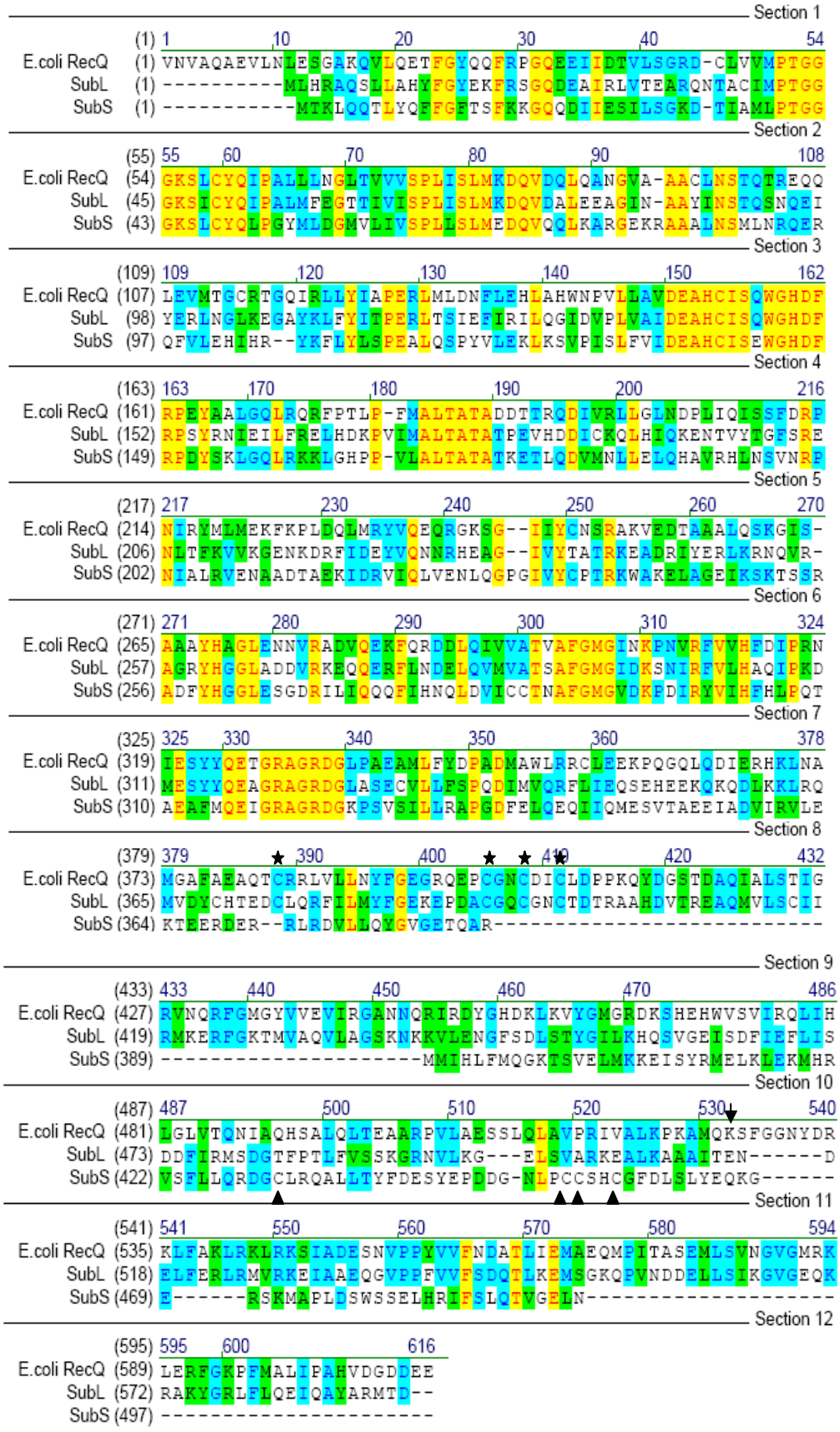
Section 1
E.coli RecQ (1) VNVAQAEVLNLESGAKQVLQETFGYQQFRPGQEEIIDTVLSGRD-CLVVMPTGG
SubL (1) ----------MLHRAQSLLAHYFGYEKFRSGQDEAIRLVTEARQNTACIMPTGG
SubS (1) ----------MTKLQQTLYQFFGFTSFKKGQQDIIESILSGKD-TIAMLPTGG
Section 2
E.coli RecQ (54) GKSLCYQIPALLLNGLTVVVSPLISLMKDQVDQLQANGVA-AACLNSTQTREQQ
SubL (45) GKSICYQIPALMFEGTTIVISPLISLMKDQVDALEEAGIN-AAYINSTQSNQEI
SubS (43) GKSLCYQLPGYMLDGMVLIVSPLLSLMEDQVQQLKARGEKRAAALNSMLNRQER
Section 3
E.coli RecQ (107) LEVMTGCRTGQIRLLYIAPERLMLDNFLEHLAHWNPVLLAVDEAHCISQWGHDF
SubL (98) YERLNGLKEGAYKLFYITPERLTSIEFIRILQGIDVPLVAIDEAHCISQWGHDF
SubS (97) QFVLEHIHR--YKFLYLSPEALQSPYVLEKLKSVPISLFVIDEAHCISEWGHDF
Section 4
E.coli RecQ (161) RPEYAALGQLRQRFPTLP-FMALTATADDTTRQDIVRLLGLNDPLIQISSFDRP
SubL (152) RPSYRNIEILFRELHDKPVIMALTATATPEVHDDICKQLHIQKENTVYTGFSRE
SubS (149) RPDYSKLGQLRKKLGHPP-VLALTATATKETLQDVMNLLELQHAVRHLNSVNRP
Section 5
E.coli RecQ (214) NIRYMLMEKFKPLDQIMRYVQEQRGKSG--IIYCNSRAKVEDTAAALQSKGIS-
SubL (206) NLTFKVVKGENKDRFIDEYVQNNRHEAG--IVYTATRKEADRIYERLKRNQVR-
SubS (202) NIALRVENAADTAEKIDRVIQLVENLQGPGIVYCPTRKWAKELAGEIKSKTSSR
Section 6
E.coli RecQ (265) AAAYHAGLENNVRADVQEKFQRDDLQIVVATVAFGMGINKPNVRFVVHFDIPRN
SubL (257) AGRYHGGLADDVRKEQQERFLNDELQVMVATSAFGMGIDKSNIRFVLHAQIPKD
SubS (256) ADFYHGGLESGDRILIQQQFIHNQLDVICCTNAFGMGVDKPDIRYVIHFHLPQT
Section 7
E.coli RecQ (319) IESYYQETGRAGRDGLPAEAMLFYDPADMAWLRRCLEEKPQGQLQDIERHKLNA
SubL (311) MESYYQEAGRAGRDGLASECVLLFSPQDIMVQRFLIEQSEHEEKQKQDLKKLRQ
SubS (310) AEAFMQEIGRAGRDGKPSVSILLRAPGDFELQEQIIQMESVTAEEIADVIRVLE
Section 8
E.coli RecQ (373) MGAFAEAQTCRRLVLLNYFGEGRQEPCGNCDICLDPPKQYDGSTDAQIALSTIG
SubL (365) MVDYCHTEDCLQRFILMYFGEKEPDACGQCGNCTDTRAAHDVTREAQMVLSCII
SubS (364) KTEERDER--RLRDVLLQYGVGETQAR----------
Section 9
E.coli RecQ (427) RVNQRFGMGYVVEVIRGANNQRIRDYGHDKLKVYGMGRDKSHEHWVSVIRQLIH
SubL (419) RMKERFGKTMVAQVLAGSKNKKVLENGFSDLSTYGILKHQSVGEISDFIEFLIS
SubS (389) ----------MMIHLFMQGKTSVELMKKEISYRMELKLEKMHR
Section 10
E.coli RecQ (481) LGLVTQNIAQHSALQLTEAARPVLAESSLQLAVPRIVALKPKAMQKSFGGNYDR
SubL (473) DDFIRMSDGTFPTLFVSSKGRNVLKG---ELSVARKEALKAAAITEN------D
SubS (422) VSFLLQRDGCLRQALLTYFDESYEPDDG-NLPCCSHCGFDLSLYEQKG------
Section 11
E.coli RecQ (535) KLFAKLRKLRKSIADESNVPPYVVFNDATLIEMAEQMPITASEMLSVNGVGMRK
SubL (518) ELFERLRMVRKEIAAEQGVPPFVVFSDQTLKEMSGKQPVNDDELLSIKGVGEQK
SubS (469) E------RSKMAPLDSWSSELHRIFSLQTVGELN----------
Section 12
E.coli RecQ (589) LERFGKPFMALIPAHVDGDDEE
SubL (572) RAKYGRLFLQEIQAYARMTD--
SubS (497) ----------

Figure 2

A

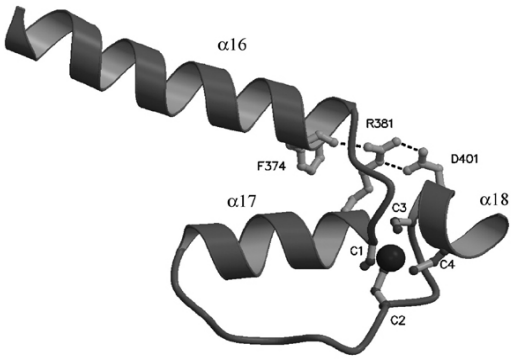

B

Protein sample	[Zinc^{2+}, nmol]/ [protein, nmol]
B.subtilis RecQL	1.096 ± 0.068
B.subtilis RecQS	1.084 ± 0.061

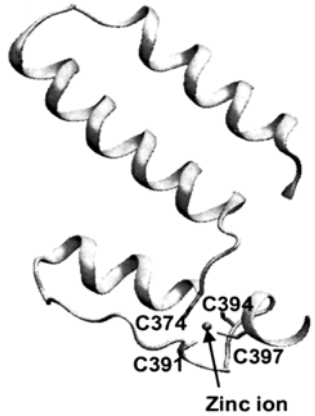

Fig. 2 Three-dimensional model of the zinc-binding motif of *E.coli* RecQ and *B. subtilis* RecQL helicase

Detail of the zinc-binding domain in the models of *E.coli* RecQ (**A**) and *B. subtilis* RecQL helicase (**B**). The four conserved cysteine residues coordinate a zinc ion. From the figure 2A, we can see that Cys^{380} (labeled as C1), Cys^{397} (labeled as C2), Cys^{400} (labeled as C3), and Cys^{403} (labelled as C4), are drawn in grey as they appear in the structure of the *E. coli* RecQ core (2;3). The homologous cysteines of Cys^{374}, Cys^{391}, Cys^{394} and Cys^{397} are formed the zinc binding motif of subtilis RecQL helicase. Quantitative analysis of the amounts of zinc atom associated with the purified *B. subtilis* RecQL and *B. subtilis* RECQS indicated that the zinc atom binds to them in a stoichiometric ratio. The values of 1.096 ± 0.068 and 1.084 ± 0.061 indicate that each molecule of *B. subtilis* RecQL or *B. subtilis* RecQL contain one zinc ion.

Cloning, Production and Purification of RecQ Helicase from *Bacillus subtilis*

To obtain the *B. subtilis recQ* gene, the 1.8 kb DNA fragment and 1.5 kb DNA carrying the open reading frame was amplified by PCR from genomic DNA of *B. subtilis* strain QST 713. These genes were fused to a sequence encoding the His tag, and the resulting construct was expressed in *E.coli* strain Rosetta and BL21 (DE3)/TrxB, respectively. A about 68 kDa (consistent with the value determined the amion acid sequence 66783Da) and about 56 kDa (56048Da) polypeptides were produced consistent with the calculated molecular weight of the His-tagged gene product (Fig. 3A). Immunoblotting with an anti-His monoclonal

antibody confirmed that the overexpressed proteins were the desired products (data not shown). Large quantities of the recombinant proteins were then purified to near homogeneity. The proteins were purified using a His-tag affinity matrix to near homogeneity and further purified on a Superdex-200 chromatography column (Fig. 3A).

Figure 3

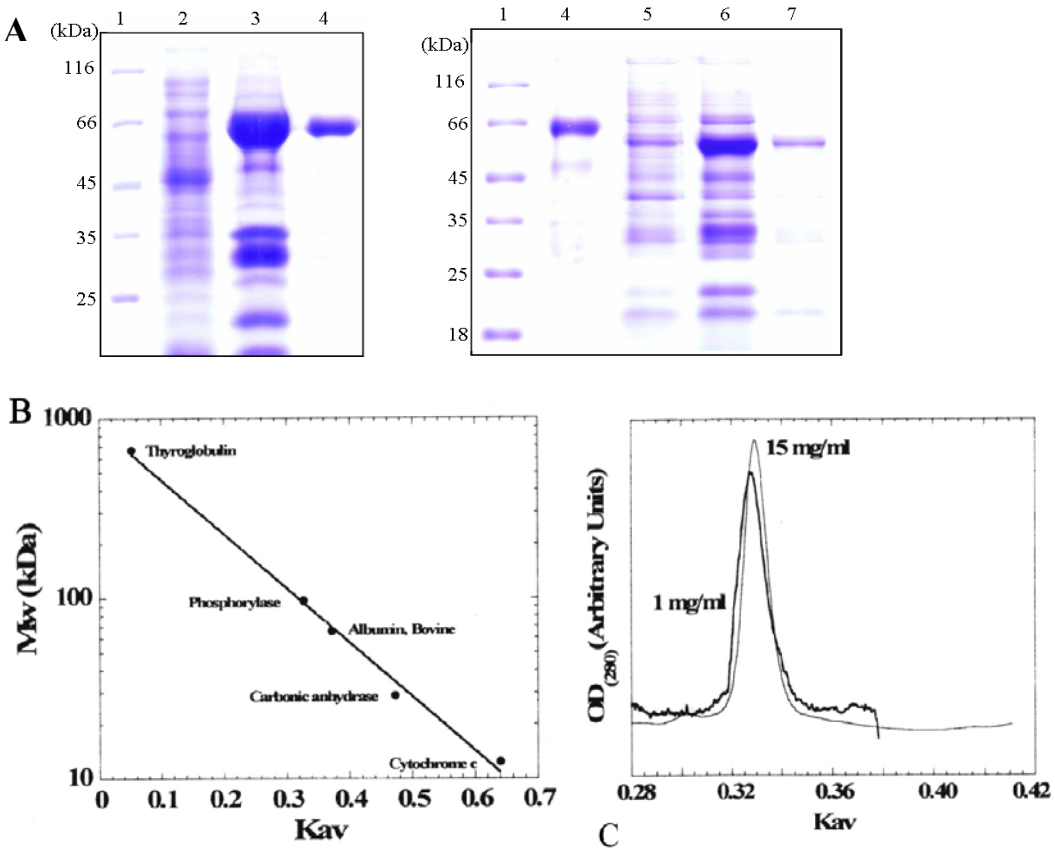

Fig. 3 Purification and gel filtration analysis of *B. subtilis* RecQ helicases

(A) 10% Commassie Blue-strained SDS-PAGE analysis of the purified *B. subtilis* RecQL (left) and *B. subtilis* RecQS (right). From left to right: lane1, protein molecular weight marker (116, 66.2, 45, 35, 25, 18 kDa); lane2: lysates from the cells before inducing SubL protein expression; line3: protein SubL purified by nickel affinity column chromatography; line4: protein SubL further purified by Superdex-200 chromatography (about 10μg); line5: lysates from the cells before inducing SubS protein expression; line6: protein SubS purified by nickel affinity column chromatography; line7: protein SubS further purified by Superdex-200 chromatography (about 2μg). **(B)** Calibration curve of the gel filtration column; the standard proteins used in this experiment are indicated in the figure. **(C)** Elution profile of the purified helicase from the chromatographic column. *B. subtilis* RecQ at two concentrations (1mg/ml and 15 mg/ml) was loaded on a Superdex-200 column and eluted as described in "Experimental procedures".

We used gel filtration to estimate the assembly state of the purified *B. subtilis* RecQL helicase in solution. Irrespective of the protein concentration used (1mg/ml and 15mg/ml), the *B. subtilis* RecQL eluted as a globular protein with a molecular mass of 69-72 kDa (Fig. 3B, C), indicating that this helicase behaved as a monomer in solution which is the same as *E.coli* RecQ (38; 39).

DNA-dependent ATPase Activity

In our laboratory, we have testified that *B. subtilis* RecQ helicases are the ATP dependent DNA helicases but not RNA helicases. The ATPase activity of *E.coli* RecQ helicase is more strongly stimulated by single-stranded DNA than double-stranded DNA, but the ATPase activities of *B. subtilis* RecQ helicases were similarly stimulated by both ssDNA and dsDNA.

The data not shown in our laboratory indicated that the ATPase activities of *B. subtilis* RecQ were influenced of pH, divalent cations and some compounds. Maximal ATP hydrolysises of these helicases were observed between pH 7.5 and pH 8.4 and much lower at pH 5.0 and at pH10. Mg^{2+} ions supported the activity most effectively and other divalent cations, in particular Mn^{2+}, Ca^{2+}, Zn^{2+}, were insufficient for activity. Most helicase shows its maximal function at 37°C as an enzyme, such as *E.coli* RecQ, PcrA, UvrD *et al.* Here we further found that *B. subtilis* RecQ helicases also show this characteristic (Fig. 4A). From the figure we can see that the ATP hydrolysis increased with the incubating temperature increasing and it reached to the maximum at 37°C, then it decreased obviously when the temperature increased continuously. When the temperature reached to 55°C, *B. subtilis* RecQ helicases almost lost its ability of ATP hydrolysis. Since ATP chelates magnesium ion, we want to confirm whether the concentration of ATP and Mg^{2+} effect on the ATP hydrolysis of helicase. The data clearly demonstrated that the ATPase activities of *B. subtilis* RecQ helicases are influenced with different ratio of the magnesium ion to ATP concentration. At both ATP concentration (1mM and 3mM), the helicase activity increased with ratio of [Mg^{2+}]: [ATP] increasing and it reached to its peak at about ratio of 2. Beyond this point, it decreased although the ratio increased continuously (Fig.4B). Thus, the concentration of magnesium ion and ATP are both appeared influence the ATP hydrolysis of *B. subtilis* RecQ helicases which was discovered formerly in *E.coli* RecQ helicase (40).

Figure 4

A

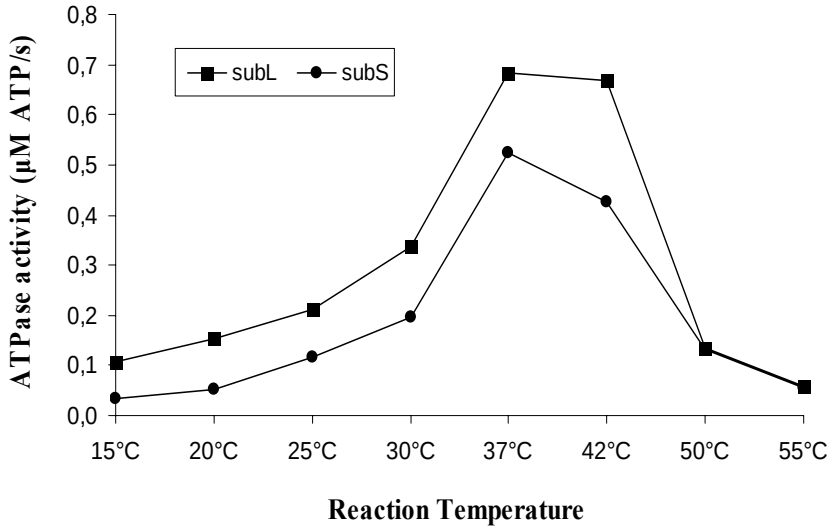

B

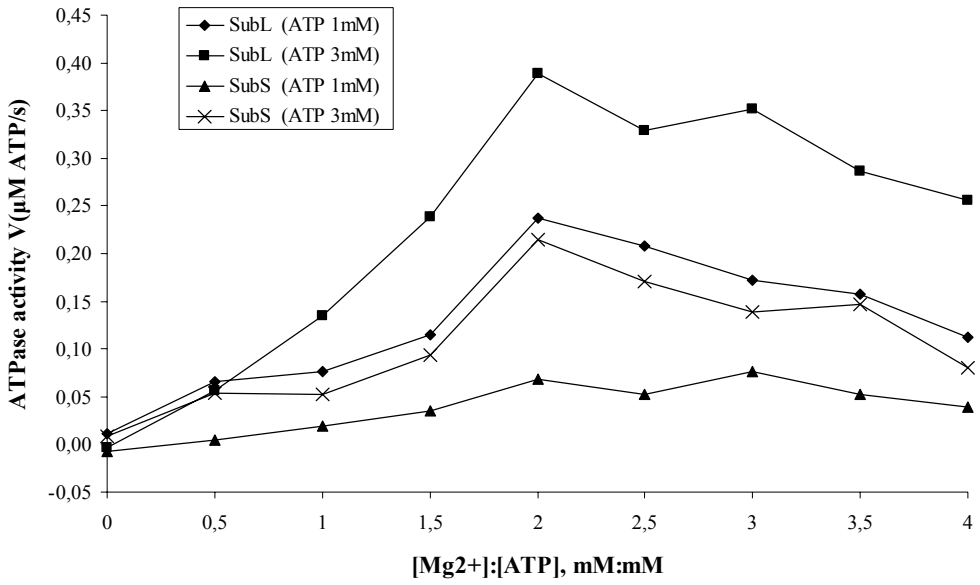

Fig. 4 Characterization of the *B. subtilis* RecQ ATPase activity

(**A**) ATPase activity at different temperature. The reactions were processed at the different temperature indicated in the figure using 0.5µM SubL or SubS for 10 min and containing 2.5mM ATP, 5mM Mg^{2+}, 200nM ssDNA (nucleotide 32 in Table 1, 53-mer oligonucleotide). (**B**) ATPase activity in the different ratio of concentration of free Mg^{2+} and ATP indicated at the X-axes. The reactions were held at 37°C for 30 min containing 1mM or 3mM ATP, 0.5µM SubL or SubS, and 200nM 53nt-ssDNA.

Figure 5

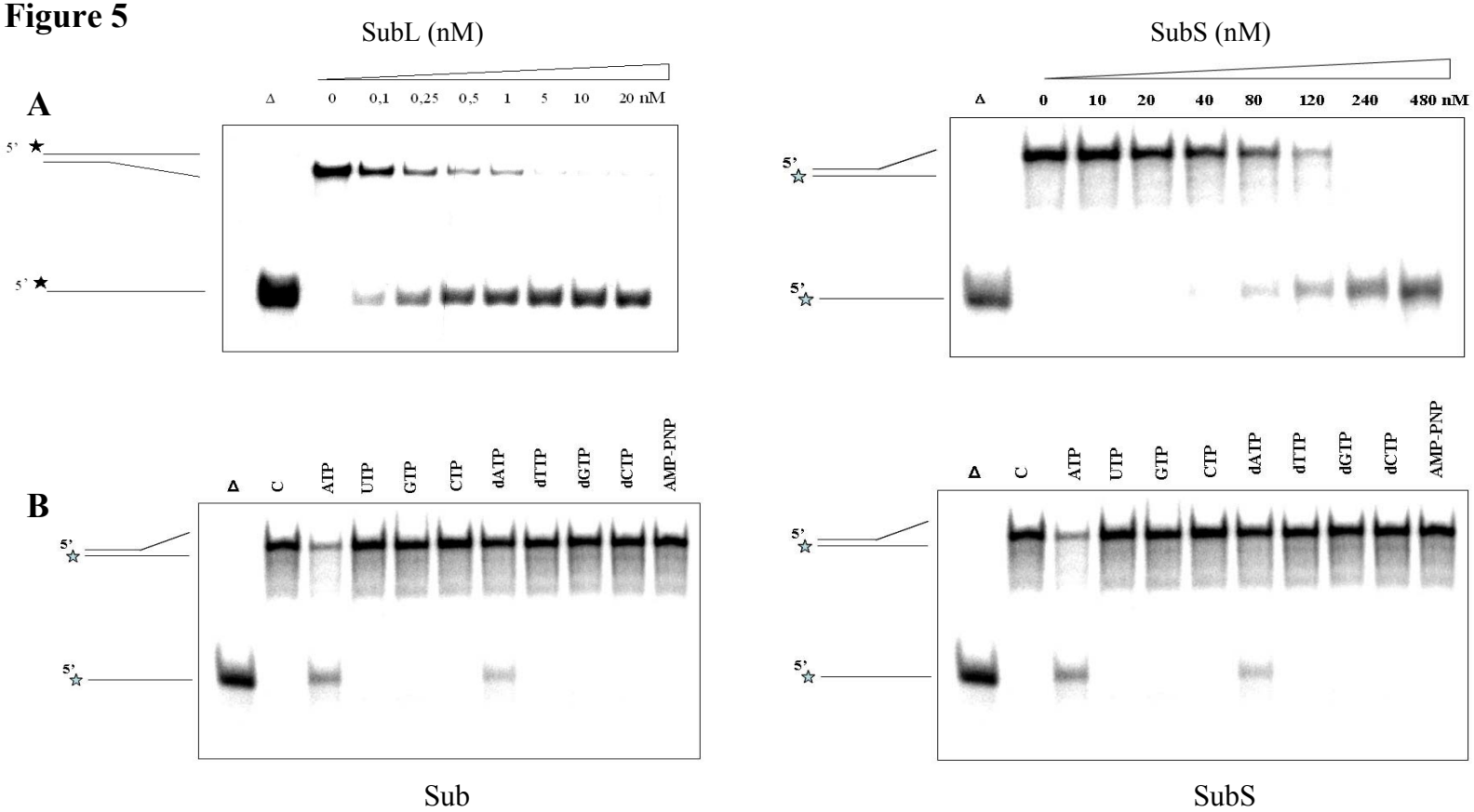

Fig. 5 Characterization of the *B. subtilis* RecQ-mediated DNA unwinding activity

(A) DNA unwinding in the presence of various concentrations of SubL (left) and SubS (left). DNA unwinding assays were as described in "Methods" using forked duplex DNA substrate (Substrate A in Table 2, 0.45nM) and 2,5mM ATP, incubate at 37°C for 30 min. The concentrations of the enzymes used are indicated at the top of the panel. The pentacle means labelled γ-^{32}P at 5' terminal of the oligo. **(B)** Effects of different nucleotides on the *B. subtilis* helicase-catalyzed DNA unwinding activity. DNA unwinding assays were performed as described in "Methods" using DNA substrate (Substrate A in Table 2, 0.45nM); each reaction contained 0.2μM helicase and one of the listed nucleotides at a final concentration of 2.5mM. Each nucleotide was noted at the each top of the panel.

DNA Unwinding Activities Assay versus *B. subtilis* RecQ Helicases Concentration

To determine the optimal amount of the RecQ protein required to unwind dsDNA, SubL concentrations of 0.1nM to 20nM and SubS concentrations of 10nM to 480nM were tested (Fig. 5A). Forked DNA (Substrate 1 in Table 1) unwinding increased with increasing the concentrations of helicase, 70~80% dsDNA substrate was unwound at 1nM SubL enzyme and 50% dsDNA was unwound at 120nM SubS. This indicates that *B. subtilis* RecQ protein is an ATP-dependent DNA helicase. The unwinding activity of SubL is stronger than that of SubS helicase. To determine the nucleotide preference of RecQ helicase, all eight kinds of nucleotides were tested for their ability to support unwinding of the 20bp forked duplex substrate (Fig. 5B). Under the reaction conditions used, only ATP and dATP allowed the helicase reaction, with ATP being preferred (100%) over dATP (90%) of SubL and (70%) over dATP (30%) of SubS. Except ATP and dATP, UTP,GTP, CTP, dTTP, dGTP and dCTP could not be used by the SubL and SubS helicases as the energy source to catalyze DNA unwinding. When AMP-PNP was included in the reaction mixture instead of ATP, no any ATPase activity was detected. Thus, ATP was preferred over other nucleotides as the nucleotide cofactor and nucleotide triphosphate hydrolysis is required for the *B. subtilis* RecQ-mediated DNA unwinding reaction.

Polarity and processivity of the *B. subtilis* RecQ Helicases

Most RecQ family helicases characterized exhibit 3' to 5' polarity. The polarity of unwinding by a helicase is defined by the strand to which the enzyme binds and the direction it moves along that strand. To test the polarity of *B. subtilis* RecQ helicase action, partial duplex DNA substrates with 5' or 3'-single-stranded tails (oligos M and N in Table 2) were used. Both SubL and SubS could only unwind the substrate with a 3'-single-stranded tail (Fig. 6A and 6B), demonstrating that the *B. subtilis* helicase is a unidirectional helicase with 3' to 5' polarity which is the same as *E coli.* RecQ.

There different substrates composed of γ-^{32}P-labelled 20-mer and 35-mer oliogonucleotide annealed to phiX174 circle ssDNA was used to assay the DNA unwinding activity of the putative *B. subtilis* RecQ helicase (Fig. 6C and 6D). One of these partial duplex substrates doesn't have any short 5' or 3' tail, the other two has 5' or 3'-single-stranded tails. As some RecQ helicases, including the Werner syndrome and Bloom

syndrome proteins, display stronger helicase activity towards DNA substrates containing a forked duplex, substrates containing 5' or 3'-end tails dsDNA were also tested. The *B. subtilis* RecQL and RecQS helicases unwound 20-mer and 3'-end-tail phiX174 partial duplex DNA substrates with similar efficiencies at 50nM SubL and 500nM SubS. However, the phiX174 partial duplex DNA substrate containing 5'-end tail couldn't be unwound by these two *B. subtilis* RecQ helicases even at high concentration of protein.

The processivity is another important characteristic of helicase-mediated DNA unwinding. Most RecQ family helicases display lower processivity than those of helicases involved in DNA replication. Two phiX174 partial duplex DNA substrates of 20 and 70bp were prepared to study the effect of duplex length on the helicase activity of *B. subtilis* RecQ helicases. A time course of the *B. subtilis* RecQ helicase-mediated strand unwinding reaction is shown in Figure 7. The labelled DNA fragment with the short partial duplex (20bp) hybridized to PhiX174 virion ssDNA was unwound within 5 min (Fig. 7A and 7C) and the amount of fragment unwound in the reaction was increased with the time by SubL. However, this substrate was unwound by the SubS weakly from 5 min. In contrast, no DNA unwinding was detected with the long partial duplex (70bp) substrate within 50 min by both two *B. subtilis* RecQ helicases (Fig. 7B and 7D). Therefore, *B. subtilis* RecQ helicase alone can unwind only short DNA substrates *in vitro*. It was reported that *E. coli* SSB protein (ESSB) stimulates *E. coli* RecQ helicase-promoted unwinding by trapping individual strands of the ssDNA product to prevent their reannealing. Therefore, we examined the effect of *E. coli* SSB protein on *B. subtilis* RecQ helicase-mediated unwinding of the 70bp duplex substrate. In control reactions, we verified that ESSB alone did not denature the 70bp DNA duplex. Then, 400nM helicases were incubated with the 70 bp duplex DNA in the presence of various concentrations of ESSB up to 4μM. The results showed that ESSB could not stimulate the unwinding activities of *B. subtilis* RecQ because of their too low processivity (data not shown).

Figure 6

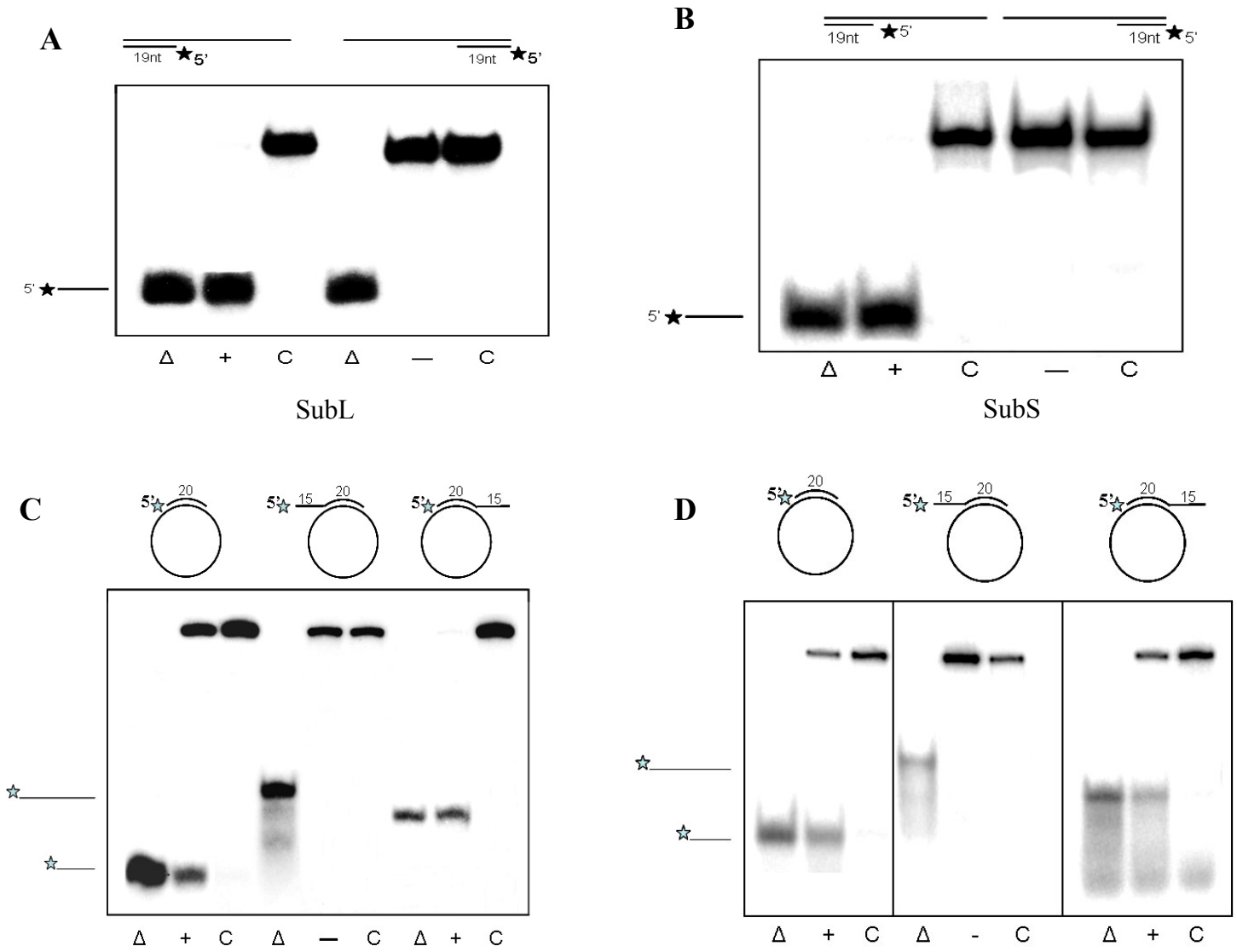
A
19nt
5'
19nt
5'
5'
Δ + C Δ — C
SubL
B
19nt
5'
19nt
5'
5'
Δ + C — C
SubS
C
5'
20
5'
15
20
5'
20
15
Δ + C Δ — C Δ + C
D
5'
20
5'
15
20
5'
20
15
Δ + C Δ - C Δ + C

Fig. 6 Polarity of DNA unwinding by the *B. subtilis* RecQ

(A, B) Reaction mixtures (20µl each) containing about 0.45nM DNA substrate and 0.4µM protein (A: SubL and B: SubS) were incubated at 37°C for 30 min. The products of the reaction were analyzed by electrophoresis in a 12% polyacrylamide gel and autoradiography. The substrate structures are shown at the top of the figures. Left lane (Δ): with heat-denatured substrate; middle lane (+/–): unwinding reaction with the enzyme; right lane (C): the control assays without enzyme. Thereinto, "+" presents DNA unwinding and "–" presents no DNA unwinding. **(C, D)** Helicase activity with three different substrates (virion Phi X174 circle ssDNA hybridized with ^{32}P-labelled oligos 29, 30, 31 respectively in Table 2) . The panel shows the structure of the substrate used and an autoradiogram of the gel. The lanes (Δ), (+/–) and (C) represent the boiled DNA substrate, the complete reaction and the DNA substrate alone (control), respectively. A reaction mixture (20µl) containing 0.45nM of the indicated substrate in the helicase assay buffer was incubated for 30min at 37°C with *B. subtilis* RecQ helicases (Fig.C: 50nM SubL and Fig.D: 0.4µM SubS). The products were analyzed by 12% nondenaturing polyacrylamide gel electrophoresis and exposed using a phosphorimager and analysed with ImageQuant softwave (Molecular Dynamics).

Figure 7

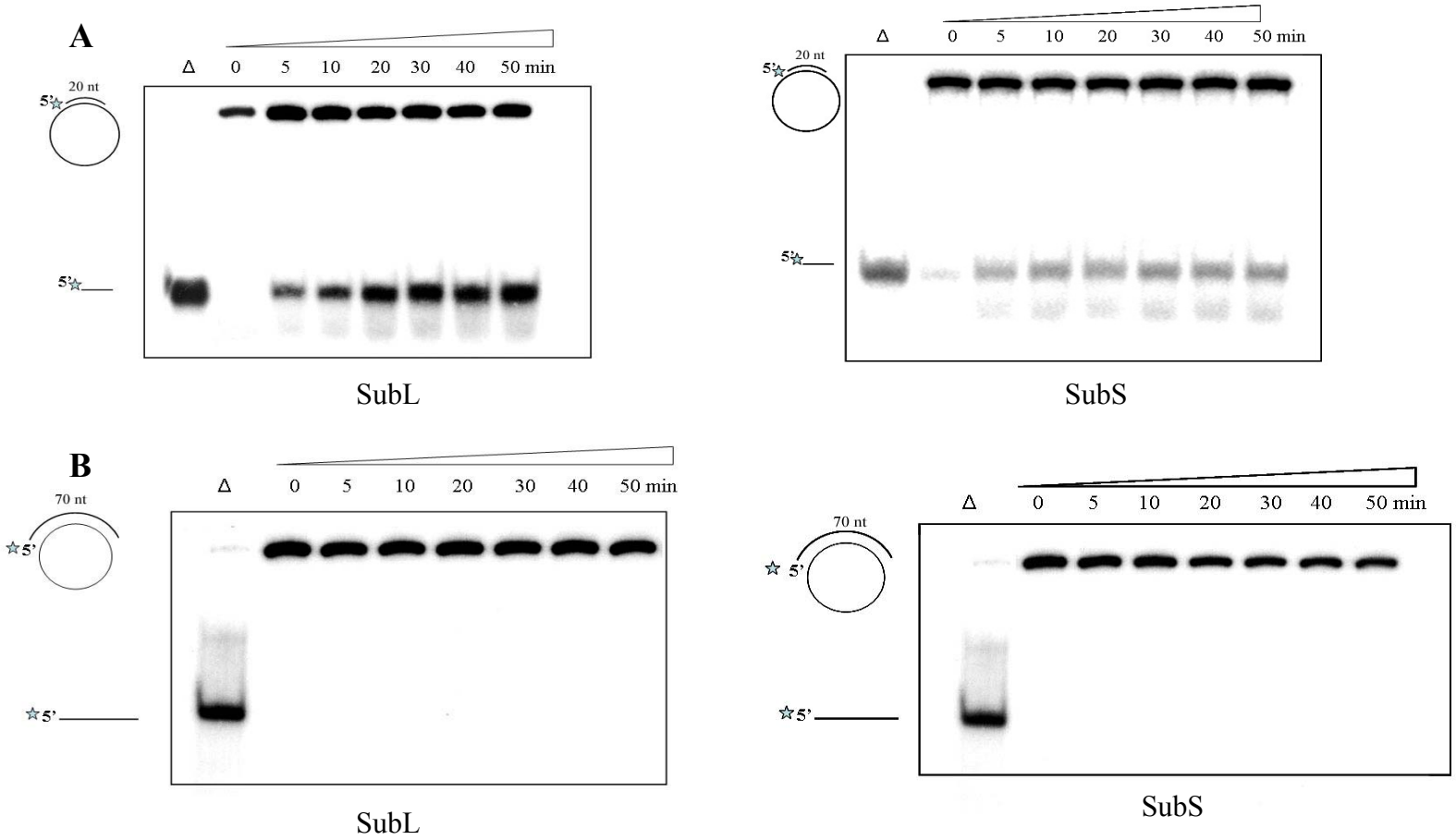

Fig. 7 Processivity of the *B. subtilis* RecQ helicases

In order to detect the processivity of the *B. subtilis* RecQ-mediated DNA unwinding, DNA substrates (0.45nM) containing virion Phi X174 circle ssDNA hybridized with ^{32}P-labelled fragments 20 (Oligo 28 hybridated with Oligo 29 in Table 1, **Fig. 7A**) or ^{32}P-labelled fragments 70 (Oligo 28 hybridated with Oligo 14 in Table 1, **Fig. 7B**) nucleotides long were incubated with 0.4µM protein in unwinding reaction buffer at 37°C. The reaction was stopped at the indicated time in the figures and the products were analyzed by electrophoresis in a 12% polyacrylamide gel and autoradiography.

B. subtilis RecQ Helicase Activity on Blunt-ended and Gapped DNA Substrates

We investigated the DNA substrate specificity of *B. subtilis* RecQ helicases. High concentrations of *E. coli* RecQ helicase can efficiently unwind a blunt-ended duplex DNA. However, the *B. subtilis* RecQ helicases, even at a high concentration of 1μM, were unable to unwind a 21bp blunt-ended DNA (Fig. 8A left and 8B left). To test whether 3' or 5' end itself might affect the unwinding activity, a series of gapped DNA molecules were constructed. When nicked DNA (gap size 0) was used as the substrates, the SubL unwound the duplex DNA with a very low efficiency (Fig. 8A right). When the DNA molecules contain a gap of 2 and 4, the DNA substrates were efficiently unwound by it. Thus, the 3' tail length is determinant for efficient DNA unwinding. However, the SubS couldn't unwind the gapped DNA substrates (Fig. 8B).

Figure 8

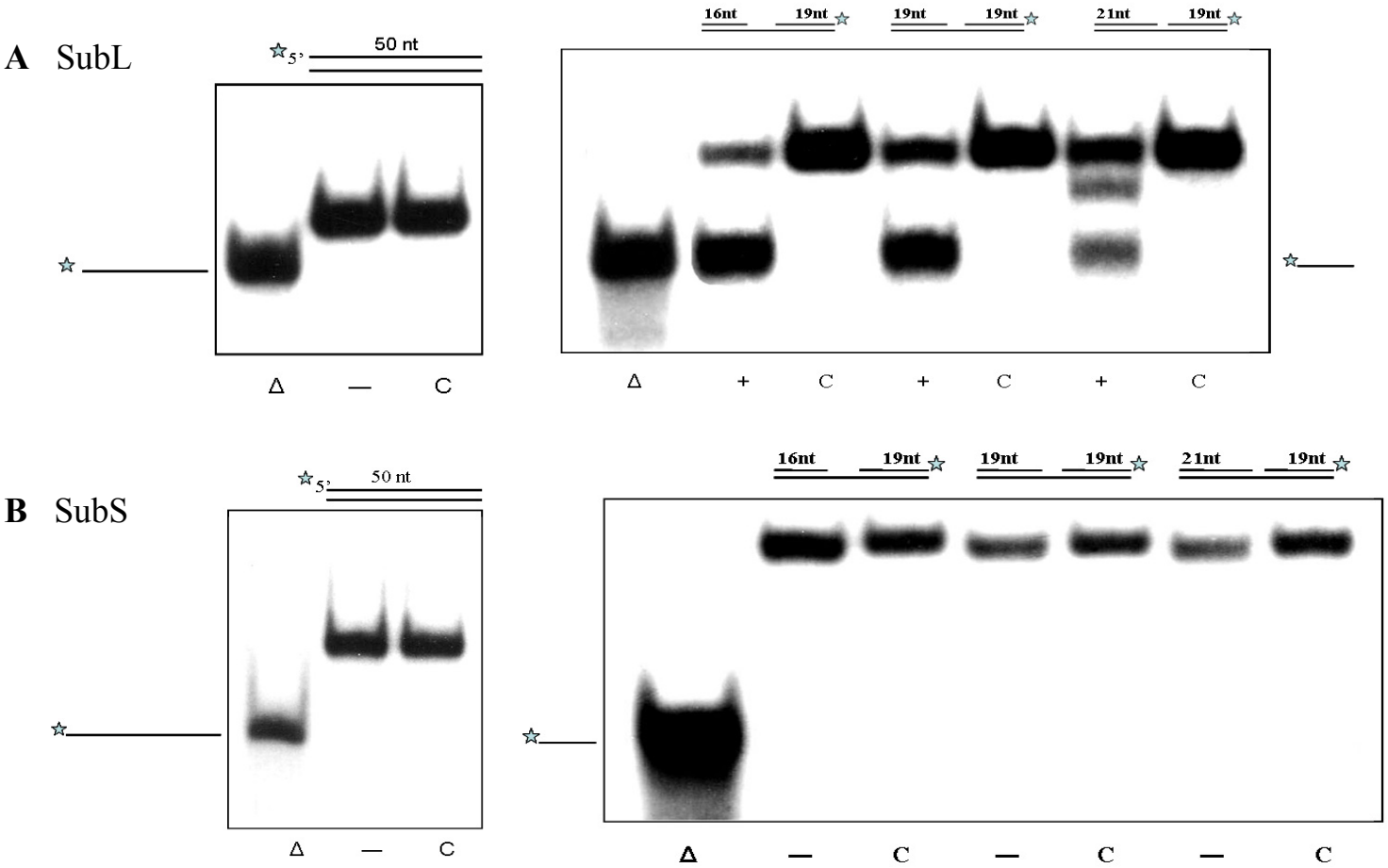

Fig. 8 Unwinding activity on the blunt substrate and nick substrates of the *B. subtilis* RecQ helicases

A reaction mixture (20μL) containing 0.45nM blunt-end substrate (substrate R in Table 2) in the unwinding reaction buffer was incubated at 37°C with the addition of the 0.4μM SubL (Fig.8A left) or SubS (Fig.8B left). Other three kinds of nick substrate (from left to right is the substrate Q, P, O in Table 2) were also analyzed in the same reaction condition discribled in "Methods" (The right two figures). Lane (Δ): with heat-denatured substrate; lane (+/–): unwinding reaction with the enzyme; lane (C): the control assays without enzyme. Thereinto, "+" presents DNA unwinding and "–" presents no DNA unwinding. The products were analyzed by 12% nondenaturing polyacrylamide gel electrophoresis and autoradiography.

B. subtilis RecQ Helicase Activity on Forked Duplex DNA with Increasing 3' and 5'- Tail Length

We have found that *B. subtilis* RecQ helicases could unwind the forked DNA duplexes, and then we were interested in the importance of the length of the no complementary 5'-ssDNA tail of the forked dsDNA substrate for the efficiency of unwinding by *B. subtilis* RecQ helicase. We tested the DNA substrate related to the forked duplex with 0, 1, 5, 10 and 26 nucleotides. As respected, all the forked substrates have been unwound by the SubL and SubS even if the 0-nucleotide forked DNA duplex used (Fig. 9A and 9B). However, the results didn't indicate that the unwinding activity of the *B. subtilis* RecQ helicases on the forked dsDNA became stronger obviously when the length of 5'-ssDNA tail increased.

On the other hand, we constructed a series of linear double substrates with 3'-ssDNA tails of 1, 5, 10, and 25 nucleotides to study the effect of 3'-tail length on the unwinding activity of the *B. subtilis* RecQ helicases. It was clearly showed from the figure that except single-nucleotide all the substrates with 3'-tails could be efficiently unwound by the SubL helicase (Fig. 10A). The DNA substrate with only a 1, 5, 10 nucleotides of 3'-tail were essentially not acted upon by the SubS (Fig. 10B); and the apparent unwinding extent of the duplex DNA was approximately 50% for the substrates with 25-nucleotides 3'-tails.

B. subtilis RecQ Helicases target DNA replication and repair intermediates

We demonstrated (above) that *B. subtilis* RecQ helicases preferentially unwind forked DNA duplexes with noncomplementary 3'- and 5'-ssDNA tails. Next, we tested whether it could unwind DNA structures resembling the DNA replication/repair intermediates, for example 5'-ssDNA flap DNA, Kappa joint molecules and synthetic replication fork DNA substrates.

5'-Flap substrates are proposed intermediates in the process of Okazaki fragment processing during lagging-strand DNA replication and also in DNA repair pathways such as base excision repair. To assess whether *B. subtilis* RecQ helicases are able to unwind a 5'-flap substrate, we tested a duplex DNA substrate containing an upstream 25-mer hybridized to the upstream ssDNA region that resides below the flap (Substrate J in Table 2; Fig. 11A, left pane 3). Only SubL helicase efficiently unwound the 5'-flap substrate (Fig. 11A, left

Figure 9

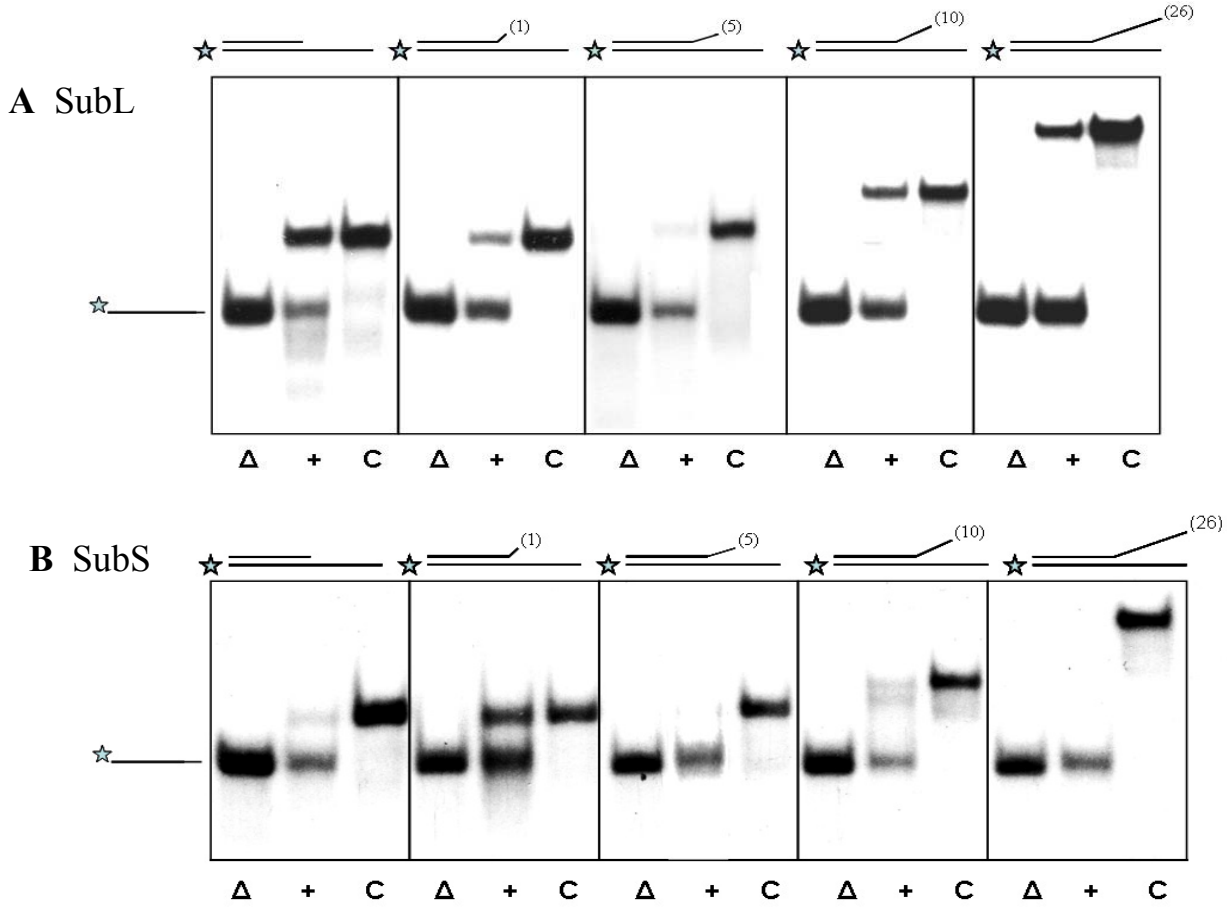

Fig. 9 3'-forked tail length dependence studies

DNA unwinding assays were performed as described in "Methods" using DNA substrates with different length of 3'-forked tail at 0.45μM (From left to right: substrate B, C, D, E and A in Table 2). Each reaction contained 50nM SubL (**A**) or 500nM SubS (**B**) helicases respectively. Lane (Δ): with heat-denatured substrate; lane (+): unwinding reaction with the enzyme; lane (C): the control assays without enzyme. The products were also analyzed by 12% nondenaturing polyacrylamide gel electrophoresis and autoradiography.

Figure 10

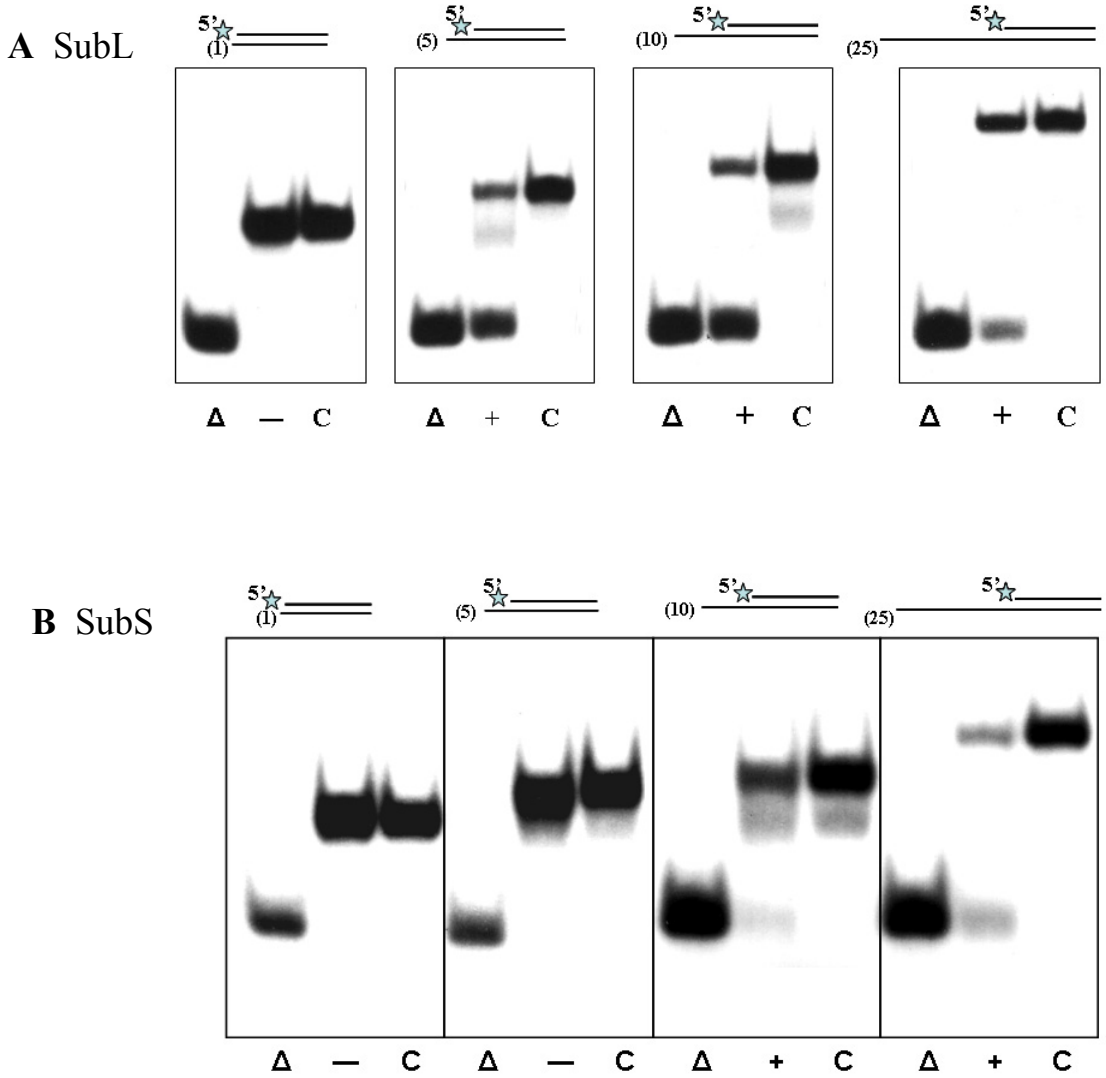

Fig. 10 3'- single tail length denpedence studies

Unwinding of the substrates which has different length of 3'-single tail (Substrate F, G and H, I in Table 2) catalyzed by SubL (Fig. 10A) and SubS (Fig. 10B). Lane (Δ): with heat-denatured substrate; lane (+): enzyme unwind dsDNA; lane (–): enzyme doesn't unwind the DNA substrate; lane (C): the control assays without enzyme. All reactions were incubated for 30 min at 37°C with 0.4μM helicase and analysed by 12% nondenaturing polyacrylamide gel electrophoresis

pane 2) and released the labelled partial duplex containing 5'-end tail, the SubS could not affected on this kind of substrate (Fig. 11B left pane 2).

The properties of the Kappa joint molecule suggest that it may be composed of a linear dsDNA molecule that has been invaded by homologous ssDNA; the resultant joint molecule would resemble the letter K and, hence, is referred to as a Kappa intermediate. Such DNA substrates are particularly relevant to DNA recombination and repair processes. To test the unwinding of a Kappa intermediate by the *B. subtilis* RecQ helicases, we prepared a substrate (Substrate K in Table 2) which mimics the Kappa joint molecule. The SubL helicase unwound the Kappa molecule (Fig. 11A middle panel) and SubS also didn't unwind the Kappa fragment synchronously (Fig. 11B middle panel).

We also tested a forked duplex in which both the 5'- and 3'-tails were double-stranded (Substrate L in Table 2). This substrate mimics a synthetic DNA replication fork with double-stranded leading and lagging strands. The duplex forked DNA substrate was unwound by the SubL not the SubS helicase at the concentration tested (0.4μM), but the duplex DNA with a labelled 5'-tail was released (Fig. 11A and 11B right panel). This is also consistent with the 3' to 5' polarity of the *B. subtilis* RecQ helicase. Hence SubL is able to unwind a synthetic replication fork.

Several RecQ homologues including BLM, WRN and *E.coli* RecQ helicase disrupt synthetic immobile four-way DNA junctions, which resemble Holliday junctions (HJ or X structure). To determine whether *B. subtilis* RecQ helicase could catalyze similar reactions, we analyzed its activity with a synthetic HJ substrate containing a 26-bp core of homologous sequences flanked by heterologous arm sequences (Substrate S in Table 2; Fig. 11 C). The result showed that SubL was able to disrupt these four-way junctions to release the component single strands, as is evident from the appearance of the free radio labelled oligonucleotide. Meanwhile, the SubS helicase could not unwind the four-way junction DNA substrate that mimics a Holliday junction.

Figure 11

A SubL

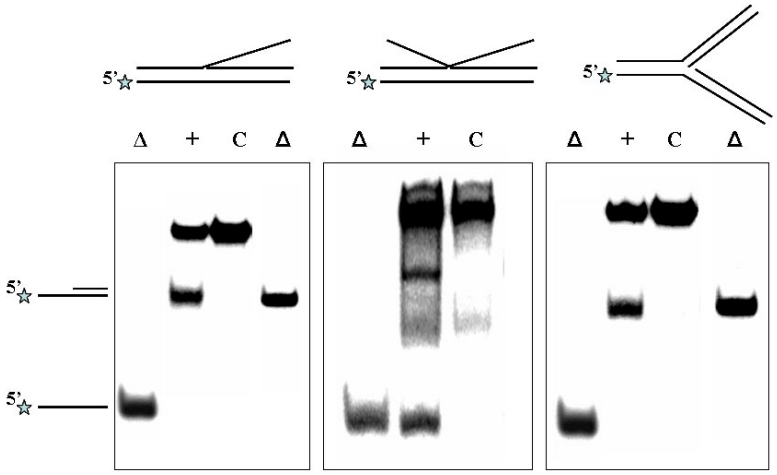

B SubS

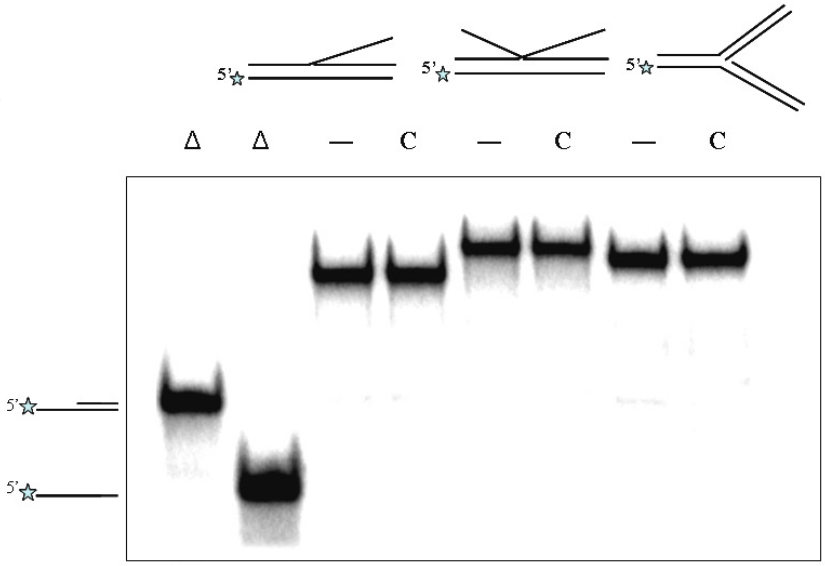

C

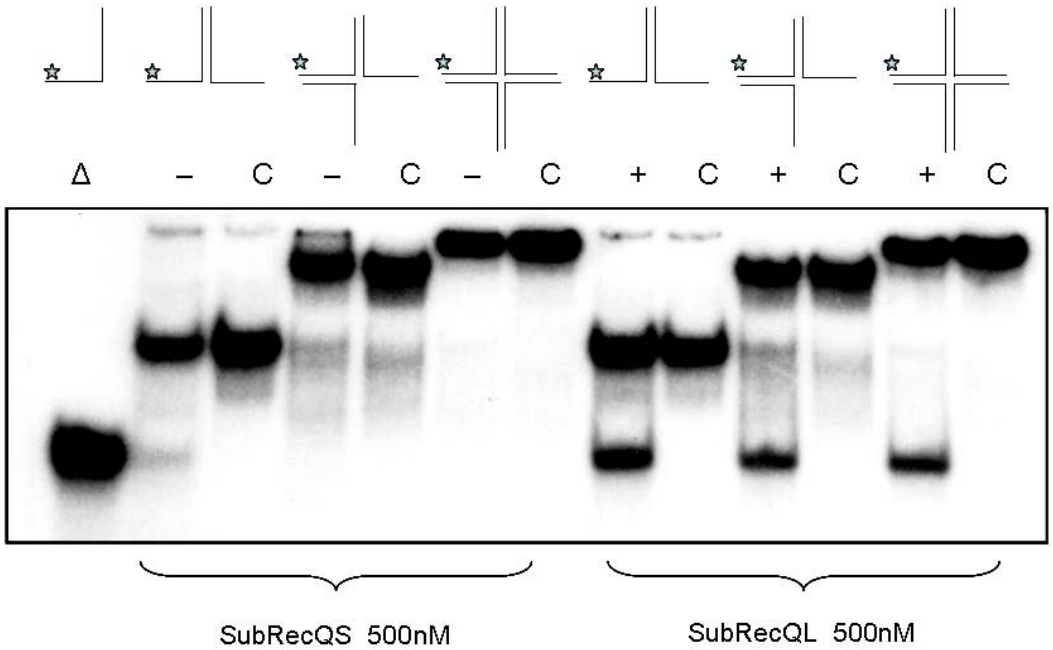

Fig. 11 (A) The SubL unwinds the 5'-flap, Kappa joint and replication fork DNA substrate (Substrate J, K and L in Table 2). **(B)** The SubS unwinds the 5'-flap, Kappa joint and replication fork DNA substrate. A reaction mixture (20 μl) containing 0.45nM of the indicated substrates (at the top of the panel) and the *B. subtilis* RecQ protein (0.5μM) in the helicase assay buffer was incubated for 30min at 37 °C. The products were analyzed by 12% nondenaturing polyacrylamide gel electrophoresis and autoradiography. **(C)** *B. subtilis* RecQ helicase unwind the four-way junction DNA substrate (recombinant Holliday junction, substrate S in Table 2). The experimental conditions are essentially identical to those described in Fig. 11 A and B. Lane (Δ): with heat-denatured substrate; lane (+/–): unwinding reaction with the enzyme; lane (C): the control assays without enzyme. Thereinto, "+" presents DNA unwinding and "–" presents no DNA unwinding.

Binding of the putative *B. subtilis* RecQ to DNA substrates

We used electrophoretic mobility shift assays (EMSA) to investigate the molecular mechanism by which the *B. subtilis* RecQ helicase preferentially unwinds the duplex DNA. The experiments were carried out using the purified protein and γ-^{32}P-labelled synthetic oligonucleotides in single-, forked double-stranded, as described under "Experimental Procedures." The *B. subtilis* RecQ helicases were able to bind ssDNA and dsDNA, but the apparent binding affinities towards these substrates were low, judged from the extent of the DNA-protein complex formation. The SubL helicases formed a more stable protein-DNA complex with forked duplex DNA than with the ssDNA (Fig. 12A). From the figure, we can see the protein-dsDNA complex clearly when SubL at 200nM. When the concentration of SubL reached to 400nM, the protein-ssDNA complex appeared. But for SubS, no visible difference can be found between binding to ssDNA and dsDNA (Fig. 12B). In addition, the SubL was found to have stronger DNA binding ability than SubS whatever in the presence of single strand or forked duplex strand. Thus, recognition of particular DNA structures by the *B. subtilis* RecQ helicases may determine the polarity and the efficiency of their helicase activities.

Figure 12

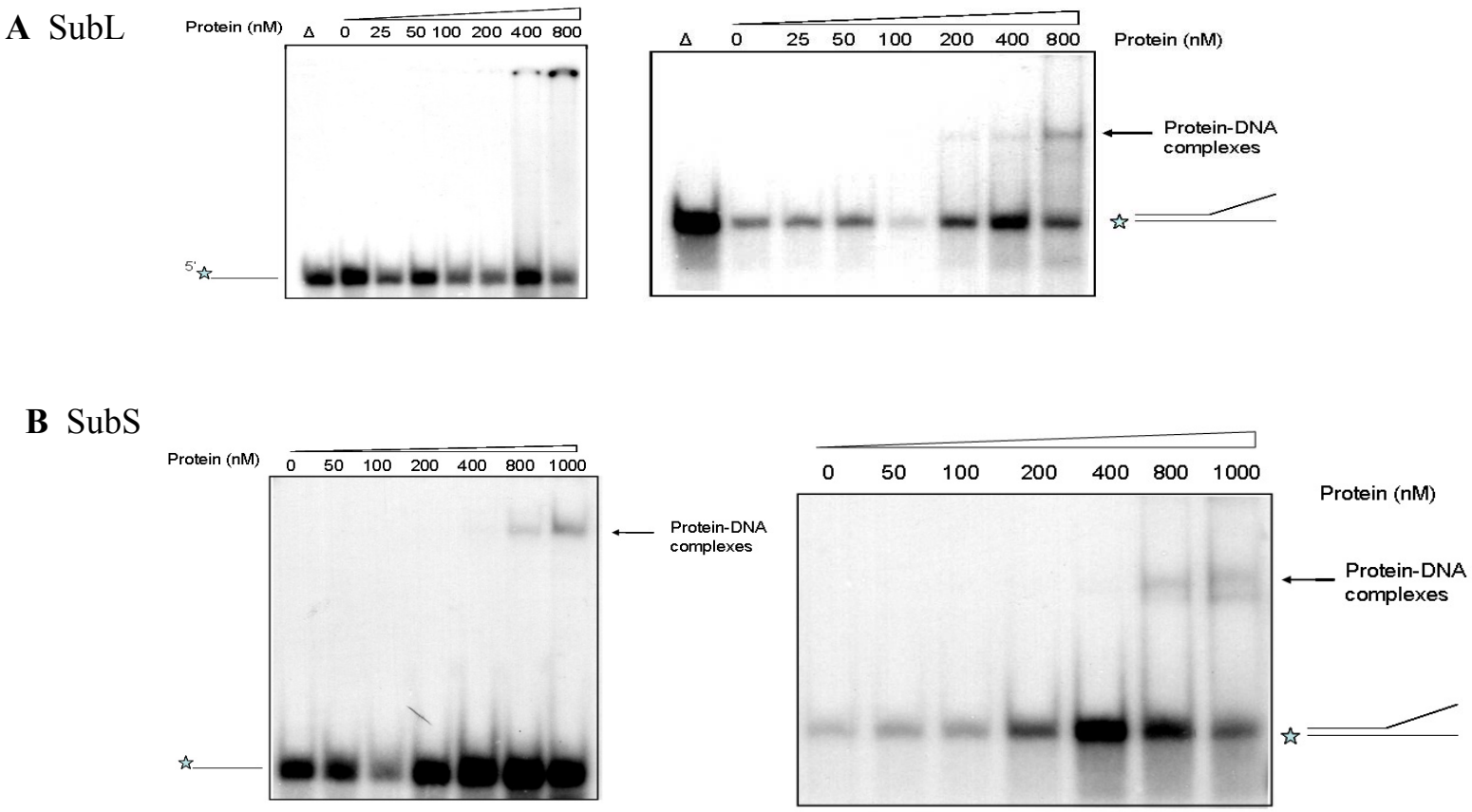

Fig. 12 DNA binding by the *B. subtilis* RecQ helicase

Electrophoretic mobility shift assays to determine the binding of the *B. subtilis* RecQ to ssDNA (Fig.12 A left and B left) and forked duplex DNA (Fig.12 A right and B right). Reaction mixtures (20µl each) contained DNA (0.45nM) and one of various concentrations of the *B. subtilis* RecQ as indicated in the figure. The binding assays were performed in binding buffer as described in "Methods." Reactions were incubated for 20 min at 37°C and then loaded onto a 6% nondenaturing polyacrylamide gel to separate the protein-DNA complexes electrophoretically. The results were visualized by autoradiography.

B. subtilis RecQ helicases possess DNA strand-annealing activity and promote DNA exchange weakly

Several human RecQ homologues, including WRN, BLM, RECQL and RECQ5, possess strand-annealing activity, and can catalyzing strand exchange by combining DNA-unwinding and strand-annealing activities. We investigated whether the *B. subtilis* RecQ might also perform this activity. To test for putative *B. subtilis* RecQ strand annealing activity, we incubated two partially complementary single stranded oligonucleotides (oligos 22 and 23 in Table 1, 0.1nM each) with a series of concentrations of the purified *B. subtilis* RecQ helicase for 15 min and analyzed the products on non-denaturing polyacrylamide gels (Fig. 13). If strand annealing occurred, a duplex strand would be formed. The *B. subtilis* RecQ indeed promoted annealing of the two complementary strands to form a duplex which co-migrated with the intact duplex control. We found that annealing was dependent on protein concentration. The SubL promoted an efficient annealing reaction at low concentration, but the SubS exhibited very low annealing activity at 160nM (Fig. 13 A and B). Meanwhile, *B. subtilis* RecQ–mediated DNA strand-annealing activity could be inhibited by ATP (data not shown), a same phenomenon observed with other RecQ family helicases. Furthermore, we studied whether the *B. subtilis* RecQ promote strand exchange. The forked double-strands (Substrate A in Table 2) and single stranded oligonucleotide (oligo 11 in Table 1) which is complementary with one of the double-strands were incubated together with SubL or SubS from increasing time up to 30 min. From the gel we could find out that the new recombinant double-strand formed when SubL was added into the reaction system and its exchange activity was increasing when the time was prolonged. Meanwhile, the SubS helicase didn't show the exchange activity.

Figure 13

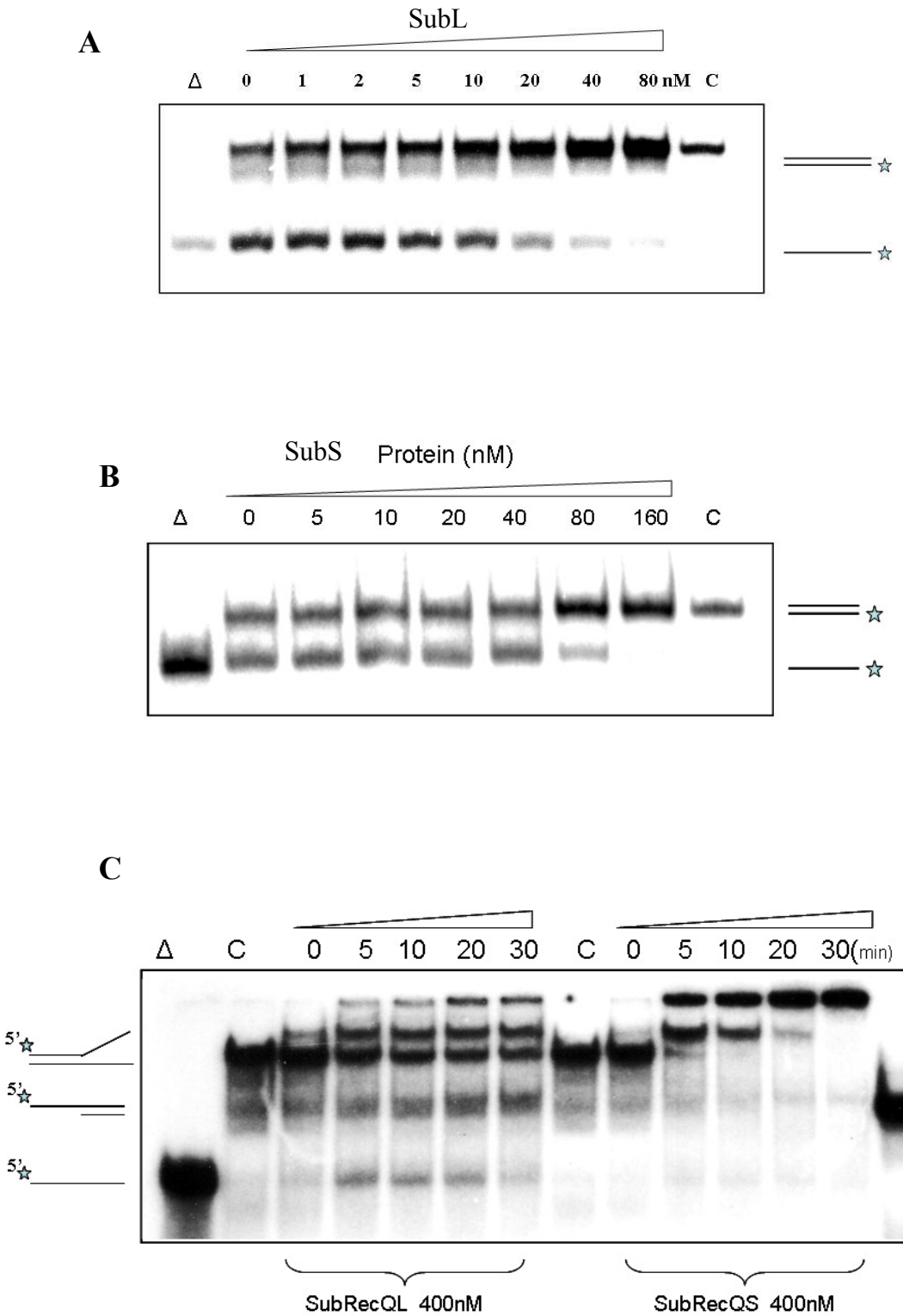
A
SubL
Δ 0 1 2 5 10 20 40 80 nM C
B
SubS Protein (nM)
Δ 0 5 10 20 40 80 160 C
C
Δ C 0 5 10 20 30 C 0 5 10 20 30(min) C
5'
5'
5'
SubRecQL 400nM
SubRecQS 400nM

Fig. 13 *B. subtilis* RecQ helicase-mediated ssDNA strand annealing

(A, B) Effect of the concentration of the *B. subtilis* RecQ protein on the annealing of the [5'-^{32}P]-labelled oligonucleotide 23 and unlabelled oligonucleotide 24 ssDNA substrates (1nM) which are indicated in Table 2 to generate duplex DNA. The reactions were incubated for 10 min at 37°C. The different concentrations of helicases were indicated at top of each panel. The reaction products were separated by 12% nondenaturing PAGE and revealed by autoradiography. **(C)** The exchange stimulated by *B. subtilis* RecQ helicase. Mix the fork substrate (substrate A in Table 2), single substrate (oligo 11 in Table 1) and 0.5μM helicases together and incubate at 37°C for indicated times at the top of the panels. Stop the reactions by adding the unwinding-stopping buffer. Load the reaction solution on 12% polyacrylamide gel and autoradiography.

DISCUSSION

In this chapter we describe structural and biochemical properties of two *B. subtilis* homologues of the *E. coli* RecQ. The predicted *B. subtilis* RecQ primary structure contains all the sequence motifs typically found in RecQ family helicases. Unlike the *E.coli* RecQ helicase family which contains only single member, there are two members that we named SubL and SubS here compose the *B. subtilis* RecQ family. Consistent with the sequence similarities, the homogeneous recombinant protein displayed many structural and functional properties found in other members of RecQ helicase family.

The gel filtration results indicate that the assembly state of the purified *B. subtilis* RecQL in solution is monomer. This is consistent with the ATP saturation curve which can be best fit by Hill equation with a Hill coefficient of 1, indicating that *B. subtilis* RecQL helicase functions as a monomer during ATP hydrolysis. We used homology modelling methods to build structural models of its 3-dimensional structure. Our models present the same overall structural features as the *E. coli* RecQ helicase. In particular, the *B. subtilis* RecQL helicase is similarly folded into four distinct domains, interestingly including a characteristic zinc binding domain. Biochemical analyses confirmed that the protein indeed contains a Zn^{2+} at a stoichiometry of 1:1 zinc/RecQ molecule. For the *E. coli* RecQ helicase and for the Bloom's syndrome helicase, the zinc finger motif of RecQ-Ct is necessary for enzymatic activity (3;41). Similarly, the probable zinc finger motif of the *B. subtilis* RecQ helicase may well be important for its function.

We have found that pH, temperature, divalent cations and some compounds can affect the ATPase ability of helicase. As most RecQ helicase, the best reaction temperature of ATP hydrolysis for *B. subtilis* RecQ helicases is 37°C. The concentration of magnesium ion and ATP both influence the ATPase activity of helicase. Generally, this ability increases with the concentration of magnesium ion or ATP increasing. Here we integrated these two factors and found that the ratio of magnesium and ATP affect the ATPase activity of *B. subtilis* RecQ helciase obviously. The optimal initial process occurred at a ratio of 2-fold magnesium than ATP. Both excess free magnesium and ATP would inhibit RecQ helicase ATPase ability. It is possible that Mg^{2+}-ATP binds to *B. subtilis* RecQ helicase as a complex to carry out the process of ATP hydrolysis. Either one of these cofactors are in the free form will inhibit this function of *B. subtilis* RecQ helicase. Frank G. Harmon and his colleagues found that the ratio of magnesium and ATP affected the unwinding activity of

E.coli RecQ helicase obviously (42). The trend of affection is similar with our findings, but the optimal condition for RecQ helicase function is very different.

We showed that the purified SubL and SubS helicases possess DNA stimulated ATPase activity and ATP-dependent helicase activities. DNA unwinding by *B. subtilis* RecQ activity is dependent on the presence of ATP or dATP which is hydrolyzed to provide the energy for the unwinding. The polarity of unwinding by the *B. subtilis* RecQ helicases is 3' to 5' with respect to the overhanging single-stranded DNA to which they bind. Consistent with this directionality, the *B. subtilis* RecQ unwind a duplex DNA substrate with a 3'-ssDNA tail but not a substrate with a 5'-ssDNA tail and they require a free 3'-ssDNA tail to initiate unwinding of duplex DNA substrates. *E.coli* RecQ protein, like several other helicases including RecBCD, can initiate duplex DNA unwinding from a blunt-ended terminus (43-45) . In contrast, unwinding of blunt-ended double-stranded DNA substrates by the *B. subtilis* RecQ helicases were undetectable under the assay conditions employed indicating that *B. subtilis* RecQ helicases cannot unwind duplex DNA with double blunt ends. The addition of a single-stranded tail (a 3'-tail for 3' to 5' helicase or a 5'-tail for a 5' to 3' helicase) to a duplex DNA is sufficient for many helicases to use the substrate, including those incapable of unwinding from blunt ends. Bennett *et al.* concluded that Sgs1p, the *Saccharomyces cerevisiae* homologue of the *B. subtilis* RecQ, had a requirement for a 3'-tail of at least 3nt and that the enzyme used the junction between single-stranded and double-stranded DNA in the substrate recognition process (46). In our studies, as expected, the *B. subtilis* RecQ helicases were unable to use a 5'-tailed duplex DNA but did unwind a 3'-tailed duplex. The SubL helicase needs at least 5-nt long 3'-tail and the SubS requires 10-nt long single strand. Further substrate specificity analyses showed that the *B. subtilis* RecQ helicases, like other RecQ family helicases including BLM and WRN, display intense helicase activity toward to a forked duplex DNA.

The efficiency of strand unwinding by the *B. subtilis* RecQ decreases sharply with increasing length of the strand to be unwound. The unwinding assay we used, however, detects only complete unwinding, and partially unwound fragments would not be scored. It is therefore plausible that the longer DNA strands re-anneal behind the translocating *B. subtilis* RecQ and thereby reduce the observed efficiency of unwinding. Alternatively, the *B. subtilis* RecQ helicases might exhibit a low processivity and might fall off the DNA before completing the unwinding action. Maybe this reason is also for why their unwinding activities cannot be increased when the length of the single tail of the forked double-strand increasing. Presumably, the SSB binds ssDNA during strand displacement reactions, and

prevent the displaced ssDNA from re-hybridizing with the DNA template, thereby increasing the processivity of the enzymes and stimulate their unwinding activities, for example, *E coli.* RecQ, NS3, UvrD *et al* (47;48). But we found that the presence of *E. coli* SSB couldn't significantly increase the extent of unwinding of the 70-bp partial duplex substrate by *B. subtilis* RecQ because ESSB cannot interact with these two helicases potentially and help them bind and process along the forked junction. Alternatively, the *B. subtilis* RecQ may fall off the DNA substrate before the complete the unwinding action.

Studies of RecQ helicases from human and yeast implicate these enzymes are involved in diverse DNA transaction processes ranging from DNA replication to DNA repair. A wide variety of DNA structures that resemble the DNA replication intermediates, including four-way Holliday-junctions at stalled replication forks, are substrates for RecQ family helicase. In accordance with previous observations, the *B. subtilis* RecQL unwind efficiently several replication and repair intermediates. The ability of SubL to unwind efficiently 5'-flap and synthetic replication fork substrates suggests that it can load onto duplex DNA due to a junction recognition property. The synthetic replication fork substrate was significantly unwound by SubL. Thus, it may initiate unwinding of DNA duplex substrates by a mechanism that requires an interaction between the protein and the forked duplex substrate. Indeed, the electrophoretic mobility shift assays indicated that the *B. subtilis* RecQ helicases have a higher affinity for a forked DNA substrate than for single-stranded DNA. This may have implications for the mechanism of DNA unwinding by the *B. subtilis* RecQ, and it has been suggested that preferential binding of the enzyme to such a junction might be important for helicase action (49). The action of the *B. subtilis* RecQ helicase on the 5'-flap substrate is interesting from a genetic viewpoint because this structure is a key DNA intermediate for lagging strand synthesis during DNA replication. The average size of an Okazaki fragment (100-150 nucleotides) (50) may be influenced by the action of the *B. subtilis* RecQ helicase on the flap structure. Here, we have demonstrated that the SubL can displace the 5'-ssDNA flap. The ability of SubL to unwind the duplex ahead of a fork structure that contains fully double-stranded leading and lagging strands may be important for the maintenance of fork progression when replication pauses. Precisely how the *B. subtilis* RecQ helicase acts *in vivo* to maintain genome stability remains to be described, but it is likely to involve helicase function and a structural intermediate of an important DNA metabolic pathway.

The SubL also acts as a helicase on a synthetic X structure (a model for the Holliday junction recombination intermediate). This structure forms a stacked X structure in the

presence of Mg^{2+} (present during the helicase assay) and therefore lacks ssDNA, even at its four arm ends. The SubL displayed no helicase activity on blunt-ended DNA, so it is at first sight surprising that it can unwind the X structure. Indeed, SubL helicase activity in the absence of a free 3'-ssDNA tail or any pre-existing ssDNA tracts in the substrate is contradictory with its substrate specificity. Possibly, this helicase initiates X-structure unwinding from the core of molecule. It has not been reported whether RecQ family helicases unwind the Holliday junction molecule from the four arm ends or from the core.

For the other RecQ helicase in *B. subtilis*, the SubS, we demonstrated that it cannot unwind these intermediate-substrates including 5'-ssDNA flap strand, Kappa structure and a model for the Holliday junction even the nicked duplex DNA. Moreover, its ATPase activity and unwinding ability are visibly lower than those of SubL. The difference between the SubL and SubS is that the latter one lack of the HRDC domain not the zinc domain in its RecQ-Ct domain. The previous study indicated that the HRDC is required for stable DNA binding and take role in the unwinding activity of helicase (51). For example, it is necessary for BLM to unwind the double Holliday junctions (52). Here, we approved again that the HRDC is one of the pivotal domain to unwind the several replication and repair intermediate substrates and Holliday function for *B. subtilis* RecQ helicases. At the same time, this important domain will also help RecQ helicase to hydrolyze ATP.

Our study revealed that the SubL protein exhibits an efficient DNA strand-annealing activity and exchange activity. This biological significance cannot be easily assessed because the phenotypic consequences of a RecQ deficiency in *Bacillus subtilis* cells are still unknown. The biochemical activities of the SubL implicate it takes role in a DNA replication and repair processes that involves cooperation between DNA unwinding and DNA strand-annealing. This action can facilitate regression of the replication fork while the annealing activity promotes base pairing of the newly synthesized strands during the fork regression (24;53). However, the SubS only has low DNA strand annealing activity and no effect on strands exchange. One reason is perhaps that there is no HRDC domain in the C terminal. Most DNA RecQ helicases such as WRN and BLM, the annealing activity were carried out using the C-terminal region of protein (24;54). Our results indicated that SubS helicase with shorten C-terminal cannot exhibit strong annealing activity like SubL. We conclude that the C-terminal region of *B. subtilis* RecQ helicase is required for its annealing ability and even contributes to single strands exchange. However, which C-terminal amino acids region determines these functions are still unknown in detail.

All the evidences in our laboratory indicated that *B. subtilis* RecQ helicases have typical biochemical functions of RecQ helicase family. They are essential in DNA metabolisms of *B. subtilis* species. But we have no idea to explain why there are two isoforms of RecQ helicase exist in *B. Subtilis* in native. Maybe they participate in different DNA metabolism processes *in vivo*. Further analysis of the roles of the *B. subtilis* RecQ *in vitro* and *in vivo* should be taken in order to understand their functions in maintaining genome integrity and stability deeply.

REFERENCES

1. Matson,S.W. and Kaiser-Rogers,K.A. (1990) DNA helicases. *Annu. Rev. Biochem.*, **59**, 289-329.

2. Liu,J.L., Rigolet,P., Dou,S.X., Wang,P.Y. and Xi,X.G. (2004) The zinc finger motif of Escherichia coli RecQ is implicated in both DNA binding and protein folding. *J. Biol. Chem.*, **279**, 42794-42802.

3. Guo,R.B., Rigolet,P., Zargarian,L., Fermandjian,S. and Xi,X.G. (2005) Structural and functional characterizations reveal the importance of a zinc binding domain in Bloom's syndrome helicase. *Nucleic Acids Res.*, **33**, 3109-3124.

4. Irino,N., Nakayama,K. and Nakayama,H. (1986) The recQ gene of Escherichia coli K12: primary structure and evidence for SOS regulation. *Mol. Gen. Genet.*, **205**, 298-304.

5. Umezu,K., Nakayama,K. and Nakayama,H. (1990) Escherichia coli RecQ protein is a DNA helicase. *Proc. Natl. Acad. Sci. U. S. A*, **87**, 5363-5367.

6. Stewart,E., Chapman,C.R., Al-Khodairy,F., Carr,A.M. and Enoch,T. (1997) rqh1+, a fission yeast gene related to the Bloom's and Werner's syndrome genes, is required for reversible S phase arrest. *EMBO J.*, **16**, 2682-2692.

7. Gangloff,S., McDonald,J.P., Bendixen,C., Arthur,L. and Rothstein,R. (1994) The yeast type I topoisomerase Top3 interacts with Sgs1, a DNA helicase homolog: a potential eukaryotic reverse gyrase. *Mol. Cell Biol.*, **14**, 8391-8398.

8. Watt,P.M., Louis,E.J., Borts,R.H. and Hickson,I.D. (1995) Sgs1: a eukaryotic homolog of E. coli RecQ that interacts with topoisomerase II in vivo and is required for faithful chromosome segregation. *Cell*, **81**, 253-260.

9. Cogoni,C. and Macino,G. (1999) Posttranscriptional gene silencing in Neurospora by a RecQ DNA helicase. *Science*, **286**, 2342-2344.

10. Kusano,K., Berres,M.E. and Engels,W.R. (1999) Evolution of the RECQ family of helicases: A drosophila homolog, Dmblm, is similar to the human bloom syndrome gene. *Genetics*, **151**, 1027-1039.

11. Fry,M. and Loeb,L.A. (1998) The three faces of the WS helicase. *Nat. Genet.*, **19**, 308-309.

12. Puranam,K.L. and Blackshear,P.J. (1994) Cloning and characterization of RECQL, a potential human homologue of the Escherichia coli DNA helicase RecQ. *J. Biol. Chem.*, **269**, 29838-29845.

13. Kitao,S., Ohsugi,I., Ichikawa,K., Goto,M., Furuichi,Y. and Shimamoto,A. (1998) Cloning of two new human helicase genes of the RecQ family: biological significance of multiple species in higher eukaryotes. *Genomics*, **54**, 443-452.

14. Kitao,S., Lindor,N.M., Shiratori,M., Furuichi,Y. and Shimamoto,A. (1999) Rothmund-thomson syndrome responsible gene, RECQL4: genomic structure and products. *Genomics*, **61**, 268-276.

15. Yu,C.E., Oshima,J., Fu,Y.H., Wijsman,E.M., Hisama,F., Alisch,R., Matthews,S., Nakura,J., Miki,T., Ouais,S. *et al.* (1996) Positional cloning of the Werner's syndrome gene. *Science*, **272**, 258-262.

16. Ellis,N.A., Groden,J., Ye,T.Z., Straughen,J., Lennon,D.J., Ciocci,S., Proytcheva,M. and German,J. (1995) The Bloom's syndrome gene product is homologous to RecQ helicases. *Cell*, **83**, 655-666.

17. Bernstein,D.A., Zittel,M.C. and Keck,J.L. (2003) High-resolution structure of the E.coli RecQ helicase catalytic core. *EMBO J.*, **22**, 4910-4921.

18. Ellis,N.A., Groden,J., Ye,T.Z., Straughen,J., Lennon,D.J., Ciocci,S., Proytcheva,M. and German,J. (1995) The Bloom's syndrome gene product is homologous to RecQ helicases. *Cell*, **83**, 655-666.

19. Yu,C.E., Oshima,J., Fu,Y.H., Wijsman,E.M., Hisama,F., Alisch,R., Matthews,S., Nakura,J., Miki,T., Ouais,S. *et al.* (1996) Positional cloning of the Werner's syndrome gene. *Science*, **272**, 258-262.

20. Kusano,K., Berres,M.E. and Engels,W.R. (1999) Evolution of the RECQ family of helicases: A drosophila homolog, Dmblm, is similar to the human bloom syndrome gene. *Genetics*, **151**, 1027-1039.

21. Bachrati,C.Z. and Hickson,I.D. (2003) RecQ helicases: suppressors of tumorigenesis and premature aging. *Biochem. J.*, **374**, 577-606.

22. Bachrati,C.Z. and Hickson,I.D. (2003) RecQ helicases: suppressors of tumorigenesis and premature aging. *Biochem. J.*, **374**, 577-606.

23. Machwe,A., Xiao,L., Groden,J., Matson,S.W. and Orren,D.K. (2005) RecQ family members combine strand pairing and unwinding activities to catalyze strand exchange. *J. Biol. Chem.*, **280**, 23397-23407.

24. Cheok,C.F., Wu,L., Garcia,P.L., Janscak,P. and Hickson,I.D. (2005) The Bloom's syndrome helicase promotes the annealing of complementary single-stranded DNA. *Nucleic Acids Res.*, **33**, 3932-3941.

25. Umezu,K. and Kolodner,R.D. (1994) Protein interactions in genetic recombination in Escherichia coli. Interactions involving RecO and RecR overcome the inhibition of RecA by single-stranded DNA-binding protein. *J. Biol. Chem.*, **269**, 30005-30013.

26. Kunst,F., Ogasawara,N., Moszer,I., Albertini,A.M., Alloni,G., Azevedo,V., Bertero,M.G., Bessieres,P., Bolotin,A., Borchert,S. *et al.* (1997) The complete genome sequence of the gram-positive bacterium Bacillus subtilis. *Nature*, **390**, 249-256.

27. Hickson,I.D. (2003) RecQ helicases: caretakers of the genome. *Nat. Rev. Cancer*, **3**, 169-178.

28. Ellis,N.A. and German,J. (1996) Molecular genetics of Bloom's syndrome. *Hum. Mol. Genet.*, **5 Spec No**, 1457-1463.

29. Kowalczykowski,S.C., Dixon,D.A., Eggleston,A.K., Lauder,S.D. and Rehrauer,W.M. (1994) Biochemistry of homologous recombination in Escherichia coli. *Microbiol. Rev.*, **58**, 401-465.

30. Bachrati,C.Z. and Hickson,I.D. (2003) RecQ helicases: suppressors of tumorigenesis and premature aging. *Biochem. J.*, **374**, 577-606.

31. Bernstein,D.A., Zittel,M.C. and Keck,J.L. (2003) High-resolution structure of the E.coli RecQ helicase catalytic core. *EMBO J.*, **22**, 4910-4921.

32. Bernstein,D.A. and Keck,J.L. (2003) Domain mapping of Escherichia coli RecQ defines the roles of conserved N- and C-terminal regions in the RecQ family. *Nucleic Acids Res.*, **31**, 2778-2785.

33. Liu,J.L., Rigolet,P., Dou,S.X., Wang,P.Y. and Xi,X.G. (2004) The zinc finger motif of Escherichia coli RecQ is implicated in both DNA binding and protein folding. *J. Biol. Chem.*, **279**, 42794-42802.

34. Altschul,S.F., Gish,W., Miller,W., Myers,E.W. and Lipman,D.J. (1990) Basic local alignment search tool. *J. Mol. Biol.*, **215**, 403-410.

35. Machwe,A., Xiao,L., Groden,J., Matson,S.W. and Orren,D.K. (2005) RecQ family members combine strand pairing and unwinding activities to catalyze strand exchange. *J. Biol. Chem.*, **280**, 23397-23407.

36. Bernstein,D.A., Zittel,M.C. and Keck,J.L. (2003) High-resolution structure of the E.coli RecQ helicase catalytic core. *EMBO J.*, **22**, 4910-4921.

37. Liu,J.L., Rigolet,P., Dou,S.X., Wang,P.Y. and Xi,X.G. (2004) The zinc finger motif of Escherichia coli RecQ is implicated in both DNA binding and protein folding. *J. Biol. Chem.*, **279**, 42794-42802.

38. Xu,H.Q., Deprez,E., Zhang,A.H., Tauc,P., Ladjimi,M.M., Brochon,J.C., Auclair,C. and Xi,X.G. (2003) The Escherichia coli RecQ helicase functions as a monomer. *J. Biol. Chem.*, **278**, 34925-34933.

39. Zhang,X.D., Dou,S.X., Xie,P., Hu,J.S., Wang,P.Y. and Xi,X.G. (2006) Escherichia coli RecQ is a rapid, efficient, and monomeric helicase. *J. Biol. Chem.*, **281**, 12655-12663.

40. Harmon,F.G. and Kowalczykowski,S.C. (2001) Biochemical characterization of the DNA helicase activity of the escherichia coli RecQ helicase. *J. Biol. Chem.*, **276**, 232-243.

41. Liu,J.L., Rigolet,P., Dou,S.X., Wang,P.Y. and Xi,X.G. (2004) The zinc finger motif of Escherichia coli RecQ is implicated in both DNA binding and protein folding. *J. Biol. Chem.*, **279**, 42794-42802.

42. Harmon,F.G. and Kowalczykowski,S.C. (2001) Biochemical characterization of the DNA helicase activity of the escherichia coli RecQ helicase. *J. Biol. Chem.*, **276**, 232-243.

43. Umezu,K., Nakayama,K. and Nakayama,H. (1990) Escherichia coli RecQ protein is a DNA helicase. *Proc. Natl. Acad. Sci. U. S. A*, **87**, 5363-5367.

44. Harmon,F.G. and Kowalczykowski,S.C. (1998) RecQ helicase, in concert with RecA and SSB proteins, initiates and disrupts DNA recombination. *Genes Dev.*, **12**, 1134-1144.

45. West,S.C. (1996) DNA helicases: new breeds of translocating motors and molecular pumps. *Cell*, **86**, 177-180.

46. Bennett,R.J., Keck,J.L. and Wang,J.C. (1999) Binding specificity determines polarity of DNA unwinding by the Sgs1 protein of S. cerevisiae. *J. Mol. Biol.*, **289**, 235-248.

47. Shereda,R.D., Bernstein,D.A. and Keck,J.L. (2007) A central role for SSB in Escherichia coli RecQ DNA helicase function. *J. Biol. Chem.*, **282**, 19247-19258.

48. Rajagopal,V. and Patel,S.S. (2008) Single strand binding proteins increase the processivity of DNA unwinding by the hepatitis C virus helicase. *J. Mol. Biol.*, **376**, 69-79.

49. Bennett,R.J., Keck,J.L. and Wang,J.C. (1999) Binding specificity determines polarity of DNA unwinding by the Sgs1 protein of S. cerevisiae. *J. Mol. Biol.*, **289**, 235-248.

50. Bae,S.H., Bae,K.H., Kim,J.A. and Seo,Y.S. (2001) RPA governs endonuclease switching during processing of Okazaki fragments in eukaryotes. *Nature*, **412**, 456-461.

51. Bernstein,D.A. and Keck,J.L. (2003) Domain mapping of Escherichia coli RecQ defines the roles of conserved N- and C-terminal regions in the RecQ family. *Nucleic Acids Res.*, **31**, 2778-2785.

52. Wu,L., Chan,K.L., Ralf,C., Bernstein,D.A., Garcia,P.L., Bohr,V.A., Vindigni,A., Janscak,P., Keck,J.L. and Hickson,I.D. (2005) The HRDC domain of BLM is required for the dissolution of double Holliday junctions. *EMBO J.*, **24**, 2679-2687.

53. Kanagaraj,R., Saydam,N., Garcia,P.L., Zheng,L. and Janscak,P. (2006) Human RECQ5beta helicase promotes strand exchange on synthetic DNA structures resembling a stalled replication fork. *Nucleic Acids Res.*, **34**, 5217-5231.

54. Muftuoglu,M., Kulikowicz,T., Beck,G., Lee,J.W., Piotrowski,J. and Bohr,V.A. (2008) Intrinsic ssDNA annealing activity in the C-terminal region of WRN. *Biochemistry*, **47**, 10247-10254.

III. The arginine finger of the Bloom syndrome protein: its structural organization and its role in energy coupling

The abbreviations used are: BS, Bloom syndrome; BLM, Bloom syndrome protein; BSA, bovine serum albumin; ssDNA, single-stranded DNA; dsDNA, double-stranded DNA; EMSA, electrophoretic mobility shift assay; FRET, fluorescence resonance energy transfer; HRDC, helicase-and-ribonuclease D-C-terminal domain; mantATP, 2′(3′)-*O*-(*N*-methlanthraniloyl) adenosine-5′-triphosphate.

ACKNOWLEDGEMENTS

This research was supported by the grant from the Institut National du Cancer to M.A.-G. and X.G.X., the National Natural Science Foundation of China, the Innovation Project of the Chinese Academy of Sciences. Part of this work was performed by HR and XGX in CNRS, UMR8113, ENS de Cachan, France. H.R. was supported by French government's scholarships. Funding to pay the Open Access publication charges for this article was provided by CNRS.

SUMMARY

RecQ family helicases are essential in maintaining chromosomal DNA stability and integrity. Despite extensive studies, the mechanisms of these enzymes and interactions between different functional domains are still poorly understood. Crystal structures of many helicases reveal that there are highly conserved arginine residues of helicase core domain are located near the γ-phosphate of ATP. This kind of residue is widely recognized as an arginine finger, and may sense ATP binding and hydrolysis, and transmit conformational changes. We investigated the existence and role of the arginine finger in the Bloom syndrome protein (BLM), a RecQ family helicase, in ATP hydrolysis and energy coupling. Our studies by combination of structural modelling, site-directed mutagenesis, and biochemical and biophysical approaches, demonstrate that mutations of residues interacting with the γ-phosphate of ATP or surrounding the ATP binding sites result in severe impairment in the ATPase activity of BLM. These mutations also impair BLM's DNA unwinding activities, but do not affect its ATP and DNA binding abilities. These data allow us to identify R982 as the residue that functions as a BLM arginine finger. Our findings further indicate how the arginine finger is precisely positioned with respect to the γ-phosphate by the conserved motifs and the relationship between this finger with other special residues of helicase core domain.

INTRODUCTION

DNA helicases play essential roles in nucleic acid metabolism by facilitating cellular processes including genome replication, DNA repair, recombination, transcription and telomere maintenance (1;2). Helicases function as molecular motors. They use the free energy of nucleotide triphosphate (NTP) binding and/or hydrolysis to translocate along and separate the two complementary strands of a nucleic acid duplex (3). A central question remaining is the manner in which energy produced by ATP binding and/or hydrolysis is coupled to helicase function.

Most SF1 and SF2 helicases are folded into two prominent domains, labelled domain 1 and domain 2, that are separated by a deep cleft. Each domain contains two sub-domains, referred as A and B (4;5). While the domains 1A and 2A are structurally similar, the domains 1B and 2B show no significant similarity to each other (4;6). Domain 1A and 2A constitute the helicase core, and share a common folding pattern and arrangement of secondary structures with RecA, the *E.coli* recombination strand exchange enzyme (Fig. 1C) (7). Domain 1A contains the ATP binding motifs 0, I, Ia, and II (the Walker A and B motifs), and the ATP hydrolysis motif III. Domain 2A contains motifs IV and V, which are believed to be involved in DNA binding. Domain 2A also contains motif VI, which may coordinate ATPase and helicase activities. These conserved motifs are present at the interface of the two domains, or at the interface with the oligonucleotide and/or ATP. ATP- and oligonucleotide-binding sites are spatially segregated, but the conserved motifs must function together to couple the ATPase cycle and the intra-molecular conformational changes that drive the processive strand displacement or duplex unwinding activity. Indeed, a comparison of the structures of PcrA helicase in apo-state and in complex with the same DNA, but different nucleotide factors revealed a significant movement of domains 1B and 2B relative to each other and a closure of the cleft between domains 1A and 2A after the binding of DNA and ATP (8). These observations have established the structural basis for ligand-induced conformational changes that are very important for the overall mechanism of helicases.

Several crystal structures of helicases have revealed that a conserved arginine residue, usually termed “arginine finger”, may be involved in the communication between the two RecA-like domains of helicases (7-10). An arginine residue that interacts the γ-phosphate of a bound nucleotide, and that is located distal to the nucleotide-binding site is known as an

arginine finger (11;12). Arginine fingers contribute to NTP hydrolysis through stabilization of the transition state of the reaction, and functions as a trigger for conformational changes after NTP hydrolysis (11-13). Depending on the enzyme, the arginine finger may be located in a separate activator protein, for example GAP-Ras (14), or it may also be located in an adjacent subunit of an oligomeric protein: F1-ATPase (15), AAV2 Rep40 (16), the bacteriophage T7 gene 4 helicase (17), the replication factor C (18) and the SV40 LTag helicase (19). The arginine finger may also be found in a distinct domain within the protein, as in most SF1 and SF2 helicases. In the structure of PcrA complexed with AMP-PNP, the guanidium groups of residue R287, located between motif III and IV, and of R610, located in motif VI, form a salt bridge with the γ-phosphate of the nucleotide. Mutation analysis has confirmed that both R287 and R610 are involved in ATP hydrolysis (20). Two arginine residues in motif VI are highly conserved in RecQ family helicases and are spatially located close to the ATP γ-phosphate (Fig. 1). In the *E. coli* RecQ atomic resolution structure, both highly conserved Arg326 and Arg329 in motif VI (equivalent to Arg979 and Arg982 in BLM) are near the γ-phosphate of the nucleotide (10;21) (Fig. 1B). Comparing the crystallographic structures, the position of Arg326 relative to the ATP binding sites in RecQ is similar to that of R610 in PcrA; however, it remains to be determined which residue is an arginine finger or whether both residues are involved in stabilizing the γ-phosphate of the nucleotide. In addition, inspection of the crystal structure of the *E. coli* RecQ helicase and the molecular modelling model of BLM protein indicated that the spatial position of the putative arginine finger residues may be further positioned by several residues at/or near the interface between the two domains. As shown in Fig. 1C, the interactions between H798 and Q975 may help to stabilize the position of R979. Similarly, the D983-R959 salt bridge could keep R982 at an appropriate spatial position to permit the interactions between the oxygen atom of the γ-phosphate of a bound nucleotide and the guanidinium amine group of R982.

Here, we describe studies of the Bloom syndrome protein (BLM) to investigate the role of the postulated "arginine finger" of RecQ family helicases in ATP hydrolysis and energy coupling. Although both arginine residues, R979 and R982, in BLM may be involved in ATP hydrolysis, R982 appears to be crucial in stabilizing the transition state and may act as an arginine finger. Our data provides new insights into how the conserved helicase motifs are spatially organized into a network monitoring the presence or absence of a γ-phosphate on the nucleotide, and how this allows communication between the two domains.

Figure 1

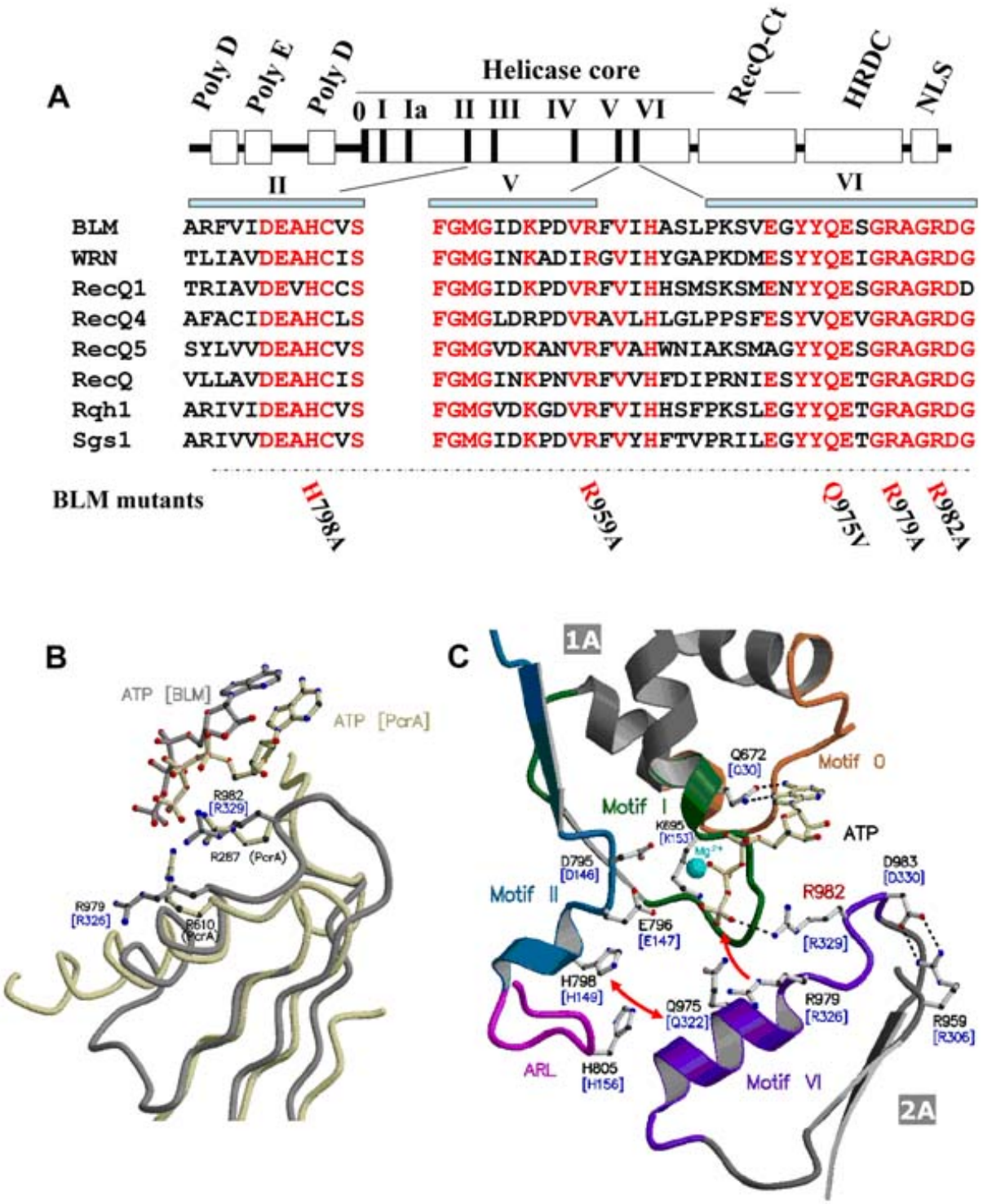
A
Poly D
Poly E
Poly D
Helicase core
0 I Ia II III IV V VI
RecQ-Ct
HRDC
NLS
II
V
VI
BLM ARFVIDEAHCVS FGMGIDKPDVRFVIHASLPKSVEGYYQESGRAGRDG
WRN TLIAVDEAHCIS FGMGINKADIRGVIHYGAPKDMESYYQEIGRAGRDG
RecQ1 TRIAVDEVHCCS FGMGIDKPDVRFVIHHSMSKSMENYYQESGRAGRDD
RecQ4 AFACIDEAHCLS FGMGLDRPDVRAVLHLGLPPSFESYVQEVGRAGRDG
RecQ5 SYLVVDEAHCVS FGMGVDKANVRFVAHWNIAKSMAGYYQESGRAGRDG
RecQ VLLAVDEAHCIS FGMGINKPNVRFVVHFDIPRNIESYYQETGRAGRDG
Rqh1 ARIVIDEAHCVS FGMGVDKGDVRFVIHHSFPKSLEGYYQETGRAGRDG
Sgs1 ARIVVDEAHCVS FGMGIDKPDVRFVYHFTVPRILEGYYQETGRAGRDG
BLM mutants
H798A
R959A
Q975V
R979A
R982A
B
ATP [BLM]
ATP [PcrA]
R982 [R329]
R287 (PcrA)
R979 [R326]
R610 (PcrA)
C
1A
Q672 [Q30]
Motif 0
Motif I
K695 [K153]
ATP
D795 [D146]
Motif II
E796 [E147]
R982
[R329]
D983 [D330]
H798 [H149]
Q975 [Q322]
R979 [R326]
R959 [R306]
ARL
H805 [H156]
Motif VI
2A

Fig. 1 (A) Schematic presentation of the conserved residues mutated in this study. BLM protein domain/motif organisations are shown above the BLM protein schema. Conserved residues are highlighted in red and the mutated residues are shown at the bottom of the figure. Alignment was performed using CLUSTALW and refined manually. (B) Superposition of the BLM modeled structure (in grey) with the PcrA crystal structure (in cream) showing the side chains of R979 and R982 from BLM (residues highlighted in grey) spatially equivalent to R610 and R287 respectively in PCRA (residues highlighted in cream). The least-squares superposition gave a RMSD of 1.25 Å. Residue numbering for PCRA is indicated besides the label PCRA. In blue and in brackets are the one letter codes of the analogous residues in RecQ from *E. coli*. (C) Detailed view of the environment of the R982 arginine finger and the ATP-binding site of the BLM-ATP modelled structure. The molecular structure of BLM in complex with ATP was modelled according Guo *et al.* (22). The conserved helicase motifs are coloured as follows: motif 0 is drawn in gold, motif I in green, motif II in blue and motif VI in purple. The conserved aromatic-rich loop is in magenta and the rest of the structure is coloured grey. ATP is drawn in cream with a ball-and-stick representation and the manganese ion is in cyan. Residues thought to be involved in ATP binding or hydrolysis are indicated. H798, H805 and Q975, possibly participating in interactions between domains II and VI, are also indicated. The salt bridge linking conserved residues R959 and D983 is indicated in dashed lines. The one letter codes and positions of the analogous residues in RecQ from *E. coli* are coloured blue and are in brackets. The red double arrow suggests a motion for R979 side chain. Highlighted in grey are the labels of subdomains 1A and 1B.

Table 1 Sequences of oligonucleotides used for site-directed mutagenesis and DNA substrates

BLM	Recombinant or mutagenic PCR primer (5'-3')
WT	F- GGAATTCATATGGAGCGTTTCCAAAGTCTTAGTTTTCCT R- CCGCTCGAGTTACGATGTCCATTCAGAGTATTTCTGTAA
H798A	F- ATTGATGAAGCAATTTGTGTCAGTCAG R- CTGACTGACACAAATTGCTTCATCAAT
R959A	F- GTACAGAAGGACACCCTGACTCAGCTG R- CAGCTGAGTCAGGGTGTCCTTCTGTAC
Q975V	F- GAGGGTTACTACGTAGAATCTGGCAGA R- TCTGCCAGATTCTACGTAGTAACCCTC
R979A	F- TACCAAGAATCTGGCGCAGCTGGAAGAGATGGG R- CCCATCTCTTCCAGCTGCGCCAGATTCTTGGTA
R982A	F- TCTGGCAGAGCTGGAGCAGATGGGGAAATATCT R- AGATATTTCCCCATCTGCTCCAGCTCTGCCAGA
R979/982A	F- TACCAAGAATCTGGCGCAGCTGGAGCAGATGGGGAAATA R- TATTTCCCCATCTGCTCCAGCTGCGCCAGATTCTTGGTA

DNA substrate	length	DNA substrate sequence (5'-3')
A	44	GCACTGGCCGTCGTTTTACGGTCGTGACTGGGAAAACCCTGGCG
B	25	CGCCAGGGTTTTCCCAGTCACGACC
C	36	ACGTGGGCAAAGTTCGTCAATGGACTGACAGCTGCA
E	19	GTAAAACGACGGCCAGTGC
F	44	CGCCAGGGTTTTCCCAGTCACGACCAACCCCTTTTTTTTTCAA
G	50	TCAAAGTCACGACCTAGACACTGCGAGCTCGAATTCACTGGAGTGACCTC-
H	50	GAGGTCACTCCAGTGAATTCGAGCTCGCAGTGTCTAGGTCGTGACTTTGA

MATERIALS AND METHODS

Plasmid construction and site-directed mutagenesis

We created a plasmid for over-producing the BLM helicase core protein, consisting of amino acid residues 642-1290. To produce a recombinant protein bearing six tandem histidine tag at N-terminus, the gene encoding BLM (642-1290) was inserted between the NdeI and XhoI cloning sites and expression of the His-tagged protein is driven by a T7 RNA polymerase promoter of the expression plasmid pET15b (Novagen). The resulting plasmid, referred to as pET-BLM$^{642-1290}$, was used as the target plasmid for site-directed mutagenesis. All point mutations were constructed by PCR with primers carrying the desired mutations (Table 1). To verify that there were no undesired mutations, the PCR products were sequenced at MWG (MWG Biotech, Germany) by the fluorescent DNA sequencing method.

Protein expression and purification

All proteins (BLM$^{642-1290}$ and its corresponding variant) were purified as described (22). Briefly, a single colony of the *E. coli* strain (BL21-CodonPlus, Stratagene) producing the corresponding protein was grown overnight in 10ml of LB containing 80μg/ml ampicillin and 34μg/ml chloramphenicol at 37°C with shaking at 200rpm.. We diluted 0.1 ml of this culture with 1 litre of pre-warmed LB. The cells were grown to mid-exponential phase (A_{600} of 0.5-0.6) at 37°C. Over-production of proteins was induced by the addition of isopropyl-1-thio-α-D-galctopyranoside to a final concentration of 0.25mM, and the culture was further shaken at 18°C for 18h. The cells were harvested by centrifugation and suspended in a final volume of 25 ml of the lysis buffer (50mM Tris-HCl, pH 7.5, 500mM NaCl, 0.1% Triton X-100, PMSF 0.1μM and 10% ethylene glycerol). Cells were lysed with a French press and the lysates were sonicated to reduce viscosity. To remove insoluble materials, the cell lysates were centrifuged twice at 15,000 g for 45 min. The soluble extract was applied to a column containing 20ml nickel-coated resin (Novagen) and the subsequent purification procedures were performed with a FPLC system (ÄKTA Purifier) at low temperature. The column was washed with lysis buffer until the UV absorbance at 280nm stabilized. Bound proteins were eluted with a 300ml linear gradient of imidazole (0.02-0.4

M). Fractions containing the proteins were identified by SDS-polyacrylamide gel electrophoresis. Pooled fractions were concentrated and further purified by FPLC size exclusion chromatography (Superdex 200, Amersham Bioscience). The collected fractions were analyzed on 10% SDS-PAGE and confirmed the aimed protein fractions. If necessary, the pooled fractions containing the aimed protein were concentrated with Amicon Ultra Centrifugal filter Devices. The purified proteins were run on SDS-polyacrylamide gels and stained with Commassie brilliant blue. The concentrations of the purified proteins were determined by the Bio-Rad dye method using bovine serum albumin as the standard.

DNA substrates preparation

PAGE-purified DNA substrates were purchased from Proligo (France) (Table 1). Duplex DNA substrates were prepared as described previously (23). Briefly, 250 μM oligonucleotides were denatured in 1×TE, containing 1 M NaCl or 1 M KCl, by incubating at 95°C for 10 min. Denatured oligonucleotide was annealed at 37°C for 48 h. The DNA substrate was further purified using 8% native PAGE containing 10mM KCl at 4°C for 12 h with constant current of 20mA. The purified duplex DNA was excised from the gel and incubated with the elution buffer (0.1% SDS, 1mM EDTA, 0.3M sodium acetate, pH=5.2) at room temperate over night. The eluted duplex DNA was concentrated with ethanol precipitation.

ATPase assay

The ATPase activity was detected by measuring the release of free phosphate during ATP hydrolysis (24;25). The reaction was carried out in ATPase reaction buffer (50mM Tris-HCl, pH 8.0, 3mM $MgCl_2$, 0.5mM DTT) at 37°C in a volume of 100μl. The reactions were initiated by the addition of enzymes into the reaction mixture contained 0.5μM ssDNA (nt, 60 mer oligonucleotide) and the indicated concentration of ATP. Eighty μl aliquots were transferred from the reaction mixture every 30s into a hydrochloric solution of ammonium molybdate, stopping the reaction. The liberated radioactive γ^{32}Pi was extracted with a solution of 2-butanol-benzene-acetoneammonium molybdate (750:750:15:1) saturated with water. An aliquot (60μl) was removed from the organic phase and the radioactivity was quantified using a liquid scintillation counter.

DNA unwinding activity assay

a) Radiometric assay.

DNA helicase reactions were incubated at 37°C. The reaction mixtures contained 25 mM HEPES-NaOH, pH 7.5, 25mM CH_3CO_2Na, 7.5mM $(CH_3CO_2)_2Mg$, 1mM ATP, 1mM DTT, 0.1mg/ml BSA, and the indicated ^{32}P-labelled partial duplex DNA substrate (10fmol, 3000c.p.m/fmol). Reactions were initiated by adding various concentrations of BLM proteins at 37°C. Reactions were terminated after 30 minutes by adding 7µl of 3× unwinding reaction stop-loading buffer (50% Glycerol, 20mM EDTA, 0.5%SDS and 0.05% Bromophenol Blue). The products of the helicase reactions were run on a 12% (w/v) polyacrylamide gel (acylamide to bis-acrylamide ratio 19:1) in TBE buffer (89mM Tris-boric acid and 2mM EDTA, pH 8) at 100V for 2 h at 4°C.

b) *Fluorometric assay.*

Stopped-flow DNA-unwinding assays were performed as described (26). Briefly, the experiments were performed using a Bio-logic SFM-400 mixer with a 1.5 mm×1.5 mm cell (Bio-Logic, FC-15) and a Bio-Logic MOS450/AF-CD optical system equipped with a 150-W mercury-xenon lamp. Fluorescein was excited at 492 nm (2-nm slit width), and its emission was monitored at 525nm using a high pass filter with 20-nm bandwidth (D525/20; Chroma Technology Co.). The experiments were conducted in two-syringe mode, where helicase and duplex DNA substrates were pre-incubated in syringe 1 for 5 min and ATP in syringe 4. Each syringe contained unwinding reaction buffer (25mM Tris-HCl, pH 7.5 at 25°C, 50mM NaCl, 1mM $MgCl_2$ and 0.1mM DTT) and the unwinding reaction was initiated by rapid mixing of the two syringes. The sequences of the two strands of the 56:16-mer DNA substrate are 5'H-AATCCGTCGAGCAGAG(dT40)-3', labelled with hexachlorofluorescein (H), and 3'F-TTAGGCAGCTCGTCTC-5', labelled with fluorescein (F). Due to the unwinding and thus the separation of the two DNA strands, the FRET (Fluorescence resonance energy transfer) between the two fluorescent molecules was reduced. As a result, the fluorescence emission, F(t), of the donor fluorescein was increased from an initial (Fini) value to a saturating value (26). Control experiment has shown that in the absence of ATP, no emission change was observed, the same as in the case of RecQ

(26). To convert the output data from volts to unwinding amplitude, we performed a calibration experiment in a four-syringe mode where the helicase was in syringe 1, H-labelled ss oligonucleotides in syringe 2, F-labelled ss oligonucleotides in syringe 3 and ATP in syringe 4. Each syringe contained unwinding reaction buffer. After mixing the solutions from the four syringes, the fluorescent signal of the mixed solution was measured, giving a value (F100%) that corresponded to 100% unwinding. The time-courses of DNA unwinding was then obtained using $A(t) = [F(t) - F_{ini}]/(F_{100\%} - F_{ini})$. The standard reaction temperature was 25°C and all concentrations listed were after mixing unless noted otherwise. Data were fitted with Equation 1

$$A(t) = A_1\left(1 - e^{-k_{obs,1}t}\right) + A_2\left(1 - e^{-k_{obs,2}t}\right), \qquad \text{(Eq. 1)}$$

Where: A_1 (A_2) and $k_{obs,1}$ ($k_{obs,2}$) represent, respectively, the unwinding amplitude and rate of the fast (slow) phase.

DNA binding assay

a) Electrophoretic mobility shift assay.

Single-strand substrate was labelled with 5'-[γ-^{32}P]ATP (oligonucleotide G in Table 1) and hybirdized with the unlabelled complementary substrate (oligonucleotide H in Table 1). Binding reactions (20 µl) were performed with 1nm single-strand substrate or double-strand substrate in standard binding buffer (40mM Tris-HCl, pH 7.0, 1mM EDTA, 20mM NaCl, 8% glycerol and 20µg/ml bovine serum albumin). Protein and DNA substrate concentrations are indicated in the figure legends. DNA-protein binding reaction mixtures were incubated at 37°C for 20 min. After adding 7µl of native loading dye (0.25% bromophenol blue in 30% glycerol), reaction mixtures were loaded on a 6% non-denaturing polyacrylamide gel (19:1). Electrophoresis was carried out at a constant voltage of 14V/cm at 10°C in 1×TBE (8mM Tris-Base, 89mM Boric acid, 2mM EDTA, pH8.0 and 1mM EDTA) for 2 h. The gel was dried and processed for autoradiography.

b) *Fluorescence polarization assay.*

DNA binding was further analyzed by fluorescence polarization as described previously (23). The assays were performed using a Bio-logic auto-titrator (TCU-250) and a Bio-Logic optical system (MOS450/AF-CD) in fluorescence anisotropy mode. Various amounts of

protein were added to 1ml of binding buffer containing 2 or 5nM DNA substrate. Each sample was allowed to equilibrate in solution for 1.5 min, after which fluorescence polarization was measured. Titrations were performed in a temperature-controlled cuvette at 25°C. The solution was stirred continuously by a small magnetic stir bar during the entire titration process. The binding isotherms were determined and fit to Equation 2.

$$A = A_{\min} + \left(A_{\max} - A_{\min}\right)\frac{\Delta - \sqrt{\Delta^2 - 4D_T NP_T}}{2D_T}, \qquad \text{(Eq. 2)}$$

Where: A is the fluorescence anisotropy at a given concentration of RecQ, $A_{\max}$ is the anisotropy at saturation, and $A_{\min}$ is the initial anisotropy. $\Delta = D_T + NP_T + K_D$, D_T is the total concentration of DNA, P_T is the concentration of the enzyme in the binding solution.

DNA annealing activity by EMSA

The DNA strand-annealing activity of the wild-type and arginine residues mutants were assayed using complementary synthetic oligonucleotides, one of the oligonucleotide of 0.2nM was labelled at the 5′-end using [γ-^{32}P]ATP and T4 polynucleotide kinase and the other unlabelled complementary oligonucleotide was at a concentration of 0.4nM. In a standard strand-annealing assay, the labelled oligonucleotide (oligonucleotide G) was added to a reaction buffer (20μl) containing 50 mM Tris-HCl (pH8,0), 5mM $MgCl_2$, 20mM NaCl, 1mM DTT, 50μg/ml BSA and the indicated protein concentration. The reaction was initiated by adding the unlabelled oligonucleotide (oligonucleotide F) and helicases which were at different concentrations, then immediately followed by incubation at 37°C for 10 min. Stop the reaction by adding 1/3 vol of 3× annealing reaction stop-loading buffer. . Analysis the result on a 12% (w/v) polyacrylamide gel (acylamide to bis-acrylamide ratio 19:1) in 1×TBE buffer and run the electrophoresis at 200V for 2 hours at 10°C. The gel was dried at 80°C for 1 hour and exposed by autoradiography.

ATP-binding assays

a) Nitrocellulose filter binding assay.

The ATP binding affinities of BLM$^{642\text{-}1290}$ and the mutants were measured by nitrocellulose filter binding as previously described (17). The assays were performed at 4 °C. A constant amount of ATP and various concentrations of the proteins were used in

the nitrocellulose assays. Nitrocellulose filters (25 mm) were washed with 0.5M NaOH for 10 min, rinsed with double-distilled water, and then equilibrated in wash buffer (40mM Tris-HCl, pH 7.5/10 mM $MgCl_2$/50 mM potassium glutamate). The proteins (from 5 to 30 μM) were mixed with 200μM ATP and [γ-^{32}P]ATP in the absence of DNA in 40mM Tris-HCl (pH 7.5)/10mM $MgCl_2$/10mM DTT/50mM potassium glutamate/10% glycerol in a total volume of 20 μl. The reaction mixtures were incubated for 30 min on ice or 10 min at room temperature, and 15μl aliquots were filtered through the nitrocellulose filters. The membranes were washed twice with 2ml of ice-cold wash buffer. The radioactivity of the nitrocellulose membrane was quantified using a liquid scintillation counter. The ATP binding stoichiometry was calculated from the radioactivity count.

b) Fluorometric mantATP binding assays.

We also used a fluorescent nucleotide analogue (mantATP) to determine the apparent dissociation values for ATP binding (27). Fluorescence spectra of the proteins were measured using FluoroMax-2 spectrofluorimeter (Jobin Yvon, Spex Instruments S.A., Inc) at 25°C. We used 0.5μM protein in 1 ml reaction buffer (25mM Tris-HCl, pH 7.5, 50mM NaCl and 0.1mM DTT) in a 10×10×40mm^3 quartz cuvette. The fluorometric mantATP binding assays were performed using a Bio-logic auto-titrator (TCU-250). Each protein was titrated with various concentrations of mantATP, during which the protein was excited at 280nm and the fluorescence of mantATP at 440nm due to fluorescence resonance energy transfer (FRET) was measured. The apparent dissociation constant K_d was determined by fitting the fluorescence intensity [corrected for the inner filter effect] to Equation 3,

$$F = F_s c_d + f_d x + f_c \frac{(x + 0.5c_d + K_d) - \sqrt{(x + 0.5c_d + K_d)^2 - 2xc_d}}{2}, \qquad \text{(Eq. 3)}$$

where: F_s is the starting fluorescence of the reaction mixture, f_d is the fluorescence coefficient of free mantATP, f_c is the fluorescence coefficient of complex formed, and x is the total concentration of mantATP. $c_d = V_0/(V_0 + V_i) \equiv 1 - x/[\text{mantATP}]$ is included to correct accurately for the sample dilution effect, where V_0 is the initial sample volume, V_i is the volume of titrant added, and [mantATP] is the mantATP concentration of the titrant.

Preparation of orthovanadate solutions

To ensure formation of a transition state with Vi, the Vi stock solution was prepared according to Ko *et al*. (28). Briefly, Na_3VO_4 powder was dissolved in water and the pH adjusted with HCl to pH 10 (orange colour). The solution was boiled for 2 min and consequently became clear. The pH was readjusted to pH 10 and boiling was repeated twice. The Vi concentration was determined using a molar extinction coefficient of 2925 $M^{-1}cm^{-1}$. The solution was covered with aluminium foil and stored at -80°C until use.

RESULTS

The previous studies have shown that a recombinant helicase of BLM protein that is composed of residues 642-1290 ($BLM^{642-1290}$) displays similar biological properties, both *in vitro* and *in vivo*, to that of the full length BLM protein (22;29). The $BLM^{642-1290}$ not only exhibited comparable ATPase, helicase activities and DNA substrates specificity to the full-length protein, but also suppresses spontaneous and UV-induced illegitimate recombination in *E. coli* (29). Since no enzymatic activity can be attributed to the N-terminal region of BLM, we used the $BLM^{642-1290}$ protein fragment in this study for the sake of facilities of the experiments.

Design, expression, and purification of BLM mutations

To better understand the role of the BLM helicase arginine finger in ATP hydrolysis and energy coupling, we introduced two categories of mutations into the $BLM^{642-1290}$ protein fragment using the structural information obtained from *E. coli* RecQ helicase and our BLM molecular modelling (Fig. 1). To explore the possibility that an arginine residue near the γ-phosphate of nucleotide acts as an arginine finger, either Arg979 or Arg982 (equivalent to Arg326 and Arg329 of *E. coli* helicase) or both were replaced by an alanine residue. To investigate how the ATP binding and hydrolysis signal is relayed to the second domain (domain 2A) via the arginine finger, residues Q975 in motif VI and H798 in motif II were replaced by valine and alanine, respectively; in this mutant the hydrogen bonds between Q975 and H798 are, obviously, altered. Also, R959 was replaced by an alanine residue to disrupt the salt bridge between Asp983 and Arg959 (Fig. 1C). The six mutants were constructed using site-directed mutagenesis. The intact *BLM* gene contains amino acids residues 642-1290 ($BLM^{642-1290}$). The intact *BLM* gene and each mutated gene were expressed in an *E. coli* pET expression system. The mutants and the wild-type $BLM^{642-1290}$ fragment were over-produced and purified using Ni-agarose affinity chromatography and the eluting procedure was performed with FPLC system. When the concentration of imidazole in eluting buffer reaches to 250mM, the aimed protein can be eluted from the affinity chromatography in a great measure and the fastigium appeared at 0.3M imidazole. For example, we can harvest most R979A mutant enzyme at 0.3M imidazole (Fig. 2 A). Then we purified these enzymes further with the gel filtration chromatography columns

(Superdex-200) to homogeneity and supervised the processes with FPLC system (ÄKTA Purifier) at UV280. Finally, the purities of proteins reached from 90 to 95% (Fig. 2 B and 2C).

Figure 2

A

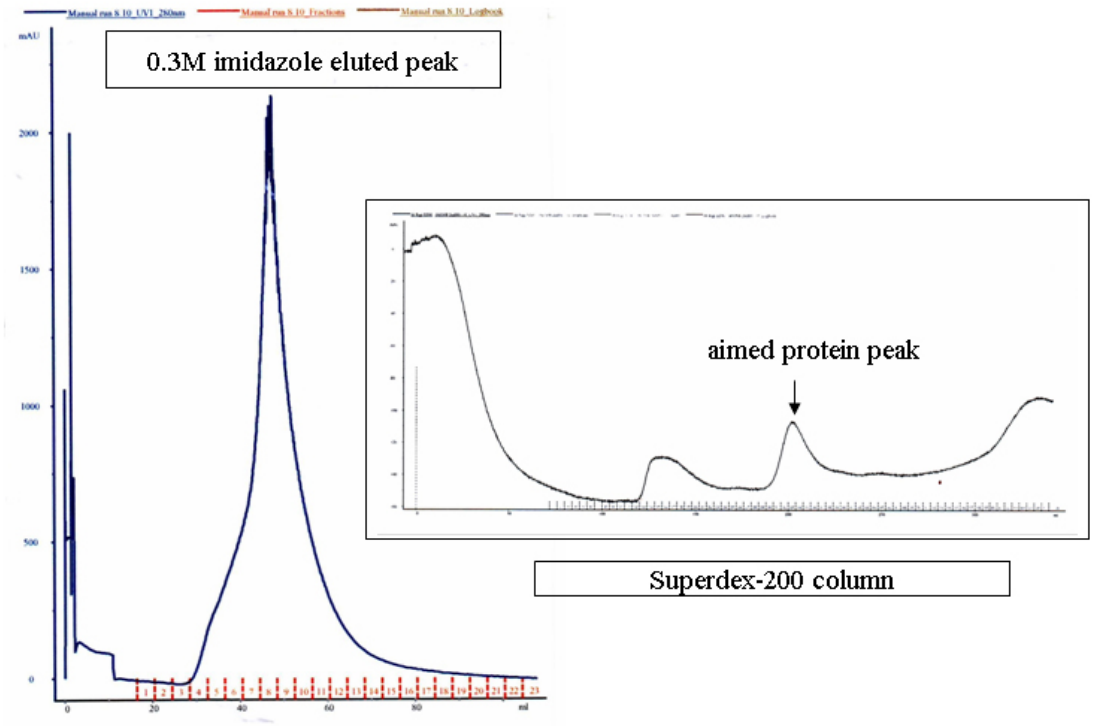

B

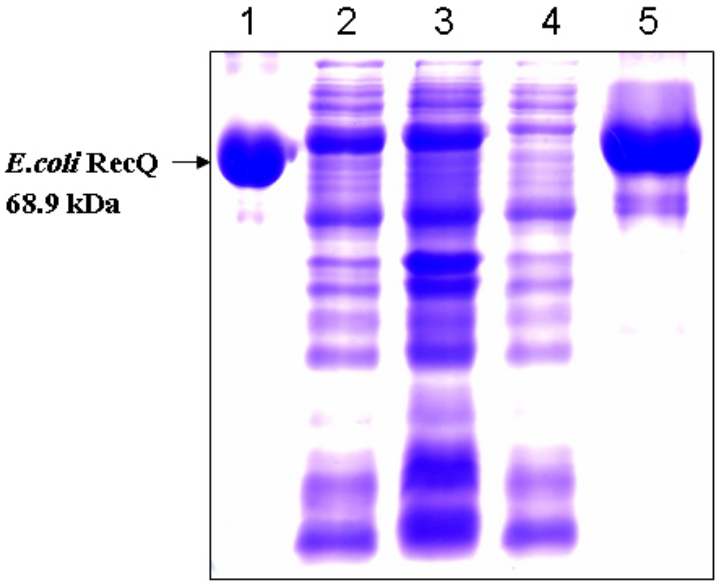

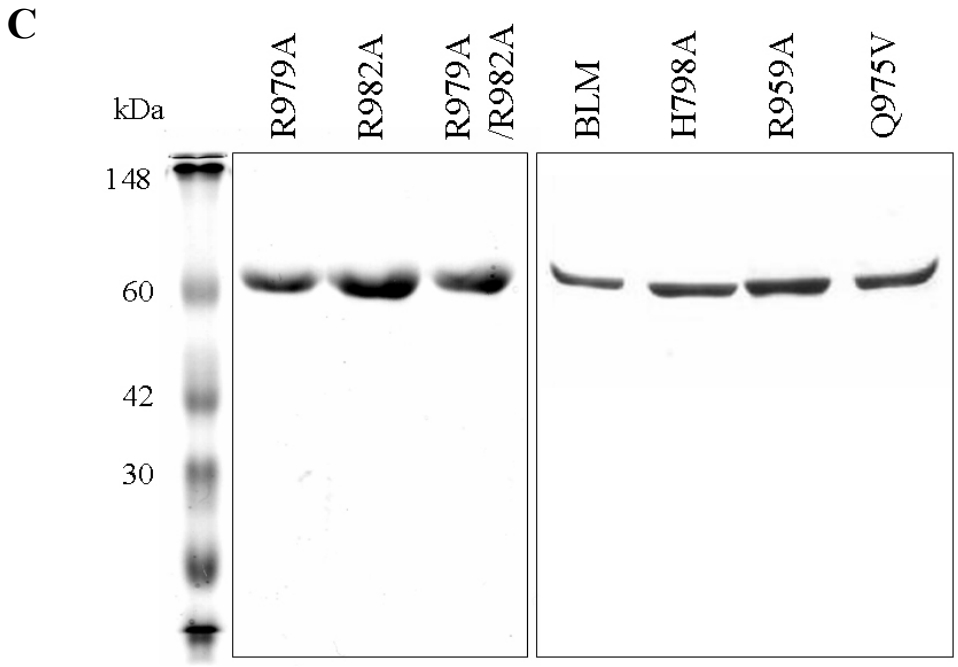

Fig. 2 (**A**) The curves under 280nm UV absorbance of R979A mutant detected with FPLC system. The left one shows the absorbent peak of the aimed protein eluted with 300mM imidazole during protein purification by nickelnitrilotriacetic acid–agarose. The right curve shows the progress of the further purification with size exclusion chromatography Superdex 200 column. The second peak presents the R979A protein. (**B**) SDS-PAGE analysis of R979A purification by nickel affinity column chromatography (stained with Coomassie blue). 1, purified *E. coli* RecQ was used as protein maker, 68.9kDa; 2, lysates from IPTG-induced cells overexpressing the His-R979A mutant protein; 3, indissolvable part after induced cells were broken; 4, lysate lysates from unindicted cells; 5, R979A protein purified by nickel affinity column chromatography with 0.3M imidazole. (C) SDS-PAGE analysis of the purified $BLM^{642-1290}$ and various mutants. The proteins (indicated above the figure) were resolved on a 10% SDS-polyacrylamide gel and stained with Coomassie blue. The concentration of the proteins used was about 15μg. The positions of the marker proteins (in kDa) are indicated on the left.

Vi inhibits and uncouples ATPase and DNA unwinding activities of $BLM^{642-1290}$

Orthovanadate (Vi) is widely used to probe the catalytic mechanism of nucleotide-5'-triphosphotase. Not all ATPases are inhibited by Vi (28); however, most ATPases that possess an arginine finger at nucleotide-binding sites, for example the F1-ATPase (13),

MutS (30) and bacteriophage T7 gene 4 helicase (17), are potentially inhibited by Vi. The inhibition involves the formation of a Mg^{2+}ADP.Vi transition-state-like complex. If the ATPase activity of a protein is efficiently inhibited by Vi, it suggests, although does not prove, that the catalytic site of the protein may shares structural features with other ATPases that have an arginine finger. We compared several ATPases with *E. coli* RecQ and the BLM molecular modelling model. BLM nucleotide-binding sites are structurally similar to ATPases that have an arginine finger (Fig. 1B, C). This structural feature should make BLM sensitive to Vi. As expected, the BLM ATPase activity was dose-dependently inhibited by vanadate, and it took 45 min to reach the maximal inhibition at 1mM Vi (Fig. 3A). In order to investigate whether Vi affects DNA unwinding, we measured the DNA unwinding activity under similar experimental conditions as used for ATPase activity in the presence of Vi. Vi inhibited the DNA unwinding activity more efficiently than the ATPase activity (Fig. 3B). Interestingly, this result is quite similar to that observed for T7 gene 4 helicase (17). As proposed previously by Crampton et colleagues (17), it suggests that the ATPase and DNA helicase activities are, at least partially, uncoupled in the presence of Vi. This probably represents a common feature of helicases possessing an arginine finger.

Figure 3

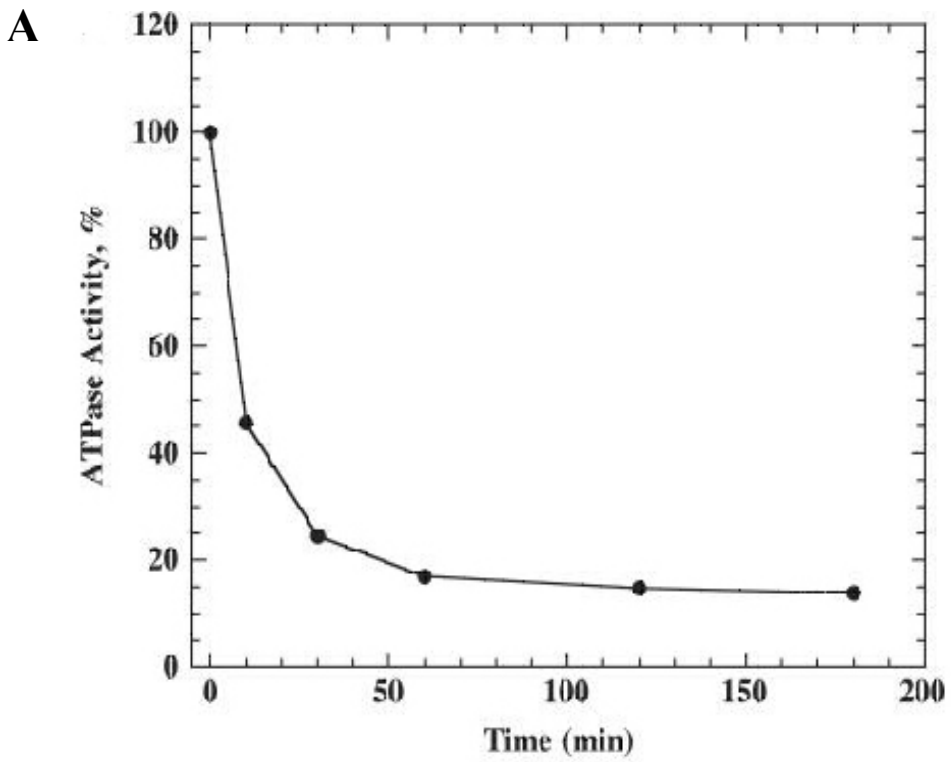

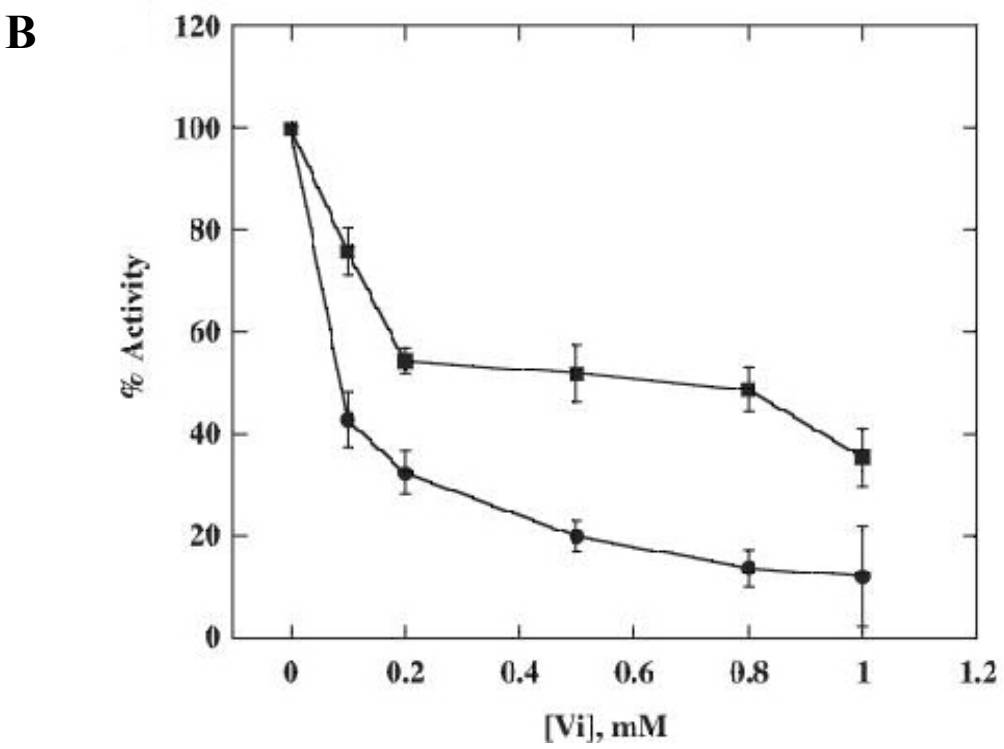

Fig. 3 (**A**) Time-dependent losses of ATPase activity upon incubation of BLM with Vi. ATP hydrolysis activity was measured with the indicated concentrations of Vi in a reaction containing 0.2 μM (bp) ssDNA, 1mM ATP, 0.1μCi[γ-^{32}]ATP, 200nM of BLM protein at the indicated times. (**B**) Uncoupling of ATPase and helicase activities in the presence of Vi. ATPase (triangle) and helicase (circle) activities were measured under similar conditions as indicated above (**A**), except that 1nM of 25bp duplex DNA was used for helicase assay. Each data point represents the mean of two or three experiments.

Helicase and ATPase activities of the mutant enzymes

We detected no helicase activity in any of the mutant enzymes using electrophoretic mobility shift assays. At first, we used the typical structures with 3'-tailed duplex (hybridism of oligonucleotides A and E in Table 1) as the substrate. The results showed that all the six mutants lose their abilities of separating the duplex strand DNA (Figs. 4A and 4B). Then we detected the unwinding abilities of arginine residues mutants using other duplex substrates (Figs. 4C~4E). We found that wild-type BLM helicase can separate not only 3'-tailed duplex but also the 5'-tailed ones, even the forked and the blunt terminal DNA. However, the arginine residues mutants showed no any capability of unwinding these different substrates. In order to confirm the results, we further measured the helicase activity of the mutant proteins with a fluorometric stopped-flow method, which is based on fluorescence resonance energy transfer. This method was used to exclude the possibility that electrophoretic mobility shift assays, which measure DNA-unwinding activity, underestimate the amount of DNA unwinding. $BLM^{642\text{-}1290}$ displayed efficient helicase activity, but all the mutant enzymes failed to unwind DNA substrates under similar experimental conditions (Fig. 4F). This is consistent with the results for electrophoretic mobility shift assays, and indicates that the DNA unwinding activity was severely impaired in mutant enzymes (Fig. 4A and B).

DNA-stimulated ATPase activities of $BLM^{642\text{-}1290}$ and the various mutants were assayed by varying the concentration of ATP substrate (Fig. 5). The resulting curves were fitted using the Michaelis-Menten equation. The rate constant (k_{cat}), K_M, and ATPase catalytic efficiency (k_{cat}/K_M) were determined from results shown in Fig. 5 and are summarized in Table 2. All mutant proteins had lower k_{cat} values for ATP hydrolysis than $BLM^{642\text{-}1290}$, and were between 5.2-fold lower for R979A to 2880-fold lower for Q975V. Mutant H798 had only a slightly high K_M value for ATP than $BLM^{642\text{-}1290.}$ Mutants R959A and R982A exhibited significantly lower ATP K_M values than $BLM^{642\text{-}1290}$. The low rate of ATP hydrolysis in Q975V made it technically impossible to determine its K_M value. These data indicate that all of the mutated residues are important for ATP hydrolysis, but are not directly implicated in ATP binding because the K_M values are not greatly increased. BLM is a DNA-stimulated ATPase, and the low ATPase activity observed with the altered BLM proteins may be due to a low affinity for either ATP or for DNA. We investigated ATP binding and DNA binding activities of both intact $BLM^{642\text{-}1290}$ and mutant proteins with various other assays.

Figure 4

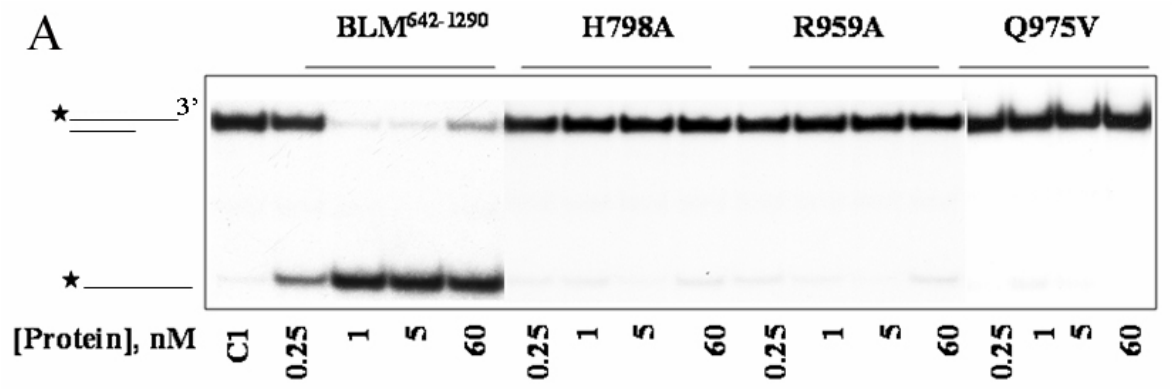
A
BLM642-1290
H798A
R959A
Q975V
3'
[Protein], nM
C1
0.25
1
5
60
0.25
1
5
60
0.25
1
5
60
0.25
1
5
60

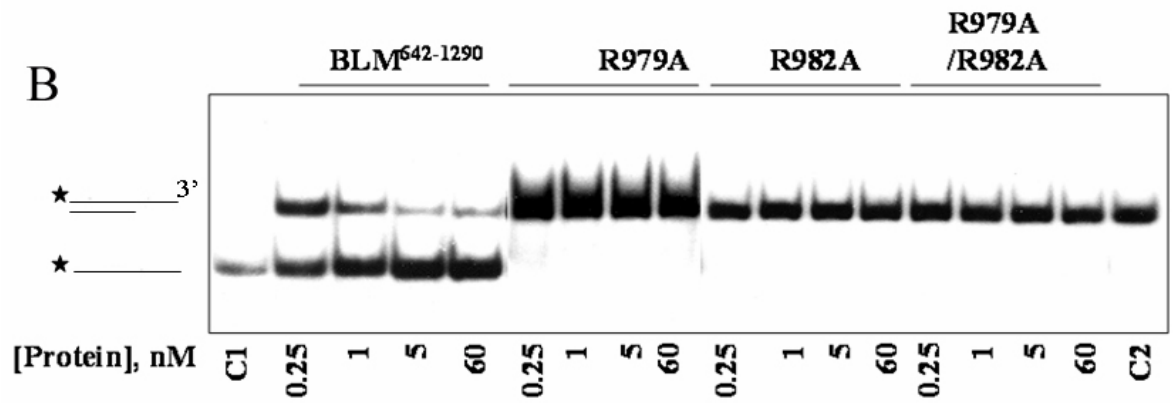
B
BLM642-1290
R979A
R982A
R979A
/R982A
3'
[Protein], nM
C1
0.25
1
5
60
0.25
1
5
60
0.25
1
5
60
0.25
1
5
60
C2

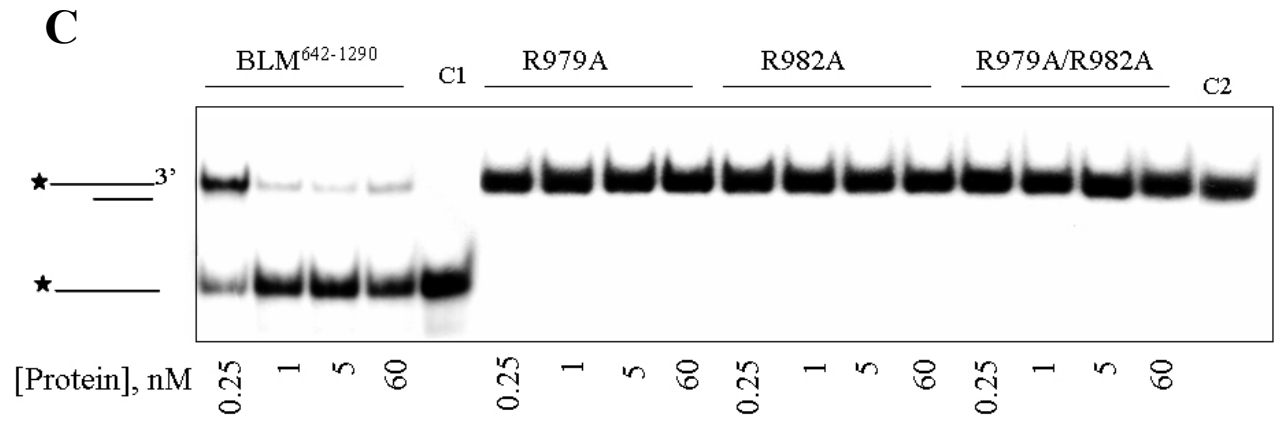
C
BLM642-1290
C1
R979A
R982A
R979A/R982A
C2
3'
[Protein], nM
0.25
1
5
60
0.25
1
5
60
0.25
1
5
60
0.25
1
5
60

D

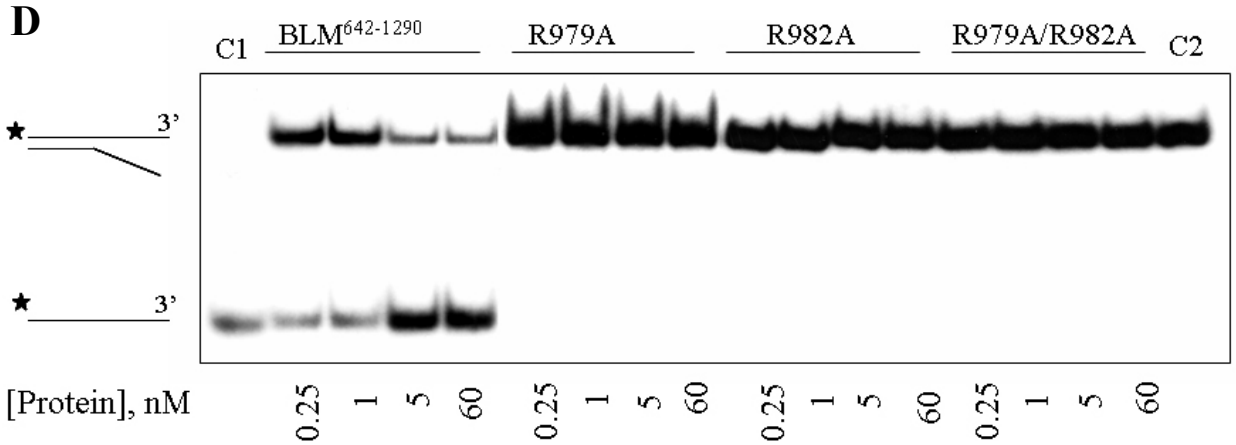
C1
BLM642-1290
R979A
R982A
R979A/R982A
C2
3'
3'
[Protein], nM
0.25
1
5
60
0.25
1
5
60
0.25
1
5
60
0.25
1
5
60

E

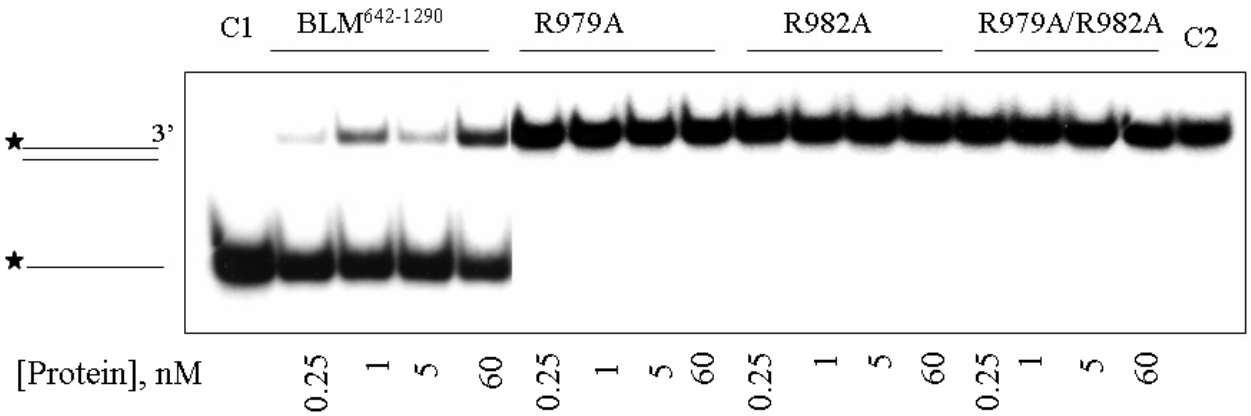
C1
BLM642-1290
R979A
R982A
R979A/R982A
C2
3'
[Protein], nM
0.25
1
5
60
0.25
1
5
60
0.25
1
5
60
0.25
1
5
60

F

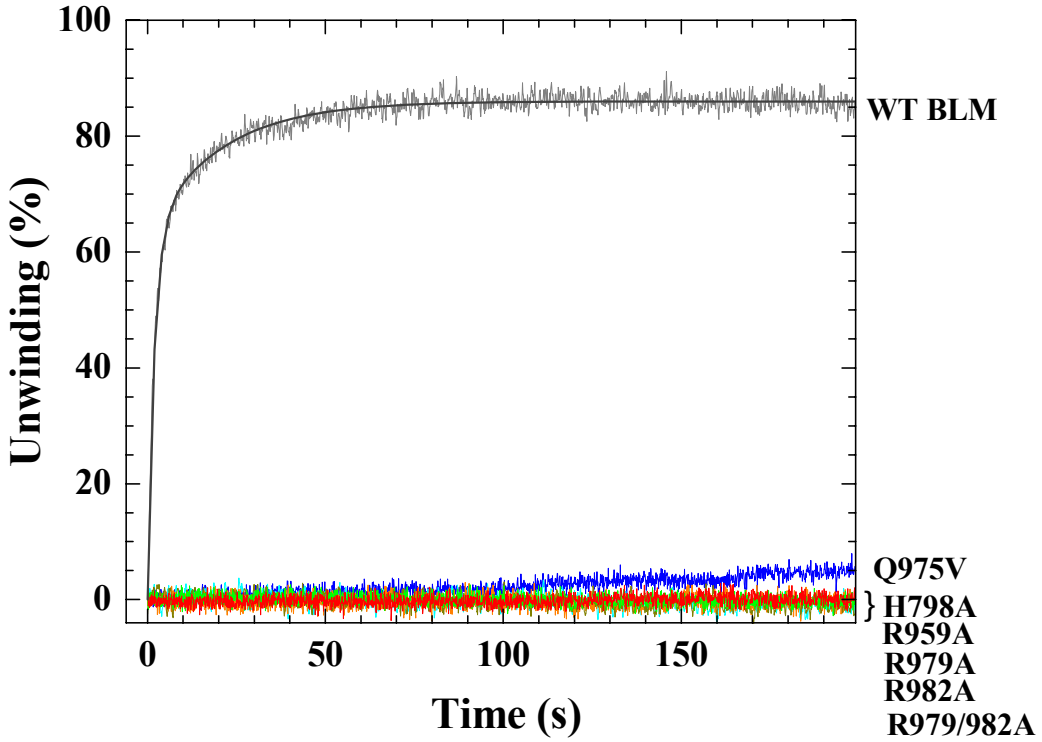
Unwinding (%)
100
80
60
40
20
0
0
50
100
150
Time (s)
WT BLM
Q975V
H798A
R959A
R979A
R982A
R979/982A

Fig. 4 (A, B) DNA unwinding activity of wild-type and mutant BLM proteins revealed by radiometric assay using duplex DNA. The DNA substrate was constructed with 5'-^{32}P-labelled oligonucleotides A and unlabelled oligonucleotide E (Table. 1). 1nM DNA substrate was incubated at 37 °C with wild-type and various mutants in the helicase assay buffer. The reactions were terminated after 30 min and the samples were analyzed by electrophoresis on a 12% non-denaturing polyacrylamide gel. The concentrations of the proteins were between 0.25 and 60nM as indicated in the bottom of the gel panel, where C1 and C2 represent the DNA substrate alone and the boiled DNA substrate, respectively. **(C, D, E)** DNA unwinding activities of wild-type and arginine residues mutants using the 5'-tailed duplex, forked duplex and blunt duplex strands which were constructed of 5'-^{32}P-labelled oligonucleotides A with unlabelled B or F, 5'-^{32}P-labelled oligonucleotides G with unlabelled H (Table. 1). Other conditions are same as described in the figure 4A and 4B. **(F)** DNA unwinding activity measured by stopped-flow DNA unwinding assay. As described in the "Materials and Methods", 2nM 56:16-mer DNA substrate was pre-incubated with 20nM helicase for 5 min at 25°C. The unwinding reaction was initiated by mixing with 1 mM ATP. The fluorescence emission of fluorescein at 520nm (excited at 492nm) was monitored. The fraction of DNA unwound was calculated by normalization of the fluorescence signal. The solid curve is the best fit of the data to Equation 1, with A_1 = 62.8±0.6 %, $k_{obs,1}$ = 0.52±0.01s^{-1}, A_2 = 3.2±0.6 %, and $k_{obs,2}$ = 0.05±0.01 s^{-1}.

Figure 5

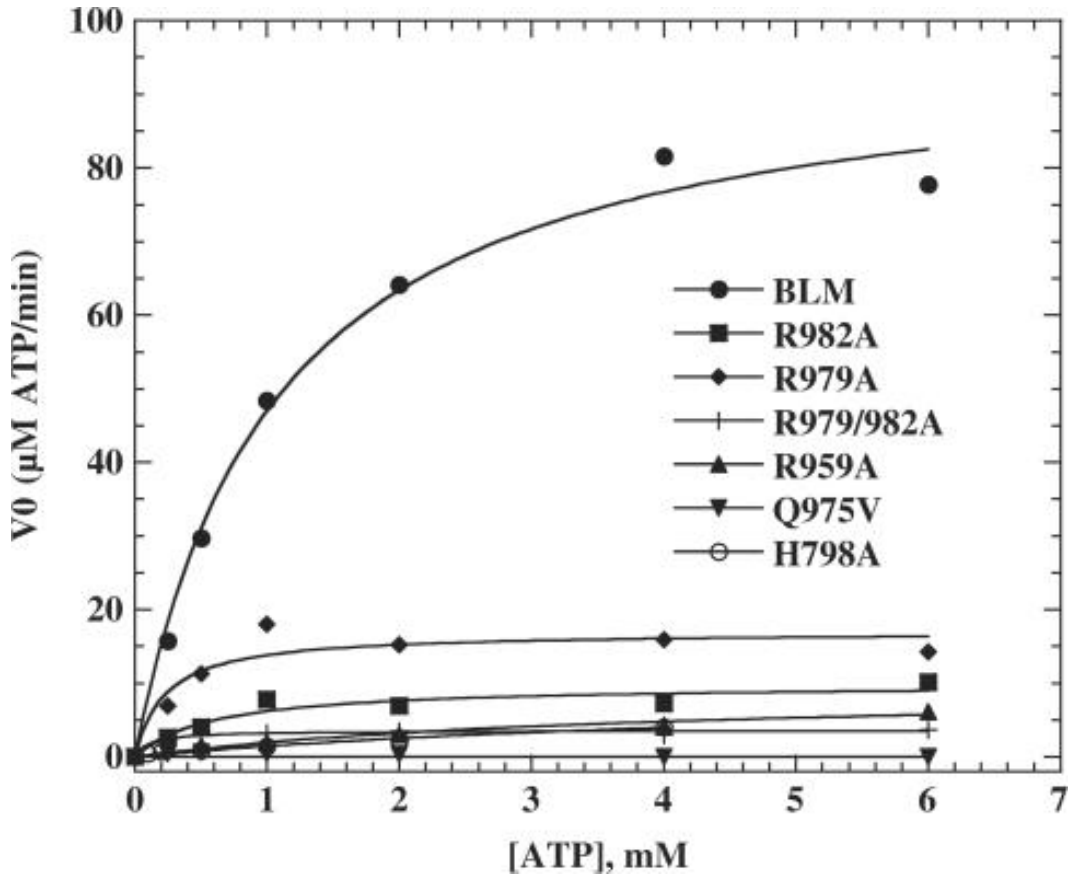

Fig. 5 ATP hydrolysis activity of wild-type and mutant BLMs as a function of ATP concentration. Experiments were performed in ATPase assay buffer at 37°C with 0.2μM ssDNA (nt, 60 mer oligonucleotide) and 0.2μM protein for each enzyme. The ATP hydrolysis was quantified as described in "Materials and Methods". Solid lines represent the best fit of the data to the Michaelis-Menten equation. The apparent k_{cat} and K_M values are summarized in Table 2.

All mutants display normal ATP and DNA binding abilities

We investigated whether altered BLM proteins bind ATP similarly to $BLM^{642-1290}$. We used a nitrocellulose filter binding assay to determine the stoichiometry of ATP binding. All mutants bound ATP with similar stoichiometry to $BLM^{642-1290}$ (Fig. 6A, Table 2). We determined the ATP binding affinities of $BLM^{642-1290}$ and mutant proteins by fluorometric titration assays which measure the equilibrium binding of mantATP, the ATP analogue. The fluorescent properties of mantATP are suitable for FRET from the intrinsic protein fluorophore (22). Our previous studies have confirmed that mantATP binds to BLM and it is a substrate of BLM protein in the presence of DNA (22), but is not a substrate in the absence of DNA, confirming that our mantATP binding experience is performed under equilibrium condition. We report the titration curves obtained with a constant amount of BLM protein and various concentrations of mantATP (Fig. 6B). The apparent K_d of mantATP for various BLM mutants were determined from the mathematical fit to these experimental curves (Table 2). Most mutants bound ATP with an affinity almost identical to that of $BLM^{642-1290}$. This is consistent with our BLM model: all mutated residues located close to the γ-phosphate of ATP or near the outer sphere of the ATP binding sites do not affect ATP binding.

In general, a combination of efficient ATP and DNA bindings may provide the maximal ATPase activity for ATPases. We investigated the DNA binding ability of these mutants to see whether the observed ATPase deficiencies result from the failure of DNA binding. We used electrophoretic mobility-shift assays to test whether BLM proteins bound DNA. All mutants displayed migration patterns similar to that of $BLM^{642-1290}$, indicating that there was no apparent defect in single-strand DNA binding (Fig. 7A and 7B). Moreover, all the arginine residues mutants also show the normal double-strand DNA binding abilities comparing with wild-type BLM helicase (Fig.7E). It is still possible that there are some subtle differences between the mutants, but these are difficult to determine using the gel shift method. Therefore, to determine the dissociation constant of DNA binding quantitatively, we used a fluorescence anisotropy assay to measure the apparent K_d values under equilibrium conditions (23). We titrated fluorescein-labelled 22 mer oligonucleotide with various concentrations of BLM protein. The resulting binding isotherms are fitted with Equation 2 (Fig. 7C, D). The apparent dissociation constants per binding site determined from the titration curves are summarized in Table 2. The K_D/N values of all mutants are

similar to those of $BLM^{642-1296}$; this is consistent with the results from the radiometric assay, and confirms that the altered proteins bind DNA in a similar manner to $BLM^{642-1290}$.

Table 2 ATPase, DNA binding and ATP-binding activities of the wild-type and mutant BLM proteins

Helicases	ATPase				DNA binding	ATP binding	
	k_{cat} (s^{-1})	k_{cat} decrease factor	K_M (mM)	k_{cat}/K_M ($s^{-1}\cdot mM^{-1}$)	K_D/N (nM)	Molar ratio ATP/Protein	K_d (μM)
$BLM^{642-1290}$	14.4	1	0.81± 0.1	18	1.11±0.11	0.88±0.12	0.47±0.06
H798A	0.82	17.6	1.5±0.2	0.54	5.03±0.55	0.86±0.17	0.52±0.06
R959A	0.61	23.6	0.52±0.1	1.21	4.15±0.40	1.02±0.18	0.62±0.04
Q975V	0.005	2880	ND[a]	ND	3.31±0.40	0.78±0.18	0.65±0.09
R982A	1.1	13.1	0.48±0.11	2.4	2.13±0.32	0.85±0.16	0.88±0.14
R979A	2.8	5.2	0.65±0.012	4.3	1.91±0.46	0.82±0.17	0.66±0.15
R979/982A	0.6	24	0.75±10.2	0.8	1.32±0.49	0.86±0.16	0.47±0.11

[a]ND: Values cannot be determined precisely

Figure 6

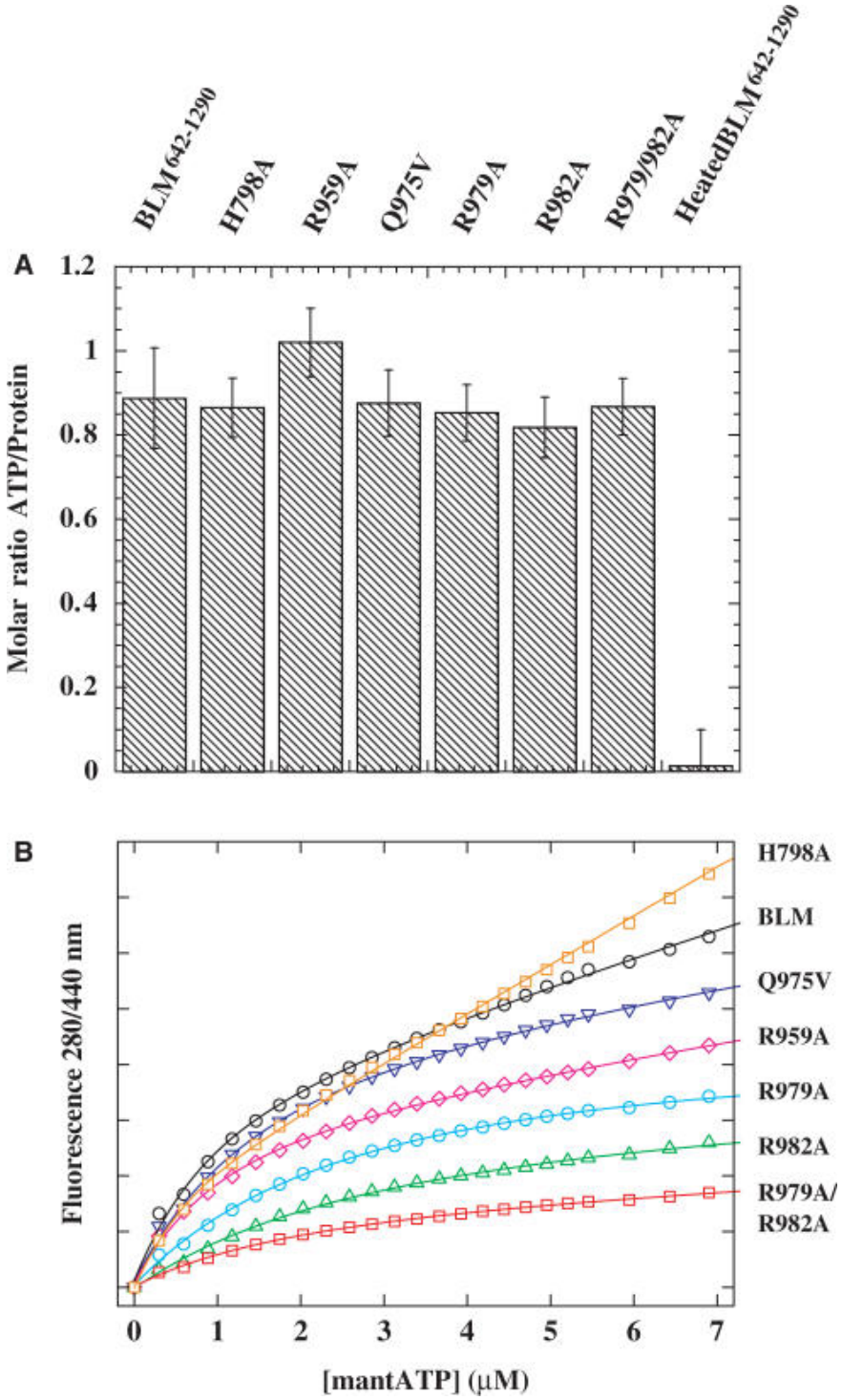

Fig. 6 ATP-binding activities as determined by nitrocellulose filter **(A)** and fluorometric **(B)** assays. **(A)** The ATP binding was determined with three concentrations of BLM$^{642\text{-}1290}$ and mutants (5, 15 and 30μM) in the presence of 200μM ATP and 0.1μCi[γ-^{32}]ATP. The data reported are means of triplicate assays. **(B)** Changes in fluorescence intensity when 0.2μM (H798A) or 0.5μM (the others) of the enzymes were titrated with various concentrations of mantATP. Data reported are means of triplicate assays. Solid lines represent the best fit of the data to Equation 3 and the apparent K_d values are summarized in Table 2.

Figure 7

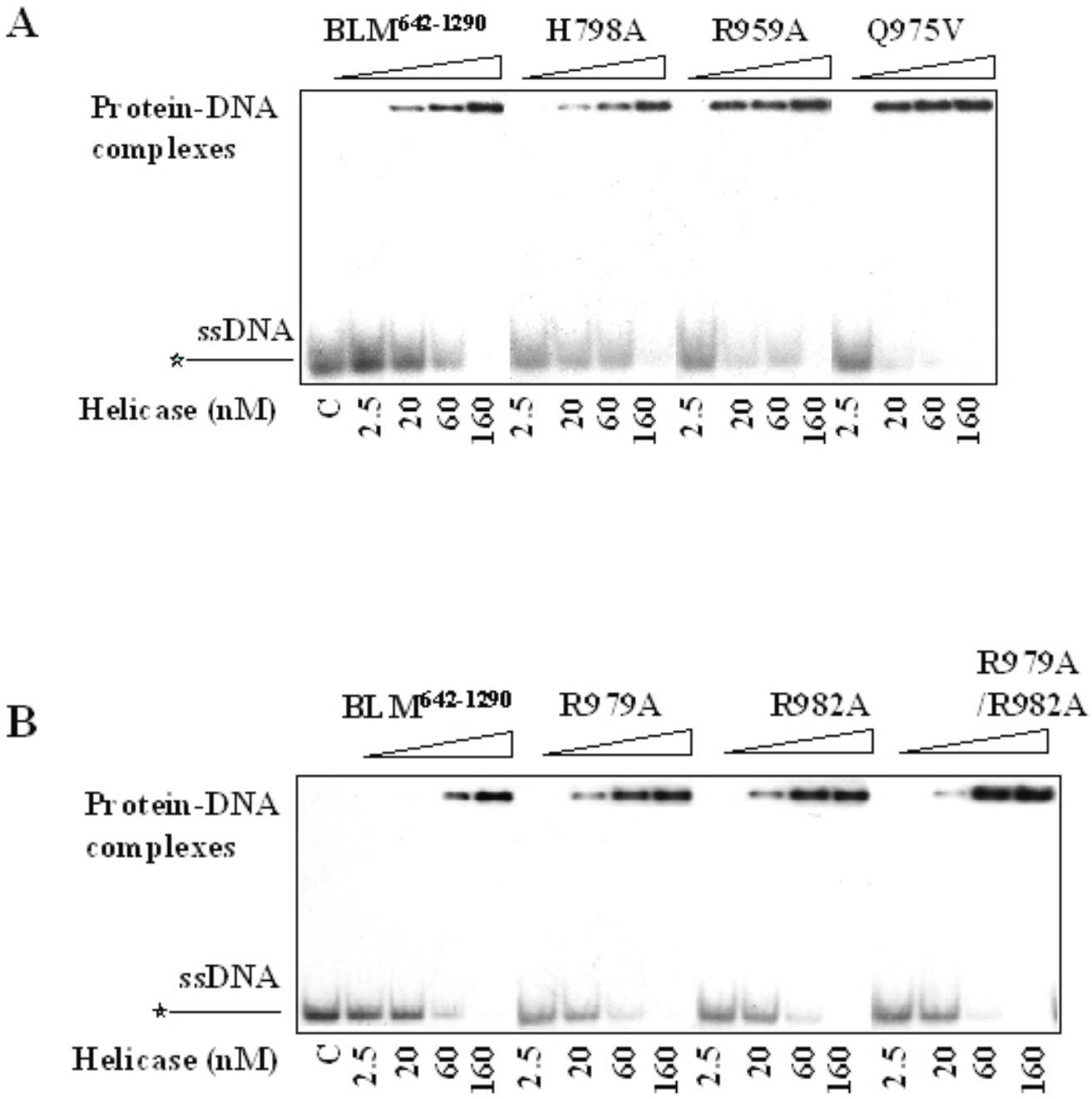
A
BLM642-1290
H798A
R959A
Q975V
Protein-DNA complexes
ssDNA
Helicase (nM)
C
2.5
20
60
160
B
BLM642-1290
R979A
R982A
R979A /R982A
Protein-DNA complexes
ssDNA
Helicase (nM)

C

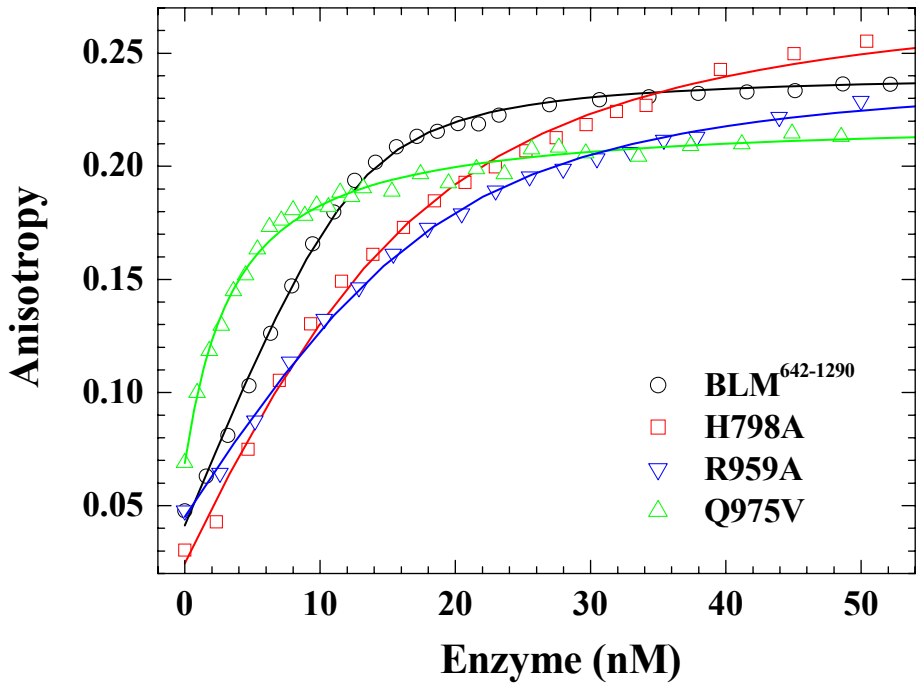
0.25
0.20
0.15
0.10
0.05
Anisotropy
0
10
20
30
40
50
Enzyme (nM)
BLM642-1290
H798A
R959A
Q975V

D

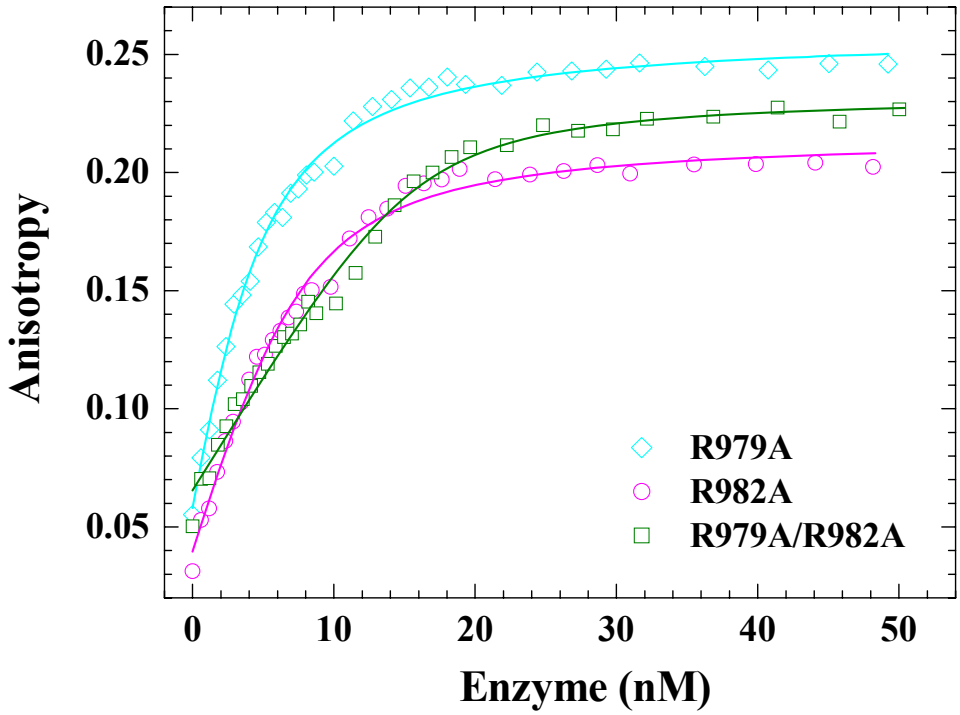
0.25
0.20
0.15
0.10
0.05
Anisotropy
0
10
20
30
40
50
Enzyme (nM)
R979A
R982A
R979A/R982A

E

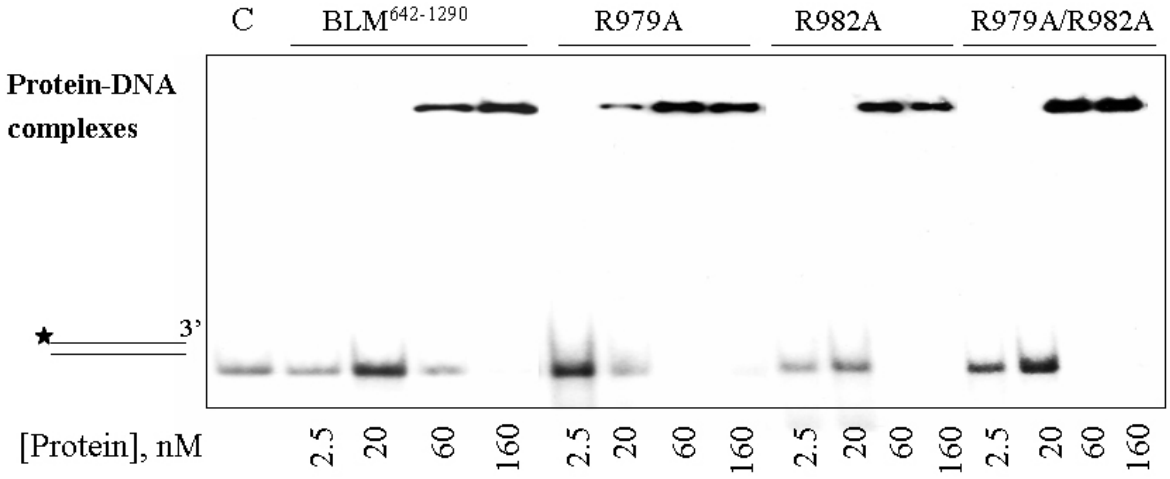

Fig. 7 (A, B) Analysis of DNA binding activity of the $BLM^{642-1290}$ and mutant BLMs using electrophoretic mobility shift assay. One nanomole of 5'-^{32}P-labelled 36 mer ssDNA (oligonucleotide C, Table 1) was incubated at 37°C for 20 min with various concentrations of protein between 2.5 and 160nM in binding reaction buffer. Bound and free DNA were separated by electrophoresis on a non-denaturing 6% polyacrylamide gel and detected by autoradiography. **(C, D)** The anisotropy-based DNA-binding isotherms of wild-type and mutant BLM proteins. Fluorescence anisotropy values were determined as a function of RecQ concentrations for 21 mer ssDNA substrates (oligonucleotide D, **Table. 2**). 2nM fluorescein-labelled DNA was titrated with various amounts of RecQ under conditions as described in "Materials and Methods". The solid lines represent the best fits of the data to Equation 2. The determined values of dissociation constant per binding site (K_D/N) are summarized in Table. 2. **(E)** Analysis of DNA binding activity of the $BLM^{642-1290}$ and arginine mutant BLMs using electrophoretic mobility shift assay. The blunt double-strand DNA at 1nM was incubated at 37°C with gradient concentration proteins from 2.5 to 60nM for 20 min. The protein-DNA complexes were separated with free substrates on a non-denaturing 6% polyacrylamide gel and detected by autoradiography.

Arginine residues mutants display normal annealing abilities

Former research showed that BLM possesses the DNA annealing ability. To gain further insight to the mechanism of BLM mediates DNA strand annealing process, we tested whether the arginine residues participate in this enzymatic ability. We incubated two partially complementary single stranded oligonucleotides with wild-type BLM and a series of arginine residues mutants and analysed the products on non-denaturing polyacrylamide gels (Figure 8). From the picture, we can see that all the mutants of arginine residues are shown the same effective annealing reactions as the wild-type BLM. At even greater protein concentration, this ability increased gradually with protein concentration. So the results suggested that conserved arginine residues which are located in the helicase core domain don't play role in annealing progress. We suppose that these mutants display normal DNA binding abilities and it increases the opportunity of two complementary single-strands to be closer. However, the mutants lose their capabilities to hydrolyze the ATP, so they possess DNA annealing abilities instead of unwinding activities. Moreover, the DNA binding capability is premises for the annealing process. . Previous results showed that the annealing ability of BLM helicase will decrease if its DNA binding domain is mutant (22).

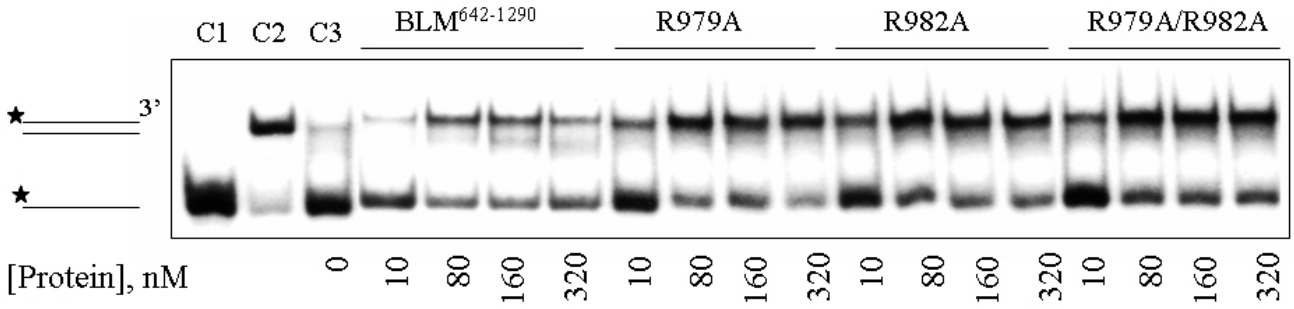

Fig. 8 Analysis of annealing activities of arginine residues mutants of BLM

5'-32P-labelled ssDNA (oligonucleotide G in Table 1) and unlabelled complementary ssDNA substrate (oligonucleotide H in Table 1) were incubated at 37°C for 10 mintues with gradient concentrations of wild-type BLM and arginine residues mutants from 10nM to 320nM in the annealing reaction buffer. Hybridated DNA and single DNA were separated by electrophoresis on a non-denatruing 12% polyacrylamide gel and detected by autoradiography. The concentrations of different proteins are indicated on the bottom of the gel. C1 presents heat-denatured substrate and C2 is hybridized substrate. C3 presents enzyme control.

Vi inhibition study reveals that R982 functions as an arginine finger

R979 and R982 are localized near the γ-phosphate of ATP and the altered proteins display defects in ATPase activity. However, R982A impaired ATPase activity more than R979A (Table. 2). We determined whether R979A and R982A are inhibited by Vi in a similar manner to identify the arginine residue involved in the transition state complex. Residual ATPase activity of the R979A mutant was inhibited by Vi, in a similar manner to that of BLM, and the residual ATPase activity of R982A was unaffected under similar experimental conditions (Fig. 9A), indicating that R982A may function as an arginine finger. We further reasoned that if the arginine residue 982 is specifically involved in the transition state complex, the other mutants such as H798A, R959A and Q975V which are structurally far from the γ-phosphate of ATP should be still sensitive to inhibition by Vi. As expected, H798A and R959A display very similar inhibition profile as that of R979A and $BLM^{642-1290}$ (Fig. 9A). The residual activity of Q975V is too low to be tested for Vi inhibition. In the above experiments, inhibition of ATPase activity by Vi was determined under turnover conditions in which ATP was present as major component. Vi inhibits ATPase activity through formation of a MgADP.Vi-BLM transition state complex; thus, we compared Vi-induced inhibition of BLM, mutant R979A and mutant R982A under the condition in which the enzymes were pre-incubated with ADP. The ATPase activities of BLM and R979A were strongly inhibited under these conditions. R982A was not inhibited by Vi, indicating that R982A cannot form this ATP hydrolysis transition state (Fig. 9B). We analyzed the type of inhibition caused by Vi. We measured Vi-induced inhibition of ATPase activity of BLM and the mutant R979A at various concentrations of ATP (Figs. 9C and D). A Lineweaver-Burk and Eadie-Hofstee analysis indicated that R979A and BLM are inhibited similarly: Vi-inhibition of ATP hydrolysis is consistent with a non-competitive mechanism and both proteins display similar inhibition constants (Ki = 1 and 1.5 for BLM and R979A, respectively). The Ki for R982A was technically difficult to determine because the variation of the residual activity of R982A was not significant in the presence of orthovanadate. These various findings indicated that the residue R982, but not the residue R979, is involved in the formation of MgATP.Vi-BLM transition state complex.

Figure 9

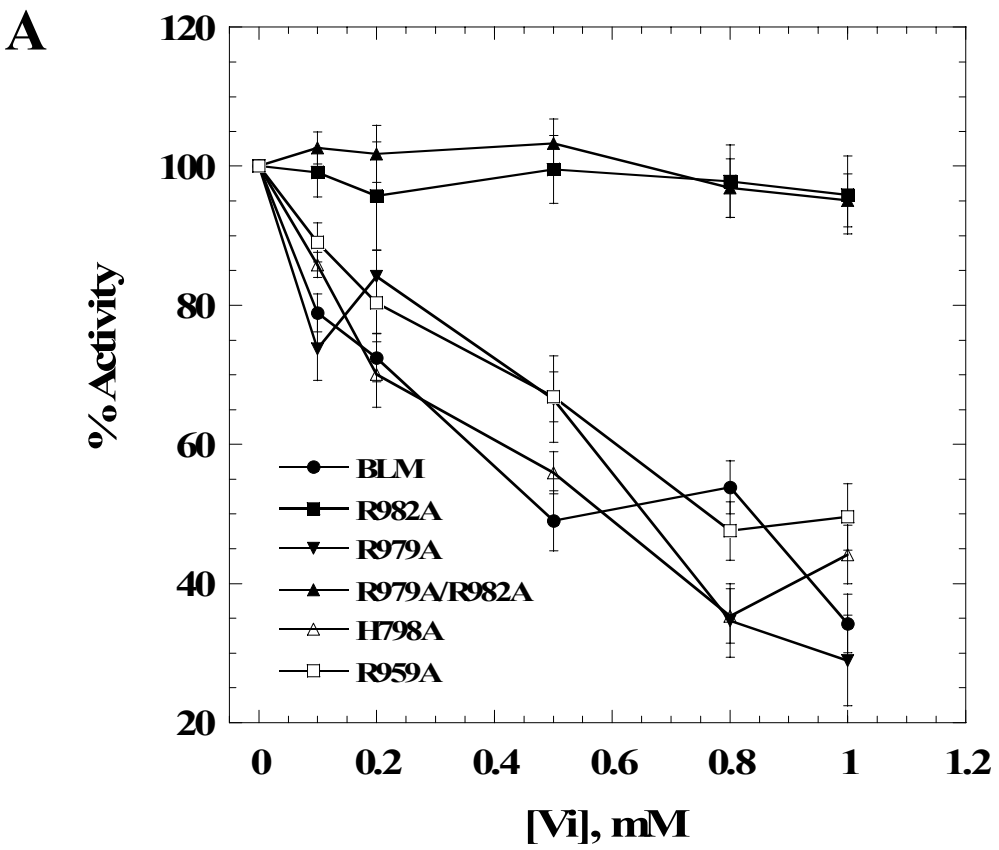
A
120
100
80
60
40
20
% Activity
0
0.2
0.4
0.6
0.8
1
1.2
[Vi], mM
BLM
R982A
R979A
R979A/R982A
H798A
R959A

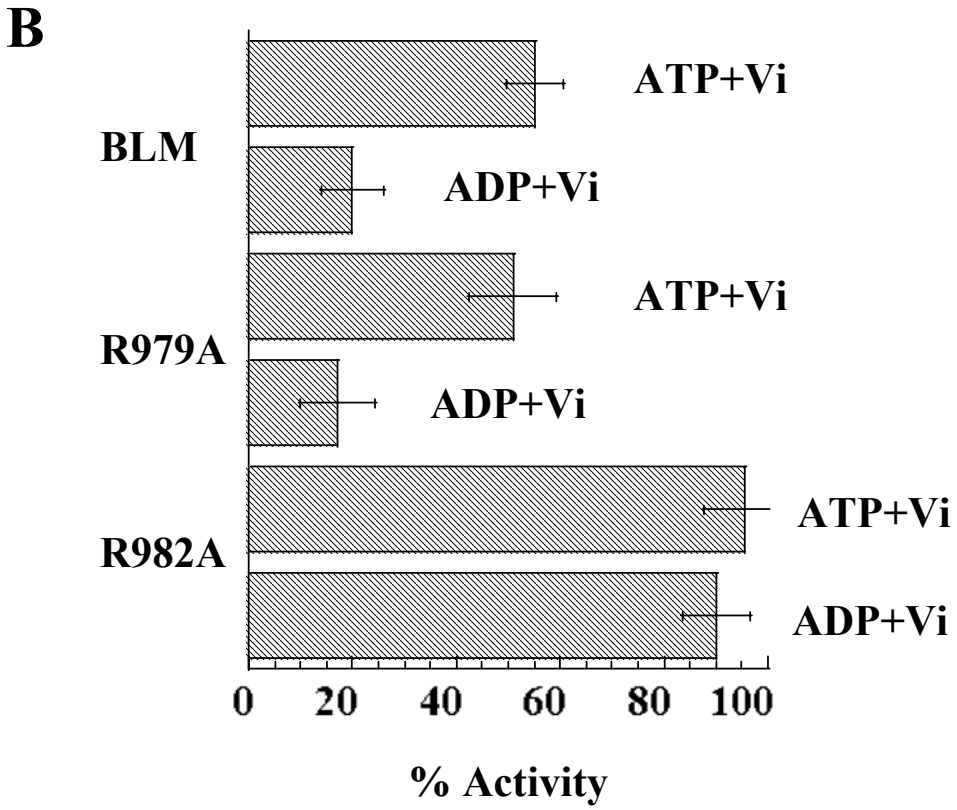
B
BLM
ATP+Vi
ADP+Vi
R979A
ATP+Vi
ADP+Vi
R982A
ATP+Vi
ADP+Vi
0
20
40
60
80
100
% Activity

C

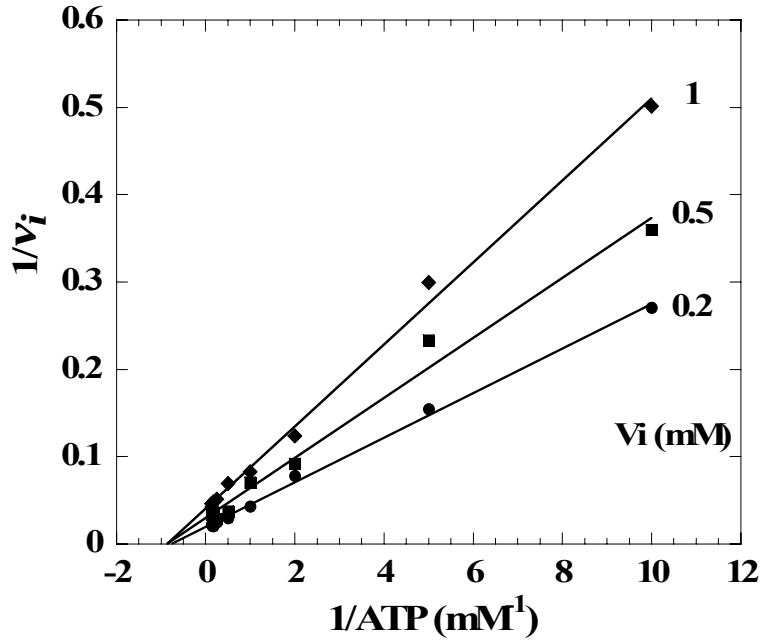
0.6
0.5
0.4
0.3
0.2
0.1
0
1/vi
-2
0
2
4
6
8
10
12
1/ATP (mM-1)
1
0.5
0.2
Vi (mM)

D

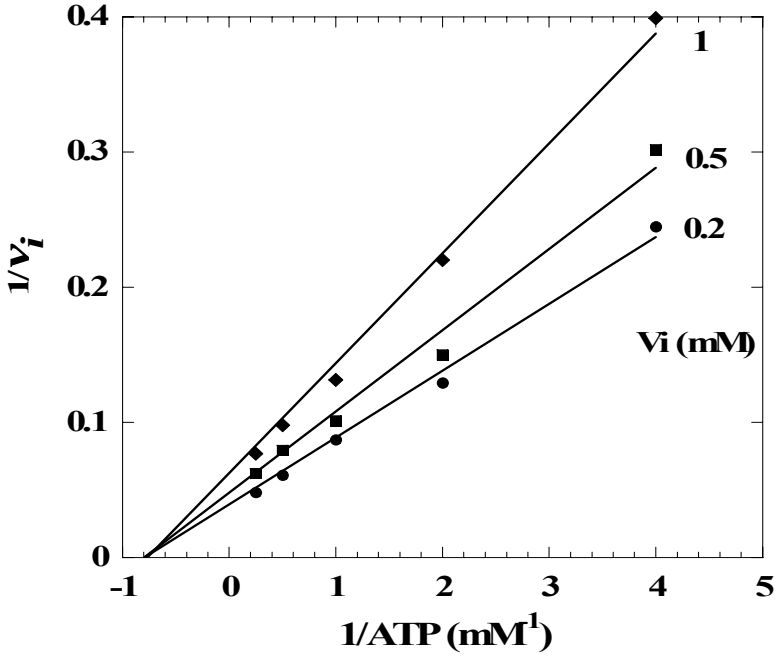
0.4
0.3
0.2
0.1
0
1/vi
-1
0
1
2
3
4
5
1/ATP (mM-1)
1
0.5
0.2
Vi (mM)

Fig. 9 R982 is insensitive to orthovanadate inhibition. (**A**) Effects of Vi on ATPase activities of $BLM^{642-1290}$ and the mutants H798A, R959A, R979A, R982A and R979A/R982A. Hydrolysis of ATP was measured in a reaction containing 0.2μM (bp) ssDNA, 1 mM ATP, 80nM of different proteins, and the indicated amounts of Vi. (**B**) Vi-induced inhibition of $BLM^{642-1290}$, mutant R982A and mutant R979A proteins in the presence of ATP and ADP. Prior incubations were carried out with 80nM protein and 0.6mM Vi in the presence of ADP or ATP as indicated in the figure. ATPase activity was assayed as described in "Materials and Methods". **(C, D)** Determination of the vanadate inhibition type for $BLM^{642-1290}$ **(C)** and mutant R979A **(D)**. The experiments were performed under similar conditions to those described in the legend to Fig. 2, with the indicated vanadate concentrations. The plot was constructed as $1/v_i$ versus 1/[ATP] to obtain the *K*i value from the intercept on the abscissa.

DISCUSSION

With the progress of helicase structure and function research, there is growing evidence that all helicases couple the energy of ATP hydrolysis to conformational changes for DNA unwinding and translocation along the DNA molecule. The mechanism of this coupling is not fully understood. It may involve a process in which ATP binding and hydrolysis are detected by the residues at the nucleotide binding pocket and the signal was transmitted to the DNA binding site. This destabilizes the duplex DNA, making the helicase translocate along the single strand product. Previous studies have identified several structural elements and/or residues essential for the coupling of ATP hydrolysis and conformational changes (20;31-33). We focused on the role of the putative arginine finger in the regulation of the RecQ family helicase activities. We used BLM as a study model for the following reasons: I) the sequence alignments of several RecQ family helicases, bacterial and human, show that the residues involved in the putative arginine finger and their organization are highly conserved (Fig. 1A); II) our BLM molecular model is based on the crystal structure of *E. coli* RecQ helicase; the root mean square deviation for 516 Cα atoms between the *E. coli* RecQ backbone and that of the recombinant BLM containing residues 642-1290 ($BLM^{642-1290}$) is 0.7 Å , indicating that $BLM^{642-1290}$ folds very similarly to *E. coli* RecQ helicase (Fig. 1B); III) we have previously used $BLM^{642-1290}$ to study the molecular consequence of several disease-causing mutations in BS patients, and this study may help understand the mechanism underlying BLM catalysis and interpret newly identified BLM-causing mutations in the future; IV) Previous study has shown that the 642-1290 fragment displayed the same or very similar properties with the full length BLM both *in vitro* and *in vivo* (22;29). The $BLM^{642-1290}$ protein fragment exhibited the same or very similar enzymatic properties and DNA substrates specificity *in vitro* as the full length BLM. Importantly, the $BLM^{642-1290}$ was able to substitute for the RecQ helicase in suppressing illegitimate recombination in *E. coli*. In order to facilitate our study and get essential information concerning the arginine finger, the $BLM^{642-1290}$ was used in this study.

We have demonstrated that BLM is sensitive to Vi; this indicates that Vi can incorporate into the catalytic sites and assist in transition-state stabilization of BLM. We mutated several residues in the helicase signature motifs clustered around the nucleotide binding pocket. We have shown that replacing R979 and R982, each by an alanine residue, does not significantly affect the ATP and DNA binding abilities, but results in lower steady-state ATP hydrolysis rates than the intact $BLM^{642-1290}$. These observations indicate that the R979 and R982 residues

play no major functional role in providing binding energy for ATP, but are crucial for ATP hydrolysis. This is consistent with the atomic resolution structure of *E. coli* RecQ and our molecular model: the guanidinium groups of both arginine residues are close to the γ-phosphate of ATP (Fig. 1C). ATP hydrolysis is impaired in mutant R982A, but the catalytic efficiency of mutant R979 is only reduced to 25%. This suggests that residue R982 plays a more crucial role in ATP hydrolysis than R979 and R982 may function as an arginine finger. To confirm this, we studied the ATPase activity of R979A and R982A in the presence of orthovanadate, which complexes with nucleotide 5'-diphosphate and mimics the catalytic transition state through the formation of a Mg^{2+}ADP-Vi-Protein complex. The residual ATPase activity of R979A was inhibited by Vi and the inhibition was similar to that of wild type $BLM^{642-1290}$ fragment in the presence of ATP or ADP. Inhibition studies demonstrated that Vi behaves as non-competitive inhibitor of both the wild-type BLM fragment and R979A; Vi presumably inhibits the two proteins by similar inhibition mechanisms. By contrast, mutant R982A was insensitive to Vi in the presence of ATP or ADP. The inability of the mutant R982A to form the transition state analogue MgADP-Vi-Protein provides firm evidence that a major role of the guanidinium group of R982 is to stabilize the catalytic transition state, and failure to do so in this mutation accounts for the loss or reduction of ATP hydrolysis. This interpretation is also consistent with the atomic resolution structures of other SF1 and SF2 helicases such as PcrA and E. coli RecQ (8;10). Although both R287 and R610 in PcrA interact with the γ-phosphate of ATP, the two arginine residues contribute differently to stabilizing the transition state. Two guanidinium amine groups of R287 can interact with the oxygen atoms on the γ-phosphate group, but only one guanidinium amine group of R610 can interact with the oxygen atoms. The configuration of the guanidinium amine group of R610 is not optimal for stabilizing the negative charge that develops in the transition and post-transition state during ATP hydrolysis. Dittrich and Schulten showed that it is R287, but not R610, that acts as an arginine finger (34). Structural comparison of the positions of R979 and R982, relative to ATP binding sites, with the arginine residues R287 and R610 in PcrA reveals that R979 is more structurally similar to R610 in PcrA (Fig. 1B). Therefore, this second arginine residue, R979, does not contribute greatly to stabilizing the transition state. Residue R979, similar to residue R610 in PcrA, may be important for the initial binding of ATP to the catalytic site and for stabilizing the hydrolysis product state (34).

Our findings also showed new light on the question of how ATP and DNA binding activate the ATPase activity, and on the mechanism transmitting chemical energy from ATP hydrolysis to DNA unwinding. For most phosphoryl transferases, the intrinsic nucleotide

hydrolysis activity is low or undetectable and needs to be activated by a separate protein/residue or other ligand. Arginine residues are crucial for many enzyme phosphoryl-transfer reactions. In the absence of DNA, the distances between the putative arginine finger and the γ-phosphate of ATP are more than 3.5 Å, RecQ and our BLM model. Such distances are quite far for the guanidinium groups of the arginine finger to interact with the γ-phosphate group. However, in PcrA helicase, ATP and DNA binding result in the closure of the cleft between domains 1A and 2A. This also positions the R287 guanidinium groups to polarize the γ-phosphate group, thereby increasing the susceptibility of the phosphorus atom to a nucleophilic attack. Although no X-ray crystal structures are available for RecQ and BLM or other RecQ family helicases in complex with ATP and DNA, these enzymes may share these properties with PcrA. If the helicase is unable to hydrolyze the ATP, it will lose the energy to make itself translocate along the substrate and then unwind the double-strand DNA; although it can bind to ATP and DNA normally. Moreover, the mutant in the domain who is charge of the ATP hydrolysis won't affect the annealing ability of helicase because the helicae can bind to substrates effectively and then increase the chance of complementary strands to meet with each other. In this case, helicase will carry out annealing progress instead of unwinding progress.

Our studies also help form a mechanistic picture of how the arginine finger is precisely positioned in relation to the γ-phosphate through the conserved motifs that stabilize the transition state complex. Both residues R979 and R982 of motif VI (equivalent to R326 and R329 in *E. coli* RecQ) are on the loop connecting α-helix 14 and β-strand 13 (Fig. 1C). This loop may be highly mobile and can assume multiple side chain positions due to the thermal fluctuation of the protein. The crystal structure of *E. coli* RecQ helicase reveals that the precise spatial arrangements of both residues R326 and R329, relative to γ-phosphate of the nucleotide, may be further positioned through a complex network of interactions between motifs II, V and VI. In the BLM model, the α-helix 14 may be spatially restricted by the interactions between Q975 of motif VI and H798 and/or H805 of motif II, thereby stabilizing the positions of both residues R979 and R982. The spatial positions of R982 may be further determined through the hydrogen bonds between R959 and D983. This proposed salt bridge would further contribute to the positioning of motif VI, thereby precisely positioning residues R979 and Q975. The importance of the interaction between R959 and D983 for enzymatic activity has been demonstrated in an analysis of polymorphism R834C in Werner syndrome protein (WRN). Residue R834 of WRN, which is equivalent to R959 in BLM, may form two side chain hydrogen bonds with D858 of WRN (corresponding to D983 in BLM) (35). This

interaction will further stabilize the residue R857, which probably acts as an arginine finger in WRN. Substitution of the residue R834 results in lower than wild-type ATPase, helicase and helicase-coupled exonuclease activities (35). Similarly, alteration of BLM R959 results in a substantial reduction in ATPase and helicase activities. Both mutants Q975V and H798A exhibit significant reduction in ATPase and helicase activities; altering Q975 leads to much more dramatic effect in enzymatic activity than H798 (the k_{cat} decreases by 2880- and 17.6-fold for Q975V and H798A, respectively). Possibly, alteration of H798 does not completely abolish transit interaction between the two domains whereas alteration of Q975 does. Hydrogen bonds between Q975-H798 and between Q975-H805 may contribute to positioning the arginine finger upon binding ATP and DNA. It will be interesting to visualize and compare the precise locations and orientations of the putative arginine finger, as well as Q975 in an apo-enzyme and in the transition state, once the X-ray structure of the protein-ATP-DNA complex is elucidated.

In view of our findings, it is plausible that the arginine finger R982, coordinating with other residues clustered around the ATP binding sites, senses ATP binding and hydrolysis and then transmits the signal for conformational changes. The cleft between domains 1A and 2A closes and, with the help of the various residues mentioned above, the arginine finger stabilizes the transition state, triggering ATP hydrolysis. After hydrolysis of ATP, the interactions between the guanidinium groups of the arginine finger and the γ-phosphate of ATP are lost. In this case, the interactions between other residues, for example Q975-H798 and Q975-H805, are not strong enough to keep the two domains close together and the enzyme returns to the initial state. RecQ family helicases may thereby couple ATP binding and hydrolysis to conformational changes and translocation along DNA as PcrA does.

Whether RecQ family helicases function as a monomer or hexamer has attracted great attention. Although BLM forms hexameric ring structure (36), the $BLM^{642-1290}$ fragment is a monomer and functions like the full length BLM both *in vivo* and *in vitro*. Similarly, a fluorometric stopped-flow assay under optimal pre-steady state conditions indicates that the oligomeric WRN functions as a monomer unwinding duplex DNA substrates (37). If an arginine finger lies in the adjacent subunits of oligomeric ATPase such as T7 gene 4 helicase (17), replication factor C (18), Adeno-associated virus type 2 helicase (16) and the structural maintenance of chromosomes (SMC) ATPase (38), oligomerization must be absolutely required for ATPase activity for such proteins. While most oligomeric ATPases harbour an arginine finger in the adjacent subunits of the protein (16-18;38), the hexameric BLM protein possesses an arginine finger that is localized within two domains of a subunit as we revealed

in this report. This structural feature may confer BLM an intrinsic ability to hydrolyze ATP as a monomer. Our data therefore provided a molecular structural explanation for BLM functions potentially as a monomer.

REFERENCES

1. Lohman,T.M. and Bjornson,K.P. (1996) Mechanisms of helicase-catalyzed DNA unwinding. *Annu. Rev. Biochem*, **65**, 169-214.

2. Soultanas,P. and Wigley,D.B. (2000) DNA helicases: 'inching forward'. *Curr. Opin. Struct. Biol.*, **10**, 124-128.

3. von Hippel,P.H. and Delagoutte,E. (2001) A general model for nucleic acid helicases and their "coupling" within macromolecular machines. *Cell*, **104**, 177-190.

4. Xi,X.G. (2007) Helicases as antiviral and anticancer drug targets. *Curr. Med. Chem.*, **14**, 883-915.

5. Singleton,M.R., Dillingham,M.S. and Wigley,D.B. (2006) Structures and Mechanism of Helicases and Nucleic Acid. *Annu. Rev. Biochem*.

6. Singleton,M.R. and Wigley,D.B. (2002) Modularity and specialization in superfamily 1 and 2 helicases. *J. Bacteriol.*, **184**, 1819-1826.

7. Story,R.M. and Steitz,T.A. (1992) Structure of the recA protein-ADP complex. *Nature*, **355**, 374-376.

8. Velankar,S.S., Soultanas,P., Dillingham,M.S., Subramanya,H.S. and Wigley,D.B. (1999) Crystal structures of complexes of PcrA DNA helicase with a DNA substrate indicate an inchworm mechanism. *Cell*, **97**, 75-84.

9. Korolev,S., Hsieh,J., Gauss,G.H., Lohman,T.M. and Waksman,G. (1997) Major domain swiveling revealed by the crystal structures of complexes of E. coli Rep helicase bound to single-stranded DNA and ADP. *Cell*, **90**, 635-647.

10. Bernstein,D.A., Zittel,M.C. and Keck,J.L. (2003) High-resolution structure of the E.coli RecQ helicase catalytic core. *EMBO J.*, **22**, 4910-4921.

11. Rittinger,K., Walker,P.A., Eccleston,J.F., Nurmahomed,K., Owen,D., Laue,E., Gamblin,S.J. and Smerdon,S.J. (1997) Crystal structure of a small G protein in complex with the GTPase-activating protein rhoGAP. *Nature*, **388**, 693-697.

12. Scheffzek,K., Ahmadian,M.R., Kabsch,W., Wiesmuller,L., Lautwein,A., Schmitz,F. and Wittinghofer,A. (1997) The Ras-RasGAP complex: structural basis for GTPase activation and its loss in oncogenic Ras mutants. *Science*, **277**, 333-338.

13. Nadanaciva,S., Weber,J., Wilke-Mounts,S. and Senior,A.E. (1999) Importance of F1-ATPase residue alpha-Arg-376 for catalytic transition state stabilization. *Biochemistry*, **38**, 15493-15499.

14. Rittinger,K., Walker,P.A., Eccleston,J.F., Smerdon,S.J. and Gamblin,S.J. (1997) Structure at 1.65 A of RhoA and its GTPase-activating protein in complex with a transition-state analogue. *Nature*, **389**, 758-762.

15. Abrahams,J.P., Leslie,A.G., Lutter,R. and Walker,J.E. (1994) Structure at 2.8 A resolution of F1-ATPase from bovine heart mitochondria. *Nature*, **370**, 621-628.

16. James,J.A., Escalante,C.R., Yoon-Robarts,M., Edwards,T.A., Linden,R.M. and Aggarwal,A.K. (2003) Crystal structure of the SF3 helicase from adeno-associated virus type 2. *Structure.*, **11**, 1025-1035.

17. Crampton,D.J., Guo,S., Johnson,D.E. and Richardson,C.C. (2004) The arginine finger of bacteriophage T7 gene 4 helicase: role in energy coupling. *Proc. Natl. Acad. Sci. U. S. A*, **101**, 4373-4378.

18. Johnson,A., Yao,N.Y., Bowman,G.D., Kuriyan,J. and O'Donnell,M. (2006) The replication factor C clamp loader requires arginine finger sensors to drive DNA binding and proliferating cell nuclear antigen loading. *J. Biol. Chem.*, **281**, 35531-35543.

19. Gai,D., Zhao,R., Li,D., Finkielstein,C.V. and Chen,X.S. (2004) Mechanisms of conformational change for a replicative hexameric helicase of SV40 large tumor antigen. *Cell*, **119**, 47-60.

20. Soultanas,P., Dillingham,M.S., Velankar,S.S. and Wigley,D.B. (1999) DNA binding mediates conformational changes and metal ion coordination in the active site of PcrA helicase. *J. Mol. Biol.*, **290**, 137-148.

21. Killoran,M.P. and Keck,J.L. (2006) Sit down, relax and unwind: structural insights into RecQ helicase mechanisms. *Nucleic Acids Res.*, **34**, 4098-4105.

22. Guo,R.B., Rigolet,P., Zargarian,L., Fermandjian,S. and Xi,X.G. (2005) Structural and functional characterizations reveal the importance of a zinc binding domain in Bloom's syndrome helicase. *Nucleic Acids Res.*, **33**, 3109-3124.

23. Dou,S.X., Wang,P.Y., Xu,H.Q. and Xi,X.G. (2004) The DNA binding properties of the Escherichia coli RecQ helicase. *J. Biol. Chem.*, **279**, 6354-6363.

24. Avron,M. (1960) Photophosphorylation by swiss-chard chloroplasts. *Biochim. Biophys. Acta*, **40**, 257-272.

25. Xu,H.Q., Deprez,E., Zhang,A.H., Tauc,P., Ladjimi,M.M., Brochon,J.C., Auclair,C. and Xi,X.G. (2003) The Escherichia coli RecQ helicase functions as a monomer. *J. Biol. Chem.*, **278**, 34925-34933.

26. Zhang,X.D., Dou,S.X., Xie,P., Wang,P.Y. and Xi,X.G. (2005) RecQ helicase-catalyzed DNA unwinding detected by fluorescence resonance energy transfer. *Acta Biochim. Biophys. Sin. (Shanghai)*, **37**, 593-600.

27. Liu,J.L., Rigolet,P., Dou,S.X., Wang,P.Y. and Xi,X.G. (2004) The zinc finger motif of Escherichia coli RecQ is implicated in both DNA binding and protein folding. *J. Biol Chem.*, **279**, 42794-42802.

28. Ko,Y.H., Bianchet,M., Amzel,L.M. and Pedersen,P.L. (1997) Novel insights into the chemical mechanism of ATP synthase. Evidence that in the transition state the gamma-phosphate of ATP is near the conserved alanine within the P-loop of the beta-subunit. *J. Biol. Chem.*, **272**, 18875-18881.

29. Janscak,P., Garcia,P.L., Hamburger,F., Makuta,Y., Shiraishi,K., Imai,Y., Ikeda,H. and Bickle,T.A. (2003) Characterization and mutational analysis of the RecQ core of the bloom syndrome protein. *J. Mol. Biol*, **330**, 29-42.

30. Pezza,R.J., Villarreal,M.A., Montich,G.G. and Argarana,C.E. (2002) Vanadate inhibits the ATPase activity and DNA binding capability of bacterial MutS. A structural model for the vanadate-MutS interaction at the Walker A motif. *Nucleic Acids Res.*, **30**, 4700-4708.

31. Dillingham,M.S., Soultanas,P. and Wigley,D.B. (1999) Site-directed mutagenesis of motif III in PcrA helicase reveals a role in coupling ATP hydrolysis to strand separation. *Nucleic Acids Res.*, **27**, 3310-3317.

32. Zittel,M.C. and Keck,J.L. (2005) Coupling DNA-binding and ATP hydrolysis in Escherichia coli RecQ: role of a highly conserved aromatic-rich sequence. *Nucleic Acids Res.*, **33**, 6982-6991.

33. Hall,M.C., Ozsoy,A.Z. and Matson,S.W. (1998) Site-directed mutations in motif VI of Escherichia coli DNA helicase II result in multiple biochemical defects: evidence for the involvement of motif VI in the coupling of ATPase and DNA binding activities via conformational changes. *J. Mol. Biol.*, **277**, 257-271.

34. Dittrich,M. and Schulten,K. (2006) PcrA helicase, a prototype ATP-driven molecular motor. *Structure.*, **14**, 1345-1353.

35. Kamath-Loeb,A.S., Welcsh,P., Waite,M., Adman,E.T. and Loeb,L.A. (2004) The enzymatic activities of the Werner syndrome protein are disabled by the amino acid polymorphism R834C. *J. Biol Chem.*, **279**, 55499-55505.

36. Karow,J.K., Newman,R.H., Freemont,P.S. and Hickson,I.D. (1999) Oligomeric ring structure of the Bloom's syndrome helicase. *Curr. Biol*, **9**, 597-600.

37. Choudhary,S., Sommers,J.A. and Brosh,R.M., Jr. (2004) Biochemical and kinetic characterization of the DNA helicase and exonuclease activities of werner syndrome protein. *J. Biol. Chem.*, **279**, 34603-34613.

38. Lammens,A., Schele,A. and Hopfner,K.P. (2004) Structural biochemistry of ATP-driven dimerization and DNA-stimulated activation of SMC ATPases. *Curr. Biol*, **14**, 1778-1782.

Chapter 3

GENERAL CONCLUSION AND PERSPECTIVE

1 The special function of zinc binding motif in RecQ family helicases

The term 'zinc finger', especially capturing the zinc atom, is derived from the original discovery of zinc-binding mini-domains in the protein transcription factor IIIA (1). After the first discovery of this motif, it has been found to be located in a lot of enzyme, especially in the DNA/or RNA-binding relative protein. Many of these proteins are transcriptional regulators of genes involved in a wide variety of cellular processes including metabolism of compounds. There are different types of the zinc finger, such C_2H_2, C_3H, C_4 and C_6, based on the number and position of cysteine residues and histidine residues. This structure of a typical motif is characterized by folding of an about 30 amino acid residue peptide into a short two-stranded antiparallel β sheet following by a α-helix with the aid of the Zn^{2+} in a tetrahedral coordination.

Sequence analyses revealed that RecQ helicases contain the zinc finger motif which belongs to the C_4 form type. This motif is usually localized on the C-terminal extension of protein. For example, the Cys^{380}, Cys^{397}, Cys^{400} and Cys^{403} form the zinc finger motif of *E.coli* RecQ (2). In human, BLM, WRN, RecQ1 and RECQ5 contain the conserved zinc finger, except RecQ4 helicase. The functions of the zinc finger motif in RecQ family helicases can be summarized according to our study and the study of other laboratories:

1) The zinc finger motif plays an essential role in DNA binding and protein folding; consequently assure the whole function of helicase (2;3). In an accordance with this interpretation, a single mutation of cysteine residue in BLM zinc finger cause BLM disease.
2) It is very well documented that RecQ family helicases play important roles at G-rich domains of the genome, including the telomeres, rDNA, and immunoglobulin switch region. How RecQ family helicase recognize this substrate? In accordance with our previous observation, Maizels and co-workers has found that the RecQ-Ct domain which contains essentially zinc finger motif functions as an independent, high affinity and conserved G4 DNA binding domain.
3) Our analysis of the isofroms of RecQ5 helicase demonstrated that the zinc finger may functions as a molecular switch to regulate transition between the strand annealing and DNA unwinding. In accordance with this view, RecQ4 helicase, the only human RecQ family helicase without the conserved zinc finger, display very strong annealing activity. Its DNA unwinding activity only can be revealed under special condition in

which a complementary ssDNA must be added in the reaction to prevent the strand annealing activity.

2 The function of the HRDC domain in RecQ helicase family

Unlike the arginine finger and the zinc binding motif, the HRDC (Helicase and RNAseD C-terminal) domain located at the C-terminal of helicases is more variational and even more is absent in some helicases. When we researched on the structures and functions of the RecQ helicase family, we are also interest in the HRDC domain in the C- terminal. During our research on the zinc binding motif of *Bacillus subtilis* RecQ helicases, we found the great difference on HRDC domain between two members in this species. The larger RecQ helicase in *Bacillus subtilis* contains the HRDC domain while the smaller one is absent in this domain naturally. The results showed that the *Bacillus subtilis* RecQ can exhibit its helicase functions without the HRDC domain, but these abilities are somehow faintness. The one which doesn't contain the HRDC domain in *Bacillus subtilis* can only unwind the complementary duplex strands not the forked duplex structures, the replication/repair intermediates and even the Holliday structures. Furthermore, it also has weaker ATPase activity correspondingly. However, the DNA binding and annealing activities are little different between these two RecQ helicases. So we presume that the HRDC domain increases the unwinding and ATPase activities of the helicase core domain, maybe it is required for unwinding the Holliday junctions not for the simple partial duplex substrates. This function of HRDC domain has been shown similar in the BLM helicase (4). The HRDC domain of BLM is required for BLM binding and unwinding the Holliday junctions, but not affects on the simple duplex DNA substrates. Other laboratories found the same function of the HRDC in other members of the RecQ helicase family such as human WRN, GcRecQ (*Neisseria gonorrhoeae* RecQ) and DrRecQ (*Deinococcus radiodurans* RecQ) (5;6). So the HRDC domain may takes an important role in the DNA repair process because helicase containing this domain can unwind some typical junctions existing at the fork stalling structures during DNA replication and repair processes. However the mechanism of the HRDC domain on DNA replication and repair is still unclear up to now.

3 The special structural feature of arginine finger of RecQ family helicase

The arginine finger usually locates near the γ-phosphate of ATP and it is distal to the nucleotide-binding site. The arginine finger can reside on a distinct activator protein (for example, GAP-Ras), an adjacent subunit of an oligomeric protein such as F1-ATPase, or a distinct domain within the protein itself which is in most SF1 and SF2 families. It contributes to the communication between the two RecA-like domains of helicases (domain 1A and 2A) and interacts with the γ-phosphate of a bound nucleotide. The finger affects on the NTP hydrolysis through stabilization of the transition state of the reaction and as a trigger for conformational changes after NTP hydrolysis.

Generally, the arginine finger in oligomeric proteins is localized in the interface between the adjacent subunits. Therefore, ATP binding and hydrolysis need the correct assembled oligomeric proteins and an isolated subunit could not be able to hydrolysis ATP. In this study, we showed that the arginine finger of BLM protein is localized in the interface of the two domains of the same subunit. This discovery may shed light on the long-standing puzzle: why heterozygote of BLM patients does not display any disease phenotype if BLM protein is hexamer. It is possible that the hexameric BLM protein will dissociate into monomer during catalysis. We will further confirm this possibility by combination of different method from Stoppted-flow to the time resolved fluorescence.

4 Perspective

The human RECQ helicases seem to play an important role in resolution of aberrant structures that arise from different repair pathways and are likely to mediate other functions as well. The fact that there are five different RecQ family members in humans, whereas unicellular organisms only contain a sole RecQ helicase, points to the evolutionary split-up and extension of the RecQ-mediated processes. Many groups have contributed to unravelling the roles of the RecQ helicases but the DNA transactions mediated by these proteins are diverse and are not fully understood yet. In fact, a very challenging task facing all DNA helicase research is how deficiency of a particular helicase gives rise to the characteristic biochemical, cellular, genetic, and organismal consequences observed in helicase mutants. The ATPase and strand displacement enzymatic activities are common to all DNA helicases; consequently, some other physical property of the helicase must govern

its functional specificity. For example, the observation that BLM and RECQ5 have non-redundant roles in suppressing crossovers is further supported by the finding that RECQ5β cannot perform the DHJ dissolution in conjunction with TOPOIIIα which is consistent with the finding that the HRDC domain of BLM absent in RECQ5β is essential for efficient binding and unwinding of DHJs. As we have found that RECQ5β exhibits strand-annealing activity in addition to its helicase activity, it may be that RECQ5 acts in the recovery of damaged replication forks by promoting fork regression, whereas BLM suppresses crossovers that would appear from the repair of non-meiotic DHJs that arise from HR-dependent repair of daughter strand gaps formed during replications. To elucidate the unique roles of the human RecQ helicases, different approaches must be combined.

It is a working hypothesis in the minds of most investigators that, by understanding the substrate specificities of a helicase and identifying the proteins or protein complexes with which a particular helicase interacts, the function of the helicase will become known.

The structure of RecQ helicase is basic for its biochemical functions. Although amino acid sequences of most RecQ helicase are clearly, few of their crystal structures have been solved up to now. Primitively, the structure of helicase was modelled according to some typical helicases which crystal structures have been determined (7;8). Now the bioinformatics system has became a key method using in determining of structure of helicase. From the model of a helicase, a lot of information can be provided on its biochemical features. But it is not the proof enough for understanding the molecular mechanisms of helicase. In order to enhance our results on RecQ helicases, the crystallizations of these helicases is an advantageous proof.

Recently, a new method, in-Cell NMR spectroscopy has been developed into observation of conformations and functions of protein in living cells (9;10). The labelled aimed protein was microinjected into living cells and the analysis protein with NMR spectroscopy. Since most RecQ helicases were expressed in *E.coli* and purified, we could use this new method to study its three-dimensional structures, dynamics, especially its interactions with nucleic acids and other protein *in vivo*. This new approaches may help us to identify the physiological substrate of RecQ helicase at different stages of cell cycle.

REFERENCES

1. Klug,A. and Schwabe,J.W. (1995) Protein motifs 5. Zinc fingers. *FASEB J.*, **9**, 597-604.

2. Liu,J.L., Rigolet,P., Dou,S.X., Wang,P.Y. and Xi,X.G. (2004) The zinc finger motif of Escherichia coli RecQ is implicated in both DNA binding and protein folding. *J. Biol. Chem.*, **279**, 42794-42802.

3. Guo,R.B., Rigolet,P., Zargarian,L., Fermandjian,S. and Xi,X.G. (2005) Structural and functional characterizations reveal the importance of a zinc binding domain in Bloom's syndrome helicase. *Nucleic Acids Res.*, **33**, 3109-3124.

4. Wu,L., Chan,K.L., Ralf,C., Bernstein,D.A., Garcia,P.L., Bohr,V.A., Vindigni,A., Janscak,P., Keck,J.L. and Hickson,I.D. (2005) The HRDC domain of BLM is required for the dissolution of double Holliday junctions. *EMBO J.*, **24**, 2679-2687.

5. Killoran,M.P., Kohler,P.L., Dillard,J.P. and Keck,J.L. (2009) RecQ DNA helicase HRDC domains are critical determinants in Neisseria gonorrhoeae pilin antigenic variation and DNA repair. *Mol. Microbiol.*, **71**, 158-171.

6. Killoran,M.P. and Keck,J.L. (2008) Structure and function of the regulatory C-terminal HRDC domain from Deinococcus radiodurans RecQ. *Nucleic Acids Res.*, **36**, 3139-3149.

7. Korolev,S., Hsieh,J., Gauss,G.H., Lohman,T.M. and Waksman,G. (1997) Major domain swiveling revealed by the crystal structures of complexes of E. coli Rep helicase bound to single-stranded DNA and ADP. *Cell*, **90**, 635-647.

8. Velankar,S.S., Soultanas,P., Dillingham,M.S., Subramanya,H.S. and Wigley,D.B. (1999) Crystal structures of complexes of PcrA DNA helicase with a DNA substrate indicate an inchworm mechanism. *Cell*, **97**, 75-84.

9. Sakakibara,D., Sasaki,A., Ikeya,T., Hamatsu,J., Hanashima,T., Mishima,M., Yoshimasu,M., Hayashi,N., Mikawa,T., Walchli,M. *et al.* (2009) Protein structure determination in living cells by in-cell NMR spectroscopy. *Nature*, **458**, 102-105.

10. Inomata,K., Ohno,A., Tochio,H., Isogai,S., Tenno,T., Nakase,I., Takeuchi,T., Futaki,S., Ito,Y., Hiroaki,H. *et al.* (2009) High-resolution multi-dimensional NMR spectroscopy of proteins in human cells. *Nature*, **458**, 106-109.

Chapter 4
APPENDIXES

I. MATERIALS AND METHODS

1. Plasmids construction

A. PCR and Gel extraction

Reagents and instruments

- Pfu DNA Polymerase 2-3U/ μL, Co.Promega
- dNTP mix, 25mM/each, Co. Fermentas
- 50×TAE buffer (1 L, pH 8.0) : 242g Tris base, 100ml 0.5 M Na_2 EDTA (pH 8.0), 57.1ml glacial acetic acid, add H_2O up to 1 litre. Sterilize by autoclaving

Note: To prepare 0.5M Na_2 EDTA (pH 8.0) add 186.1g of disodium ethylenediaminetetraacetate·$2H_2O$ to 800ml of H_2O. Stir vigorously. Adjust the pH to 8.0 with NaOH (ca. 20g of NaOH). The disodium salt of EDTA will not go into solution until the pH of the solution is adjusted to 8.0 by the addition of NaOH.

- λ DNA-BstEII Digest : 117bp to 8,454bp, Co. Biolabs
- PCR clean-up Gel extraction NuCleoSpin Extract II Kit, Co. MACHEREY-NAGEL
- Termal Cyclers/ DOUCYCLER, Co. VWR
- UV Transilluminator, Co. Major Science

Protocol

1. In a sterile, nuclease-free microcentrifuge tube (0.2mL), and in ice bath, combine the following components:

		Volume (μL)
DNA template (plasmids)	~0.5μg/μL	0.5
Upstream primer	100μM	0.1
Downstream primer	100 μM	0.1
dNTP mix	25mM each	0.4
Pfu DNA polymerase 10 X buffer with $MgSO_4$		5
Pfu DNA polymerase	2-3U/μL	0.8
Nuclease-free water to final volume of		50

Note: It is critical to add the Pfu DNA polymerase lastly; otherwise, the proofreading activity of the polymerase may degrade the primers. Assemble on ice before running the PCR program.

2. If using a thermal cycler without a heated lid, overlay the reaction mix with 1-2 drops (approximately 50μL) of mineral oil to prevent evaporation during thermal cycling. Centrifuge the reaction mix in a microcentrifuge for 5 seconds.

3. Immediately place the reactions in a thermal cycler and operate the PCR program.

Step	Temperature	Time	Number of Cycles
Initial Denaturation	95 °C	1-2min	1 cycle
Denaturation	95 °C	30s	35 cycles
Annealing	~55 °C	30s	
Extension	72 °C	approximately 1min for every 1kb	
Final Extension	72 °C	7min	1 cycle
Soak	4 °C	Indefinite	1 cycle

4. Analysis the PCR fragments on a 0.7 % 1×TAE agarose gel. The recovery was estimated by comparison with a fragment ladder.

5. If we get the aimed PCR fragments, purify the DNA fragments from the agarose gel.

6. Load all the PCR reaction on a 0.7% agarose gel and run the electrophoresis with fresh 1×TAE buffer and a clean groove to avoid the other nucleic acid contamination.

7. Take a clean scalpel to excise the DNA segment from the agarose gel in the 365-wavelength ultraviolet lamp. Excise gel slic containing the fragment carefully to minimize the gel volumne. Determine the weight of the gel slice and transfer it to a clean tube.

8. Purification the DNA extraction using NucleoSpin ExTractII kit. Generally, elte the DNA fragment with 50μL sterile and nuclease-free water. Analyze the eluted DNA on a 0.7% 1×TAE agarose gel and keep at -20°C.

B. Plasmid construction

Reagents and instruments

• Endonucleases (NedI, XhoI), Co. Biolabs

• pET-15b vector (5708bp), Co. Novagen

• 5×transformation buffer(KCM buffer): 0.5M KCl, 0.15M $CaCl_2$, 0.25M $MgCl_2$, 0.22μM filter and sterilize. Keep at -20°C.

• LB medium: 10g/L bacto-tryptone, 5g/L bacto-yeast extract, 10g/L NaCl, adjust pH to 7.0 with NaOH. Sterilize using autoclave.

• LB agar plate: Prepare LB medium as described above, before autoclaving, add agar (15g/L).

• LB agar plate with antibiotics: After sterilized LB agar medium, cool down at room temperature till it is cool enough to hold, and then add additional appropriate antibiotics at the concentration needed. Mix and pour the liquid agar medium into the plates to a depth of 4 or 5 mm. Let plates set under the super-clean bench until the agars solidify. Store the plates upside down in the fridge (4°C) or cold room until needed.

• Ampicillin sodium salt¨(AMP), Co. Sigma

• SURE® 2 Supercompetent Cells, Co. STRATAGENE

• TSS Solution: 85% LB medium, 10%PEG (wt/vol; mw 8000, Sigma), 5%DMSO (vol/vol, sigma) and 50mM $MgCl_2$, pH6.5, autoclaved or 0.22μM filter sterilized

• *Taq* DNA Polymerase (5U/μL), Co. STRATAGENE

• MF disc MCE philic 0.025μm 25mm, Co. Millipore

• DNA ligation Kit (T4 DNA ligase), Co. STRATAGENE

• Plasmid purification Kit, Co. STRATAGENE

Protocol

1. Microdialysis of the PCR purified products with 0.025μM membrane filter:

Fill the bottom of a Petri dish with sterile water, float the membrane filter disc on the surface of the buffered solution, then deposit 50μL of the PCR products solutions on the center of the membrane and place a tight-fitting lid on the Petri dish to prevent evaporation. After 30 ~60 min recover the desalted sample.

Note: Endonucleases and T4 ligase is strongly inhibited by high NaCl concentration. This step is in order to remove NaCl, so Endonucleases and T4 ligase can work in the best salt condition.

2. Digest the insert DNA with endonuclease:

In a sterile, nuclease-free microcentrifuge tube (0.5mL), and in ice bath, combine the following components to digest the desalted PCR products with NdeI and Xhol endonucleases.

Mix and incubate at 37°C for about 5 hours.

	Volume (μL)
PCR products	20
NdeI (20U/ μL)	5
XhoI (20U/ μL)	3
10× NEBuffer 4	4
Nuclease-free water to final volume of	40

3. Digest the vector with endonuclease:

Digest the pET15b vector with NdeI and XhoI endonucleases at 37°C for at least 5 hours. Analysis on the 0.7% agarose gel and purified the linearized vector from the gel using the NucleoSpin ExTract II kit. Keep the digested vector at -20°C.

4. Estimate the concentration between the vector and the target by DNA by loading them on a 0.7 % 1×TAE agarose gel.

5. Ligation system:

Add the following components to a clear microcentrifuge tube:

	Volume (μL)
Insert DNA (digested by NdeI and XhoI)	X
Vector (pET15b digested by NdeI and XhoI)	X
Nuclease-free water to final volume of	7.5

Mix and incubate at 75°C for 1~3min to break undesired ligations intra-vector or intra-target DNA. After cooling in ice bath for several minutes, centrifuge the reaction mix for 5 seconds. Add the rest ligation components, 10 × ligase buffers 1 μL, rATP (10mM) 0.5μL and T4 ligase (4U/μL) 0.5μL which are from the ligation kit. Mix gently and incubate the ligation reaction system at 4°C overnight.

Note: To obtain optimum results, it recommends using various vector-to-insert ratios from 2/1 to 10:1 to ensure the highest ligation efficiency.

6. Competent cells preparation:

Take out about 5 μL stock of competent cells or purchased cells and incubate in 5mL LB at 37°C with shaking at 200rpm overnight. Transfer 1mL of the saturated overnight culture of cells to a fresh, sterile 500mL flask containing 100mL LB medium (do not add any antibiotic in this step). Incubate the cells at 37°C with shaking at 200rpm, until OD_{600} reaches 0.5±0.03, Check the OD frequently when it gets beyond 0.4 to avoid overgrowth. When the culture reaches the exponential phase, chill the flask on ice for 20min and then collect the cells by centrifugation at 1,200×g for 30min at 4°C. During the centrifugation, prepare 10mL fresh TSS Solution under the super-clean bench and keep on ice. After centrifugation, decant the LB medium supernatant carefully and completely. Resuspend the cells with 10mL of ice-cold TSS solution gently. The prepared competent cells are stored at -80°C at volume of 100μL in each microtube.

Note: When pre-incubate the cells in 5mL LB medium overnight, don't add any antibiotic into medium for Sure-2 cells. But for Rosetta cells and Codonplus cells, we should add 50μg/mL Chloramphenicol into the pre-incubation system. We should use the fresh TSS Solution.

7. Chemical transformation

Mix the components as following in ice bath and incubate the reactions on ice for 30min:

ligation reaction system	10μL
5×KCM buffer	20μL
Sterile water	80μL
Sure-2 competent cells	100μL

Note: It's better to swirling transformation reactions gently every several minutes during the ice incubation to let the transformation more efficiently. Store the competent cells on ice at all times during the whole operation.

Heat-pulse the reaction in a 42°C water bath for 1 minute, then incubate on ice for 2 minutes. Add 0.8mL LB medium to the reaction and incubate at 37°C for 1 hour with shaking at 200~220rpm. Centrifuge the reaction at 14,000rpm for 2 minutes to collect all the cells. Decant a majority of LB medium supernatants and resuspend the cells gently with the rest LB medium (about 200μL). Using a sterile spreader or glass beads, spread of the cells transformed with experimental DNA onto LB agar plate which contain the appropriate antibiotic (80μg/mL Ampicillin). Transformation will appear as colonies following overnight incubation at 37°C.

Note: The duration of the heat pulse is critical for optimal transformation efficiencies. When adding LB medium and spreading the cells onto plate, it is better operate under the super-clean bench to avoiding contamination.

8. Colony screening by PCR

(1) DNA extracts

Pick out several colonies from the plate and incubate in 500 μL LB containing 100μg/mL AMP at 37°C for with shaking at 220rpm until the medium appears turbid about 5 hours). Take out half volume of the incubating medium, centrifuge at 14,000rpm for 5min to collect the cells. Decant the supernatant and resuspend the cells with about 50 μL sterile water. Heat the cells at 95°C for 10min to destroy the cells and let all DNA release. Centrifuge at 14,000rpm at 4°C for 20min to remove the fragments of cells. Transfer out the supernatant containing the DNA extraction with pipette carefully.

(2) PCR screening

In a sterile, nuclease-free microcentrifuge tube (0.2mL), and in ice bath, mix the following components:

		Volume (μL)
DNA extraction solution		2
Upstream primer	100μM	0.1
Downstream primer	100 μM	0.1
dNTP mix	25mM each	0.2
10× Taq polymerase buffer with $MgSO_4$		2.5
Taq DNA polymerase	5U/μL	0.5
Nuclease-free water to final volume of		25

Immediately place the reactions in a thermal cycler and operate the PCR program.

Step	Temperature	Time	Number of Cycles
Initial Denaturation	95 °C	1-2min	1 cycle
Denaturation	95 °C	30s	25 cycles
Annealing	~55 °C	30s	
Extension	72 °C	approximately 1min for every 1kb	
Final Extension	72 °C	7min	1 cycle
Soak	4 °C	Indefinite	1 cycle

Analysis the PCR segments on a 0.7 % 1×TAE agarose gel. The recovery was estimated by comparison with the purified target DNA obtained on step A-3. If the sizes of them are same, we can make sure that we get the correct plasmid primary.

9. Plasmids purification and screening by digestion

Transfer the rest half volume of the incubating medium into 5mL LB medium containing 100μg/mL AMP and incubate at 37°C overnight with shaking at 200rpm. Collect the cells with centrifugation and purify the plasmid using Plasmid Purification Kit. Finally elute the plasmid with 50μL sterile water. After analysis the eluted plasmid on a 0.7% 1×TAE agarose gel, digest the plasmid at 37°C for 2 hours with NdeI and XhoI endonucleases to check whether the target DNA has inserted into the vector. Mix the following components on ice:

	Volume (μL)
plasmid	8
NdeI (20U/ μL)	0.5
XhoI (20U/ μL)	0.3
10× NEBuffer4	1
Nuclease-free water to final volume of	10

Compare the result of digested plasmid with the purified target DNA obtained on step A-3 on a 0.7 % 1×TAE agarose gel. If the target DNA is released by digesting, it testifies that we obtain the aim constructed plasmid.

Note: If necessary, analysis the recombined plasmid sequence and then compare with the original sequence of cDNA.

2. Protein expression and purification

Reagents and instruments

- Chloramphenicol (CAM), Co. VWR (34mg/mL in absolute ethanol)
- Rosetta^{TM}(DE3) Competent cells, Co. Novagen
- Phenylmethanesulfon (PMSF), Co. Sigma
- Isopropyl-β-D-thiogalactopyranoside (IPTG), Co. EUROMEDEX
- His•tag affinity Resin Co. Novagen
- 1×Binding Buffer: 0.5M NaCl, 20mM Tris-HCl, 5mM imidazole, 10% Glycerol, pH 7.9
- 1×Wash Buffer: 0.5M NaCl, 20mM Tris-HCl, 60mM imidazole, 10% Glycerol, pH 7.9
- 1×Elute Buffer : 0.5M NaCl, 20mM Tris-HCl, 500mM imidazole, 10% Glycerol, pH 7.9
- 1×Charge Buffer : 50mM $NiSO_4$
- Superdex-200 buffer: 0.5M NaCl, 20mM Tris-HCl pH 7.9, 10% Glycerol, 1mMDTT

- Acrylamide/bis-acrylamide 40%, 37.5/1, Co.EUROMEDEX
- Econo-Column Chromatography Columns, 2.5 × 10cm, Co. Biorad
- Econo-Column Flow Adaptor Instruction, Co. Biorad
- Mini-PROTEAN Tetra Electrophoresis System, Co. Biorad
- HPLC system (ÄKTA Purifier), Co. GE Healthcare
- Amicon Ultra Centrifugal filter Devices, Co.MILLIPORE
- Bio-Rad Protein Assay Dye Reagent Concentrate, Co. Biorad

Note: All buffers should be filtrated with 0.22μM membrane and degased additionally for Superdex-200 column. The pH value of buffer should be far away from the pI value of target protein and better higher than pI because the protein binding capacity demonstrates in alkalescent condition.

Protocol

(1) Transformation of expression host

Using chemical transformation method (See protocol B-7), transfer the recombinant plasmid into Rosetta competent cells and spread the cells DNA onto LB agar plate which contain the appropriate antibiotic (80μg/mL Ampicillin + 34μg/mL Chloramphenicol). Transformation will appear as colonies following overnight incubation at 37°C.

Note: The expression host is selective: the BL21 (DE3) needed 50~100μg/mL Ampicillin, BL21 (DE3)/TrxB (50μg/mL ampicillin + 15μg/mL kanamycin) or BL21 codonplus (80μg/mL Ampicillin + 34μg/mL Chloramphenicol). The results of expression of the aim protein in these host is variable, so we should do small scale protein expression to choose the best condition and host to express the aim protein.

(2) Small scale protein expression

Pick out one single colon from the plate and incubate in 50mL LB (80μg/mL AMP + 34μg/mL CAM) at 37°C with shaking at 200rpm until OD_{600} reaches 0.6(mid-exponential phase). Induce the protein expression in addition of 0.5mM IPTG to the growing culture at 18°C overnight with shaking of 200rpm. The cells are harvested by centrifugation at 10,000g at 4°C for 15min and suspended in a final volume of 5mL of the lysis buffer (0.5M NaCl, 20mM Tris-HCl pH 7.9, 5mM imidazole, 10% Glycerol, 0.1μM PMSF). Cells are sonicated on ice to reduce viscosity and then centrifuged at 15,000g at 4°C for 45min to remove insoluble materials. Transfer the soluble part; resuspend the insoluble part with appropriate volume of 1%SDS. The insoluble part and the soluble part are run on 10% SDS-polyacrylamide gels at 100V for about 2 hours. The gel is stained with Coomassie brilliant blue to estimate whether the protein has been induced express.

Note: It's better to compare the crude cell extracts before inducing and after inducing on SDS-PAGE to help us to evaluate the expression easily. The condition of expression is optional, we choose 37°C for 3 hours or 18°C overght. The culture can be stored at -80°C.

(3) Strain storage

It's necessary that we store the strain of target protein for further research. Pick out one single colon from the plate and incubate in 5mL LB (80μg/mL AMP + 34μg/mL CAM) at 37°C overnight with shaking of 200rpm. Mix the bacterial liquid and 100% sterile glycerol of equivalent volume (1mL/1mL) in microtube. Store at -80°C.

(4) Protein purification using His tag resin

Incubate the conserved stain or single colon from plate in 5mL LB (80μg/mL AMP + 34μg/mL CAM) medium at 37°C overnight with shaking of 200rpm. Transfer out 1mL culture into 1L LB (80μg/mL AMP + 34μg/mL CAM) medium and incubate at 37°C until OD_{600} reaches 0.6, then add 0.5mM IPTG to induce protein expression at 18°C overnight with shaking of 200rpm.

Harvest cells by centrifugation at 10,000×g for 10min. Decant supernatant. Allow cell pellet to drain as completely. Resuspend cells in 30mL ice-cold 1×Binding buffer contain 0.1μM PMSF per 1L culture.

Note: If resuspension is difficult, blender and soicator can be used to break up cell pellet well. The cells can be stored at -80°C after centrifugation.

Frech press and sonicate the cell suspenion in tube on ice until sample is no longer viscous. Divide sonication into bursts and allow cooling between treatments to avoid long sonication times to prevent sample heating. Centrifuge lysate twice at 14,000×g for 45min to remove cell debris. Filter post-centrifugation supernatant though a 0.45μM membrane (syringe-end filters) to prevent clogging of resins.

During centrifugation, install the His·Bind column chromatography charged with Ni^{2+} (10mL resin per 1L culture volume). Equilibrate the column with at least 3 times volume 1× Binding buffer. Load the filtrated supernatant onto the column. Apply vacuum and adjust flow rate to about 1mL/min.

Note: Passing flow-through over the same column to cartridge a second time can increase yields.

Wash the column with 10 volumes of 1×Binding buffer, at flow rate of 1~2mL/min.

Wash the column with 6 volumes of 1×Wash buffer, at1~2mL/min.

Elute the bound protein with at lease 3 volumes of 1×Elute buffer, at 1mL/min.

Analysis the protein solution pooled on each step on SDS-PAGE using standard methods.

Note: The whole process can be manipulated using HPLC system and monitored at UV280. Manipulations are done on ice or in 4°C cold room. A obvious peak appears at UV280 on each step, at the end of eluting, the

UV280 curve won't be back to the base level because imidazole has the absorption value related to its concentration. The binding capacity to His•Bind resin is various for different protein. It's better to wash and elute the sample with gradient concentration of imidazole monitored at UV280. Analyze all the collected solution of each peak on SDS-PAGE to estimate the eluting concentration of imidazole for the aim protein.

(5) Protein purification further with Superdex-200 column Chromatography

Harvest eluted protein sample and concentrate using Centrifugal Filter Devices at 4000×g at 4°C to final volume of about 2mL (>2mg/mL). Centrifuge the concentrated protein sample at 14,000×g at 4°C for 30min to remove denatured pellet, or filtrate with 0.22μM filter before loading onto Superdex-200 column Chromatography.

Note: The molecular weight limit of concentrate device is chosen according to that of aim protein. Remove concentrated sample immediately after centrifugation.

Load the filtrated protein sample onto Superdex-200 equilibrated with at least 1vol of Superdex-200 buffer monitoring on UV280 using HPLC system (ÄKTA Purifier).

General program of Superdex-200:

Sample volume: 2mL (≤ 1/100 of column volume) Superdex-200 column volume: 350mL Equilibrate Volume: 80mL Flow rate: 0.3~0.5mL/min, 4°C Fraction Size: 4mL/tube End volume: 400mL

(6) Protein concentration detection and storage

Collect fractions of each peak and check on SDS-PAGE. Pool and concentrate the aim protein solution with Centrifugal Filter Devices. Determination of the concentration of the aim protein using Bio-Rad Protein Assay Dye Reagent at OD_{595} comparing with the standard linear of BSA (0.5 μg/μL) from 0 μg to 10 μg. Allot the protein to 10 or 20μL per microtube and store at -80°C. Make sure that there is 5~10% glycerol in protein storage.

Note: Before store the protein into -80°C refrigerator, the sample should be freeze quickly by Liquid Nitrogen to avoid form the ice crystal during temperature decreasing.

3. Western blot

Reagents and instruments

- 10×PBS(pH7.4): NaCl 80g, KCl 2g, Na2HPO4.7H2O 26.8g, KH2PO4 2.4g, add H_2O to 1L and adjust pH to 7.4 with HCl
- PBST: 1×PBS+ 0.1% Tween20
- Blocking solution: 1×PBS, 0.1% Tween20, 10% degreased milk powder

• Primary Antibody solution: 1×PBS, 0.05% Tween20, 1%BSA, His-tag monoclonal antibody (1:2500)

• Secondary Antibody solution: 1×PBS, 0.05% Tween20, 5% degreased milk powder, Peroxidase labelled secondary antibody (1:2000)

• Ponceau Staining Solution: 0.25% ponceau S, 3.5% TCA

• Transfer buffer: 25mM Tris Base, 192mM Glycine, 20% Methanol (v/v), 0.01% SDS

• Trans-blot SD SEMI-DRY TRANSFER CELL, Co.Biorad

• Inrocellulose membrane, Co.Sigma

• His-Tag monoclonal Mouse IgG (100 μg/μL), Co.ONCOGENE

• Peroxidase labelled anti-rabbit antibody,Co.GE Healthcare

• ECL Western blotting detection reagents and analysis system, Co.GE Healthcare

• Hyperfilm ECL 18×24cm film, Co. GE Healthcare

• Amersham Hypercassette™ Autoradiography Cassettes, Co. GE Healthcare

Protocol

We estimate the quality of target protein during each step of purification process using Western blot assay.

(1) Run the SDS-PAGE using standard methods. When the electrophoresis is finished, take out the gel and remove the stacking gel and cut the gel in about 7cm×8cm large.

(2) Sock the SDS gel, inrocellulose membrane and whatman papers in transfer buffer for 5min. Remove the demi-dry transfer apparatus, place 9 sheets of pre-soaked whatman papers one by one onto the platinum anode. Roll a pipette or test tube over the surface of the whatman paper (like a rolling pin) when adding each paper to exclude all air bubbles. Place the pre-wetted inrocellulose membrane on top of the whatman paper and roll out all air bubbles. Carefully place the equilibrated gel on top of the transfer membrane, aligning the gel on the center of the membrane. Transfer will be incomplete if any portion of the gel is outside the blotting media. Roll out all air bubbles. Place another 9 sheets of whatman papers on top of the gel, carefully removing air bubbles from between the gel and filter papers (Fig 1). Install the transfer apparatus carefully and transfer at 25V for 1h30. The transfer efficiency can be monitored by staining the membrane with ponceau stain.

Note: Do not reverse polarity. Put the transfer membrane on the anode polarity.

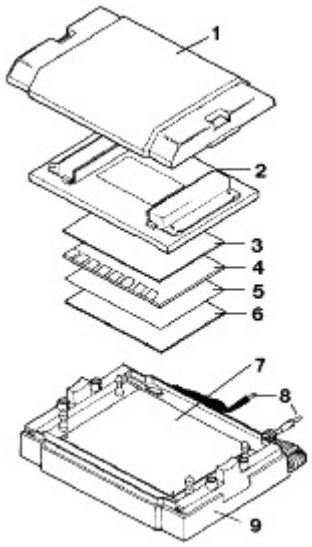

Fig 1: Install the western system in demi-dry transfer apparatus

1. cover
2. stainless steel cathode assembly
3. whatman paper (9 sheets)
4. gel
5. transfer membrane
6. whatman paper (9 sheets)
7. anode assembly
8. pluge
9. base

(3) Wash the membrane with 1×PBST for 5min at room temperature with shaking of 120rpm/min. Block non-specific binding sites by immersing the membrane in the Block Solution at room temperature for 1~3 hours or at 4°C overnight with shaking of 120rpm/min.

(4) Rinse the membrane in 1×PBST for 4×5min with shaking of 120rpm/min. Incubate the membrane in fresh Primary Antibody solution at 4°C overnight with shaking of 120rpm/min.

(5) Rinse the membrane in 1×PBST for 4×5min with shaking of 120rpm/min. Incubate the membrane in fresh Secondary Antibody solution at room temperature for 1~3 hours with shaking of 120rpm/min. Rinse the membrane as the above method.

(6) Mix an equal volume of detection solution 1 with detection solution 2 of ECL kit allowing sufficient total volume to cover the membranes. The final volume required is 0.125 ml/cm^2 membrane. (7mL solution 1 with 7mL solution 2 for each 7cm×8cm membrane in this protocol)

(7) Drain the excess PBST buffer from the washed membranes and place them, protein side up, incubate in the detection solution at room temperature for 1~5min in the dark room.

(8) In the dark room, place the wrapped blots, protein side up, in an X-ray film cassette. Place a sheet of autoradiography film (for example, Hyperfilm ECL) on top of the membrane. Close the cassette and expose for 15 seconds. Remove the film and replace with a second sheet of unexposed film. Develop the first piece of film immediately, and on the basis of its appearance estimate how long to continue the exposure of the second piece of film. Second exposures can vary from 1 minute to 1 hour, even overnight.

Note: The Block Solution, Primary Antibody solution and Secondary Antibody solution should be prepared freshly. The membrane is immersed in all the solutions completely.

4. ATPase activity

Reagents and instruments

- [γ-^{32}P]-ADENOSINE 5'-TRIPHOSPHATE (6000Ci/mmol), Co. PerkinElmer
- Solution A : Ammonium molybdate $(NH_4)_2MoO_4$ 5g, HCl 37% 40mL, add H_2O to 500mL
- Solution B: cyclohexane 250mL, butanol-2 250mL, Acetone 50mL, Solution A 10mL
- ATPase reaction buffer: 50mM Tris-HCl pH7.5, 50μg/mL BSA, 20mM NaCl, 5mM $MgCl_2$, 1mM DTT (usually prepared as 5×ATPase reaction buffer)
- Phosphoric acid solution, Co. Fluka
- 1414 Liquid scintillation counter WALLAC WINSPECTRAL, Co. CMI

Protocol

Note: All operations should be done in the radiation laboratory and observe the safty rules.

(1) Prepare ATP solution contains ATP, γ^{32}-Pi, reaction buffer, substrate (DNA or RNA), detect CPM value of 1μL solution, usually 1mM ATP possesses 3000~10000 CPMA.

(2) Add the helicase to ATP solution in final volume of 40μL, mix and incubate at 37°C for desired time (from 10min to 30min), Transfer out 35μL reaction system into a 2mL microtube containing 600μL Solution A to terminate the reaction and then add 6μL Phosphate acid. Agitate vigorously for 30s, centrifuge at 14,000×g for 30s. Add 1mL Buffer B to extract the hydrolyte Pi, agitate vigorously for 30s, centrifuge at 14,000×g for 1 min to

distribute the organic phase and the aqueous phase. Take out 400μL of organic solution on the upper into a fresh microtube.

(3) Count the CPM value of radioactivity with Liquid scintillaton counter.

(4) Determine hydrolysis rate by following equation:

$$V = \frac{(CPM_{sample} - CPM_{control}) \times C_{ATP}}{v_{sample} \times CPM_{ATP} \times T}$$

Where V is the hydrolysis rate (μM ATP/min), CPM_{sample} is the radioactive value of sample, $CPM_{control}$ is the radioactive value of blank control without protein, C_{ATP} is the concentration of ATP (μM), v_{sample} is the final relative volume taken out from total reaction system to count the radioactive value multiplying with the percentage of volume taken from the 40μL reaction to add into Solution A, C_{PMATP} presents the radioactive value of 1μL ATP, and T is the reaction time (min). Measure the data with Microsoft Office Excel and Soft KaleidaGraph4.0.

5. Helicase activity examination

Reagents and instruments

- Sephadex^{TM}-G25 resin (superfine), Co. GE Healthcare
- Whatman glass microfiber filter, Co. Millipore
- T4 Polynucleotide Kinase(10U/μL) with reaction buffer, Co. Biolabs
- 1×TE buffer: 10mM Tris-HCl, pH7.5, 1mM EDTA
- 10×TBE buffer (1L): Tris base 108g, Boric acid 55g, 0.5M EDTA (pH 8.0) 40mL
- 5×Hybridation buffer: 5× (95mM NaCl, 5mM $MgCl_2$, 50mMTris-HCl pH7.5)
- 5×unwinding reaction buffer: 5× (50mM Tris-HCl pH7.5, 5mM $MgCl_2$, 6mM NaCl, 50μg/mL BSA, 5% Glycerol, 1mM DTT)
- 5×binding reaction buffer: 5× (50mM Tris-HCl pH7.5, 6mM NaCl, 5% Glycerol, 1mM DTT)
- 5×annealing reaction buffer: 5× unwinding reaction buffer

• 3×unwinding reaction stop-loading buffer: 50% Glycerol, 20mM EDTA, 0.5%SDS, 0.05% Bromophenol Blue

• 3×binding reaction stop-loading buffer: 50% Glycerol, 0.05% Bromophenol Blue

• 3×annealing reaction stop-loading buffer: 3×unwinding reaction stop-loading buffer

• Gel fixing solution: 6% acetic acid, 10% ethanol

• Acrylamide/bis-acrylamide 40%, 19.5/1, Co. EUROMEDEX

• Hoefer™ SE 600 electrophoresis Series, Co. Hoefer

• Storage Phosphor Screens and Cassettes 35 × 43 cm, Co. GE Healthcare

• Storm® gel and blot imaging system, Co. GE Healthcare

• GD 2000 Vacuum Gel Dryer System 115 VAC, Co. GE Healthcare

Protocol

Note: All operations should be done in the radiation laboratory and observe the safty rules.

(1) Labeled-DNA substrates preparation

A. Label the oligos

Mix the following components in a microtube and incubate at 37°C for 1 hour:

Oligonucleotide (50μM)	1.5μL
10×T4 kinase reaction buffer	1.5μL
T4 polynucleotide Kinase	1.5μL
[γ-^{32}P]ATP (6000ci/mmol)	3 μL
Add sterile H2O to final volume of	15 μL

Note: It is better to heat the oligos at 95°C for 2min before adding T4 kinase and radio material to let the DNA structure be open, then chill on ice for 5min.

B. Prepare the purification column

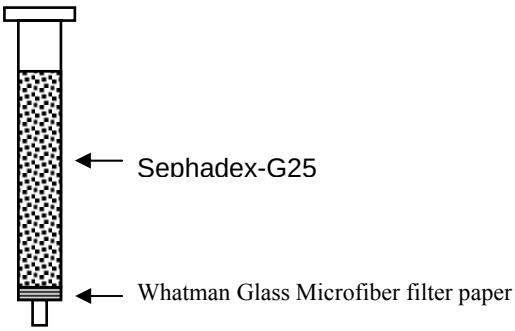

Figue 2 : Self-install Sephadex-G25

Install the Sephadex-G25 resin equilibrated with 1×TE buffer into 1mL-style syringe column using two sheets of Whatman Glass Microfiber filter paper (Fig 2). Finally we get about 0.8~1mL free settling and centrifuge it at 1400×g at room temperature for 5min in order to remove TE buffer and make the resin tight.

C. Labeled- oligo purification

Load the radioactive labeling reaction onto the Sephadex-G25 column, centrifuge at 1400×g at room temperature for 5min. Collect the flow-through solution. Wash the column with another 4×15μL H_2O and centrifuge to collect the flow-through. Count the CPM value of each fraction and pool the fractions at highest CPM values, usually we collect the first three fractions, then calculate the proximate concentration of labelled-oligo as following expressions:

$$C_{label} = \frac{C_0 \times V_0 \times CPM_P / CPM_T}{V_P}$$

Where the C_{label} is the concentration of labeled oligo; C_0 is the original concentration of oligo; V_0 presents the original volume of oligo before add into reaction system; CPM_P is thetotal count of CPM of pooled fractions; CPM_T is the total count of CPM of all fractions; V_P is the volume of oligo pooled.

The labelled oligo can be store at -20°C for two weeks.

D. Hybridation

Mix the labeled and unlabelled ssDNA at ratio of 1:5 (μmol/ μmol). After heated at 95°C for 5min and chilled on ice for 2min, add 1/5 volume of 5×hybridation buffer and incubate at 37°C for 1hour. Detect the count of CPM value and calculate the CPM value per μL of hybridized DNA and check whether the hybridation is complete using electrophoresis mobility shift assay (EMSA). Store at -20°C.

Note: We find that repeated freezing and thawing is helpful to single DNA hybridation.

(2) DNA binding assays by electrophoresis mobility shift assay (EMSA)

Mix the labeled substrates, binding reaction buffer and enzyme of needed concentration to final volume of 20μL on ice. Incubate at 37°C for 20min, add 7μL 3×binding reaction stop-loading buffer. Mix completely and centrifuge for 5 seconds. Load the reaction samples onto 1×TBE 6% nondenaturing polyacrylamide gel (19:1, 18cm×18cm) to separate the protein-DNA complexes electrophoretically and run at 200V for about 90~120min at 10°C. Fix the gel in 6% acetic acid and 10% ethanol for 10min, and then dry it at 80°C for 1h. Exposure of the gel in the cassette with the storage phosphor screens at room temperature overnight or even for longer time. The image is visible by scanning the screen with Storm system.

Note: When mix the all the reaction components, it is better operate on ice and add the enzyme lastly. Amount of labelled substrates are determined according to its CPM value in each reaction sample. Usually we add the substrates of 1000~2000 CPM value per reaction. Before loading the sample, the gel should be run without any sample at 200V for 30min at 8°C. To estimate the results more believably, the blank control without enzyme and labelled ssDNA, labelled hybridized DNA are necessary for EMSA assay.

(3) DNA unwinding activity assays by EMSA

The unwinding reaction system (20μL) contains the labeled substrates of 1000~2000 CPM value, appropriate ATP (usually 2 or 2.5 mM), unwinding reaction buffer with Mg^{2+} and helicase protein. The reaction processes at 37°C for 30min and is stopped by adding 7μL 3×unwinding reaction stop-loading buffer. Mix and load onto 1×TBE 12% nondenaturing polyacrylamide gel (19:1, 18cm×18cm). The gel is run at 8°C for 90~120min at 200V. Dry the gel after fixing for 10min, the image is autoradiography by storage phosphor screen and Strom system.

(4) DNA annealing activity assays by EMSA

For the annealing activity reaction, the labeled ssDNA and unlabeled ssDNA should be added directly at radio of 1:2 (w/w). ATP is not necessary for annealing activity and even sometimes it will inhibit the annealing activity of helicase. The annealing reaction buffer is the same as unwinding reaction buffer. Incubate 20μL reaction system at 37°C for 10~15min and then add 7μL 3×unwinding reaction stop-loading buffer to stop the reaction. Analysis the result in the same condition of unwinding activity assay by EMSA and autoradiography.

6. Determine zinc ion concentration of helicase

Reagents and instruments

- Buffer A: 20mM Tris-HCl, pH8.0, 500mM NaCl
- PAR, Co. Sigma, (PAR solution: PAR 0.2mM in buffer A)
- Trypsin, Co. Sigma (prepare at 20mg/ml)

Protocol

(1) Preparing gradient $ZnCl_2$ solution with buffer A. Usually, we use the $ZnCl_2$ of 1nmol/μl for preparing the gradient solutions because it's easy to convert to the mole number of

$ZnCl_2$ in solutions. The gradient of $ZnCl_2$ that I used is 0, 0.1, 0.2, 0.4, 0.6, 1, 2, 3, 4, 5 nmol, each in 500μl.

(2) Prepare 500μl protein solution which contains a certain mole number of protein. (Attention: here we use "mole number" not the "mole concentration") with buffer A from 1nmol of protein. For each mole number of protein we prepare two samples, one of them is prepared by diluting the original protein solution directly in Buffer A; Another needs to adding 10μl of 20mg/ml of trypsin and digests at 37°C water-bath for 2 hours.

Note: after boiling the samples, it is better to give samples a flash centrifuge and let it cool down to nearly the room temperature.

(3) Add equal volume of PAR to samples, mixing well, detect at OD_{490} value from the spectrophotometer.

Note: The PAR may break some of the structure of protein, therefore, you should measure as soon as possible after adding it.

(4) Calculate the OD_{490} given out by the trapped zinc ion ($OD_{trapped}$) as the following formula:

$$OD_{total} - OD_{free} = OD_{trapped}$$

Then, calculate the standard curve and convert the $OD_{trapped}$ to the mole number of Zinc ion.

II. List of Publications

1. **Ren, H**., Dou, S.X., Rigolet, P., Yang, Y., Wang, P.Y., mor-Gueret, M. and Xi, X.G. (2007) The arginine finger of the Bloom syndrome protein: its structural organization and its role in energy coupling. *Nucleic Acids Res.*, **35**, 6029-6041.

2. Guo,R.B., Rigolet,P., **Ren,H**., Zhang,B., Zhang,X.D., Dou,S.X., Wang,P.Y., mor-Gueret,M. and Xi,X.G. (2007) Structural and functional analyses of disease-causing missense mutations in Bloom syndrome protein. *Nucleic Acids Res.*, **35**, 6297-6310.

3. **Ren,H**., Dou,S.X., Zhang,X.D., Wang,P.Y., Kanagaraj,R., Liu,J.L., Janscak,P., Hu,J.S. and Xi,X.G. (2008) The zinc-binding motif of human RECQ5beta suppresses the intrinsic strand-annealing activity of its DExH helicase domain and is essential for the helicase activity of the enzyme. *Biochem. J.*, **412**, 425-433.

4. Yang, Y., Dou, S.X., **Ren, H**., Wang, P.Y., Zhang, X.D., Qian, M., Pan, B.Y. and Xi, X.G. (2008) Evidence for a functional dimeric form of the PcrA helicase in DNA unwinding. *Nucleic Acids Res.*, **36**, 1976-1989.